
**Università degli Studi di Verona**

FACOLTÀ DI SCIENZE MATEMATICHE, FISICHE E NATURALI
Dipartimento di Biotecnologie

Dottorato di Ricerca in
Biotecnologie Molecolari, Industriali ed Ambientali
XXII CICLO

# The function of monomeric Lhcb proteins of Photosystem II analyzed by reverse genetic

Coordinatore:
**Ch.mo Prof. Roberto Bassi**

Supervisore:
**Ch.mo Prof. Roberto Bassi**

Dottoranda:
**Silvia de Bianchi**

**Anni Accademici 2007–2009**

A Stefano

# Contents

# Summary

In eukaryotes the photosynthetic antenna system is composed by subunits encoded by the light harvesting complex (Lhc) multigene family. These proteins play a key role in photosynthesis and are involved in both light harvesting and photoprotection. In particular, antenna protein of PSII, the Lhcb subunits, have been proposed to be involved in the mechanism of thermal dissipation of excitation energy in excess (NPQ, non-photochemical quenching). Elucidating the molecular details of NPQ induction in higher plants has proven to be a major challenge. In my phD work, I decided to investigate the role of Lhcbs in energy quenching by using a reverse genetic approach: I knocked out each subunit in order to understand their involvement in the mechanism. Here below the major results obtained are summarized.

**Section A. Mutants of monomeric Lhc and photoprotection: insights on the role of minor subunits in thermal energy dissipation.** In this section I investigate the function of chlorophyll *a/b* binding antenna proteins, CP26, CP24 and CP29 in light harvesting and regulation of photosynthesis by isolating *Arabidopsis thaliana* knockout (ko) lines that completely lacked one or two of these proteins.
In particular in Section A.1 I focused on single mutant koCP24, koCP26 and double mutant koCP24/26. All these three mutant lines have a decreased efficiency of energy transfer from trimeric light-harvesting complex II (LHCII) to the reaction center of photosystem II (PSII) due to the physical disconnection of LHCII from PSII and formation of PSII reaction center depleted domains in grana partitions. We observed that photosynthetic electron transport is affected in koCP24 plants but not in plants lacking CP26: the former mutant has decreased electron transport rates, a lower pH gradi-

ent across the grana membranes, a reduced capacity for non-photochemical quenching, and a limited growth. Furthermore, the PSII particles of these plants are organized in unusual two-dimensional arrays in the grana membranes. Surprisingly, the double mutant koCP24/26, lacking both CP24 and CP26 subunits, restores overall electron transport, non-photochemical quenching, and growth rate to wild type levels. We further analysed the koCP24 phenotype to understand the reasons for the photosynthetic defection. Fluorescence induction kinetics and electron transport measurements at selected steps of the photosynthetic chain suggested that koCP24 limitation in electron transport was due to restricted electron transport between $Q_A$ and $Q_B$, which retards plastoquinone diffusion. We conclude that CP24 absence alters PSII organization and consequently limits plastoquinone diffusion. The limitation in plastoquinone diffusion is restore in koCP24/26.
In Section A.2 I characterized the function of CP29 subunits, extending the analyses to the different CP29 isoforms. To this aim, I have constructed knock-out mutants lacking one or more Lhcb4 isoforms and analyzed their performance in photosynthesis and photoprotection. We found that lacks of CP29 did not result in any significant alteration in linear/cyclic electron transport rate and maximal extent of state transition, while PSII quantum efficiency and capacity for NPQ were affected. Photoprotection efficiency was lower in koCP29 plants with respect to either WT or mutants retaining a single Lhcb4 isoform. Interestingly, while deletion of either isoforms Lhcb4.1 or Lhcb4.2 get into a compensatory accumulation of the remaining subunit, photoprotection capacity in the double mutant Lhcb4.1/4.2 was not restored by Lhcb4.3 accumulation.

**Section B. Membrane dynamics and re-organization for the quenching events: B4 dissociation and identification of two distinct quenching sites.**

Antenna subunits are hypothesized to be the site of energy quenching, while the trigger of the mechanism is mediated by PsbS, a PSII subunit that is involved in detection of lumenal acidification.
In this section we investigate the molecular mechanism by which PsbS regulates light harvesting efficiency by studying *Arabidopsis* mutants specifically devoid of individual monomeric Lhcbs.
In Section B.1 we showed that PsbS controls the association/dissociation of a five-subunit membrane complex, composed of two monomeric Lhcb proteins, CP29 and CP24 and the trimeric LHCII-M (namely Band 4 Complex - B4C). We demonstrated that the dissociation of this supercomplex is indispensable for the onset of non-photochemical fluorescence quenching in high light. Consistently, we found that knock-out mutants lacking the two subunits participating to the B4C, namely CP24 and CP29, are strongly

affected in heat dissipation. Direct observation by electron microscopy and image analysis showed that B4C dissociation leads to the redistribution of PSII within grana membranes. We interpret these results proposing that the dissociation of B4C makes quenching sites, possibly CP29 and CP24, available for the switch to an energy-quenching conformation. These changes are reversible and do not require protein synthesis/degradation, thus allowing for changes in PSII antenna size and adaptation to rapidly changing environmental conditions.

In Section B.2 we studied this quenching mechanism by ultra-fast Chl fluorescence analysis. Recent results based on fluorescence lifetime analysis "*in vivo*" (Holzwarth et al., 2009) proposed that two independent quenching sites are activated during NPQ: Q1 is located in the major LHCII complexes, which are functionally detached from the PSII/RC (reaction centre) supercomplex with a mechanism that strictly requires PsbS but not Zea; Q2 is located in and connected to the PSII complex and is dependent on the Zea formation (Miloslavina et al., 2008). These two quenching events could well originate in each of the two physical domains of grana revealed by electron microscopy analysis previously reported (see Section B.1). We thus proceeded to investigate the modulation of energy quenching in knock out mutants by comparing the fluorescence lifetimes under quenched and unquenched conditions in intact leaves: we obtained results that are consistent with the model of two quenching sites located, respectively, in the $C_2S_2$ domain and in the LHCII-enriched domain. Data reported suggest that Q1 site is released in the koCP24 mutant while Q2 is attenuated in the koCP29 mutant.

On the bases of the results of this section, we conclude that during the establishment of NPQ *in vivo* the PSII supercomplex dissociates into two moieties, which segregates into distinct domain of the grana membrane and are each protected from over-excitation by the activity of quenching sites probably located in CP24 and CP29.

**Section C. Excitation energy transfer and membrane organization: role of PSII antenna subunit.**

In this section we investigated the role of individual photosynthetic antenna complexes of PSII both in membrane organization and excitation energy transfer, by using the knock out mutants previously isolated (Section A). Thylakoid membranes from wild-type and three mutants lacking light-harvesting complexes CP24, CP26 or CP29 respectively, were studied by picosecond-fluorescence spectroscopy on thylakoids, using different combination of excitation and detection wavelengths in order to separate PSI and PSII kinetics. Spectroscopic measurements revealed that absence of CP26 did not alter PSII organization, as evidenced by very similar excitons migra-

tion times in both wild-type and koCP26 samples. In contrast, the absence of CP29 and especially CP24 lead to substantial changes in the PSII organization as evidenced by a significant increase of the apparent migration time, demonstrating a bad connection between a significant part of the peripheral antenna and the RCs.

**Section D. A mutant without minor antenna proteins: towards a solution of the differential role of monomeric Lhcb proteins vs major LHCII in Non Photochemical Quenching.**

In this section we attempt to answer to the question on the localization of the quenching site(s) in the major LHCII or in monomeric Lhcb proteins. In order to verify the implication of monomeric antenna CP24, CP26 and CP29 in quenching we tried to isolate a mutant knocked out for all the three subunit. Lhcb5 (CP26) and Lhcb6 (CP24) are coded by a single gene while three isoforms of Lhcb4 (CP29) are present in the *Arabidopsis* genome, we thus looked for a five-gene mutant. We tried to isolate such a mutant from the screening of two different populations but without success. In particular, we found that is not possible to obtain a mutant lacking both CP26 and CP29 at the same time. We verified that is not a problem of seed germination but instead a defect of the embryo development. This unexpected genetic evidence shows that, for a correct and functional organization of the PSII supercomplexes, either Lhcb5 or Lhcb4.1 must be present: probably these two subunits can replace themselves each other when one lacks, while none of the other monomeric antenna (Lhcb6, Lhcb4.2, Lhcb4.3) are able to takes their place in PSII.

Two mutants obtained in these screenings allowed us to make some considerations about the role of monomeric antenna proteins in NPQ: mutants koCP29/24 which differ for the condition at the Lhcb5 locus, either homozygous WT or heterozygous. We observed a dose effect for the expression of Lhcb5, that is lower in the heterozygous since one allele only is functional. Interestingly, the amount of CP26 on thylakoid membrane strictly correlated with the quenching amplitude measured at 1200 $\mu$mol photons $m^{-2}s^{-1}$ of actinic light. These results suggest that the residual quenching in koCP29/24 plants is largely due to the capacity of CP26 subunit to mediate energy quenching. This is a further indication of the primary role of monomeric Lhcb in NPQ, as recently stated by CT (charge transfer) quenching models (Avenson et al., 2008; Ahn et al., 2008).

**Reference List**

**Ahn,T.K.,** Avenson,T.J., Ballottari,M., Cheng,Y.C., Niyogi,K.K., Bassi,R., and Fleming,G.R. (2008). Architecture of a charge-transfer state regulating light harvesting in a plant antenna protein. Science 320, 794-797.

**Avenson,T.J.,** Ahn,T.K., Zigmantas,D., Niyogi,K.K., Li,Z., Ballottari,M., Bassi,R., and Fleming,G.R. (2008). Zeaxanthin radical cation formation in minor light-harvesting complexes of higher plant antenna. J. Biol. Chem. 283, 3550-3558.

**Holzwarth,A.R.,** Miloslavina,Y., Nilkens,M., and Jahns,P. (2009). Identification of two quenching sites active in the regulation of photosynthetic light-harvesting studied by time-resolved fluorescence. Chemical Physics Letters 483, 262-267.

**Miloslavina,Y.,** Wehner,A., Lambrev,P.H., Wientjes,E., Reus,M., Garab,G., Croce,R., and Holzwarth,A.R.(2008). Far-red fluorescence: A direct spectroscopic marker for LHCII oligomer formation in non-photochemical quenching. FEBS Letters 582, 3625-3631.

# Chapter 1

# Introduction

## 1.1 Oxygenic photosynthesis

Photosynthesis is one of the most important chemical processes on Earth: most organisms depend directly or indirectly from the solar energy. In particular autotrophic organisms as plants, algae and some kind of bacteria, harvest light and convert it into chemical energy in order to produce biomass, which constitutes food for heterotrophic organisms. The photosynthetic reactions enable the absorption of light energy and its conversion into chemical energy. In oxygenic photosynthesis, performed by green plants, algae, and cyanobacteria, water is used as electron donor to reduce $CO_2$ to carbohydrates, generating molecular oxygen as a secondary product. The overall equation of the photosynthetic reaction is the following:

$$\mathbf{nH_2O + nCO_2 + light \rightarrow (CH_2O)n + nO_2}$$

The whole photosynthetic process can be divided into a light and a dark phase (Figure 1.1). The light phase is strictly dependent from the presence of solar energy, while dark phase occurs also in the dark, provided that ATP and NADPH are available. Light phase is triggered by the absorption of sunlight by photosynthetic pigments (chlorophylls (Chls) and carotenoids), followed by transfer of the energy to the reaction centre of the two photosystems where charge separation occurs, thus converting light energy into chemical form. This event induces a set of electron transfer reactions across the thylakoid membrane, leading to the formation of a trans-membrane proton gradient used for ATP formation. Water is the primary electron donor during this process and oxygen is formed as a consequence. Finally, free energy and reducing power, in the form of ATP and NADPH plus proton ($H^+$), are generated. Light reaction can be summarized by the following equations:

$$\mathbf{2\ NADP^+ + 2\ H_2O + light \rightarrow 2\ NADPH + O_2 + 2H^+}$$
$$\mathbf{ADP + P_{\mathit{i}} + energy \rightarrow ATP}$$

In dark reactions, ATP and NADPH produced during the light reactions are used to reduce $CO_2$ to the carbohydrate GAP (Glyceraldehyde-3-Phosphate). GAP is then used for the synthesis of various cellular compounds. The process of the dark reactions can be summarized in the following equation:

$$\mathbf{3\ CO_2 + 9\ ATP + 6\ NADPH \rightarrow GAP + 9\ ADP + 8\ P_i + 6\ NADP^+}$$

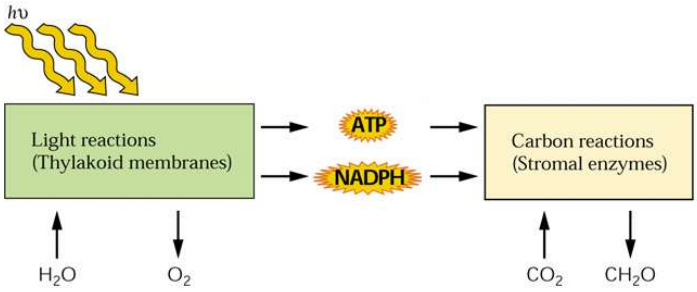


**Figure 1.1:** *Schematic representation of light and dark reactions in photosynthesis.*

## The chloroplast

Chloroplast is the specialized organelle in photosynthetic eukaryotes, in which both light and dark reactions take place (Figure 1.2). This organelle is limited by two membranes (called together envelope): the first one is highly permeable, while the second one contains specific transporters, which mediate the flux of metabolites with the cytoplasm. The soluble phase delimited by the envelope membranes is called stroma and contains all enzymes catalyzing the dark reactions, included Rubisco, the most abundant soluble protein on Earth, as well as the plastidial DNA, RNA and ribosomes. A third membrane system, the thylakoids, is found in the stroma confining a second compartment, the lumen. Thylakoids are organized into two membrane domains: cylindrical stacked structures called grana, and interconnecting regions, the stroma lamellae. The thylakoid membranes carry a negative charge, but the presence of cations, especially divalent cations like $Mg^{2+}$, keeps the thylakoid membranes stacked (Barber, 1980). In vascular plants, chloroplast are found especially in leaves mesophyll cells and their number is variable between a few to hundreds per cell, depending on species, growth conditions and developmental stage.

## The light phase

Four major protein complexes embedded into the thylakoids membrane catalyze the light reactions: Photosystem I (PSI), cytochrome $b_6f$ complex (Cyt-$b_6f$), Photosystem II (PSII) and ATP synthase. These complexes

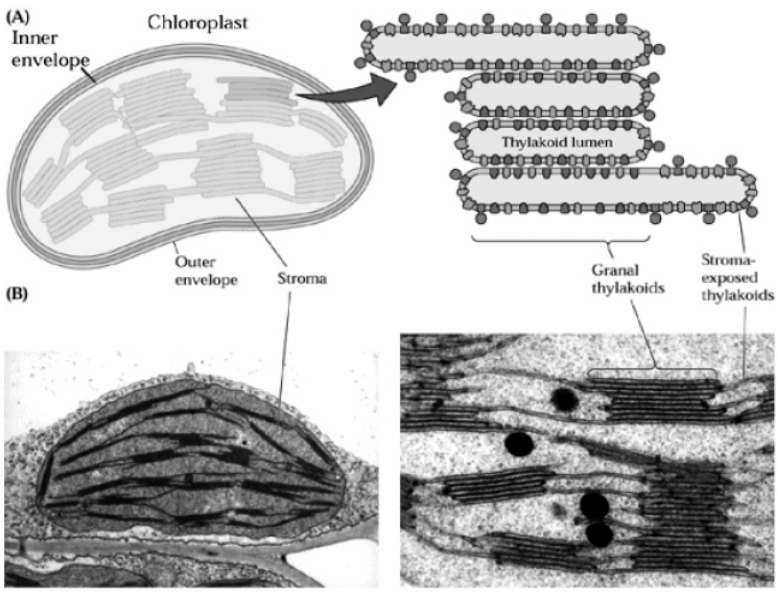


**Figure 1.2:** *The chloroplast.*
*A) Schematic diagram of a plant chloroplast. Thylakoids are distinguished in grana, stromal and stroma lamellae. B) Electronic micrographs of a chloroplast. Images from (Malkin and Niyogi, 2000).*

catalyze the processes of light harvesting, electron transport and photophosphorylation, leading to the conversion of light energy to chemical free energy (ATP and NADPH) (Figure 1.3).

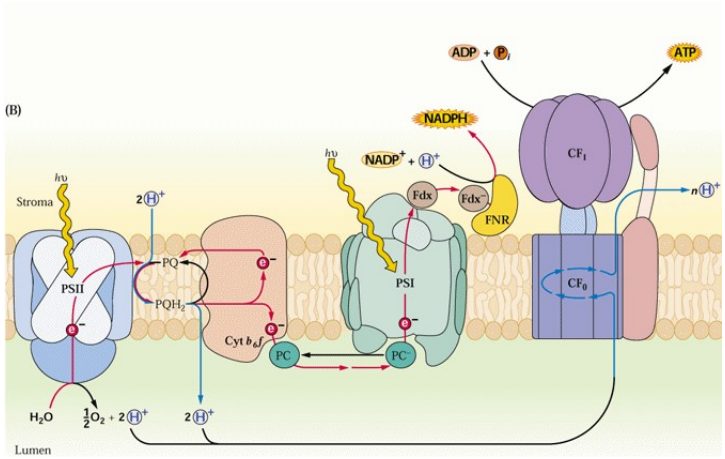


**Figure 1.3:** *Schematic representation of light reactions in photosynthesis.*
*Organization of the major protein complexes in the thylakoid membrane is also shown.*

PSI and PSII bind pigments that harvest light and funnel excitation energy to the reaction center (RC), where charge separation takes place. Taking account of the redox potential of reagents and products, the energy required for the generation of NADPH cannot be provided by only one photon in the visible range of light (Figure 1.4): this is the reason why two photosystems act in series, as described in the so called Z-scheme (Hill and Bendall, 1960).

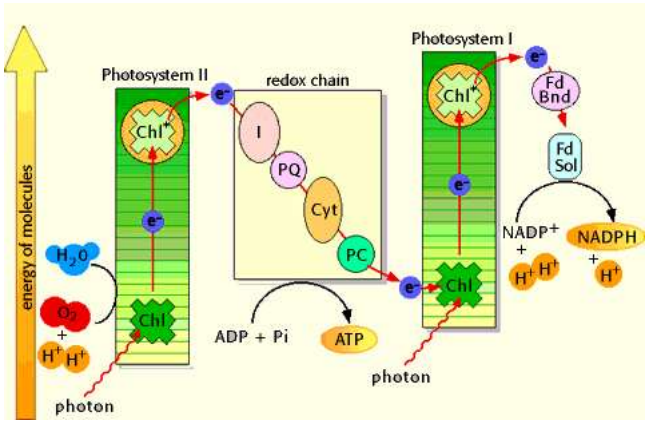


**Figure 1.4:** *The Z-scheme of Bendall and Hill.*
*Cofactors involved in electron translocation between $H_2O$ and $NADP^+$, and their redox potential, are indicated.*

After absorption of light by light-harvesting antenna of PSII, the excitation energy is transferred to a special pair of Chls in the PSII-RC, P680 (Primary electron donor absorbing at 680 nm). Upon receiving the excitation an electron is released from P680 and transported to other side of the thylakoid membrane, where it is donated to a plastoquinone (PQ) molecule. After receiving a second electron, from the next photocycle of P680, PQ takes up two protons from the stromal space to form plastoquinol ($PQH_2$), which diffuses into the membrane toward the Cyt-$b_6f$ complex. $P680^+$ is a very strong oxidant, which extracts electron from water, leading to the formation of $O_2$, the release of protons in the inner thylakoid space and the return of P680 to the neutral space. Between PSI and PSII, electrons flow through the Cyt-$b_6f$ complex that oxidize plastoquinol and transfer two electrons to plastocyanin (PC), a small, copper-containing protein, while two protons are released into the inner thylakoid space. The resulting PQ is recycled to PSII and in addition, the Cyt-$b_6f$ complex pumps another pair of protons across the membrane. These reactions are called Q-cycle (Figure 1.5): overall, the Q-cycle oxidizes two plastoquinols, reduces one PQ and one PC, and translocates 4 $H^+$ for every 2 electrons transported to PSI (Trumpower, 1990).

In PSI, light is absorbed by the antenna pigments and the excitation energy is transferred to the RC. As in PSII, a special pair of Chls is present in the PSI-RC. The special pair, designated as P700 (Primary electron donor absorbing at 700 nm), upon excitation releases an electron that reduces ferredoxin (Fd) on the stroma side. Reduced Fd is subsequently used in numerous regulatory cycles and reactions, like nitrate and $CO_2$ assimilation, fatty-acid desaturation and NADPH production through a $NADP^+$ oxidoreductase (FNR) (Buchanan, 1991). Both photosystems operate with a very high quantum yield: PSI works with an almost perfect quantum yield

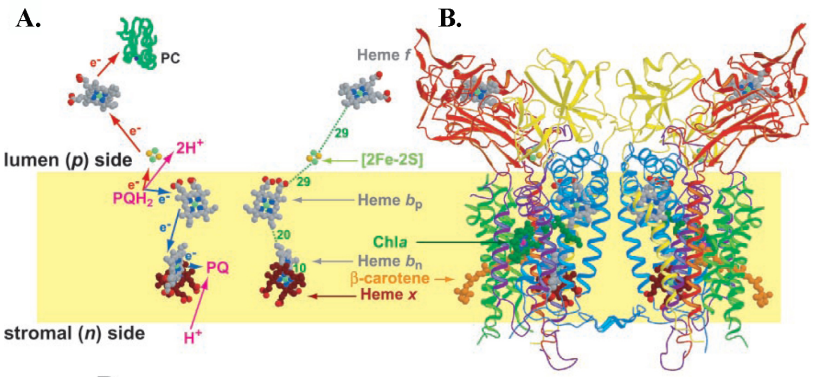


**Figure 1.5:** *The cytochrome-$b_6f$ complex.*
*(A) Schematic model of the proposed molecular mechanism of the Q-cycle. (B) 3D structure of cytochrome-$b_6f$ from cyanobacteria resolved by Stroebel et al. (2003).*

of 1.0, while PSII operates with a lower efficiency (about 0.85). An alterative electron transport, not involving PSII supercomplex, is used when the NADPH/$NADP^+$ ratio is high, known as cyclic electron flow. This process is referred to a cyclic photophosphorylation and involves the transfer of electrons from Fd to the Cyt-$b_6f$ complex, probably through the extra haem $c_i$ (haem x) (Stroebel et al., 2003; Kurisu et al., 2003) producing a proton gradient during the reduction of plastocyanin that regenerate the P700 reaction centre (Harbinson and Foyer, 1991). This process generates a proton gradient (and thus ATP), without producing NADPH or oxygen. The charge separation in PSI and PSII, together with the electron transfer through the Cyt-$b_6f$ and cyclic electron transport, leads to the formation of an electrochemical potential gradient, between the stromal and the lumenal side of the membrane, which powers ATP synthesis by the ATP-ase, a fourth protein complex (Mitchell, 1961). The ATP-ase enzyme is a multimeric complex with both stromal and transmembrane regions, known as $CF_1$ and $CF_0$, respectively, and represents a molecular motor that is driven by a proton motive force (Figure 1.6). Proton movement through $CF_0$ is coupled to ATP synthesis/hydrolysis in the $\beta$-subunits of $CF_1$. In chloroplasts, $CF_0$ contains four subunits I, II, III and IV (in a probable stoichiometry of 1:1:14:1; the 14 III subunits form a ring-like structure). The whole $CF_0$-$CF_1$ complex is thought to function as a rotary proton-driven motor, in which the stationary subunits are I, II, IV, $\delta$, $\alpha$ and $\beta$, and the rotary subunits are III (c), $\gamma$ and $\epsilon$ (McCarty et al., 2000).

### The dark phase

The dark phase of photosynthesis includes different reactions, on the whole indicated as Calvin cycle (Benson and Calvin, 1950): through these reactions, atmospheric $CO_2$ is reduced to carbohydrates, using the chemical free energy (ATP and NADPH) produced during the light reactions (Figure 1.7).

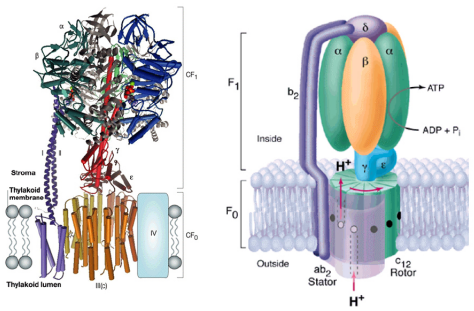


**Figure 1.6:** *3D structure of the multimeric complex ATP-ase (Abrahams et al., 1994). Resolution of the complex draws a representation of rotary and stationary subunits acting in ATP synthesis.*

The Calvin cycle allows the synthesis of one GAP from three $CO_2$ molecules and the regeneration of Ru5P to preserve the cyclic character of the process. It can be summarized with the following reactions:

$$\mathbf{3\ CO_2 + 3\ Ru5P + 9\ ATP + 6\ NADPH \rightarrow 6\ GAP + 9\ ADP + 6\ NADP^+ + 8\ P_i}$$

$$\mathbf{5\ GAP \rightarrow 3\ Ru5P}$$

In Figure 1.7, all biosynthetic step of Calvin cycle are summarized.

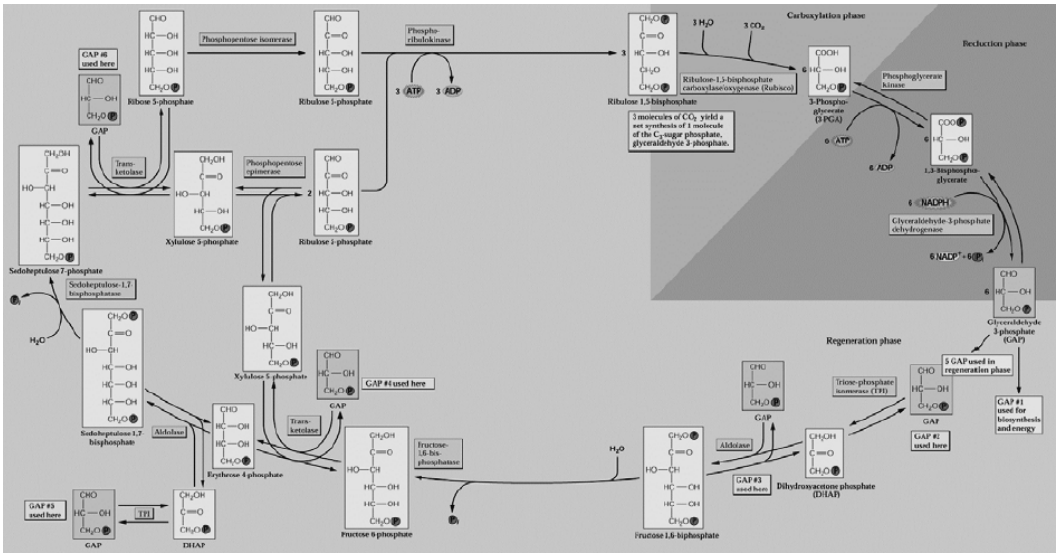


**Figure 1.7:** *Enzymatic steps involved in Calvin cycle.*

## 1.2 Photosynthetic pigments in higher plants

Two main classes of pigments are responsible for light absorption, charge separation and energy transfer toward the reaction centre in both photosystems: chlorophylls (Chls) and carotenoids.

### Chlorophylls

The basic component of all different types of chlorophylls is a porphyrin (a cyclic tetrapyrrole) in which the four nitrogen atoms of the pyrroles coordinate a magnesium (Mg) atom. A fifth ring and the phytyl, a chain of 20 carbon atoms responsible for hydrophobicity properties, are also present. Different chlorophylls are distinguished from their substitutions. In higher plants, two types of molecules are present, differing in a group in the second pyrrhole ring: a methyl for the Chl *a*, an aldehyde for the Chl *b* (Figure 1.8 A). The characteristic ability of Chls to absorb light in the visible region is due to the high number of conjugated double bonds present in these molecules. The Chl *a* and Chl *b* absorption spectra in solution do not completely overlap, this increase the spectral range over which light is absorbed, thus increasing the efficiency of light-harvesting.
The absorption spectra of the Chl present two main bands, the Qy transition in the red part of the spectrum and the Soret transition in the blue/violet part of the spectrum; another absorption band, called Qx is visible, even if it is partly masked by the Qy vibronic transitions (Figure 1.8 B). The Qy transition corresponds to the transition of an electron from the ground state (S0) to the first excited state (S1) and peaks around 640-670 in Chl *b* and Chl *a* in organic solvent, respectively. Less clear from the spectrum (580-640nm) is the weakly Qx, corresponding to the transition of a S0 electron to the second excited state (S2). The transition to higher states corresponds to the Soret band, visible in the blue region of the absorption spectrum and whose maximum is around 430-460 nm for Chl *a* and Chl *b*.
Chls are mainly present in the chloroplast bound by proteins. A key interaction for the stabilization of Chl binding to proteins, is the coordination of the central Mg: in most cases it is bound by nucleophilic amino acids residues, like histidine (Jordan et al., 2001; Liu et al., 2004); however, Chls bound to proteins by water or lipid molecules was also shown (Liu et al., 2004). Chl *a* and *b* absorption properties are well known to be modulated by the protein environment in which they are located. Moreover these pigments are indispensable for the correct folding of some photosynthetic proteins, as the light harvesting complexes (*Lhc*) proteins (Paulsen et al., 1993).

### Carotenoids

Carotenoids are among the most widespread of all natural pigments and fulfill a variety of functions (Straub O, 1987; Kull D. and Pfander, 1995); they are synthesized by bacteria, algae, fungi and plants and play many essential roles in organisms performing oxygenic photosynthesis.
Carotenoids are poly-isoprenoid compounds containing 40 carbon atoms. The atomic structure of these pigments is constituted by a long chain of

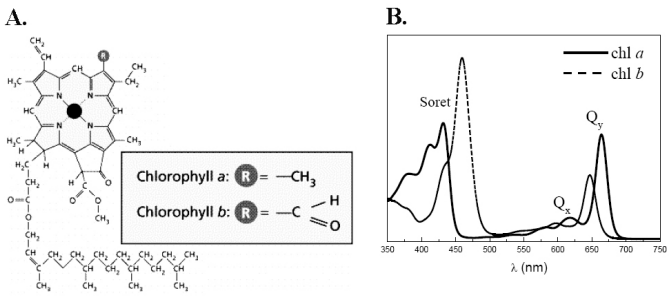


**Figure 1.8:** *A) Structure and (B) absorption spectra in acetone 80% of Chl a and b.*

conjugated double bonds in the central part of the molecule and cyclic groups and the extremities. Different level of hydrogenation and introduction of oxygen-containing functional groups create a large family of carotenoids, composed by over 600 natural compounds. In higher plants, two different classes are found into thylakoid: (i) carotenes (as for example $\beta$-carotene), which are hydrocarbons with linear structure and with cyclic groups in one or both extremities, and (ii) xanthophylls (as for example lutein) which are oxygenated derivatives of carotenes.

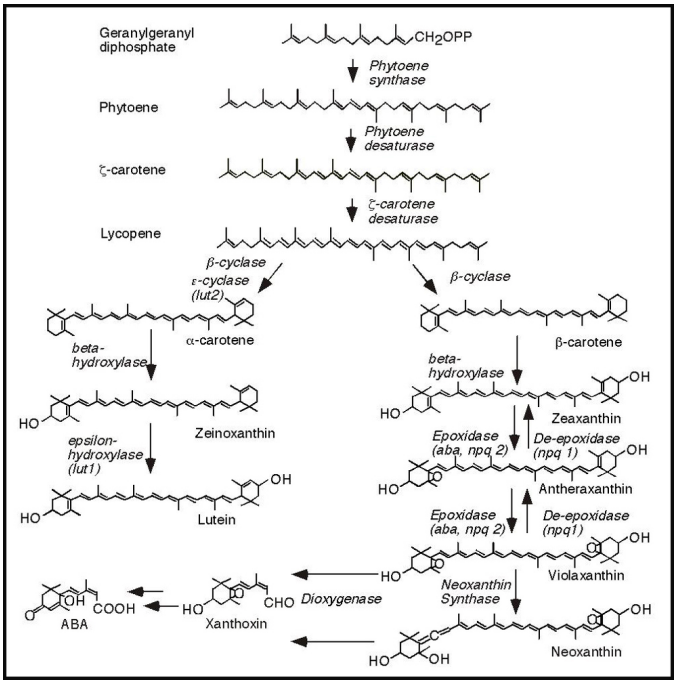


**Figure 1.9:** *Biosynthetic pathway of carotenoids in higher plants, with enzymes involved.*

In higher plants the most abundant carotenoids associated with thylakoid membranes are the $\alpha$ and $\beta$ carotene and the xanthophylls lutein, violaxanthin, neoxanthin and zeaxanthin. Carotenoids are non-covalently bound to the protein complexes, probably involving hydrophobic interactions (Gastaldelli et al., 2003). Carotenes are bound especially to the core complex of both photosystems, while xanthophylls are mainly located in the antenna complexes (Bassi et al., 1993; Caffarri et al., 2001; Ruban et al.,

1999).
Carotenoids are all synthesized from the terpenoid pathway and derive from the condensation of 8 IPP (isopentenyl diphosphate) molecules, thus producing phytoene. Phytoene undergoes several reduction steps, introducing four more double bonds and generating lycopene. The following reactions of the pathway are reported in Figure 1.9. At this point the biosynthesis splits into two branches: one leads to the formation of $\beta$-carotene, zeaxanthin, violaxanthin and neoxanthin, while the other to $\alpha$-carotene and lutein (Pogson et al., 1996).
The light absorption characteristics, the photochemical properties and the chemical reactivity of the carotenoids are mainly determined by the conjugated double bond system of these molecules. The $\pi$-electrons delocalisation in the conjugated double bonds system leads to the light absorption in the visible range 400-500 nm. When carotenoids absorb light, S0 electrons are raised to the second excited singlet state S2; this strongly dipole-dipole allowed transition is responsible for the characteristic absorption spectrum. The first excited singlet state S1 cannot be populated from the ground state by photon absorption due to symmetry reasons.
The absorption spectra of carotenoids are strongly red-shifted *in vivo*, compared to their spectra in organic solvents. This shift represents a lowering of the S2 energy level, which has been ascribed to the mutual polarisability of the carotenoid and protein environment (Andersson et al., 1991; Cogdell et al., 1992). In contrast to S2, the S1 level is little affected by the surrounding environment (Andersson et al., 1991).
Carotenoids have several role in photosynthesis: a) structure stabilization and assembly of protein complexes in the thylakoid membrane (Paulsen et al., 1993; Plumley and Schmidt, 1987); b) light absorption and excited state energy transfer to the Chls (Gradinaru et al., 2000; Mimuro and Katoh, 1991); c) protection against photo-oxidative damages (Havaux and Niyogi, 1999). Carotenoids are important antioxidant in the thylakoid membrane and are involved in dissipation of excited states of Chls in overexcitation conditions.

### Xanthophyll cycle

Carotenoids composition of thylakoid is not constant: it can undergo modifications during long-term acclimation of plants to stressing condition, as well as rapidly changes following fluctuations of solar light intensity (Demmig-Adams et al., 1989).
This observation is well explained since different carotenoids, even if sharing a similar structure, are characterized by specific functions. An example of carotenoids composition changing in response to a variation of the environ-

mental conditions is the xanthophylls cycle. The xanthophyll cycle involves the three xanthophylls violaxanthin, antheraxanthin and zeaxanthin, and consists in a light-dependent, reversible de-epoxidation of violaxanthin to zeaxanthin via the intermediate antheraxanthin.
Zeaxanthin lowers the light use efficiency and, if present constitutively, decreases plant growth (Dall'Osto et al., 2005). Thus, the regulation of the xanthophyll cycle has an important physiological influence. The de-epoxidation reactions converting violaxanthin to zeaxanthin are catalyzed by violaxanthin de-epoxidase (VDE) (Yamamoto and Kamite, 1972), a lumenal enzyme activated by acidification of the lumenal compartment (Gilmore and Yamamoto, 1992): this event occurs when high illumination of leaf induces the build-up of a high transmembrane proton gradient (Figure 1.10). Xanthophyll cycle is a key component in the activation of several photoprotective mechanisms as thermal dissipation of excitation energy in excess (Holt et al., 2004; Niyogi, 1999) or Chls triplets excited state quenching. Carotenoids involved in the xanthophyll cycle are localized in the peripheral antenna proteins of PSII and PSI (Bassi et al., 1993; Bassi and Caffarri, 2000; Ruban et al., 1999), even if a certain photoprotective role has been assigned also to zeaxanthin in the free lipid phase (Yokthongwattana et al., 2005).

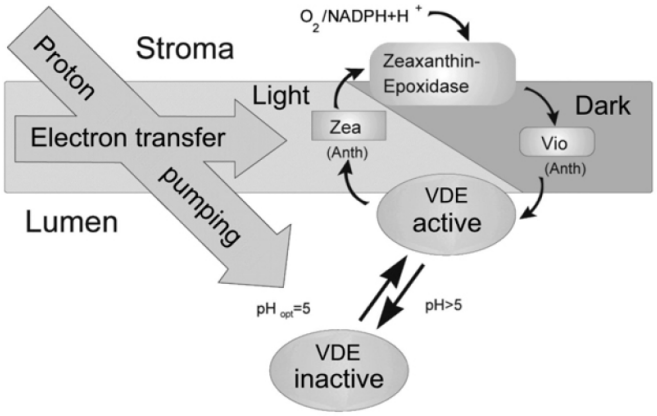


**Figure 1.10:** *The xanthophyll cycle.*
*Schematic representation of electron transfer events leading to of $\Delta pH$ and activation of enzymes involved in the cycle.*

## 1.3 The light absorbing units

Photosystems I and II (PSI, PSII) are two multi-protein complexes binding the pigments responsible for light harvesting and charge separation. Moreover in PSI and PSII are present some co-factors constituting the electron acceptor and donor in the electron transfer reactions from water to NADPH. PSI and PSII are located in the thylakoids membranes but their distribution

is not homogenous: PSII is mainly located in the stacked grana membranes, while PSI is present in the unstacked stroma lamellae membranes.
PSI and PSII are structurally different, however in both complexes can be identified two moieties: a) a core complex, in which are located the Chl special pair and the cofactors involved in electron transport; and b) a peripheral antenna system, composed by Chls binding proteins responsible for light harvesting and energy transfer to the reaction center. Chls and carotenoids are bound both by core complex and antenna system, however core complexes bind only Chl *a* and carotenes, while antenna proteins bind Chl *a*, Chl *b* and xanthophylls. Core complexes are composed by the polypeptides denominated *Psa* and *Psb* respectively for PSI and PSII. Among Psa and Psb proteins there are gene products encoded from both nuclear or plastidic genes. Their sequences are generally well conserved during evolution and similar polypeptides are found in bacteria and eukaryotic organisms.
The antenna system is instead more variable in different organisms: in higher plants, it is composed by polypeptides belonging to the multigenic family of *Lhc*. All these polypeptides share the same evolutionary origin and a common structural organization (Durnford et al., 1999).
They are encoded by the nuclear genome and denominated Lhca and Lhcb, respectively for the antenna proteins of PSI and PSII (Jansson, 1999). In vascular plants 10 different isoforms have been identified to be associated to PSs, respectively Lhca1-4 to PSI and Lhcb1-6 to PSII (Jansson, 1999); each class can be composed by one or more genes and their number depend on the species, as a result of gene duplication events occurred quite late in evolution. Lhcb1 is the largest class: 5 different Lhcb1 genes have been identified in *Arabidopsis thaliana* (Jansson, 1999), and at least 14 in barley (Caffarri et al., 2004).
Lhcb1-3 proteins form LHCII trimers, the major PSII antenna complex, with different combinations between the three isoforms. Lhcb 4-6 instead are present in PSII supercomplexes as monomers and they are also referred to as "minor complexes".
Four additional isoforms (Lhca5, Lhca6, Lhcb7 and Lhcb8) have been identified from gene sequences but their functional significance is still uncertain (Jansson, 1999; Klimmek et al., 2006).
The cladogram of *lhc* genes sequence form *Arabidopsis thaliana* shows that Lhca and Lhcb cluster in two different groups, with Lhcb6 and Lhca1 located in the middle (Figure 1.11). In fact, evolutionary studies suggested that antenna proteins of PSI and PSII diverged soon, before the separation of individual classes (Durnford et al., 1999). This separated evolution leaded to different characteristics of PSI and PSII antenna proteins, as specificity in carotenoids binding or the presence/absence of long-wavelength absorption forms. In between the two Lhca and Lhcb proteins group some proteins

appeared at different evolutionary steps: Lhca4, Lhcb3 and Lhcb6 are not present in green algae, while are present in bryophytes and vascular plants, indicating a possible role of this proteins in water to land transition of photosynthetic organisms (Alboresi et al., 2008).

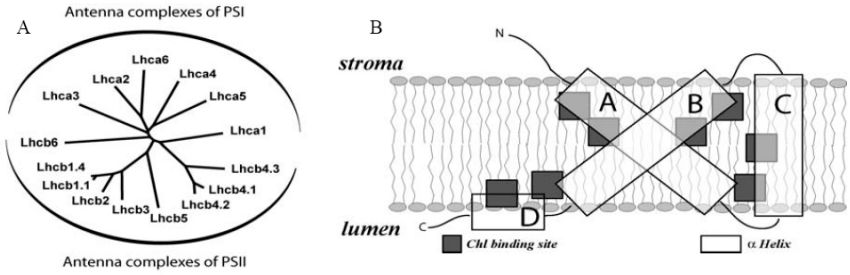


**Figure 1.11:** *A) Cladogram of Lhc sequences from Arabidopsis thaliana. 2 out of the 5 Lhcb1 and one out of 4 Lhcb2 sequences are reported. The association to Photosystem I or II is indicated. B) Schematic representation of the structure of Lhc complexes. α-helices and putative conserved Chl binding residues are indicated.*

## Photosystem II

The PSII complex (Figure 1.12) is a multiproteic complex that catalyses the electron transfer from water to plastoquinone (water-plastoquinone oxidoreductase) producing oxygen. PSII activity appearance is thus a key feature for the evolution of aerobic organisms. The mechanism of oxygen production involves the oxidation of two water molecules to make molecular oxygen ($O_2$) triggered by absorption of four light quanta.

The PSII core complex contains the reaction centre where a Chl special pair, named P680, undergoes charge transfer triggered by light energy absorbed. After absorption of the first light quanta, an electron is translocated from P680 to a pheophytin and then to the quinone $Q_A$. Quinone $Q_A$ is stably bound to PSII and reduces a mobile quinone PQ at site $Q_B$ (Figure 1.12). The $P680^+$ oxidizes a nearby tyrosine ($Y_Z$); it then extracts an electron from a cluster of four manganese (Mn) ions (OEC, oxygen-evolving complex), which binds two substrate water molecules. On the lumenal side of the complex, three extrinsic proteins of 33, 23 and 17 KDa (OEC1-3) compose the OEC (Zouni et al., 2001), and have a calcium ion, a chloride ion and a bicarbonate ion as necessary cofactors.

Upon an additional photochemical cycle, the doubly reduced PQ ($PQ^{2-}$) takes up two protons from the stroma to form $PQH_2$ and is released into the lipid bilayer; an oxidized PQ from the lipid-freemembrane pool will then replace it. After two more photochemical cycles, the Mn cluster is provided with four oxidizing equivalents, which are used to oxidize two water molecules to produce $O_2$ (Ferreira et al., 2004).

CP43 and CP47 form the inner antenna of PSII, and bind respectively 14 and

16 Chl *a* molecules. Up to 12 other small subunits are associated with the PSII core; some are involved in the dimerization or in Chl and carotenoids binding stabilization, but they do not all have a well-clarified function (Zheleva et al., 1998; Nakazato et al., 1996; Ballottari et al., 2007).

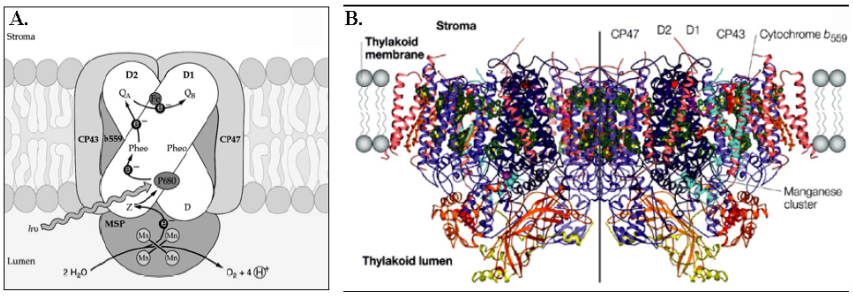


**Figure 1.12:** *(A) Schematic model for PSII and (B) 3D crystal structure of PSII core complex. Crystal structure of photosystem II from cyanobacterium T. elongatus was resolved by Ferreira et al. (Ferreira et al., 2004).*

## Antenna complex of Photosystem II

The peripheral antenna of photosystem II is composed of two classes of light-harvesting complexes: a) the trimeric major light-harvesting complexes of PSII, called LHCII (Thornber et al., 1967) and b) the monomeric minor antennae (Bassi et al., 1996).
PSII antenna proteins bind Chl *a*, Chl *b* and xanthophylls and their function is to harvest light energy and transfer it to the P680, but they are also involved in photoprotection.

Crystal structure of **LHCII** has been recently resolved (Liu et al., 2004) at 2.72 Å therefore it is now a model for the other antenna protein encoded by the *Lhc multigene* family (Jansson, 1999). The term LHCII defines a very heterogeneous class of proteins: several subpopulations of the complex can be separated by native isoelectrofocusing (Bassi et al., 1996). Indeed, LHCII proteins are encoded by a large number of highly homologous nuclear genes; these genes have been found in several species and they are subdivided into three types known as Lhcb1, Lhcb2 and Lhcb3 (Jansson, 1999). LHCII trimers are heterotrimers constituted by Lhcb1, Lhcb2 and Lhcb3 subunits. These complexes are coded by different isoforms and are present with different ratio in the PSII antenna, depending from numerous factors as environmental conditions and the plant species (Caffarri et al., 2001). In *Arabidopsis*, the products of these genes have an average length of 232, 228 and 223 aminoacids respectively (after removal of the chloroplast import signal).
In the trimeric complex of LHCII, each monomer is constituted of 3 transmembrane domains with $\alpha$-helix conformation (helices A, B and C)

(Kühlbrandt et al., 1994; Liu et al., 2004). The N-terminal is fully hydrophilic, thus protruding into the stroma space and the C-terminal peptides is exposed on the lumenal space. Two amphipathic helixes, named D and E, were found respectively on the C-terminal peptide and in the BC loop region; both helices lie on the lumenal surface (Liu et al., 2004) (Figure 1.13).

The trimerization domain covers: the amino-terminal domain, the carboxy terminus, the stromal end of helix B, several hydrophobic residues from helix C and also pigments and lipid as phosphatidylglycerol (PG), bound to these parts of the polypeptide chain. Six Chl *a* (two from each monomer) constitute the core of the trimer (Liu, Z. et al. 2004).

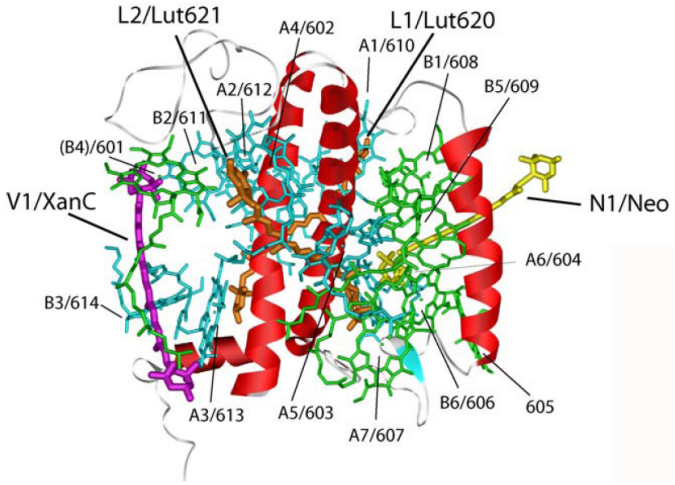


**Figure 1.13:** *3D Structure of the light-harvesting complex II (LHCII). Structure of LHCII from spinach was resolved by Liu et al. Cofactors bound (chlorophylls and carotenoids) are indicated with nomenclatures from Kühlbrandt et al., 1994 and Liu et al., 2004.*

Each monomer binds 14 Chls and 4 xanthophylls. All ligands of the 14 Chls have been identified as side chains of seven amino-acid residues, two backbone carbonyls, four water molecules and the phosphodiester group of a PG. Part of the chlorophylls binding sites are selective for Chl *a* or Chl *b*, while in other cases Chl binding sites with mixed occupancy are present. The spectroscopic properties of each Chl bound by Lhcb1 monomer has been investigated through a mutational approach in the Chl binding sites and reconstitution *in vitro* of recombinant Lhcb1 mutants (Remelli et al., 1999).

Two central lutein molecules are bound in the grooves on both sides of the helices A and B cross-brace, forming the internal L1 and L2 carotenoid binding sites; the polyene chains are firmly fixed in two hydrophobic cavities, providing strong linkage between helices A and B. The third xanthophyll, 9'-cis neoxanthin is located in the Chl *b*-rich region around helix C in the carotenoid binding site N1; side chains from helices B and C as well as phytyl chains form a hydrophobic space that accommodates the hook-

shaped polyene chain of neoxanthin, while ring on the other ends stretches into the exterior solvent region. Recently a Tyr residue in the lumenal loop has been found to form hydrogen bound with neoxanthin, stabilizing N1 site (Caffarri et al., 2007; Hobe et al., 2006). The fourth carotenoid is located in a peripheral site named V1 (Caffarri et al., 2001; Liu et al., 2004). V1 site is constituted by a hydrophobic pocket at the interface monomer-monomer, formed by several Chls, hydrophobic residues and the PG; part of the xanthophyll is located inside this pocket, while the opposite end group is located outside, toward the stromal surface.
As its name indicates, LHCII fulfils the role of light-harvesting for PSII, transferring it in a highly efficient manner to the PSII reaction centre where primary photochemistry takes place. Another important function of LHCII complexes concerns their role in photoprotective mechanisms in excess light conditions. Depending on environmental conditions, a subpopulation of LHCII trimers can be phosphorylated and migrate from PSII, docking to PSI. This process is called state transition (Allen, 1992; Andersson and Anderson, 1980): when electron transport between the two photosystems is inhibited because of an insufficient light absorption of PSI, state transitions provide a mechanism for the equilibration of the excitation energy between PSs, thus increasing the efficiency of the whole process. In higher plants this mechanism was demonstrated to depend on the presence of the specific kinase STN7 (Bellafiore et al., 2005). As discussed, LHCII are deeply involved in mechanisms established by plants during short-term and long-term stress that causes over-excitation of PSII and generation of harmful reactive oxygen species (Niyogi, 1999).

Three Chl *a*/*b*- and xanthophyll-binding proteins constitute monomeric minor antennae, named also minor complexes: CP29, CP26 and CP24, named from their apparent mass in non-denaturing SDS-PAGE gels (Bassi et al., 1987; Peter and Thornber, 1991). They are encoded respectively by the nuclear genes *Lhcb4*, *Lhcb5* and *Lhcb6*, which are highly homologous to each other and to the other members of the *Lhc* multigene family.
The three subunits are probably monomeric proteins that are present in one copy per PSII unit, and bind about 10% of the total Chls and 20% of the violaxanthin of the total complex (Nield et al., 2000). Single genes encode Lhcb5 (CP26) and Lhcb6 (CP24), while three *lhcb4* genes are present in *Arabidopsis*. The expression levels of minor antennae are similar and the proteins are found in equimolar amounts in the thylakoid (Jansson, 1999). However recently the expression profile of the third gene coding for CP29, *lhcb4.3*, was shown to be different than *lhcb4.1* and *lhcb4.2*. *Lhcb4.3* was then re-named into *lhcb8* (Klimmek et al., 2006). Another gene similar to the genes coding for minor complexes is *lhcb7*. An *lhcb7* ortholog was

found in *Physcomitrella* which shows the Lhcb7-specific motif identified in *Arabidopsis*, poplar and rice, in agreement with the suggestion that it represents a distinct isoform (Klimmek et al., 2006; Alboresi et al., 2008). In the case of Lhcb8, no ortholog was found in *Physcomitrella*, although this was expected since this polypeptide was only identified in dicots (Klimmek et al., 2006; Alboresi et al., 2008). However Lhcb8 and Lhcb7 proteins are not present in substantial amount into thylakoids membranes and the role of *lhcb8* and *lhcb7* genes is still unclear.

**CP29** is composed by 256-258 amino acids in its mature form in *Arabidopsis*, and it is the largest among Lhc encoded proteins. The overall sequence identity between CP29 and LHCII is 34%, but most of the substitutions are conservative, especially in the helix regions. CP29 binds 6 Chl *a*, 2 Chl *b*. As for Lhcb1, CP29 Chls spectroscopic properties has been analyzed through site-specific mutagenesis on residues responsible for Chl binding and *in vitro* reconstitution of recombinant mutants (Bassi et al., 1999). The results obtained demonstrated the presence of 4 Chl binding sites specific for Chl *a*, and 4 with mixed occupancy. About carotenoids CP29 binds one molecule of lutein and substoichiometric amounts of violaxanthin and neoxanthin (for a total of 2 xanthophylls) (Dainese and Bassi, 1991). Recently a third carotenoid binding sites specific for neoxanthin, equivalent to the N1 site in LHCII, has been proposed also for CP29, since the Tyr residue responsible for N1 stabilization is present. However native and recombinant CP29 was found with only 2 carotenoids bound, revealing a probable low stability of N1 due to the absence of most of the Chl binding sites nearby helix C involved in N1 stabilization (Caffarri et al., 2007). CP29 can be phosphorylated, especially when plants are exposed to low temperature and high light stress (Croce et al., 1996). The N-terminal portion of the protein protrudes into the stroma space and can be reversibly phosphorylated on Thr83 (Testi et al., 1996). CP29 phosphorylation is supposed to induce conformational rearrangement or modification in the PSII supercomplex that could facilitate thermal energy dissipation.

**CP26** is 243 amino acids long in *Arabidopsis*, shows 48% identity with respect to LHCII and coordinates 7 Chl *a*, 3 Chl *b* and 2-3 xanthophylls (lutein, violaxanthin and neoxanthin) (Bassi et al., 1996; Croce et al., 2002a). CP26, as Lhcb1 and CP29, presents a Tyr residue which is suggested to stabilize the third carotenoid binding site N1 (Caffarri et al., 2007).

**CP24** is the smallest of *Lhc* proteins (211 amino acids in *Arabidopsis*), due to the lack of the major part of the C-terminal region of the protein. Sequence homology and absorption spectra suggest that 5 Chl *a*, 5 Chl *b* and

2 xanthophylls are bound (Bassi et al., 1996; Pagano et al., 1998). CP24, differently from other Lhcb proteins doesn't bind neoxanthin; indeed the Tyr residue involved in N1 stabilization is absent (Caffarri et al., 2007).

## Supramolecular organization of PSII

Photosystem II forms a supramolecular complex together with its antenna. Electron microscopy measurements provided 2D and 3D structures of PSII supercomplexes at around 2 nm resolution (Boekema et al., 1999b; Nield et al., 2000); from these measurements we have the better description of the PSII structure, due to absence till now of a crystallographic structure. Electron micrographs show that organisation of PSII is very different from PSI: PSII is dimeric, while PSI in higher plants is a monomer.
*Lhc* subunits are organized into two layers around the PSII core: the inner one is composed of CP29, CP26 and one LHCII trimer (S-type LHCII), forming the so-called $C_2S_2$ particle together with PSII core (Boekema et al., 1999a; Morosinotto et al., 2006). The outer layer is made of LHCII trimers and CP24, to build up the large $C_2S_2M_2Lx$ complex in which the number of LHCII-L trimers depends on the light intensity during growth (Bailey et al., 2001) (Figure 1.14). In particular CP29, CP24 and a LHCII trimer form a stable supercomplex bound to PSII core (Bassi and Dainese, 1992). Moreover part of LHCII-L trimers can be phosphorylated by STN7 kinase and move to PSI, during the state transitions, in order to balance the excitation energy receipt by PSI and PSII.

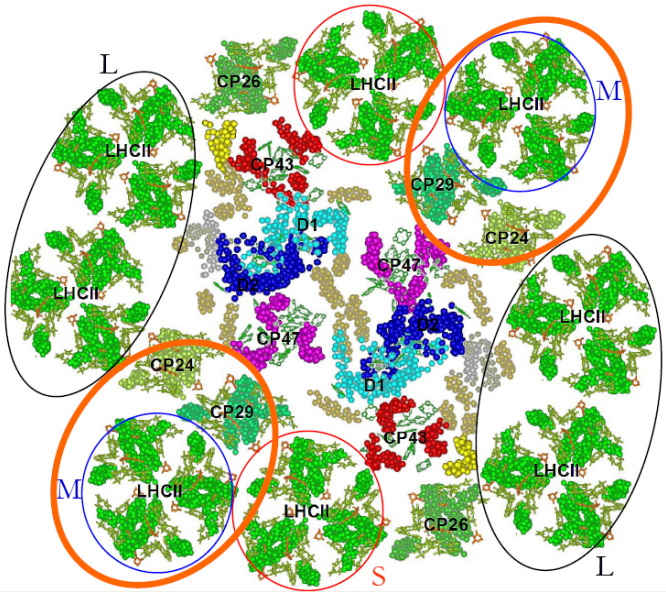


**Figure 1.14:** *Schematic rappresentation of higher plant PSII supercomplex. Structural model shows the core dimmer, trimeric outer antennae (LHCII) and the monomeric minor complexes (CP24, CP26 and CP29). Different trimers L, S and M are indicated. Orange circles indicate the supramolecular complexes CP24-CP29-LHCII-M.*

## Photosystem I

Photosystem I of higher plants is a light-dependent plastocyanin-ferredoxin oxidoreductase. Higher plants PSI consists of at least 18 polypeptides (Scheller et al., 2001) and binds about 180 Chls and 35 carotenoid molecules (Amunts et al., 2007; Ben Shem et al., 2003; Boekema et al., 2001). It is composed of a core complex (PSI core) and the antenna system responsible for light harvesting (LHCI). In the core complex is bound the P700 special Chl pair which undergoes charge separation occurs; core complex includes also the primary electron acceptors A0 (Chl-$a$), A1 (phylloquinone) and $F_X$ (a Fe4-S4 cluster) Figure 1.15.
The reaction centre comprises 12 subunits that are denoted PsaA-PsaL, PsaN and PsaO (Scheller et al., 2001).
PsaG, PsaH, PsaN and PsaO subunits are present only in plants and green algae, not in cyanobacteria (Scheller et al., 2001). The PsaA-PsaB heterodimer forms the inner core of PSI, binding the P700 special Chl pair: here the light-driven charge separation occurs, and it includes the primary electron acceptors A0 (Chl-$a$), A1(phylloquinone) and $F_X$ (a Fe4-S4 cluster). This heterodimer binds 80 Chls that function as inner light harvesting antenna.

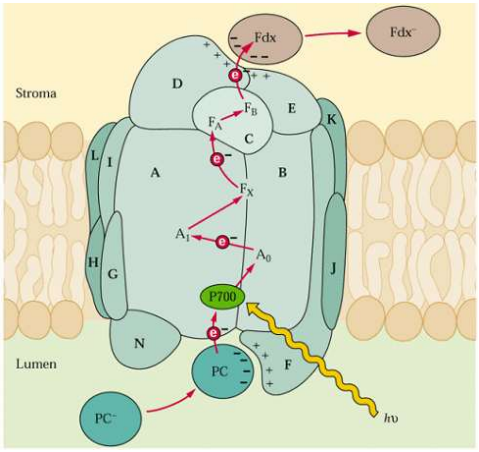


**Figure 1.15:** *Schematic model of photosystem I.*
*Subunits organization and cofactors involved in electron transfer are indicated.*

## Antenna complex of photosystem I

Lhca 1-4 are the 4 polypeptides constituting LHCI complex, the major component of PSI antenna system (Ben Shem et al., 2003; Croce et al., 2002b; Jansson, 1999). These polypeptides are assembled into two dimers, Lhca1-Lhca4 and Lhca2-Lhca3, arranged in half-moon shaped belt (Ben Shem et al., 2003), and they are bound to the core complex mainly through interactions with PsaG subunit. The characterization of the individual LHCI components has been difficult, due to the inability to separate different

polypeptides in LHCI preparations. A recent study allowed characterization of individual Lhca1-4 complexes following a different method, expressing the apoprotein in *E.coli* and reconstituting the protein *in vitro* (Croce et al., 2002b).
Lhca5 has been identified at the polypeptide level, with both mass spectrometry and specific antibodies (Ganeteg et al., 2004; Storf et al., 2004). However, it was detected only in very low amounts and not tightly associated to PSI and its physiological relevance is still under debate (Ganeteg et al., 2004): recent results showed a peripherally interaction between Lhca5 and Lhca2-3 dimer and possibly a presence of Lhca5 homodimer as substitute of Lhca1-4 eterodimer (Lucinski et al., 2006). The *lhca6* gene, instead, is expressed in very low levels and the polypeptide has never been detected. Since its sequence is very similar to *lhca2*, *lhca6* could result from a recent duplication (Jansson, 1999), being a pseudogene, without any physiological function.
Photosystem I from both eukaryotic and prokaryotic organisms has a peculiar spectroscopic feature, the presence of "red forms", chlorophylls adsorbing at lower energies with respect to the reaction centre P700 (Gobets and van Grondelle, 2001). Red forms are generally found in the PSI core complex, but higher plants are peculiar in this respect: in fact, while they still have red forms in the core complex, the red-most Chls are found in the antenna complex LHCI (Mullet et al., 1980).

### Supramolecular organization of PSI

The structure of PSI-LHCI complex from higher plants was resolved at 4.4 Å (Ben Shem et al., 2003) and recently at 3.4 Å resolution (Amunts et al., 2007) by 3D crystallography giving details on the supramolecular organization of the complex (Figure 1.16). It shows that Lhca1-4 polypeptides are bound to one side of the PSI core complex and that PsaH is located on the opposite side with respect to LHCI. Since this protein was shown to be necessary for state transition (Lunde, C. et al. 2000), its localization suggests that LHCII should dock to PSI in this part of the core complex, on the opposite side of LHCI. Higher plants PSI is present as monomers, while in cyanobacterial PSI trimers are found (Jordan et al., 2001).

## 1.4 Reactive Oxygen Species (ROS)

Plants need light to trigger the photosynthetic reactions, however it can also be dangerous for the photosynthetic apparatus. Plants growth conditions are often dynamic, involving diurnal and seasonal fluctuations in light intensities, temperatures and availability of nutrients. In all these situations

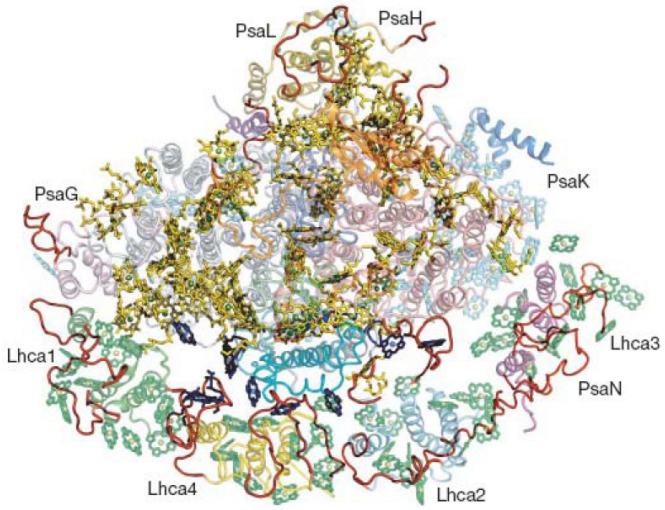


**Figure 1.16:** *Crystal structure of higher plant Photosystem I. Supramolecular organization of Photosystem I from Pisum sativum (Ben Shem et al., 2003).*

the absorbed light energy can exceed the capacity for its utilization for photochemistry and the excitation energy in excess can induce the formation of dangerous molecules as ROS (Prasil, O. et al. 1992, Tjus, S. E. et al. 1998, Tjus, S. E. et al. 2001), which can damage the thylakoids membranes. The whole process in which light damages some photosynthetic structures is called "photoinhibition", since these photo-oxidative damages can decrease the rate of photosynthesis (Aro et al., 1993; Hideg et al., 1998; Powles and Bjorkman, 1982).

Oxidizing, dangerous molecules can be generated at three major sites in the photosynthetic apparatus: light-harvesting complex (LHC) of PSII, PSII reaction center and PSI acceptor side.

Chlorophyll and carotenoid molecules, bound to the light-harvesting complexes, absorb light: excited pigments rapidly (<ps time scale) transfer the excitation energy to the reaction centres, in order to drive electron transport.

Absorption of excess photons can cause accumulation of excitation energy in the LHCs and thereby increase the lifetime of singlet Chl ($^1$Chl*, lifetime ∼ns time scale): $^1$Chl* can thus convert into triplet chlorophyll ($^3$Chl*), through intersystem crossing. $^3$Chl* excited state is a long-lived state (∼ms time scale) and thus can react with triplet oxygen ($^3O_2$), converting it to singlet oxygen ($^1O_2$*), a highly ROS (Knox and Dodge, 1985; Krieger-Liszkay, 2005). Production of $^1O_2$* within the Lhcs causes oxidation of lipids (Tardy and Havaux, 1996), proteins and pigments (Formaggio et al., 2001). Thylakoid membrane lipids, with their abundance in unsaturated fatty acid side chains, are susceptible of singlet oxygen attack: products are hydroperoxides and peroxyl radical chain reactions in the thylakoid membrane(Havaux

and Niyogi, 1999).
Another site for ROS production is the PSII reaction centre. After primary charge transfer, $P680^+$ and $Ph^-$ species are formed; $Ph^-$ is reconverted to Ph after electron transfer to $Q_A$, while $P680^+$ is reconverted to P680 through YZ oxidation. However if $Q_A$ is already reduced and electron transport is blocked, which is the case of excess light absorption, a charge recombination can occur between $P680^+$ and $Ph^-$, producing a triplet P680 ($^3P680^*$). $^3P680^*$ can generate singlet oxygen (Melis, 1999) inducing photoinhibition, and photo-damages in particular on the D1 subunit of PSII (Aro et al., 1993).
In the case of PSI, the oxidized reaction centre $P700^+$ is more stable than $P680^+$ and behaves as a quencher of excitation energy (Dau, 1994). Nevertheless, at the acceptor side of PSI, ferrodoxin can reduce molecular oxygen to the superoxide anion ($O_2^-$). This short-living specie can be metabolized to hydrogen peroxide ($H_2O_2$) or hydroxyl radical (OH•), the latter one being an extremely aggressive ROS.
ROS produced on the acceptor side of PSI are able to damage key enzymes of photosynthetic carbon metabolism such as phosphoribulokinase and NADP-glyceraldehyde-3-phosphate dehydrogenase, as well as subunits of PSI reaction centre. There are evidences that also PSII can be photoinhibited by PSI-produced ROS *in vivo* (Tjus et al., 2001).

## 1.5 Photoprotection mechanisms

Plants evolved mechanisms to use light avoiding as much as possible ROS formation, in order to prevent photoinihibition.
These photoprotective mechanisms can be divided into two different classes, depending on the time-scale of action: a. short-term photoprotective mechanisms and b. long-term photoprotective mechanisms.
In the short-term photoprotective mechanisms the absorbed energy is dissipated as heat, in order to prevent ROS formation, while in long-term photoprotective mechanisms plants adjust their photosynthetic machineries to the disposable light. In particular short-term photoprotective mechanisms don't need synthesis of proteins *de novo*, while in long-term photoprotective mechanisms proteins are modulated in order to adapt their amount and composition to the energy requirements for photochemistry reactions.

### a. Short term responses

#### NON-PHOTOCHEMICAL QUENCHING (NPQ).

Since production of $^3Chl^*$ is a constitutive, intrinsic properties of chlorophylls, plants evolved a rapidly inducible mechanism, termed NPQ (Non-

Photochemical Quenching), that allows the harmless thermal dissipation of excess absorbed photons in PSII (Demmig-Adams and Adams, 1992; Frank et al., 2000). NPQ is a feed-back regulation mechanism for excitation energy in excess (Figure 1.17), since it's activation and modulation depend on the extent of thylakoid transmembrane ΔpH deriving from photosynthetic electron transport (Horton, 1996). Triggering of NPQ is accompanied by a change in Chl fluorescence lifetime distribution that leads PSII into a quenched state. This energy quenching process involves several processes and its mechanism is still unclear. In the Section 1.6 is discussed in detail the current knowledge about the role of gene products involved in NPQ, the phenotype of *npq* mutants found and the molecular models proposed for this process.

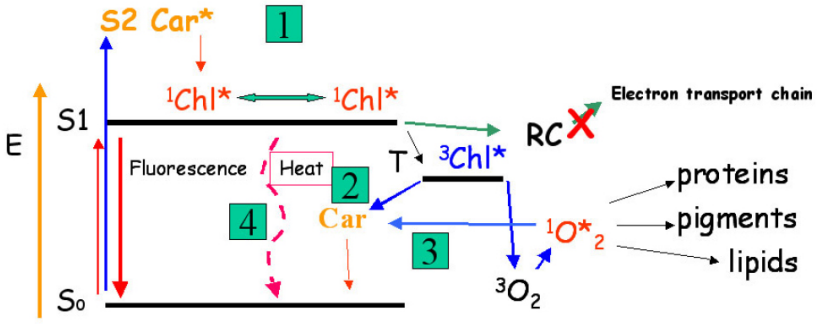


**Figure 1.17:** *Scheme of de-excitation pathway for $^1Chl^*$. Photochemistry, fluorescence emission, intersystem crossing and thermal energy emission compete for de-excitation of excited singlet state of Chls. Light is absorbed by Cars and Chls bound to Lhcs; an excited Chl ($^1Chl^*$) goes back to its ground state S0 through rapid transfer of excitation energy to a neighbouring Chl, toward the RC [1], through fluorescence emission or by heat dissipation of excitation energy (NPQ) [4]. $^1Chl^*$ can be converted into $^3Chl^*$ by intersystem crossing; in this form, $^3Chl^*$ can interact with molecular oxygen, producing the aggressive species $^1O_2$. Carotenoids are able to quench $^3Chl^*$ [2] and scavenge singlet oxygen [3].*

### STATE TRANSITIONS

Depending on environmental conditions, a subpopulation of LHCII trimers can be phosphorylated and migrate from PSII, docking to PSI. This process is called state transition (Allen, 1992; Andersson and Anderson, 1980): when electron transport between the two photosystems is inhibited because of an insufficient light absorption of PSI, state transitions provide a mechanism for the equilibration of the excitation energy between photosystems, thus increasing the efficiency of the whole process. The state transition takes several minutes to be activated, since it involves also the migration of LHCII from grana to stroma lamellae. In higher plants this mechanism was demonstrated to depend on the presence of the specific kinase STN7 (Bellafiore et al., 2005). The importance of state-transition mechanism in photoprotection is still a subject of debates (Wollman, 2001).

**NON-ASSIMILATORY ELECTRON TRANSPORT MECHANISMS**

Especially under conditions of $CO_2$ limitation, non-assimilatory electron transport to oxygen acts as important photoprotection mechanism. In C3 plants, photorespiratory metabolism can sustain linear electron transport, and thus allowing utilization of excitation energy; this feature has been verified showing that mutants blocked in photorespiration undergo inhibition of photosynthesis and photoxidative damages (Wallsgrove et al., 1987).

The so-called pseudocyclic electron transport, or water-water cycle, consists in an alternative electron transport pathway starting with direct reduction of $O_2$ by PSI, that acts as another important photoprotective mechanism (Ruuska et al., 2000). On the acceptor side of PSI, reduction of $O_2$ leads to superoxide ($O_2^-$) production; this aggressive ROS is readily metabolized by thylakoid-bound superoxide dismutase (SOD) and ascorbate peroxidase (APX) to generate $H_2O$ and monodehydroascorbate (Figure 1.19); the latter product can be directly reduced by PSI to yield ascorbate. This pseudocyclic pathway, in which electrons produced from water oxidation (in PSII) are used to reduce $O_2$ to $H_2O$, generate $\Delta$pH for ATP synthesis without production of $O_2$ or NADPH (Schreiber and Neubauer, 1990); this process allows dissipation of excitation energy in excess through electron transport (Asada, 1999).

SOD and APX isoforms have a key role as ROS scavengers: thylakoid-bound form of SOD and PAX are able to efficiently detoxify $O_2^-$ and $H_2O_2$ at their site of production; soluble forms react with the ROS that diffuse into the stroma from the thylakoid membrane (Karpinski et al., 1999).

**ANTIOXYDANT SPECIES**

ROS production is often unavoidable for plants. Reactive species produced during photooxidative stress can be deactivated by several antioxidant species present in the chloroplast as ascorbate, glutathione, tocopherols and especially carotenoids (Figure 1.18);

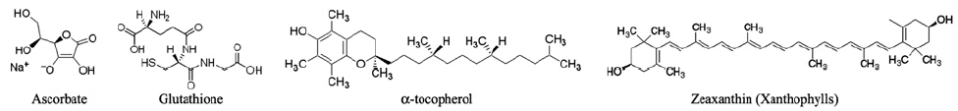


**Figure 1.18:** *Molecular structures of the most common chloroplastic antioxidants.*

Carotenoids play a key role as photoprotective agents: they are membrane-bound antioxidant able to quench both $^3Chl^*$ and $^1O_2^*$, thus stabilizing membrane by inhibition of lipid peroxidation. Carotenoids bound to Lhcs and PSII core complex are involved in efficient quenching respectively of antenna $^3Chl^*$ (Formaggio et al., 2001) and singlet oxygen produced by

$^3$P680* (Telfer et al., 1994). This is an antioxidant function of carotenoids in addition to the role of xanthophyll cycle: they have a role in both rapid and sustained thermal energy dissipation, as previously described (Yamamoto et al., 1999). Furthermore, their essential role in photoprotection has been demonstrated by the bleached phenotypes of mutant green algae that are unable to synthesize any carotenoids (Sager and Zalokar, 1958).

Other antioxidant molecules acting into the chloroplast are tocopherols, ascorbate and glutathione.

Tocopherols are thylakoid antioxidant molecules, free into the membrane, able to chemically scavenge $^1O_2^*$, $O_2^-$ and OH•; through their action, plants can prevent lipid peroxidation and damages to the other chloroplast structures. Recently, isolation of a mutant depleted in $\alpha$-tocopherol, the most abundant tocopherol in chloroplast, has addressed the importance of this molecule in photoprotection (Havaux et al., 2005).

Ascorbate (vitamin C) is a soluble antioxidant molecule; it can prevent oxidative damage both by direct quenching of major ROS and as substrate for VDE and APX reactions. Importance of ascorbate in photoprotection, as well as its overlapping function with zeaxanthin in ROS deactivation has been described (Muller-Moule et al., 2003).

Glutathione has a key role in detoxifying singlet oxygen and hydroxyl radical, and is involved in regeneration of both $\alpha$-tocopherol and ascorbate, through the glutathione-ascorbate cycle (Figure 1.19) (Foyer et al., 1991).

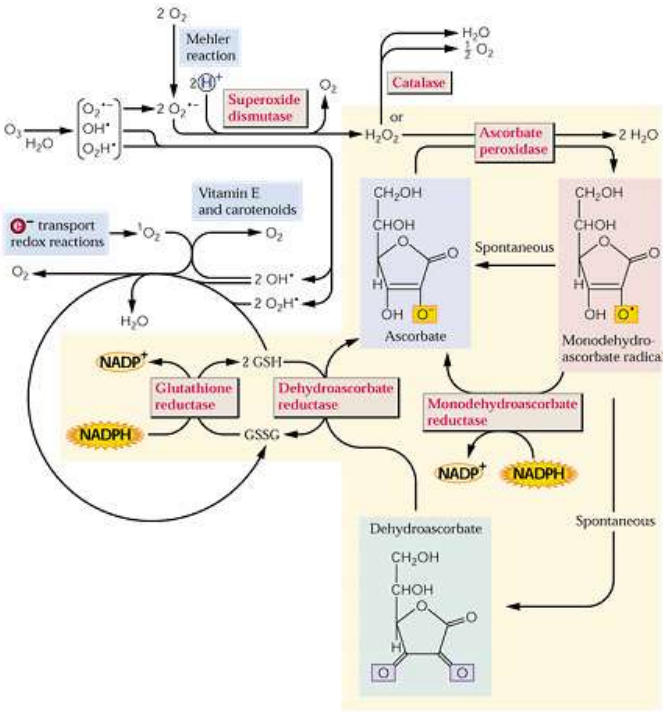


**Figure 1.19:** *Schematic representation of antioxidant system network acting in higher plants. Detailed description of enzymatic and non-enzymatic antioxidants is provided.*

### b. Long-term photoprotective mechanisms

When plants are exposed for a long time to stress conditions, long-term photoprotective mechanisms are activated.
These adaptations involve several phenomena, for instance the expression or repression of specific proteins, but also chloroplast movements and modification of plant morphology.
One of the mechanisms involves adjustment of changes in *Lhc* gene expression or *Lhc* protein degradation (Escoubas et al., 1995), yielding a reduction of light-harvesting antenna size.
Maximum rate of photosynthesis is a dynamic parameter too: during acclimation is possible to increase the capacity for photosynthetic electron transport and $CO_2$ fixation. These mechanisms involve the regulation of nuclear and chloroplast gene expression by redox potentials and/or ROS production (Pfannschmidt et al., 1999). In some over-wintering evergreen plants, that undergo prolonged cold-stress conditions, mechanisms of sustained thermal dissipation of excess photons have been described (Gilmore and Ball, 2000). Because these mechanisms allow a decrease in the quantum efficiency of photosynthesis, they have been termed photoinhibitory quenching (qI). This kind of persistent thermal dissipation is reversed only slowly with warming; levels of zeaxanthin accumulation have been correlated with qI, and recovery from qI is accompanied by epoxidation of zeaxanthin accumulated during winter (Adams, III et al., 2001; Verhoeven et al., 1999).

## Abbreviations

*Chl*, Chlorophyll; Fd, ferredoxin; $H^+$, proton; Lhc, Light harvesting complex; LHCI, antenna system of Photosystem I; LHCII, Major antenna complex of Photosystem II; Lhca, antenna polypeptides of Photosystem I; Lhcb, antenna polypeptides of Photosystem II; PSI (II); Photosystem I (II); Cyt-$b_6f$, Cytochrome $b_6f$ complex; PQ, plastoquinone; PC, plastocyanin; OEC, oxygen-evolving complex; PG, phosphatidylglycerol; RC, reaction center; ROS Reactive Oxygen Species; $^1Chl^*$, singlet Chl; $^3Chl^*$, triplet chlorophyll; $^3O_2$, triplet oxygen; $^1O_2^*$, singlet oxygen; $O_2^-$, oxygen superoxide anion; $H_2O_2$, hydrogen peroxide; OH•, hydroxyl radical; NPQ, Non-Photochemical Quenching; qI photoinhibitory quenching.

## Reference List

**Abrahams,J.P.,** Leslie,A.G.W., Lutter,R., and Walker,J.E. (1994). Structure at 2.8A resolution of F1-ATPase from bovine heart mitochondria. Nature 370, 621-628.

**Adams,W.W.,** III, Demmig-Adams,B., Rosenstiel,T.N., and Ebbert,V. (2001). Dependence of photosynthesis and energy dissipation activity upon growth form and light environment during the winter. Photosynth. Res. 67, 51-62.

**Alboresi,A.,** Caffarri,S., Nogue,F., Bassi,R., and Morosinotto,T. (2008). In silico and biochemical analysis of Physcomitrella patens photosynthetic antenna: identification of subunits which evolved upon land adaptation. PLoS. One. 3, e2033.

**Allen,J.F.** (1992). Protein phosphorylation in regulation of photosynthesis. Biochim. Biophys. Acta 1098, 275-335.

**Amunts,A.,** Drory,O., and Nelson,N. (2007). The structure of a plant photosystem I supercomplex at 3.4 A resolution. Nature 447, 58-63.

**Andersson,B.** and Anderson,J.M. (1980). Lateral heterogeneity in the distribution of chlorophyll-protein complexes of the thylakoid membranes of spinach chloroplasts. Biochim. Biophys. Acta 593, 427-440.

**Andersson,P.O.,** Gillbro,T., Ferguson,L., and Cogdell,R.J. (1991). Absorption Spectral Shifts of Carotenoids Related to Medium Polarizability. Photochem. Photobiol. 54, 353-360.

**Aro,E.-M.,** Virgin,I., and Andersson,B. (1993). Photoinhibition of Photosystem-2 - Inactivation, Protein Damage and Turnover. Biochim. Biophys. Acta 1143, 113-134.

**Asada,K.** (1999). THE WATER-WATER CYCLE IN CHLOROPLASTS: Scavenging of Active Oxygens and Dissipation of Excess Photons. Annu. Rev. Plant Physiol Plant Mol. Biol. 50, 601-639.

**Bailey,S.,** Walters,R.G., Jansson,S., and Horton,P. (2001). Acclimation of Arabidopsis thaliana to the light environment: the existence of separate low light and high light responses. Planta 213, 794-801.

**Ballottari,M.,** Dall'Osto,L., Morosinotto,T., and Bassi,R. (2007). Contrasting behavior of higher plant photosystem I and II antenna systems during acclimation. Journal of Biological Chemistry 282, 8947-8958.

**Barber,J.** (1980). Membrane surface charges and potentials in relation to photosynthesis. Biochim. Biophys. Acta 594, 253-308.

**Bassi,R.** and Caffarri,S. (2000). Lhc proteins and the regulation of photosynthetic light harvesting function by xanthophylls. Photosynthesis Research 64, 243-256.

**Bassi,R.,** Croce,R., Cugini,D., and Sandona,D. (1999). Mutational analysis of a higher plant antenna protein provides identification of chromophores bound into multiple sites. Proc. Natl. Acad. Sci. USA 96, 10056-10061.

**Bassi,R.** and Dainese,P. (1992). A Supramolecular Light-Harvesting Complex from Chloroplast Photosystem-II Membranes. Eur. J. Biochem. 204, 317-326.

**Bassi, R.,** Giuffra, E., Croce, R., Dainese, P., and Bergantino, E. Biochemistry and molecular biology of pigment binding proteins.Jennings, R. C., Zucchelli, G., Ghetti, F., and Colombetti, G. NATO ASI series[287], 41-63. 1996. New York, Plenum Press. Life Science. Ref Type: Serial (Book,Monograph)

**Bassi,R.,** Hoyer-hansen,G., Barbato,R., Giacometti,G.M., and Simpson,D.J. (1987). Chlorophyll-proteins of the photosystem-II antenna system. J. Biol. Chem. 262, 13333-13341.

**Bassi,R.,** Pineau,B., Dainese,P., and Marquardt,J. (1993). Carotenoid-Binding Proteins of Photosystem-II. Eur. J. Biochem. 212, 297-303.

**Bellafiore,S.,** Bameche,F., Peltier,G., and Rochaix,J.D. (2005). State transitions and light adaptation require chloroplast thylakoid protein kinase STN7. Nature 433, 892-895.

**Ben Shem,A.,** Frolow,F., and Nelson,N. (2003). Crystal structure of plant photosystem I. Nature 426, 630-635.

**Benson,A.A.** and Calvin,M. (1950). Carbon Dioxide Fixation by Green Plants. Annual Review of Plant Physiology and Plant Molecular Biology 1, 25-42.

**Boekema,E.J.,** Jensen,P.E., Schlodder,E., van Breemen,J.F., van Roon,H., Scheller,H.V., and Dekker,J.P. (2001). Green plant photosystem I binds light-harvesting complex I on

one side of the complex. Biochemistry 40, 1029-1036.

**Boekema,E.J.,** van Roon,H., Calkoen,F., Bassi,R., and Dekker,J.P. (1999a). Multiple types of association of photosystem II and its light- harvesting antenna in partially solubilized photosystem II membranes. Biochemistry 38, 2233-2239.

**Boekema,E.J.,** van Roon,H., van Breemen,J.F., and Dekker,J.P. (1999b). Supramolecular organization of photosystem II and its light-harvesting antenna in partially solubilized photosystem II membranes. Eur. J. Biochem. 266, 444-452.

**Buchanan,B.B.** (1991). Regulation of $CO_2$ assimilation in oxygenic photosynthesis: the ferredoxin/thioredoxin system. Perspective on its discovery, present status, and future development. Arch. Biochem. Biophys. 288, 1-9.

**Caffarri,S.,** Croce,R., Breton,J., and Bassi,R. (2001). The major antenna complex of photosystem II has a xanthophyll binding site not involved in light harvesting. J. Biol. Chem. 276, 35924-35933.

**Caffarri,S.,** Croce,R., Cattivelli,L., and Bassi,R. (2004). A look within LHCII: differential analysis of the Lhcb1-3 complexes building the major trimeric antenna complex of higher-plant photosynthesis. Biochemistry 43, 9467-9476.

**Caffarri,S.,** Passarini,F., Bassi,R., and Croce,R. (2007). A specific binding site for neoxanthin in the monomeric antenna proteins CP26 and CP29 of Photosystem II. FEBS Lett. 581, 4704-4710.

**Cogdell,R.J.,** Andersson,P.O., and Gillbro,T. (1992). Carotenoid Singlet States and Their Involvement in Photosynthetic Light-Harvesting Pigments. J. Photochem. Photobiol. B 15, 105-112.

**Croce,R.,** Breton,J., and Bassi,R. (1996). Conformational Changes Induced by Phosphorylation in the CP29 Subunit of Photosystem II. Biochemistry 35, 11142-11148. Croce,R., Canino,g., Ros,F., and Bassi,R. (2002a). Chromophore organization in the higher-plant photosystem II antenna protein CP26. Biochemistry 41, 7334-7343.

**Croce,R.,** Morosinotto,T., Castelletti,S., Breton,J., and Bassi,R. (2002b). The Lhca antenna complexes of higher plants photosystem I. Biochimica et Biophysica Acta-Bioenergetics 1556, 29-40.

**Dainese,P.** and Bassi,R. (1991). Subunit Stoichiometry of the Chloroplast Photosystem-II Antenna System and Aggregation State of the Component Chlorophyll-a/b Binding Proteins. J. Biol. Chem. 266, 8136-8142.

**Dall'Osto,L.,** Caffarri,S., and Bassi,R. (2005). A mechanism of nonphotochemical energy dissipation, independent from Psbs, revealed by a conformational change in the antenna protein CP26. Plant Cell 17, 1217-1232.

**Dau,H.** (1994). Molecular mechanisms and quantitative models of variable photosystem II fluorescence. Photochem. Photobiol. 60, 1-23.

**Demmig-Adams,B.** and Adams,W.W. (1992). Photoprotection and other responses of plants to high light stress. Ann. Rev. Plant Physiol. Plant Mol. Biol. 43, 599-626.

**Demmig-Adams,B.,** Winter,K., Kruger,A., and Czygan,F.-C. (1989). Light stress and photoprotection related to the carotenoid zeaxanthin in higher plants. In Photosynthesis. Plant Biology Vol.8, W.R.Briggs, ed. (New York: Alan R. Liss), pp. 375-391.

**Durnford,D.G.,** Deane,J.A., Tan,S., McFadden,G.I., Gantt,E., and Green,B.R. (1999). A phylogenetic assessment of the eukaryotic light-harvesting antenna proteins, with implications for plastid evolution. J. Mol. Evolution 48, 59-68.

**Escoubas,J.M.,** Lomas,M., LaRoche,J., and Falkowski,P.G. (1995). Light intensity regulation of cab gene transcription is signaled by the redox state of the plastoquinone pool. Proc. Natl. Acad. Sci. U. S. A 92, 10237-10241.

**Ferreira,K.N.,** Iverson,T.M., Maghlaoui,K., Barber,J., and Iwata,S. (2004). Architecture of the photosynthetic oxygen-evolving center. Science 303, 1831-1838.

**Formaggio,E.,** Cinque,G., and Bassi,R. (2001). Functional architecture of the major Light-harvesting Complex from Higher Plants. J. Mol. Biol. 314, 1157-1166.

**Foyer,C.,** Lelandais,M., Galap,C., and Kunert,K.J. (1991). Effects of Elevated Cytosolic Glutathione Reductase Activity on the Cellular Glutathione Pool and Photosynthesis in Leaves under Normal and Stress Conditions. Plant Physiol 97, 863-872.

**Frank,H.A.,** Bautista,J.A., Josue,J.S., and Young,A.J. (2000). Mechanism of nonphotochemical quenching in green plants: Energies of the lowest excited singlet states of violaxanthin and zeaxanthin. Biochemistry 39, 2831-2837.

**Ganeteg,U.,** Klimmek,F., and Jansson,S. (2004). Lhca5 - an LHC-Type Protein Associated with Photosystem I. Plant Mol. Biol. 54, 641-651.

**Gastaldelli,M.,** Canino,g., Croce,R., and Bassi,R. (2003). Xanthophyll binding sites of the CP29 (Lhcb4) subunit of higher plant photosystem II investigated by domain swapping and mutation analysis. Journal of Biological Chemistry 278, 19190-19198.

**Gilmore,A.M.** and Ball,M.C. (2000). Protection and storage of chlorophyll in overwintering evergreens. Proc. Natl. Acad. Sci. U. S. A 97, 11098-11101.

**Gilmore,A.M.** and Yamamoto,H.Y. (1992). Dark induction of zeaxanthin-dependent nonphotochemical fluorescence quenching mediated by ATP. Proc. Natl. Acad. Sci. USA 89, 1899-1903.

**Gobets,B.** and van Grondelle,R. (2001). Energy transfer and trapping in Photosystem I. Biochim. Biophys. Acta 1057, 80-99.

**Gradinaru,C.C.,** van Stokkum,I.H.M., Pascal,A.A., van Grondelle,R., and Van Amerongen,H. (2000). Identifying the pathways of energy transfer between carotenoids and chlorophylls in LHCII and CP29. A multicolor, femtosecond pump - probe study. J. Phys. Chem. B 104, 9330-9342.

**Harbinson,J.** and Foyer,C.H. (1991). Relationships Between the Efficiencies of Photosystem-I and Photosystem-II and Stromal Redox State in $CO_2$- Free Air - Evidence for Cyclic Electron Flow In Vivo. Plant Physiol. 97, 41-49.

**Havaux,M.,** Eymery,F., Porfirova,S., Rey,P., and Dormann,P. (2005). Vitamin E Protects against Photoinhibition and Photooxidative Stress in Arabidopsis thaliana. Plant Cell 17, 3451-3469.

**Havaux,M.** and Niyogi,K.K. (1999). The violaxanthin cycle protects plants from photooxidative damage by more than one mechanism. Proc. Natl. Acad. Sci. U. S. A 96, 8762-8767.

**Hideg,E.,** Kalai,T., Hideg,K., and Vass,I. (1998). Photoinhibition of photosynthesis in vivo results in singlet oxygen production detection via nitroxide-induced fluorescence quenching in broad bean leaves. Biochemistry 37, 11405-11411.

**Hill,R.** and Bendall,F. (1960). Function of the two cytochrome components in chloroplasts: A working hypothesis. Nature 186, 136-137.

**Hobe,S.,** Trostmann,I., Raunser,S., and Paulsen,H. (2006). Assembly of the major light-harvesting chlorophyll-a/b complex: Thermodynamics and kinetics of neoxanthin binding. J. Biol. Chem. 281, 25156-25166.

**Holt,N.E.,** Fleming,G.R., and Niyogi,K.K. (2004). Toward an understanding of the mechanism of nonphotochemical quenching in green plants. Biochemistry 43, 8281-8289.

**Horton,P.** (1996). Nonphotochemical quenching of chlorophyll fluorescence. In Light as an Energy Source and Information Carrier in Plant Physiology, R.C.Jennings, ed. (Plenum Press: New York), pp. 99-111.

**Jansson,S.** (1999). A guide to the Lhc genes and their relatives in Arabidopsis. Trends Plant Sci. 4, 236-240.

**Jordan,P.,** Fromme,P., Witt,H.T., Klukas,O., Saenger,W., and Krauss,N. (2001). Three-dimensional structure of cyanobacterial photosystem I at 2.5 A resolution. Nature 411,

909-917.

**Karpinski,S.,** Reynolds,H., Karpinska,B., Wingsle,G., Creissen,G., and Mullineaux,P. (1999). Systemic signaling and acclimation in response to excess excitation energy in Arabidopsis. Science 284, 654-657.

**Klimmek,F.,** Sjodin,A., Noutsos,C., Leister,D., and Jansson,S. (2006). Abundantly and rarely expressed Lhc protein genes exhibit distinct regulation patterns in plants. Plant Physiol 140, 793-804.

**Knox,J.P.** and Dodge,A.D. (1985). The photodynamic action of eosin, a singlet-oxygen generator. Some effects on leaf tissue of Pisum sativum L. Planta 164, 22-29.

**Krieger-Liszkay,A.** (2005). Singlet oxygen production in photosynthesis. J. Exp. Bot. 56, 337-346.

**Kühlbrandt,W.,** Wang,D.N., and Fujiyoshi,Y. (1994). Atomic model of plant light-harvesting complex by electron crystallography. Nature 367, 614-621.

**Kull D.** and Pfander,H. (1995). Appendix: List of new carotenoids. In Carotenoids: isolation and analysis., G.Britton, S.Liaaen-Jensen, and H.Pfander, eds. (Birkhauser, Basel)

**Kurisu,G.,** Zhang,H., Smith,J.L., and Cramer,W.A. (2003). Structure of the cytochrome $b_6f$ complex of oxygenic photosynthesis: tuning the cavity. Science 302, 1009-1014.

**Liu,Z.,** Yan,H., Wang,K., Kuang,T., Zhang,J., Gui,L., An,X., and Chang,W. (2004). Crystal structure of spinach major light-harvesting complex at 2.72 A resolution. Nature 428, 287-292.

**Lucinski,R.,** Schmid,V.H., Jansson,S., and Klimmek,F. (2006). Lhca5 interaction with plant photosystem I. FEBS Lett. 580, 6485-6488.

**Malkin,R.** and Niyogi,K.K. (2000). Photosynthesis. In Biochemistry and Molecular Biology of Plants, B.B.Buchanan, W.Gruissem, and R.Jones, eds. American Society of Plant Biologists), pp. 521-575.

**McCarty,R.E.,** Evron,Y., and Johnson,E.A. (2000). THE CHLOROPLAST ATP SYNTHASE: A Rotary Enzyme? Annu. Rev. Plant Physiol Plant Mol. Biol. 51, 83-109.

**Melis,A.** (1999). Photosystem-II damage and repair cycle in chloroplasts: what modulates the rate of photodamage ? Trends Plant Sci. 4, 130-135.

**Mimuro,M.** and Katoh,T. (1991). Carotenoids in photosynthesis: Absorption, transfer and dissipation of light energy. Pure Appl. Chem. 63, 123-130.

**Mitchell,P.** (1961). Coupling of phosphorylation to electron and hydrogen transfer by a chemi-osmotic type of mechanism. Nature 191, 144-148.

**Morosinotto,T.,** Bassi,R., Frigerio,S., Finazzi,G., Morris,E., and Barber,J. (2006). Biochemical and structural analyses of a higher plant photosystem II supercomplex of a photosystem I-less mutant of barley. Consequences of a chronic over-reduction of the plastoquinone pool. FEBS J. 273, 4616-4630.

**Muller-Moule,P.,** Havaux,M., and Niyogi,K.K. (2003). Zeaxanthin deficiency enhances the high light sensitivity of an ascorbate-deficient mutant of Arabidopsis. Plant Physiol 133, 748-760.

**Mullet,J.E.,** Burke,J.J., and Arntzen,C.J. (1980). Chlorophyll proteins of photosystem I. Plant Physiol. 65, 814-822.

**Nakazato,K.,** Toyoshima,C., Enami,I., and Inoue,Y. (1996). Two-dimensional Crystallization and Cryo-electron Microscopy of Photosystem II. J. Mol. Biol. 257, 225-232.

**Nield,J.,** Orlova,E.V., Morris,E.P., Gowen,B., van Heel,M., and Barber,J. (2000). 3D map of the plant photosystem II supercomplex obtained by cryoelectron microscopy and single particle analysis. Nat. Struct. Biol. 7, 44-47.

**Niyogi,K.K.** (1999). Photoprotection revisited: Genetic and molecular approaches. Annu. Rev. Plant Physiol. Plant Mol. Biol. 50, 333-359.

**Pagano,A.,** Cinque,G., and Bassi,R. (1998). In vitro reconstitution of the recombinant

photosystem II light-harvesting complex CP24 and its spectroscopic characterization. J. Biol. Chem. 273, 17154-17165.

**Paulsen,H.,** Finkenzeller,B., and Kuhlein,N. (1993). PIGMENTS INDUCE FOLDING OF LIGHT-HARVESTING CHLOROPHYLL ALPHA/BETA-BINDING PROTEIN. Eur. J. Biochem. 215, 809-816.

**Peter,G.F.** and Thornber,J.P. (1991). Electrophoretic Procedures for Fractionation of Photosystem-I and Photosystem-II Pigment-Proteins of Higher Plants and for Determination of Their Subunit Composition. In Methods in Plant Biochemistry. 5, L.J.Rogers, ed. (New York: Academic Press), pp. 195-210.

**Pfannschmidt,T.,** Nilsson,A., Tullberg,A., Link,G., and Allen,J.F. (1999). Direct transcriptional control of the chloroplast genes psbA and psaAB adjusts photosynthesis to light energy distribution in plants. IUBMB. Life 48, 271-276.

**Plumley,F.G.** and Schmidt,G.W. (1987). Reconstitution of chloroform a/b light-harvesting complexes: Xanthophyll-dependent assembley and energy transfer. Proc. Natl. Acad. Sci. USA 84, 146-150.

**Pogson,B.,** McDonald,K.A., Truong,M., Britton,G., and DellaPenna,D. (1996). Arabidopsis carotenoid mutants demonstrate that lutein is not essential for photosynthesis in higher plants. Plant Cell 8, 1627-1639.

**Powles,S.B.** and Bjorkman,O. (1982). Photoinhibition of photosynthesis: Effect on chlorophyll fluorescence at 77k in intact leaves and in chloroplast membranes of nerium oleander. Planta 156, 97-107.

**Remelli,R.,** Varotto,C., Sandona,D., Croce,R., and Bassi,R. (1999). Chlorophyll binding to monomeric light-harvesting complex. A mutation analysis of chromophore-binding residues. J. Biol. Chem. 274, 33510-33521.

**Ruban,A.V.,** Lee,P.J., Wentworth,M., Young,A.J., and Horton,P. (1999). Determination of the stoichiometry and strength of binding of xanthophylls to the photosystem II light harvesting complexes. J. Biol. Chem. 274, 10458-10465.

**Ruuska,S.A.,** von Caemmerer,S., Badger,M.R., Andrews,T.J., Price,G.D., and Robinson,S.A. (2000). Xanthophyll cycle, light energy dissipation and electron transport in transgenic tobacco with reduced carbon assimilation capacity. Aust. J. Plant Physiol. 27, 289-300.

**SAGER,R.** and ZALOKAR,M. (1958). Pigments and photosynthesis in a carotenoid-deficient mutant of Chlamydomonas. Nature 182, 98-100.

**Scheller,H.V.,** Jensen,P.E., Haldrup,A., Lunde,C., and Knoetzel,J. (2001). Role of subunits in eukaryotic Photosystem I. Biochim. Biophys. Acta 1507, 41-60.

**Schreiber,U.** and Neubauer,C. (1990). $O_2^-$ dependent electron flow, membrane energization and the mechanism of non-photochemical quenching of chlorophyll fluorescence. Photosynth. Res. 25, 279-293.

**Storf,S.,** Stauber,E.J., Hippler,M., and Schmid,V.H. (2004). Proteomic analysis of the photosystem I light-harvesting antenna in tomato (Lycopersicon esculentum). Biochemistry 43, 9214-9224.

**Straub O** (1987). Key to carotenoids., H.Pfander, ed.

**Stroebel,D.,** Choquet,Y., Popot,J.L., and Picot,D. (2003). An atypical haem in the cytochrome b(6)f complex. Nature 426, 413-418.

**Tardy,F.** and Havaux,M. (1996). Photosynthesis, chlorophyll fluorescence, light-harvesting system and photoinhibition resistance of a zeaxanthin- accumulating mutant of Arabidopsis thaliana. J. Photochem. Photobiol. B 34, 87-94.

**Telfer,A.,** Dhami,S., Bishop,S.M., Phillips,D., and Barber,J. (1994). -carotene quenches singlet oxygen formed by isolated photosystem II reaction centers. Biochemistry 33, 14469-14474.

**Testi,M.G.,** Croce,R., Polverino-De Laureto,P., and Bassi,R. (1996). A CK2 site is reversibly phosphorylated in the photosystem II subunit CP29. FEBS Lett. 399, 245-250.

**Thornber,J.P.,** Stewart,J.C., Hatton,M.W., and Bailey,J.L. (1967). Studies on the nature of chloroplast lamellae. II. Chemical composition and further physical properties of two chlorophyll-protein complexes. Biochemistry 6, 2006-2014.

**Tjus,S.E.,** Scheller,H.V., Andersson,B., and Moller,B.L. (2001). Active oxygen produced during selective excitation of photosystem I is damaging not only to photosystem I, but also to photosystem II. Plant Physiol 125, 2007-2015.

**Trumpower,B.L.** (1990). The protonmotive Q cycle. Energy transduction by coupling of proton translocation to electron transfer by the cytochrome bc1 complex. J. Biol. Chem. 265, 11409-11412.

**Verhoeven,A.S.,** Adams,W.W., Demmig-Adams,B., Croce,R., and Bassi,R. (1999). Xanthophyll cycle pigment localization and dynamics during exposure to low temperatures and light stress in Vinca major. Plant Physiology 120, 727-737.

**Wallsgrove,R.M.,** Turner,J.C., Hall,N.P., Kendall,A.C., and Bright,S.W. (1987). Barley Mutants Lacking Chloroplast Glutamine Synthetase-Biochemical and Genetic Analysis. Plant Physiol 83, 155-158.

**Wollman,F.A.** (2001). State transitions reveal the dynamics and flexibility of the photosynthetic apparatus. EMBO J. 20, 3623-3630.

**Yamamoto,H.Y.,** Bugos,R.C., and Hieber,A.D. (1999). Biochemistry and molecular biology of the xanthophyll cycle. In The Photochemistry of Carotenoids., H.A.Frank, A.J.Young, G.Britton, and R.J.Cogdell, eds., pp. 293-303.

**Yamamoto,H.Y.** and Kamite,L. (1972). The effects of dithiothreitol on violaxanthin deepoxidation and absorbance changes in the 500nm region. Biochim. Biophys. Acta 267, 538-543.

**Yokthongwattana,K.,** Savchenko,T., Polle,J.E., and Melis,A. (2005). Isolation and characterization of a xanthophyll-rich fraction from the thylakoid membrane of Dunaliella salina(green algae). Photochem. Photobiol. Sci. 4, 1028-1034.

**Zheleva,D.,** Sharma,J., Panico,M., Morris,H.R., and Barber,J. (1998). Isolation and characterization of monomeric and dimeric CP47- reaction center photosystem II complexes. J. Biol. Chem. 273, 16122-16127.

**Zouni,A.,** Witt,H.T., Kern,J., Fromme,P., Krauss,N., Saenger,W., and Orth,P. (2001). Crystal structure of photosystem II from Synechococcus elongatus at 3.8 A resolution. Nature 409, 739-743.

## 1.6 Regulation of plant light harvesting by thermal dissipation of excess energy.

S. de Bianchi, M. Ballottari, L. Dall'Osto and R Bassi.

This article has been written in my last year of phD in order to summarize the current knowledge about the thermal dissipation of excess light energy, and came from the exigence of arrange our work in this field in a more general scientific view. Under the supervision of the prof. Bassi, I wrote this article describing the phenotype of *npq* (non-photochemical quenching)-knockout mutants, the role of gene products involved in the qE process and I compared the molecular models proposed for this mechanism. Discussion with dr Dall'Osto and dr Ballottari helped me to better describe the scientific knowledge and to improve my drafting capacity.

# Regulation of plant light harvesting by thermal dissipation of excess energy

**Silvia de Bianchi, Matteo Ballottari, Luca Dall'Osto and Roberto Bassi**[1]
Dipartimento di Biotecnologie, Università di Verona, I-37134 Verona, Italy

## Abstract

**Elucidating the molecular details of qE (energy quenching) induction in higher plants has proven to be a major challenge. Identification of qE mutants has provided initial information on functional elements involved in the qE mechanism; furthermore, investigations on isolated pigment–protein complexes and analysis *in vivo* and *in vitro* by sophisticated spectroscopic methods have been used for the elucidation of mechanisms involved. The aim of the present review is to summarize the current knowledge of the phenotype of *npq* (non-photochemical quenching)-knockout mutants, the role of gene products involved in the qE process and compare the molecular models proposed for this process.**

## Introduction

### Organization of PS (Photosystem) I and II supercomplexes

Plants use light as the energy source for their metabolism. During the early steps of photosynthesis, solar energy is absorbed efficiently, and excitons are transferred to the photosynthetic reaction centres by a complex array of pigment-binding proteins, the LHCs (light-harvesting antenna complexes), localized at the periphery of each PS [1,2]. LHC proteins not only are involved in light harvesting, but also act in photoprotection by multiple mechanisms, including Chl (chlorophyll) singlet energy dissipation, Chl triplet quenching and scavenging of ROS (reactive oxygen species). The antenna system thus has a dual function: on one hand, it harvests photons and extends the cross-section for light absorption under light-limiting conditions; on the other hand, it limits damage to the photosynthetic apparatus when light is in excess. In higher plants, two classes of proteins compose the antenna system, which can be divided into two moieties. The inner antenna is made by the plastid-encoded proteins, CP43 and CP47, which bind Chl *a* and $\beta$-carotene, whereas the outer moiety is composed by the nuclear-encoded LHC proteins, which bind Chl *a*, Chl *b* and xanthophylls. In plants the PSII outer antenna consists of one copy each of three monomeric proteins called CP29 (Lhcb4), CP26 (Lhcb5) and CP24 (Lhcb6) and two to four copies, depending on light conditions during growth, of the major antenna complex, called LHCII. The latter is a heterotrimer of the Lhcb1, Lhcb2 and Lhcb3 subunits in different combinations [3–6]. The D1/D2/cytochrome $b_{559}$ subunits constitute a 'core' complex with the inner antenna moiety and a core dimer, which also includes many small transmembrane subunits [7], forms a supramolecular complex together with two copies each of the monomeric Lhcb4, Lhcb5 and Lhcb6 subunits and, more peripherally, with several LHCII trimers [2,8,9]. PSI is simpler, with electron-transport domains fused with the inner antenna in a core complex composed of PsaA/PsaB large subunits and many small elements. The outer antenna is smaller than in PSII with only four Lhca subunits organized as a crescent on one side of the monomeric core moiety [10,11].

**Key words:** charge-transfer quenching, light-harvesting antenna complex protein (LHC protein), minor antenna protein, non-photochemical quenching (NPQ), photoprotection, xanthophyll mutant.

**Abbreviations used:** AA, antimycin A; CET, cyclic electron transport; Chl, chlorophyll; CT, charge-transfer; DCCD, *N*,*N*′-dicyclohexylcarbodi-imide; DTT, dithiothreitol; HL, high light; LET, linear electron transport; LHC, light-harvesting antenna complex; Neo, neoxanthin; NPQ, non-photochemical quenching; PGR, protein gradient regulation; PS, Photosystem; qE, energy quenching; qI, inhibitory quenching; ROS, reactive oxygen species; VDE, violaxanthin de-epoxidase; Viola, violaxanthin; WT, wild-type; Zea, zeaxanthin.

### The need for photoprotection and the role of xanthophylls

Under normal stable light conditions, the efficiency of the photosynthetic machinery is optimal for a given light intensity once plants are acclimatized to it. Nevertheless, in the natural environment, plants often experience rapid fluctuations in light intensity, temperature and water availability that easily lead to overexcitation of photosystems. Therefore, since absorbed light may exceed the capacity to use reducing equivalents for $CO_2$ fixation and primary metabolic roles, such conditions lead to over-reduction of the $NADP^+$ pool and to superoxide ($O_2^-$) production in the chloroplast by the Mehler's reaction [12,13]. $O_2^-$ can be metabolized to hydrogen peroxide ($H_2O_2$) or hydroxyl radical ($OH^\bullet$), the latter being a very aggressive ROS [14–16]. Furthermore, incomplete photochemical quenching leads to an increased lifetime of Chl excited state ($^1Chl^*$), increasing the probability of Chl *a* triplet formation ($^3Chl^*$) by intersystem crossing. $^3Chl^*$ promptly reacts with oxygen ($^3O_2$) to form single oxygen ($^1O_2$), a harmful ROS. Thus PSII and LHCs, when overexcited, became an important source of $^1O_2$ [17,18]. These harmful events are counteracted by photoprotection mechanisms that either detoxify the ROS produced or prevent their formation. ROS can be deactivated

**Figure 1** | **Carotenoid biosynthetic pathway in higher plants**

Enzymes involved and corresponding knockout mutants are indicated. ABA, abscisic acid.

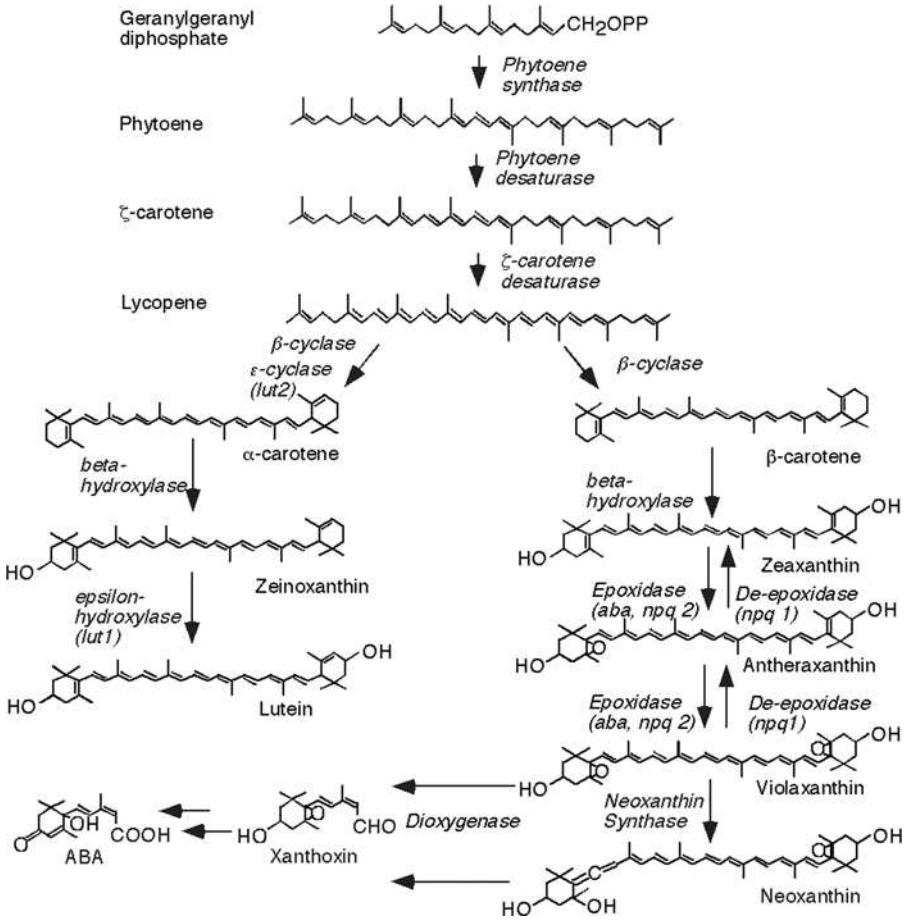


by small chloroplast antioxidant molecules, including α-tocopherol, glutathione and carotenoids, or enzymes, such as the thylakoid-bound superoxide dismutase and ascorbate peroxidase. Carotenoids, and their oxygenated derivatives, xanthophylls, play a key role as photoprotective agents. The biosynthetic pathway of carotenoids is shown in Figure 1. The carotenoid composition of thylakoids is not constant and undergoes modifications during long-term acclimatization of plants to stress conditions, as well as during rapid fluctuations of solar light intensity, owing to the operation of the xanthophyll cycle [19]. The xanthophyll cycle involves the xanthophylls violaxanthin (Viola) and zeaxanthin (Zea), and consists of a light-dependent reversible de-epoxidation of Viola to Zea via the intermediate antheraxanthin; the reaction is catalysed by VDE (violaxanthin de-epoxidase), a luminal enzyme activated by the build-up of a high transmembrane proton gradient, which is a good indicator for the presence of light in excess [20,21].

Plants have evolved several mechanisms in order to minimize ROS production. Chloroplasts are able to relocate their positions in a cell in response to the incident light intensity, moving to the side wall of the cell to avoid strong light, but gathering at the front face under low light in order to maximize light harvesting [22]. Within the chloroplast, both PSII antenna size and composition are adjusted through changes in gene expression and protein turnover [23–25] or through covalent modification of LHCII proteins by phosphorylation, which modulates the interaction of LHCII with PSII and PSI [26–28] thus balancing the energy pressure between the two PSs (state transition). Mechanisms acting as alternative sinks for excess electrons, such as photorespiration [29,30], water–water cycle [31] or cyclic electron transport [32], appear as photochemical strategies to relieve overexcitation.

## Excess energy dissipation into heat

Since $^3$Chl* production is a constitutive intrinsic property of Chls, the capacity to control its formation is essential for plant survival. This is obtained by preventing the formation of the $^3$Chl*, derived from excess $^1$Chl*, through a set of inducible mechanisms, collectively referred to as NPQ (non-photochemical quenching). NPQ allows for the harmless thermal dissipation of excess absorbed photons by PSII [33] and can be monitored as a light-dependent quenching

of leaf Chl fluorescence [34], whereas thermal dissipation can be evaluated by measuring the heat production by photo-acoustic spectroscopy [35]. The predominant NPQ component is triggered by the pH change across the thylakoid membrane and rapidly reversible. It is thus depending on the 'energization' of the chloroplast and defined as qE (energy quenching) [36–38]. In addition to qE, a slowly relaxing component of the NPQ process is known as qI (inhibitory quenching), which relaxes with a half-time of approx. 30 min. This component has been attributed to photoinhibition and its relaxation is suggested to be dependent on D1 re-synthesis [39]. Although this attribution is justified when NPQ is induced by very HL (high light), qI is also observed under intermediate light conditions, where it depends on the accumulation of Zea [40]. A third quenching component (qT) component, relaxing within minutes has been reported [39]. Its attribution to the establishment of state 1–state 2 transitions appears unlikely on the basis of an unchanged NPQ in the *stn7* mutant lacking the LHCII kinase. Moreover, LHCII phosphorylation is saturated at 200 $\mu Em^{-2} \cdot s^{-1}$ [41], a light intensity rather inefficient for NPQ induction.

Overall, the ability of plants to modulate light-utilization efficiency to the fluctuating light intensity, through a feedback mechanism coupled to pH changes in the chloroplast lumen, is determinant for plant fitness in natural environments [42,43].

In the following sections, we summarize the current knowledge regarding the photoprotective mechanism of excess energy dissipation (NPQ) in higher plants and discuss the different models proposed.

## Genetic analysis of qE

A number of studies have used genetic analysis in order to identify mutants in NPQ. qE mutants can be classified into three major groups: (i) mutants with altered capacity of build-up of the ΔpH gradient or detect luminal pH; (ii) mutants affected in pigment composition; (iii) knockout mutants lacking external antenna protein subunits of PSII (Lhcbs).

### Mutants altered in ΔpH building or luminal pH sensing

The excess proton concentration in the thylakoid lumen is perceived as a signal that the absorbed light exceeds the capacity of electron transport to $NADP^+$ and/or the capacity of ATPase to use the proton gradient for ATP synthesis, thus requiring thermal energy dissipation. Treatment with the ionophore nigericin collapses ΔpH and prevents the activation of NPQ otherwise activated within a few seconds of exposure to HL [44], thus mutations that reduce ΔpH building capacity also affect qE amplitude and kinetic. LET (linear electron transport) and CET (cyclic electron transport) are both coupled to the generation of a trans-thylakoid ΔpH that drives ATP synthesis [45], whereas only LET produces NADPH. It has long been discussed whether CET around PSI is involved in regulating photosynthesis via lumen acidification [32], and, in the last few years, isolation of several mutants defective in CET and with altered qE phenotype got further clues. In vascular plants, PSI CET consists of two partially redundant pathways: the PGR (protein gradient regulation) 5-dependent pathway, which is inhibited by AA (antimycin A), and the AA-resistant NAD(P)H dehydrogenase-dependent pathway [46]. *Arabidopsis* mutants *pgr5* and *pgr1* were identified owing to their low qE phenotype by Chl fluorescence imaging [47,48]. Deletion of subunits involved in the PGR5-dependent pathway revealed that it is essential for qE induction [49], whereas the contribution of the NAD(P)H dehydrogenase-dependent pathway to ΔpH building is not significant for qE induction [46].

Signal transduction of lumen over-acidification involves the PSII subunit PsbS that is essential for qE induction (Figure 2), as demonstrated by the phenotype of the *npq4* mutant [50,51]. PsbS belongs to the LHC protein superfamily, but differs from other members for having four transmembrane helices rather than the three generally found in most LHC proteins [50] and for not binding pigments as shown from the non-conservation of Chl-binding residues [52]. Typical of this protein is the presence of two lumen-exposed glutamate residues, $Glu^{122}$ and $Glu^{226}$, that bind DCCD (*N*,*N*′-dicyclohexylcarbodi-imide), a protein-modifying agent that covalently binds to protonatable residues in hydrophobic environment [53]. In *Arabidopsis,* mutation of each glutamate to a non protonatable residue e.g. E122Q and E226Q, decreased by 50% both qE and DCCD-binding capacity, whereas the double mutant has a qE-null phenotype like *npq4* [54].

Altogether, phenotypes of qE-triggering mutant (*npq4*) and CET mutant (*pgr*) confirmed the tight dependence of NPQ on the low luminal pH and the detection of acidification through PsbS.

### Xanthophyll biosynthesis mutants

Single and multiple mutations targeting genes encoding enzymes in the carotenoid biosynthesis pathway have been produced by several laboratories, yielding mutants with altered xanthophyll composition. Most of these mutations affect both qE amplitude and kinetics, thus suggesting that xanthophylls have important roles in qE.

The *npq1* mutant lacks VDE activity and is thus unable to convert Viola into Zea upon exposure to HL [55]; qE in *npq1* has approx. 30–40% amplitude with respect to WT (wild-type), showing that Zea synthesis is need for full expression of qE in *Arabidopsis*. Moreover, quenching in *npq1* is saturated within 1 min, whereas WT, in addition, develops a slower phase of quenching, proceeding for up to 30 min [56], which is related to Zea accumulation (Figure 2). Upon its synthesis, Zea binds to specific binding sites in Lhcb proteins, namely the site L2 in monomeric Lhcb4–Lhcb6 [57,58] and the peripheral V1 site of LHCII [59,60]: the slow kinetics of the Zea-dependent qE component reflects the replacing of Viola bound to sites L2 and/or V1 in Lhcb proteins with Zea, a process limited by diffusion in the

**Figure 2** |

(**A**) NPQ kinetics upon transition from the dark to HL (1100 $\mu Em^{-2} \cdot s^{-1}$) and subsequent relaxation in the dark of WT *Arabidopsis* and mutants with modified xanthophyll composition or lacking PsbS. Npq1, npq2, lut2, npq4 lacks respectively the xanthophylls Zea, Viola, lutein and the PsbS protein. Note that residual qE in lut2 is due to the presence of Zea, whose synthesis is inhibited by leaf infiltration with DTT (5 mM). (**B**) Maximal value of NPQ amplitude of WT and xanthophyll biosynthesis mutants. Horizontal lines indicates the level of NPQ measured in the absence of qE (npq4), in the absence of lutein with constitutive presence of Zea (npq2lut2) and in WT. Residual NPQ in npq4 is attributed to quenching in the PSII core complex [79].

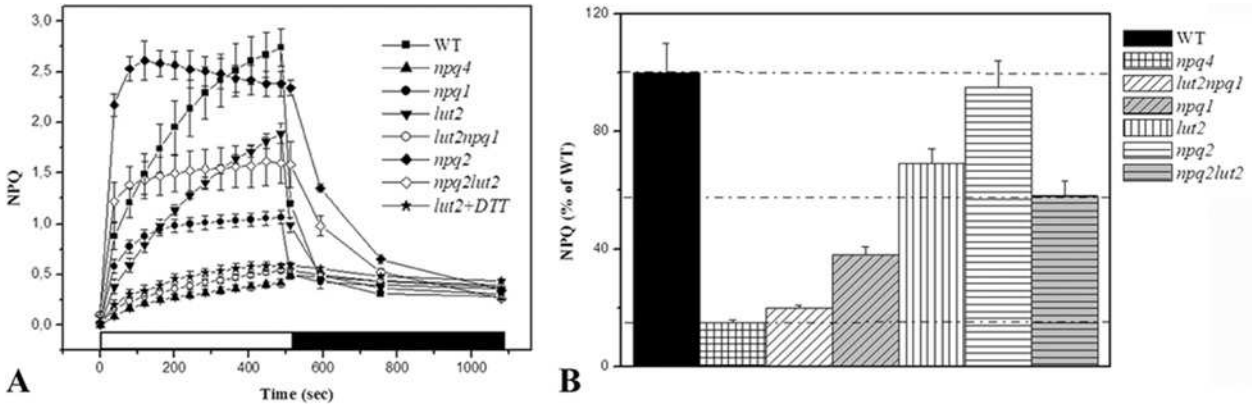


lipid phase. This suggestion is consistent with results of experiments in which DTT (dithiothreitol) is used as VDE activity inhibitor: DTT blocks the slow phase of NPQ rise [61,62], while retaining the fast, initial, phase of quenching. Thus a component of qE is activated independently of the presence of a functional xanthophyll cycle [63] and is due to the action of a xanthophyll species already bound to Lhcb proteins in the dark, before NPQ induction. This xanthophyll appears to be lutein, the most abundant among plant xanthophylls: the *lut2npq1* double mutant, lacking both Zea and lutein, have a NPQ-null phenotype [64]. Residual qE measured in *lut2* plants has been attributed to Zea. In fact, the *lut2* mutant has both a low NPQ and slower kinetics [65–68], whereas DTT treatment of *lut2* plants (Figure 2) phenocopy *lut2npq1*, implying that the slowly developing quenching is produced from newly synthesized Zea. The mutation *szl1* (*suppressor of zeaxanthinless1*), identified on the *npq1* genetic background and promoting a higher lutein/$\beta$-xanthophyll ratio, is effective in partially releasing the qE restriction owing to the *npq1* mutation, suggesting that lutein can replace Zea and perform quenching binding to site L2 of monomeric Lhcb4 and Lhcb6 as proved using recombinant proteins with lutein in L2 [69]. The above evidence suggests that: (i) lutein, in addition to Zea, has a key role in qE modulation and for the full expression of qE [70]; (ii) lutein and Zea modulate distinct kinetic components of qE. lutein is stably bound to several LHC, whereas Zea is accumulated upon de-epoxidation of Viola, released by peripheral xanthophyll-binding sites on LHCII. The rapid phase in qE induction kinetics, retained in *npq1* plants, together with the effect of *szl1* mutation, indicate that the functional component responsible for the retained qE in *npq1* is lutein, already bound to photosynthetic complexes before light exposure. This is in accordance with the lack of the rapid component of NPQ induction in *lut2* plants. The slower phase of fluorescence quenching measured in *lut2* leaves is due to Zea. Indeed, by infiltrating *lut2* leaves with DTT, the qE amplitude decreases to levels of *lut2npq1* (Figure 2).

The primary role of Zea in qE induction is confirmed by the phenotype of *npq2* mutants; in these plants, blocking the Zea epoxidation reaction leads to accumulation of high levels of Zea, even in dark-adapted plants [55,71], which leads to a more rapid saturation of qE maximal amplitude respect to WT, with kinetics presumably limited only by the build-up of a trans-thylakoid $\Delta$pH (Figure 2).

Altogether, lutein and Zea appear to be determinant for qE amplitude, whereas Viola and neoxanthin (Neo) are not involved [72]. This suggests the presence of two distinct quenching sites, either lutein- or Zea-specific. The specificity is proved by the fact that lutein-only plants [72] or Zea-only plants [73] cannot reach the maximal amplitude of NPQ. Indeed, the double mutant *lut2npq2*, in which all xanthophylls are replaced by Zea [73] shows NPQ amplitude similar to *lut2* (Figure 2).

## Knockout mutants lacking single or multiple PSII Lhcbs

The sections above showed that PsbS is essential for triggering of NPQ, whereas both lutein and Zea are needed for the full activation of the mechanism. The *npq4* mutation is epistatic over mutations in the xanthophyll biosynthesis pathway [74,75], implying that both lutein and Zea act downstream of the mechanistic step controlled by pH sensing trough PsbS. In order for PsbS protonation yielding into dissipation of

$^1$Chl* and fluorescence quenching, this event must affect a Chl binding protein. Such a protein should also bind lutein and Zea as shown above or, at least, should interact tightly with a xanthophyll-binding protein, thus providing a quenching effect. Early works proposed that PsbS might bind both Chls and xanthophylls [76] or Zea alone [77], making it a candidate for the role of quencher. Nevertheless, further work pointed to the non-conservation of Chl-binding residues in PsbS [52], while its properties both *in vivo* and *in vitro* are not consistent with binding of xanthophylls [75]. Once PsbS is ruled out, Lhcb proteins appear to be ideal candidates for the role of quenching sites owing to their capacity to bind Chls and xanthophylls, with lutein and Zea binding to distinct sites, which could well catalyse the two distinct and complementary quenching events identified above. Indeed, the *ch1* mutant of *Arabidopsis* that lacks Chl *b*, thus leading to degradation of LHC proteins [78], exhibits a strongly reduced capacity of NPQ in the presence of both lutein and Zea, suggesting that LHCs are needed for the lutein/Zea-quenching events. Indeed, the small residual fluorescence quenching measured on *ch1* and *npq4* mutants has been attributed to a quenching mechanism located within the PSII core complex [79].

Lhcb proteins fall into two groups with respect to the sites where they bind lutein and Viola/Zea: the first group includes Lhcb1, Lhcb2 and Lhcb3, the components of the major trimeric LHCII, binding lutein at sites L1 and L2, whereas Viola/Zea bind at site V1 [60,80,81]. The second group includes monomeric Lhcb4, Lhcb5 and Lhcb6 which bind lutein at site L1, with Viola/Zea binding at site L2 [82–84]. These proteins do not have a V1 site and exchange Viola with Zea in site L2 [85,86], whereas Lhcb1–Lhcb3 do not. This feature is consistent with the slow kinetics of the Zea-dependent quenching component of NPQ and with the need for *de novo* synthesis of Zea for quenching (Figure 2). Zea binding to Lhcb4–Lhcb6 results in a conformational change [40] and into a decrease in the fluorescence lifetime [73,87–89]. The presence of a Zea-binding site effective in providing enhancement of NPQ is not a property of a single LHC protein since Zea-dependent enhancement of NPQ has been observed in plants depleted in Lhcb6, Lhcb4 and LHCII [90].

The role of individual LHCs has been investigated using reverse genetics. Down-regulation of Lhcb1 + Lhbc2 and knockout of Lhcb3 did not significantly decrease NPQ amplitude or slow down its kinetics [91,92]. Targeting monomeric Lhcbs yielded into different results: Lhcb5-knockout plants retained qE [93,94], whereas the qI component of NPQ was down-regulated [40]. qE was affected in Lhcb6- and Lhcb4-knockout plants [56,93–95]. In summary, depletion of a single monomeric Lhcb protein could not completely abolish NPQ, implying redundancy within the subfamily members. The making of a mutant lacking all three monomeric Lhcb4–Lhcb6 proteins is awaited in order to verify whether NPQ can be sustained in the absence of these gene products. Nevertheless, the work accomplished so far highlights the role of Lhcb4–Lhcb6 gene products on NPQ, whereas Lhcb1–Lhcb3 antisense or Lhcb3-knockout had little effect on NPQ.

## Molecular mechanisms of excess energy dissipation

Elucidating the molecular details of qE induction in higher plants has proven to be a major challenge. Reverse genetics has focused the attention on Lhcb proteins; nevertheless, systems simpler than the whole plant have been used in order to perform spectroscopy aiming to identify the underlying mechanism(s) that catalyse energy dissipation into heat. At present, investigations by several groups worldwide have contributed to the formulation of three mechanistic models for excess energy dissipation.

(i) Aggregation-dependent LHCII quenching. According to this model, qE occurs upon aggregation of the major trimeric LHCII complex of PSII. This produces a conformational change within the protein and promotes energy transfer from Chl *a* to a low-lying S1 excited state of lutein bound to site L1 of LHCII [96–98].

(ii) CT (charge-transfer) quenching model. Energy absorbed in excess induces formation of a carotenoid radical cation by charge separation within a Chl *a*–Zea heterodimer followed by charge recombination at the ground state [99]. The process is located in monomeric Lhcb4–Lhcb6 proteins and does not occur in LHCII [63,100]. Lutein can also be active in this process [69].

(iii) Zea radical cation in Lhcb–PsbS oligomers. This model agrees with the second model as for the involvement of carotenoid radical cations in quenching, but proposes that the interaction between Chl *a* and Zea is promoted by the binding of a Zea–PsbS complex with either LHCII or a monomeric Lhcb subunit [101,102].

### Aggregation-dependent LHCII quenching

This hypothesis was proposed based on experimental evidence that aggregation of isolated LHCII trimers or monomers, induced in solution by low detergent concentration and/or low pH, causes a decrease in Chl fluorescence lifetime [103–105]. This early model has been refined over the years and presently incorporates a detailed description of the conformational changes induced by aggregation within the LHCII molecule [106], yielding a tight interaction between lutein bound into the L1 site and Chl *a* chromophores [98,107]. Evidence that the process as observed in purified LHCII is related to NPQ *in vivo* relies on the similar spectral changes, attributed to Chl *a* and Neo, detected in leaves during establishment of NPQ and aggregation of LHCII [97,98,103]. Recently, support for this model was provided by the observation of a red-shifted fluorescence lifetime component in both aggregated LHCII trimers binding Zea and quenched leaves [108]. Zea bound at site V1 of LHCII, acts as an allosteric modulator of lutein-dependent quenching [108,109], whereas aggregation *in vitro* has been propose to entrain an intrinsic conformational transition

in LHCII, in turn responsible for establishment of the quenching reaction [110]. Car S1–Chl excited state coupling was recently measured in isolated LHCII and correlated with the NPQ amplitude *in vivo* in different mutants such as *npq1*, *npq2*, *lut2* and *PsbS*-over-accumulating line [111].

Criticisms of this model have been raised on the basis that: (i) the effect of down-regulating the components of LHCII *in vivo*, namely Lhcb1 + Lhcb2 [91] or Lhcb3 [92] is, at best, very small; (ii) quenching and other spectral changes attributed to LHCII occurs in monomeric Lhcb4 and Lhcb5 proteins as well, even more rapidly than in LHCII [104,112]; (iii) lutein cannot be the only quencher during NPQ, since the *lut2npq2* mutant having Zea as the only xanthophyll is active in NPQ as well as the lutein-less mutant *lut2* (Figure 2).

## CT quenching in minor complexes

The proposal that NPQ is based on the formation of a CT state between Chl *a* and Zea has been proposed based on quantum chemical calculations [113] and ultra-fast pump-probe experiments on isolated thylakoid membranes [99]. The CT mechanism, which accounts for a large fraction of qE [100], involves energy transfer from bulk Chl molecules to a Chl–Zea heterodimer that undergoes charge separation followed by recombination, thereby transiently producing a Zea radical cation ($Zea^{\bullet+}$) with a very short relaxation time (50–200 ps), as expected for an efficient quencher. Formation of $Zea^{\bullet+}$ in thylakoids depends on the three components needed for qE *in vivo*: lumen acidification, PsbS activation and Zea production [99,100]. The signal from $Zea^{\bullet+}$ formation has been found in isolated monomeric Lhcbs, but not in LHCII [63,100,114–116], consistent with reverse genetic data showing that no single LHC subunit is essential for qE [93,95,100]; furthermore, the localization of these complexes between LHCII and the reaction centre makes a perfect setting for regulating excitation energy transfer from the peripheral LHCII to the core subunits. Mutation analysis of Chl-binding sites in Lhcb4 [63] showed that a Chl pair (Chl A5 and Chl B5) rather than a single Chl *a* chromophore, is critical for CT quenching. The involvement of a Chl pair is reasonable since charge delocalization over the Chl pair would stabilize the CT state. Chl A5–B5 are located in close proximity to the L2 domain, whereas Zea binding to this site induces a conformational change, bringing Chl A5 into excitonic interaction with Chl B5, switching the protein to a dissipative state by $Zea^{\bullet+}$ formation. Also, Lhcb6 antenna complexes shows $Zea^{\bullet+}$ formation, whereas in the Lhcb5 complex, two distinct CT quenching sites are detected, involving Zea and lutein radical cation species respectively, depending on Zea binding to the L2 binding site. Thus Zea in the L2 site acts both as a quencher and as an allosteric modulator of lutein CT efficiency into site L1 [115]. $Lutein^{\bullet+}$ was also recently detected in Lhcb6 and Lhcb4 complexes binding lutein as the only xanthophyll [69]. This result, combined with the rescuing of the NPQ phenotype of *npq1* in the double mutant *slz/npq1*, exhibiting increased lutein content, implies that not only Zea, but also lutein, is involved in CT quenching and accounts for the presence of partial NPQ in Zea-less mutants.

Unanswered questions by the CT model include: (i) a double mutant lacking both Lhcb5 and Lhcb6 and reduced in Lhcb4 still retains most NPQ activity; (ii) a low level (~1%) *in vitro* of minor complexes undergoing CT quenching compared with *in vivo* (30%), implying the presence of factors, possibly PsbS, ΔpH or interactions with protein partners, which stabilize the dissipative conformation [115] *in vivo*; (iii) the LHC protein conformational change induced by interaction with PsbS has not been reproduced *in vitro*, so far; and (iv) the relationship between CT quenching and the S1 population, as a consequence of charge recombination upon carotenoid radical cation formation.

## PsbS–Zea complex interaction with Lhcbs

The model proposed from Kuhlbrandt and co-workers is a variant of the above-described CT model [101,102]. They agree that $Zea^{\bullet+}$ formation has a primary role in modulating qE amplitude and propose that trimeric LHCII or monomeric LHCs are involved in the catalysis of NPQ, despite the fact that LHCII trimers in solution could not form $Zea^{\bullet+}$ [100–102], by postulating that Zea is brought to LHCII by interaction with PsbS. However, PsbS has not been found as a cross-linking product of LHCII [117] and cannot bind Zea *in vivo* or *in vitro* [52,75].

## Triggering of qE

Chloroplast lumen acidification is the original event activating NPQ. The signal transduction into a quenching state appears to be obtained by two independent, although complementary, pathways. The first event is the activation of VDE in the chloroplast lumen. VDE is a monomer soluble in the luminal space at neutral pH, whereas it becomes a dimer bound to the thylakoid membrane at low pH [118], where it catalyses the synthesis of Zea from pre-existing Viola [119]. This is bound to the V1 site of LHCII which becomes labile at low pH [60,120]. Newly formed Zea binds to site L2 of monomeric Lhcbs [85] where it induces the conformational change which allows the interaction between Chl A5 and Chl B5 in Lhcb4 and probably in Lhcb5 and Lhcb6 [63,121], and the Chl *a*–lutein interaction in the Lhcb5 L1 site [115].

The second pathway is more direct: low pH protonates two glutamate residues on the luminal loops of PsbS [50,54], each responsible for 50% of the NPQ amplitude, thus implying that PsbS somehow interacts with LHC proteins binding Chl *a* and xanthophylls responsible for quenching by one or more of the above-described mechanisms. Nevertheless, the mode of interaction is still obscure. In one proposal, PsbS would promote LHCII aggregation [122], whereas the level of quenching thus induced, is allosterically regulated by the de-epoxidation state of site V1 [109]. An alternative model (by Kuhlbrandt and co-workers) postulates that PsbS, a dimer at neutral pH, dissociates at acidic pH into monomers [117,123]. This dimer–monomer transition might uncover the Zea-binding site on the hydrophobic surface of PsbS; PsbS monomers could transiently bind pigments (Zea) under

**Figure 3** | **Model of the PsbS-dependent qE mechanism in the PSII supercomplex**

Low luminal pH leads to: (**A**) binding of newly formed Zea to site L2 of monomeric Lhcbs where it induces conformational change, and (**B**) protonation of the two glutamate residues on the luminal loops of PsbS. (**C**) Reorganization of PSII–LHCII supercomplexes upon the two triggering events: activated PsbS induces the dissociation of a pentameric complex composed of CP24, CP29 and LHCII trimer M. CP29 remains bound to PSII core together with CP26 and LHCII trimer S, whereas CP24 and timers M plus L segregates into different domains with respect to PSII RC-containing complexes towards grana margins. Quenching of PSII supercomplex is provided by CP29 and CP26, whereas quenching of LHCII M + L is provided by CP24 [56].

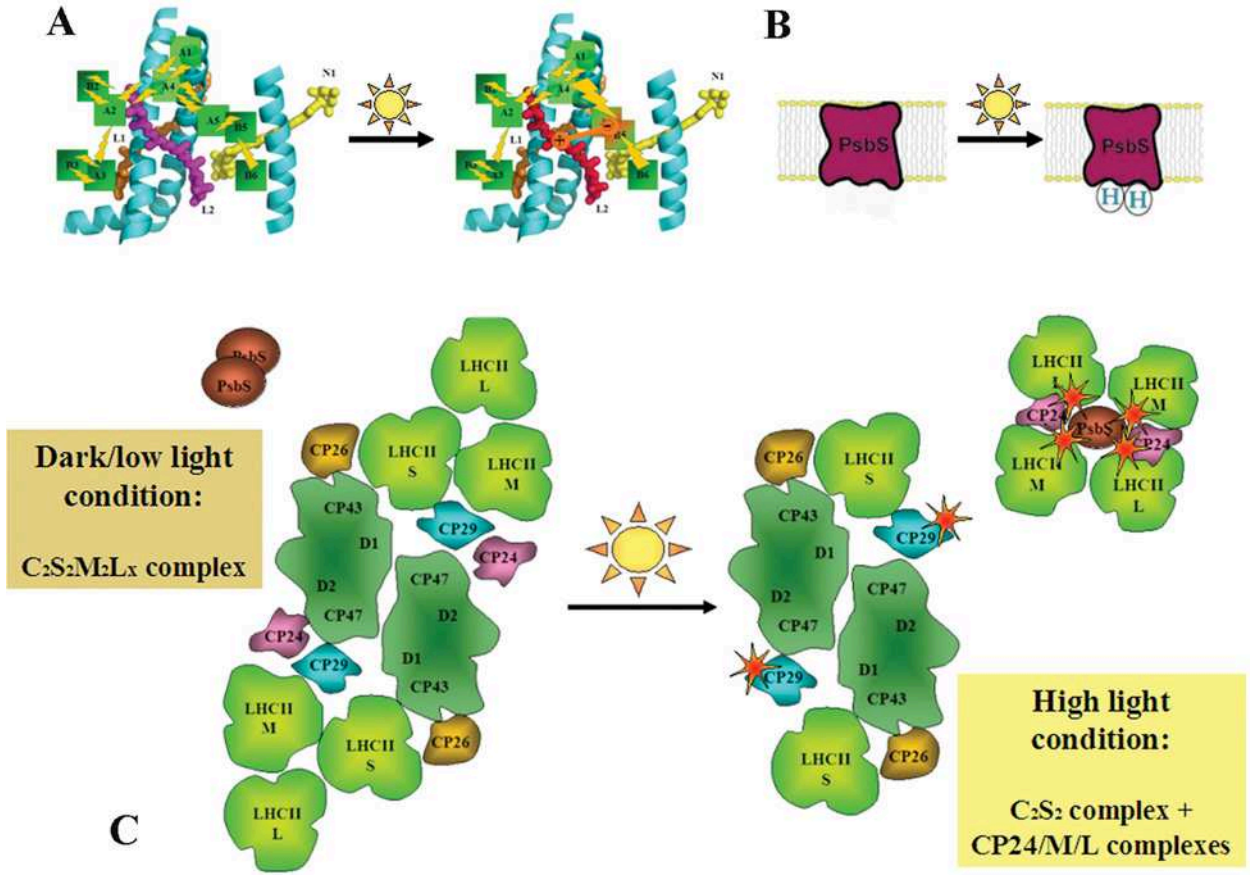


qE conditions and bring pigments into close proximity with either LHCII or a minor Lhcb, forming a Chl–Zea heterodimer. A third model for the triggering of quenching by PsbS has been advanced on the basis of the observation that any physiological conditions or chemical treatment that prevents dissociation of a pentameric complex, including Lhcb4 and Lhcb6, together with a LHCII trimer also blocks NPQ. Thus the unquenched conformation of Lhcb proteins is stabilized by their inclusion in this large complex, while its dissociation by PsbS would allow transition to the quenching state, also promoted by Zea binding [56]. Indeed, mutations inducing constitutive dissociation of the pentameric complex (designated as 'B4 complex' from its order of migration in sucrose gradients) show formation of two-dimensional arrays of C2S2 particles in the centre of grana discs, whereas LHCII is segregated out towards grana margins. The two triggering pathways and the reorganization of PSII–LHCII supercomplexes are outlined in Figure 3.

## References


1 Ben Shem, A., Frolow, F. and Nelson, N. (2003) Crystal structure of plant Photosystem I. Nature **426**, 630–635

2 Caffarri, S., Kouril, R., Kereiche, S., Boekema, E.J. and Croce, R. (2009) Functional architecture of higher plant Photosystem II supercomplexes. EMBO J. **28**, 3052–3063

3 Jansson, S. (1994) The light-harvesting chlorophyll *a*/*b*-binding proteins. Biochim. Biophys. Acta **1184**, 1–19

4 Bassi, R., Giuffra, E., Croce, R., Dainese, P. and Bergantino, E. (1996) Biochemistry and molecular biology of pigment binding proteins. in Light as Energy Source and Information Carrier in Plant Photophysiology (Jennings, R.C., Zucchelli, G., Ghetti, F. and Colombetti, G., eds), pp. 41–63, Plenum Press, New York

5 Jackowski, G. and Jansson, S. (1998) Characterization of Photosystem II antenna complexes separated by non-denaturing isoelectric focusing. Z. Naturforsch. C J. Biosci. **53**, 841–848

6 Ballottari, M., Dall'Osto, L., Morosinotto, T. and Bassi, R. (2007) Contrasting behavior of higher plant Photosystem I and II antenna systems during acclimation. J. Biol. Chem. **282**, 8947–8958

7 Ferreira, K.N., Iverson, T.M., Maghlaoui, K., Barber, J. and Iwata, S. (2004) Architecture of the photosynthetic oxygen-evolving center. Science **303**, 1831–1838
8 van Roon, H., van Breemen, J.F., de Weerd, F.L., Dekker, J.P. and Boekema, E.J. (2000) Solubilization of green plant thylakoid membranes with n-dodecyl-$\alpha$,D-maltoside: implications for the structural organization of the Photosystem II, Photosystem I, ATP synthase and cytochrome $b_6f$ complexes. Photosynth. Res. **64**, 155–166
9 Harrer, R. (2003) Associations between light-harvesting complexes and Photosystem II from *Marchantia polymorpha* L. determined by two- and three-dimensional electron microscopy. Photosynth. Res. **75**, 249–258
10 Amunts, A., Drory, O. and Nelson, N. (2007) The structure of a plant Photosystem I supercomplex at 3.4 Å resolution. Nature **447**, 58–63
11 Ben Shem, A., Frolow, F. and Nelson, N. (2004) Light-harvesting features revealed by the structure of plant Photosystem I. Photosynth. Res. **81**, 239–250
12 Wise, R.R. and Naylor, A.W. (1987) Chilling-enhanced photooxidation: evidence for the role of singlet oxygen and superoxide in the breakdown of pigments and endogenous antioxidants. Plant Physiol. **83**, 278–282
13 Mehler, A.H. (1951) Studies on reactions of illuminated chloroplasts. I. Mechanism of the reduction of oxygen and other Hill reagents. Arch. Biochem. **33**, 65–77
14 Barber, J. and Andersson, B. (1992) Too much of a good thing: light can be bad for photosynthesis. Trends Biochem. Sci. **17**, 61–66
15 Aro, E.-M., Virgin, I. and Andersson, B. (1993) Photoinhibition of Photosystem-2: inactivation, protein damage and turnover. Biochim. Biophys. Acta **1143**, 113–134
16 Osmond, C.B. (1994) What is photoinhibition? Some insights from comparisons of shade and sun plants. In Photoinhibition of Photosynthesis: from Molecular Mechanisms to the Field (Baker, N.R. and Bowyer, J.R., eds), pp. 1–24, Bios Scientific Publishers, Oxford
17 Melis, A. (1999) Photosystem-II damage and repair cycle in chloroplasts: what modulates the rate of photodamage? Trends Plant Sci. **4**, 130–135
18 Dall'Osto, L., Fiore, A., Cazzaniga, S., Giuliano, G. and Bassi, R. (2007) Different roles of $\alpha$- and $\beta$-branch xanthophylls in photosystem assembly and photoprotection. J. Biol. Chem. **282**, 35056–35068
19 Demmig-Adams, B., Winter, K., Kruger, A. and Czygan, F.C. (1989) Light response of $CO_2$ assimilation, dissipation of excess excitation energy, and zeaxanthin content of sun and shade leaves. Plant Physiol. **90**, 881–886
20 Gilmore, A.M. and Yamamoto, H.Y. (1992) Dark induction of zeaxanthin-dependent nonphotochemical fluorescence quenching mediated by ATP. Proc. Natl. Acad. Sci. U.S.A. **89**, 1899–1903
21 Yamamoto, H.Y. and Kamite, L. (1972) The effects of dithiothreitol on violaxanthin deepoxidation and absorbance changes in the 500 nm region. Biochim. Biophys. Acta **267**, 538–543
22 Kagawa, T., Sakai, T., Suetsugu, N., Oikawa, K., Ishiguro, S., Kato, T., Tabata, S., Okada, K. and Wada, M. (2001) *Arabidopsis* NPL1: a phototropin homolog controlling the chloroplast high-light avoidance response. Science **291**, 2138–2141
23 Escoubas, J.M., Lomas, M., LaRoche, J. and Falkowski, P.G. (1995) Light intensity regulation of cab gene transcription is signaled by the redox state of the plastoquinone pool. Proc. Natl. Acad. Sci. U.S.A. **92**, 10237–10241
24 Maxwell, D.P., Laudenbach, D.E. and Huner, N. (1995) Redox regulation of light-harvesting complex II and *cab* mRNA abundance in *Dunaliella salina*. Plant Physiol. **109**, 787–795
25 Montane, M.H., Tardy, F., Kloppstech, K. and Havaux, M. (1998) Differential control of xanthophylls and light-induced stress proteins, as opposed to light-harvesting chlorophyll *a*/*b* proteins, during photosynthetic acclimation of barley leaves to light irradiance. Plant Physiol. **118**, 227–235
26 Allen, J.F. (1992) Protein phosphorylation in regulation of photosynthesis. Biochim. Biophys. Acta **1098**, 275–335
27 Allen, J.F. and Forsberg, J. (2001) Molecular recognition in thylakoid structure and function. Trends Plant Sci. **6**, 317–326
28 Haldrup, A., Jensen, P.E., Lunde, C. and Scheller, H.V. (2001) Balance of power: a view of the mechanism of photosynthetic state transitions. Trends Plant Sci. **6**, 301–305
29 Osmond, C.B. and Grace, SC (1995) Perspectives on photoinhibition and photorespiration in the field: quintessential inefficiencies of the light and dark reactions of photosynthesis? J. Exp. Bot. **46**, 1351–1362
30 Niyogi, K.K. (2000) Safety valves for photosynthesis. Curr. Opin. Plant Biol. **3**, 455–460
31 Asada, K. (1999) The water–water cycle in chloroplasts: scavenging of active oxygens and dissipation of excess photons. Annu. Rev. Plant Physiol. Plant Mol. Biol. **50**, 601–639
32 Heber, U. and Walker, D. (1992) Concerning a dual function of coupled cyclic electron-transport in leaves. Plant Physiol. **100**, 1621–1626
33 Frank, H.A., Bautista, J.A., Josue, J.S. and Young, A.J. (2000) Mechanism of nonphotochemical quenching in green plants: energies of the lowest excited singlet states of violaxanthin and zeaxanthin. Biochemistry **39**, 2831–2837
34 Hideg, E. and Schreiber, U. (2007) Parallel assessment of ROS formation and photosynthesis in leaves by fluorescence imaging. Photosynth. Res. **92**, 103–108
35 Buschmann, C., Langsdorf, G. and Lichtenthaler, H.K. (2000) Imaging of the blue, green, and red fluorescence emission of plants: an overview. Photosynthetica **38**, 483–491
36 Briantais, J.-M., Vernotte, C., Picaud, M. and Krause, G.H. (1980) Chlorophyll fluorescence as a probe for the determination of the photoinduced proton gradient in isolated chloroplasts. Biochim. Biophys. Acta **591**, 198–202
37 Niyogi, K.K. (1999) Photoprotection revisited: genetic and molecular approaches. Annu. Rev. Plant Physiol. Plant Mol. Biol. **50**, 333–359
38 Horton, P. (1996) Nonphotochemical quenching of chlorophyll fluorescence. In Light as Energy Source and Information Carrier in Plant Photophysiology (Jennings, R.C., Zucchelli, G., Ghetti, F. and Colombetti, G., eds), pp 99–111, Plenum Press, New York
39 Horton, P., Ruban, A.V. and Walters, R.G. (1996) Regulation of light harvesting in green plants. Annu. Rev. Plant Physiol. Plant Mol. Biol. **47**, 655–684
40 Dall'Osto, L., Caffarri, S. and Bassi, R. (2005) A mechanism of nonphotochemical energy dissipation, independent from Psbs, revealed by a conformational change in the antenna protein CP26. Plant Cell **17**, 1217–1232
41 Rintamaki, E., Salonen, M., Suoranta, U.M., Carlberg, I., Andersson, B. and Aro, E.M. (1997) Phosphorylation of light-harvesting complex II and Photosystem II core proteins shows different irradiance-dependent regulation *in vivo*: application of phosphothreonine antibodies to analysis of thylakoid phosphoproteins. J. Biol. Chem. **272**, 30476–30482
42 Ganeteg, U., Kulheim, C., Andersson, J. and Jansson, S. (2004) Is each light-harvesting complex protein important for plant fitness? Plant Physiol. **134**, 502–509
43 Kulheim, C., Agren, J. and Jansson, S. (2002) Rapid regulation of light harvesting and plant fitness in the field. Science **297**, 91–93
44 Ruban, A.V. and Horton, P. (1995) An investigation of the sustained component of nonphotochemical quenching of chlorophyll fluorescence in isolated chloroplasts and leaves of spinach. Plant Physiol. **108**, 721–726
45 Joliot, P. and Joliot, A. (2002) Cyclic electron transfer in plant leaf. Proc. Natl. Acad. Sci. U.S.A. **99**, 10209–10214
46 Shikanai, T., Endo, T., Hashimoto, T., Yamada, Y., Asada, K. and Yokota, A. (1998) Directed disruption of the tobacco *ndhB* gene impairs cyclic electron flow around Photosystem I. Proc. Natl. Acad. Sci. U.S.A. **95**, 9705–9709
47 Munekage, Y., Hojo, M., Meurer, J., Endo, T., Tasaka, M. and Shikanai, T. (2002) PGR5 is involved in cyclic electron flow around Photosystem I and is essential for photoprotection in *Arabidopsis*. Cell **110**, 361–371
48 DalCorso, G., Pesaresi, P., Masiero, S., Aseeva, E., Nemann, D.S., Finazzi, G., Joliot, P., Barbato, R. and Leister, D. (2008) A complex containing PGRL1 and PGR5 is involved in the switch between linear and cyclic electron flow in *Arabidopsis*. Cell **132**, 273–285
49 Munekage, Y.N., Genty, B. and Peltier, G. (2008) Effect of PGR5 impairment on photosynthesis and growth in *Arabidopsis thaliana*. Plant Cell Physiol. **49**, 1688–1698
50 Li, X.P., Bjorkman, O., Shih, C., Grossman, A.R., Rosenquist, M., Jansson, S. and Niyogi, K.K. (2000) A pigment-binding protein essential for regulation of photosynthetic light harvesting. Nature **403**, 391–395

51 Li, X.P., Gilmore, A.M. and Niyogi, K.K. (2002) Molecular and global time-resolved analysis of a *psbS* gene dosage effect on pH- and xanthophyll cycle-dependent nonphotochemical quenching in Photosystem II. J. Biol. Chem. **277**, 33590–33597
52 Dominici, P., Caffarri, S., Armenante, F., Ceoldo, S., Crimi, M. and Bassi, R. (2002) Biochemical properties of the PsbS subunit of Photosystem II either purified from chloroplast or recombinant. J. Biol. Chem. **277**, 22750–22758
53 Jahns, P., Polle, A. and Junge, W. (1988) The photosynthetic water oxidase: its proton pumping activity is short-circuited within the protein by DCCD. EMBO J. **7**, 589–594
54 Li, X.P., Gilmore, A.M., Caffarri, S., Bassi, R., Golan, T., Kramer, D. and Niyogi, K.K. (2004) Regulation of photosynthetic light harvesting involves intrathylakoid lumen pH sensing by the PsbS protein. J. Biol. Chem. **279**, 22866–22874
55 Niyogi, K.K., Grossman, A.R. and Björkman, O. (1998) *Arabidopsis* mutants define a central role for the xanthophyll cycle in the regulation of photosynthetic energy conversion. Plant Cell **10**, 1121–1134
56 Betterle, N., Ballottari, M., Zorzan, S., de Bianchi, S., Cazzaniga, S., Dall'Osto, L., Morosinotto, T. and Bassi, R. (2009) Light-induced dissociation of an antenna hetero-oligomer is needed for non-photochemical quenching induction. J. Biol. Chem. **284**, 15255–15266
57 Morosinotto, T., Baronio, R. and Bassi, R. (2002) Dynamics of chromophore binding to Lhc proteins *in vivo* and *in vitro* during operation of the xanthophyll cycle. J. Biol. Chem. **277**, 36913–36920
58 Jahns, P., Wehner, A., Paulsen, H. and Hobe, S. (2001) De-epoxidation of violaxanthin after reconstitution into different carotenoid binding sites of light-harvesting complex II. J. Biol. Chem. **276**, 22154–22159
59 Walters, R.G. and Horton, P. (1999) Structural and functional heterogeneity in the major light- harvesting complexes of higher plants. Photosynth. Res. **61**, 77–89
60 Caffarri, S., Croce, R., Breton, J. and Bassi, R. (2001) The major antenna complex of Photosystem II has a xanthophyll binding site not involved in light harvesting. J. Biol. Chem. **276**, 35924–35933
61 Demmig-Adams, B. (1990) Carotenoids and photoprotection in plants: a role for the xanthophyll zeaxanthin. Biochim. Biophys. Acta **1020**, 1–24
62 Johnson, G.N., Young, A.J. and Horton, P. (1994) Activation of non-photochemical quenching in thylakoids and leaves. Planta **194**, 550–556
63 Ahn, T.K., Avenson, T.J., Ballottari, M., Cheng, Y.C., Niyogi, K.K., Bassi, R. and Fleming, G.R. (2008) Architecture of a charge-transfer state regulating light harvesting in a plant antenna protein. Science **320**, 794–797
64 Niyogi, K.K., Shih, C., Soon, C.W., Pogson, B.J., Dellapenna, D. and Bjorkman, O. (2001) Photoprotection in a zeaxanthin- and lutein-deficient double mutant of *Arabidopsis*. Photosynth. Res. **67**, 139–145
65 Pogson, B.J., Niyogi, K.K., Björkman, O. and DellaPenna, D. (1998) Altered xanthophyll compositions adversely affect chlorophyll accumulation and nonphotochemical quenching in *Arabidopsis* mutants. Proc. Natl. Acad. Sci. U.S.A. **95**, 13324–13329
66 Dall'Osto, L., Lico, C., Alric, J., Giuliano, G., Havaux, M. and Bassi, R. (2006) Lutein is needed for efficient chlorophyll triplet quenching in the major LHCII antenna complex of higher plants and effective photoprotection *in vivo* under strong light. BMC Plant Biol. **6**, 32
67 Lokstein, H., Tian, L., Polle, J.E. and DellaPenna, D. (2002) Xanthophyll biosynthetic mutants of *Arabidopsis thaliana*: altered nonphotochemical quenching of chlorophyll fluorescence is due to changes in Photosystem II antenna size and stability. Biochim. Biophys. Acta **1553**, 309–319
68 Kalituho, L., Rech, J. and Jahns, P. (2007) The roles of specific xanthophylls in light utilization. Planta **225**, 423–439
69 Li, Z., Ahn, T.K., Avenson, T.J., Ballottari, M., Cruz, J.A., Kramer, D.M., Bassi, R., Fleming, G.R., Keasling, J.D. and Niyogi, K.K. (2009) Lutein accumulation in the absence of zeaxanthin restores nonphotochemical quenching in the *Arabidopsis thaliana npq1* mutant. Plant Cell **21**, 1798–1812
70 Gilmore, A.M. and Yamamoto, H.Y. (1993) Linear models relating xanthophylls and lumen acidity to non-photochemical fluorescence quenching: evidence that antheraxanthin explains zeaxanthin-independent quenching. Photosynth. Res. **35**, 67–78
71 Rock, C.D. and Zeevaart, J.A. (1991) The *aba* mutant of *Arabidopsis thaliana* is impaired in epoxy-carotenoid biosynthesis. Proc. Natl. Acad. Sci. U.S.A. **88**, 7496–7499
72 Dall'Osto, L., Cazzaniga, S., North, H., Marion-Poll, A. and Bassi, R. (2007) The *Arabidopsis aba4-1* mutant reveals a specific function for neoxanthin in protection against photoxidative stress. Plant Cell **19**, 1048–1064
73 Havaux, M., Dall'Osto, L., Cuine, S., Giuliano, G. and Bassi, R. (2004) The effect of zeaxanthin as the only xanthophyll on the structure and function of the photosynthetic apparatus in *Arabidopsis thaliana*. J. Biol. Chem. **279**, 13878–13888
74 Li, X.P., Muller-Moule, P., Gilmore, A.M. and Niyogi, K.K. (2002) PsbS-dependent enhancement of feedback de-excitation protects Photosystem II from photoinhibition. Proc. Natl. Acad. Sci. U.S.A. **99**, 15222–15227
75 Bonente, G., Howes, B.D., Caffarri, S., Smulevich, G. and Bassi, R. (2008) Interactions between the Photosystem II subunit PsbS and xanthophylls studied *in vivo* and *in vitro*. J. Biol. Chem. **283**, 8434–8445
76 Funk, C., Schröder, W.P., Napiwotzki, A., Tjus, S.E., Renger, G. and Andersson, B. (1995) The PSII-S protein of higher plants: a new type of pigment-binding protein. Biochemistry **34**, 11133–11141
77 Aspinall-O'Dea, M., Wentworth, M., Pascal, A., Robert, B., Ruban, A.V. and Horton, P. (2002) *In vitro* reconstitution of the activated zeaxanthin state associated with energy dissipation in plants. Proc. Natl. Acad. Sci. U.S.A. **99**, 16331–16335
78 Havaux, M., Dall'Osto, L. and Bassi, R. (2007) Zeaxanthin has enhanced antioxidant capacity with respect to all other xanthophylls in *Arabidopsis* leaves and functions independent of binding to PSII antennae. Plant Physiol. **145**, 1506–1520
79 Finazzi, G., Johnson, G.N., Dall'Osto, L., Joliot, P., Wollman, F.A. and Bassi, R. (2004) A zeaxanthin-independent nonphotochemical quenching mechanism localized in the Photosystem II core complex. Proc. Natl. Acad. Sci. U.S.A. **101**, 12375–12380
80 Croce, R., Weiss, S. and Bassi, R. (1999) Carotenoid-binding sites of the major light-harvesting complex II of higher plants. J. Biol. Chem. **274**, 29613–29623
81 Liu, Z., Yan, H., Wang, K., Kuang, T., Zhang, J., Gui, L., An, X. and Chang, W. (2004) Crystal structure of spinach major light-harvesting complex at 2.72 Å resolution. Nature **428**, 287–292
82 Bassi, R. and Dainese, P. (1992) A supramolecular light-harvesting complex from chloroplast Photosystem-II membranes. Eur. J. Biochem. **204**, 317–326
83 Croce, R., Cinque, G., Holzwarth, A.R. and Bassi, R. (2000) The Soret absorption properties of carotenoids and chlorophylls in antenna complexes of higher plants. Photosynth. Res. **64**, 221–231
84 Jahns, P., Latowski, D. and Strzalka, K. (2009) Mechanism and regulation of the violaxanthin cycle: the role of antenna proteins and membrane lipids. Biochim. Biophys. Acta **1787**, 3–14
85 Morosinotto, T., Caffarri, S., Dall'Osto, L. and Bassi, R. (2003) Mechanistic aspects of the xanthophyll dynamics in higher plant thylakoids. Physiol. Plant. **119**, 347–354
86 Wehner, A., Storf, S., Jahns, P. and Schmid, V.H. (2004) De-epoxidation of violaxanthin in light-harvesting complex I proteins. J. Biol. Chem. **279**, 26823–26829
87 Moya, I., Silvestri, M., Vallon, O., Cinque, G. and Bassi, R. (2001) Time-resolved fluorescence analysis of the Photosystem II antenna proteins in detergent micelles and liposomes. Biochemistry **40**, 12552–12561
88 Gastaldelli, M., Canino, G., Croce, R. and Bassi, R. (2003) Xanthophyll binding sites of the CP29 (Lhcb4) subunit of higher plant Photosystem II investigated by domain swapping and mutation analysis. J. Biol. Chem. **278**, 19190–19198
89 Croce, R., Canino, G., Ros, F. and Bassi, R. (2002) Chromophore organization in the higher-plant Photosystem II antenna protein CP26. Biochemistry **41**, 7334–7343

90 Johnson, M.P., Perez-Bueno, M.L., Zia, A., Horton, P. and Ruban, A.V. (2009) The zeaxanthin-independent and zeaxanthin-dependent qE components of nonphotochemical quenching involve common conformational changes within the Photosystem II antenna in *Arabidopsis*. Plant Physiol. **149**, 1061–1075
91 Andersson, J., Wentworth, M., Walters, R.G., Howard, C.A., Ruban, A.V., Horton, P. and Jansson, S. (2003) Absence of the Lhcb1 and Lhcb2 proteins of the light-harvesting complex of Photosystem II: effects on photosynthesis, grana stacking and fitness. Plant J. **35**, 350–361
92 Damkjaer, J.T., Kereiche, S., Johnson, M.P., Kovacs, L., Kiss, A.Z., Boekema, E.J., Ruban, A.V., Horton, P. and Jansson, S. (2009) The Photosystem II light-harvesting protein Lhcb3 affects the macrostructure of Photosystem II and the rate of state transitions in *Arabidopsis*. Plant Cell **21**, 3245–3256
93 Andersson, J., Walters, R.G., Horton, P. and Jansson, S. (2001) Antisense inhibition of the photosynthetic antenna proteins CP29 and CP26: implications for the mechanism of protective energy dissipation. Plant Cell **13**, 1193–1204
94 de Bianchi, S., Dall'Osto, L., Tognon, G., Morosinotto, T. and Bassi, R. (2008) Minor antenna proteins CP24 and CP26 affect the interactions between Photosystem II subunits and the electron transport rate in grana membranes of *Arabidopsis*. Plant Cell **20**, 1012–1028
95 Kovacs, L., Damkjaer, J., Kereiche, S., Ilioaia, C., Ruban, A.V., Boekema, E.J., Jansson, S. and Horton, P. (2006) Lack of the light-harvesting complex CP24 affects the structure and function of the grana membranes of higher plant chloroplasts. Plant Cell **18**, 3106–3120
96 Berera, R., van Stokkum, I.H., Kodis, G., Keirstead, A.E., Pillai, S., Herrero, C., Palacios, R.E., Vengris, M., van Grondelle, R., Gust, D. et al. (2007) Energy transfer, excited-state deactivation, and exciplex formation in artificial caroteno-phthalocyanine light-harvesting antennas. J. Phys. Chem. B **111**, 6868–6877
97 Pascal, A.A., Liu, Z., Broess, K., van Oort, B., Van Amerongen, H., Wang, C., Horton, P., Robert, B., Chang, W. and Ruban, A. (2005) Molecular basis of photoprotection and control of photosynthetic light-harvesting. Nature **436**, 134–137
98 Ruban, A.V., Berera, R., Ilioaia, C., van Stokkum, I.H., Kennis, J.T., Pascal, A.A., Van Amerongen, H., Robert, B., Horton, P. and van Grondelle, R. (2007) Identification of a mechanism of photoprotective energy dissipation in higher plants. Nature **450**, 575–578
99 Holt, N.E., Zigmantas, D., Valkunas, L., Li, X.P., Niyogi, K.K. and Fleming, G.R. (2005) Carotenoid cation formation and the regulation of photosynthetic light harvesting. Science **307**, 433–436
100 Avenson, T.J., Ahn, T.K., Zigmantas, D., Niyogi, K.K., Li, Z., Ballottari, M., Bassi, R. and Fleming, G.R. (2008) Zeaxanthin radical cation formation in minor light-harvesting complexes of higher plant antenna. J. Biol. Chem. **283**, 3550–3558
101 Barros, T. and Kuhlbrandt, W. (2009) Crystallisation, structure and function of plant light-harvesting complex II. Biochim. Biophys. Acta **1787**, 753–772
102 Barros, T., Royant, A., Standfuss, J., Dreuw, A. and Kuhlbrandt, W. (2009) Crystal structure of plant light-harvesting complex shows the active, energy-transmitting state. EMBO J. **28**, 298–306
103 Horton, P., Ruban, A.V., Rees, D., Pascal, A.A., Noctor, G. and Young, A.J. (1991) Control of the light-harvesting function of chloroplast membranes by aggregation of the LHCII chlorophyll–protein complex. FEBS Lett. **292**, 1–4
104 Ruban, A.V., Young, A.J. and Horton, P. (1996) Dynamic properties of the minor chlorophyll *a*/*b* binding proteins of Photosystem II, an *in vitro* model for photoprotective energy dissipation in the photosynthetic membrane of green plants. Biochemistry **35**, 674–678
105 Horton, P., Ruban, A.V. and Wentworth, M. (2000) Allosteric regulation of the light-harvesting system of Photosystem II. Philos. Trans. R. Soc. London Ser. B **355**, 1361–1370
106 Berera, R., Herrero, C., van Stokkum, L.H.M., Vengris, M., Kodis, G., Palacios, R.E., van Amerongen, H., van Grondelle, R., Gust, D., Moore, T.A. et al. (2006) A simple artificial light-harvesting dyad as a model for excess energy dissipation in oxygenic photosynthesis. Proc. Natl. Acad. Sci. U.S.A. **103**, 5343–5348
107 van Stokkum, I.H.M., Larsen, D.S. and van Grondelle, R. (2004) Global and target analysis of time-resolved spectra. Biochim. Biophys. Acta **1657**, 82–104
108 Miloslavina, Y., Wehner, A., Lambrev, P.H., Wientjes, E., Reus, M., Garab, G., Croce, R. and Holzwarth, A.R. (2008) Far-red fluorescence: a direct spectroscopic marker for LHCII oligomer formation in non-photochemical quenching. FEBS Lett. **582**, 3625–3631
109 Horton, P. and Ruban, A. (2005) Molecular design of the Photosystem II light-harvesting antenna: photosynthesis and photoprotection. J. Exp. Bot. **56**, 365–373
110 Ilioaia, C., Johnson, M.P., Horton, P. and Ruban, A.V. (2008) Induction of efficient energy dissipation in the isolated light-harvesting complex of Photosystem II in the absence of protein aggregation. J. Biol. Chem. **283**, 29505–29512
111 Bode, S., Quentmeier, C.C., Liao, P.N., Hafi, N., Barros, T., Wilk, L., Bittner, F. and Walla, P.J. (2009) On the regulation of photosynthesis by excitonic interactions between carotenoids and chlorophylls. Proc. Natl. Acad. Sci. U.S.A. **106**, 12311–12316
112 Mozzo, M., Passarini, F., Bassi, R., van Amerongen, H. and Croce, R. (2008) Photoprotection in higher plants: the putative quenching site is conserved in all outer light-harvesting complexes of Photosystem II. Biochim. Biophys. Acta **1777**, 1263–1267
113 Schiffer, R., Neis, M., Holler, D., Rodriguez, F., Geier, A., Gartung, C., Lammert, F., Dreuw, A., Zwadlo-Klarwasser, G., Merk, H. et al. (2003) Active influx transport is mediated by members of the organic anion transporting polypeptide family in human epidermal keratinocytes. J. Invest. Dermatol. **120**, 285–291
114 Amarie, S., Standfuss, J., Barros, T., Kuhlbrandt, W., Dreuw, A. and Wachtveitl, J. (2007) Carotenoid radical cations as a probe for the molecular mechanism of nonphotochemical quenching in oxygenic photosynthesis. J. Phys. Chem. B **111**, 3481–3487
115 Avenson, T.J., Ahn, T.K., Niyogi, K.K., Ballottari, M., Bassi, R. and Fleming, G.R. (2009) Lutein can act as a switchable charge transfer quencher in the CP26 light-harvesting complex. J. Biol. Chem. **284**, 2830–2835
116 Amarie, S., Wilk, L., Barros, T., Kuhlbrandt, W., Dreuw, A. and Wachtveitl, J. (2009) Properties of zeaxanthin and its radical cation bound to the minor light-harvesting complexes CP24, CP26 and CP29. Biochim. Biophys. Acta **1787**, 747–752
117 Teardo, E., De Laureto, P.P., Bergantino, E., Dalla, V.F., Rigoni, F., Szabo, I. and Giacometti, G.M. (2007) Evidences for interaction of PsbS with photosynthetic complexes in maize thylakoids. Biochim. Biophys. Acta **1767**, 703–711
118 Arnoux, P., Morosinotto, T., Saga, G., Bassi, R. and Pignol, D. (2009) A structural basis for the pH-dependent xanthophyll cycle in *Arabidopsis thaliana*. Plant Cell **21**, 2036–2044
119 Yamamoto, H.Y., Chang, J.L. and Aihara, M.S. (1967) Light-induced interconversion of violaxanthin and zeaxanthin in New Zealand spinach-leaf segments. Biochim. Biophys. Acta **141**, 342–347
120 Ruban, A.V., Pascal, A.A. and Robert, B. (2000) Xanthophylls of the major photosynthetic light-harvesting complex of plants: identification, conformation and dynamics. FEBS Lett. **477**, 181–185
121 Cheng, Y.C., Ahn, T.K., Avenson, T.J., Zigmantas, D., Niyogi, K.K., Ballottari, M., Bassi, R. and Fleming, G.R. (2008) Kinetic modeling of charge-transfer quenching in the CP29 minor complex. J. Phys. Chem. B **112**, 13418–13423
122 Kiss, A.Z., Ruban, A.V. and Horton, P. (2008) The PsbS protein controls the organization of the Photosystem II antenna in higher plant thylakoid membranes. J. Biol. Chem. **283**, 3972–3978
123 Bergantino, E., Segalla, A., Brunetta, A., Teardo, E., Rigoni, F., Giacometti, G.M. and Szabo, I. (2003) Light- and pH-dependent structural changes in the PsbS subunit of Photosystem II. Proc. Natl. Acad. Sci. U.S.A. **100**, 15265–15270

Received 10 December 2009
doi:10.1042/BST038xxxx

# Section A

# Mutants of monomeric Lhcb proteins and photoprotection: insight on the role of monomeric subunits in thermal energy dissipation

## A.1 Minor Antenna Proteins CP24 and CP26 Affect the Interactions between Photosystem II Subunits and the Electron Transport Rate in Grana Membranes of *Arabidopsis*

S. de Bianchi, L. Dall'Osto, G. Tognon, T. Morosinotto, and R. Bassi.

This is the first article written during my phD and it deals with the characterization of the first mutants that I isolated during my work. In the experiments' design I received important suggestions from prof. Bassi and dr Dall'Osto as also in the setting up of the experiments. The electron microscopy images were done in the university of Padua by dr. Morosinotto and Mr Tognon, but the results were analyzed and interpreted in Verona.

This article is a *Plant Cell* Advance Online Publication. The date of its first appearance online is the official date of publication. The article has been edited and the authors have corrected proofs, but minor changes could be made before the final version is published. Posting this version online reduces the time to publication by several weeks.

# Minor Antenna Proteins CP24 and CP26 Affect the Interactions between Photosystem II Subunits and the Electron Transport Rate in Grana Membranes of *Arabidopsis* [W]

**Silvia de Bianchi,[a,1] Luca Dall'Osto,[a,1] Giuseppe Tognon,[b] Tomas Morosinotto,[b] and Roberto Bassi[a,2]**

[a] Dipartimento Scientifico e Tecnologico, Università di Verona, I-37134 Verona, Italy
[b] Dipartimento di Biologia, Università di Padova, 35131 Padova, Italy

**We investigated the function of chlorophyll *a/b* binding antenna proteins Chlorophyll Protein 26 (CP26) and CP24 in light harvesting and regulation of photosynthesis by isolating *Arabidopsis thaliana* knockout lines that completely lacked one or both of these proteins. All three mutant lines had a decreased efficiency of energy transfer from trimeric light-harvesting complex II (LHCII) to the reaction center of photosystem II (PSII) due to the physical disconnection of LHCII from PSII and formation of PSII reaction center depleted domains in grana partitions. Photosynthesis was affected in plants lacking CP24 but not in plants lacking CP26: the former mutant had decreased electron transport rates, a lower ΔpH gradient across the grana membranes, reduced capacity for nonphotochemical quenching, and limited growth. Furthermore, the PSII particles of these plants were organized in unusual two-dimensional arrays in the grana membranes. Surprisingly, overall electron transport, nonphotochemical quenching, and growth of the double mutant were restored to wild type. Fluorescence induction kinetics and electron transport measurements at selected steps of the photosynthetic chain suggested that limitation in electron transport was due to restricted electron transport between $Q_A$ and $Q_B$, which retards plastoquinone diffusion. We conclude that CP24 absence alters PSII organization and consequently limits plastoquinone diffusion.**

## INTRODUCTION

In plants, photosynthetic reaction centers (RCs) exploit solar energy to drive electrons from water to $NADP^+$. This transport is coupled to $H^+$ transfer from the chloroplast stroma to the thylakoid lumen, which builds a proton gradient for ATP synthesis. The capacity of light absorption is increased by the pigment binding proteins composing the antenna system. In higher plants, the antenna system surrounding the plastid-encoded photosystem II (PSII) core is composed of the nuclear-encoded chlorophyll *a/b* binding light-harvesting complexes (Lhc). LHCII is the major component of the outer antenna and comprises different heterotrimers of *LHCB1*, *LHCB2*, and *LHCB3* gene products, while minor antenna complexes (Chlorophyll Protein 29 [CP29], CP26, and CP24) are encoded by *LHCB4*, *LHCB5*, and *LHCB6* genes, respectively, and are found as monomers (Bassi et al., 1996; Jansson, 1999). Structural analysis of PSII and Lhcb supercomplex organization within grana membranes has revealed that minor complexes CP26 and CP29 are located in between the core complex and the trimeric LHCII (Harrer et al., 1998; Boekema et al., 1999). Additional LHCII trimers, depending on growth light intensity (Dekker and Boekema, 2005; Morosinotto et al., 2006; Ballottari et al., 2007), complete the PSII structure and require CP24 for connection to PSII core by forming a complex with CP29 (Bassi and Dainese, 1992; Yakushevska et al., 2003; Dekker and Boekema, 2005). Similarly, PSI has four Lhca antenna proteins, yielding a total of 10 distinct Lhc isoforms in higher plants (Jansson, 1999). These gene products have been conserved during at least 350 million years of evolution, strongly indicating that each pigment-protein complex has a specific function in the highly variable conditions of the natural subaerial environment (Durnford, 2003; Ganeteg et al., 2004).

Rapid changes in light intensity, temperature, and water availability easily lead to overexcitation of photosystems when the absorbed light exceeds the capacity to use reducing equivalents. Incomplete photochemical quenching leads to an increased chlorophyll excited state ($^1$Chl*) lifetime and increased probability of chlorophyll *a* triplet formation ($^3$Chl*) by intersystem crossing. Chlorophyll triplets react with oxygen ($^3O_2$) and form harmful reactive oxygen species responsible for photoinhibition and oxidative stress (Barber and Andersson, 1992). These harmful events are counteracted by photoprotection mechanisms that either scavenge the reactive oxygen species produced (Asada, 1999) or prevent their production through deexcitation of excessive $^1$Chl* (Niyogi, 2000). This latter process is known as nonphotochemical quenching (NPQ) since it is observed as light-dependent quenching of Chl fluorescence. The largest NPQ component is rapidly reversible and dependent on the formation of a low thylakoid lumen pH and is thus defined as energy quenching (qE; Briantais et al., 1980; Niyogi, 1999).

The qE developing within the first minute after overexcitation is largely zeaxanthin (Zea) independent and is followed by a slower

[1] These authors contributed equally to this work.
[2] Address correspondence to bassi@sci.univr.it.
The author responsible for distribution of materials integral to the findings presented in this article in accordance with the policy described in the Instructions for Authors (www.plantcell.org) is: Roberto Bassi (bassi@sci.univr.it).
[W] Online version contains Web-only data.
www.plantcell.org/cgi/doi/10.1105/tpc.107.055749

component that depends on Zea synthesis (Horton et al., 1996), which is promoted by acidic pH in the lumen through the activation of violaxanthin deepoxidase. Zea is rapidly produced under conditions of high light intensity and is bound to Lhc proteins, mainly to CP24 and CP26 (Morosinotto et al., 2002), where it displaces violaxanthin (Viola) and induces conformational changes that result in a quenched state (Crimi et al., 2001). This event is coupled to the rise of a slower component of the NPQ process and to a sustained dissipation of light energy known as qI (Dall'Osto et al., 2005). Besides violaxanthin deepoxidase activation, low lumenal pH exerts control over the thylakoid membrane by reversibly protonating exposed acidic residues, as suggested by the inhibition of NPQ by dicyclohexylcarbodiimide (DCCD), a reagent that modifies acidic residues that undergo reversible protonation (Ruban et al., 1992). Whereas $^{14}C$ DCCD binding antenna proteins CP26 and CP29 are located between the inner antenna and the LHCII (Walters et al., 1996, Pesaresi et al., 1997), the site of DCCD inhibition of qE is located in PsbS (Li et al., 2004), an Lhc-like protein (Li et al., 2000) that likely does not bind pigments (Sundaresan et al., 1995; Dominici et al., 2002) but exerts its function by interacting with Lhc proteins (Bonente et al., 2007; Teardo et al., 2007).

Consistently, antenna proteins are needed for full expression of NPQ (Briantais, 1994). Functional dissection of individual Lhc isoforms has been undertaken using antisense and knockout approaches. Antisense inhibition of CP29, CP26 (Andersson et al., 2001), and Lhcb1+Lhcb2 (Andersson et al., 2003) expression did not disrupt NPQ, while deletion of the *Lhcb6* gene encoding CP24 did reduce this function (Kovacs et al., 2006). We have isolated and characterized CP24 and CP26 knockout (koCP24 and koCP26) plants and confirmed the phenotype described in previous work for koCP24. Surprisingly, the limitation in NPQ and growth rate of koCP24 was reversed in the double koCP24/26 mutant, suggesting that the koCP24 phenotype was not due to specific properties of CP24 but rather to an effect on the organization of photosynthetic complexes within grana partitions, which affected electron transport rate (ETR) and proton pumping into the thylakoid lumen.

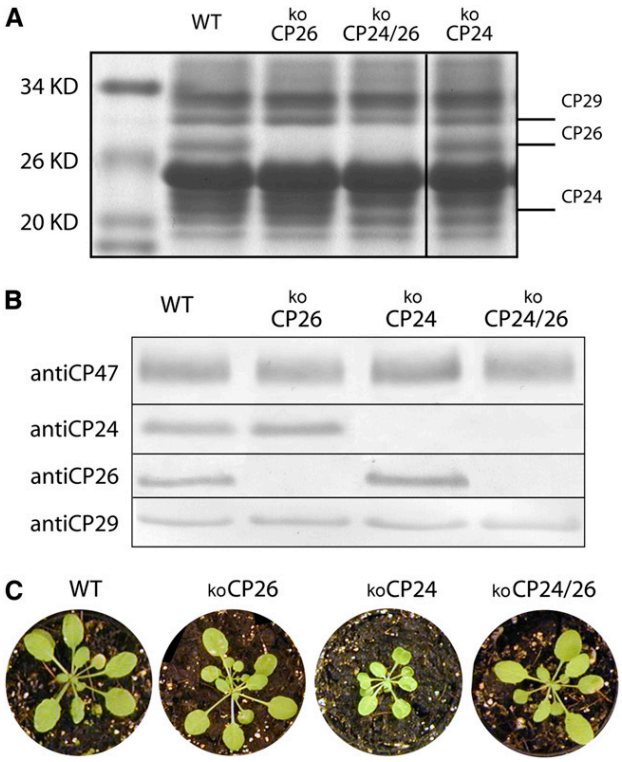


**Figure 1.** Polypeptide Composition of Thylakoid Membranes from Wild-Type and Knockout Mutants.

**(A)** SDS/PAGE analysis of wild-type and mutants thylakoid proteins. Selected apoprotein bands are marked. Fifteen micrograms of chlorophylls were loaded in each lane.
**(B)** Immunoblot analysis of thylakoid membranes with antibodies directed against minor antenna proteins CP29, CP26, and CP24 and against the PSII core subunit CP47.
**(C)** Phenotype of wild-type and mutant plants grown in control conditions for 3 weeks (100 μmol photons $m^{-2}$ $s^{-1}$, 25°C, 8/16 h day/night).

## RESULTS

We identified *kolhcb6* and *kolhcb5* homozygous lines in seed pools obtained from the Nottingham Arabidopsis Stock Centre (NASC) by immunoblot analysis using specific antibodies raised against CP26 and CP24 antenna proteins (Di Paolo et al., 1990). Similarly, the *kolhcb5 kolhcb6* double mutant was obtained by selection of the progeny of single mutant crossings. Thylakoid membranes from kolhcb5, kolhcb6, and kolhcb5 kolhcb6 were depleted in the corresponding gene products (Figures 1A and 1B). We will henceforth refer to these genotypes as koCP26 (kolhcb5), koCP24 (kolhcb6), and koCP24/26 (kolhcb5 kolhcb6). Single knockouts did not differ in chlorophyll content per leaf area compared with wild-type plants in regular lighting, but koCP24/26 showed a small decrease in chlorophyll content (Table 1). Pigment composition was similar in all dark-adapted plants. Nevertheless, when plants were exposed to high light intensity for 30 min to induce Zea synthesis, deepoxidation was significantly lower in koCP24 than in wild-type, koCP26, and koCP24/26 plants (Table 1). When grown in control conditions (100 μmol photons $m^{-2}$ $s^{-1}$, 24°C, 8/16 day/night) for 3 weeks, koCP26 plants did not show significant reduction in growth with respect to the wild type, while koCP24 plants were much smaller than wild-type plants (Figure 1C). Surprisingly, koCP24/26 plants were less affected in their growth than koCP24 plants and appeared more similar to the wild type.

### Chloroplast Organization

Chloroplast structure was analyzed by transmission electron microscopy on leaf samples harvested at the middle of the light period (Figure 2). Under these growth conditions, wild-type chloroplasts showed a characteristic organization of stroma membranes, interconnecting grana stacks, and large starch granules in most sections. koCP24 plants differed in that a large number of their stroma membranes had blunt ends not engaged in grana stacks and they completely lacked starch granules. koCP26 chloroplasts, on the other hand, had starch granules and

**Table 1.** Photosynthetic Pigment Content of the Wild Type and Mutants

| | | Wild Type | koCP24 | koCP26 | koCP24/26 |
|---|---|---|---|---|---|
| | Chlorophyll (mg $cm^{-2}$) | 16.8 ± 1.0 | 16.4 ± 0.6 | 15.9 ± 1.7 | 14.3 ± 0.8* |
| | Chlorophyll *a*/*b* | 3.04 ± 0.06 | 3.20 ± 0.10 | 3.06 ± 0.10 | 2.96 ± 0.09 |
| | Chlorophyll/Carotenoid | 3.29 ± 0.04 | 3.23 ± 0.05 | 3.19 ± 0.13 | 3.18 ± 0.16 |
| Dark-Adapted Leaves | Neo | 4.7 ± 0.2 | 4.9 ± 0.1 | 4.8 ± 0.1 | 5.1 ± 0.2 |
| | Viola | 3.9 ± 0.9 | 4.1 ± 0.2 | 3.6 ± 0.1 | 4.0 ± 0.1 |
| | Anthera | – | – | – | – |
| | Lute | 14.5 ± 0.5 | 14.4 ± 0.3 | 15.4 ± 0.4 | 15.7 ± 1.0 |
| | β-Carotenoid | 7.1 ± 0.1 | 7.3 ± 0.1 | 7.2 ± 0.1 | 6.3 ± 0.5 |
| Light-Treated Leaves | Viola | 1.4 ± 0.1 | 2.1 ± 0.5 | 1.3 ± 0.1 | 1.4 ± 0.1 |
| | Anthera | 1.0 ± 0.1 | 1.3 ± 0.1 | 0.8 ± 0.1 | 1.2 ± 0.1 |
| | Zea | 1.2 ± 0.1 | 0.7 ± 0.2* | 1.3 ± 0.1 | 0.9 ± 0.1 |
| | (Z + 0.5A)/(V + A + Z) | 0.47 ± 0.04 | 0.32 ± 0.08* | 0.51 ± 0.06 | 0.42 ± 0.05 |

Pigment content is expressed as mol/100 mol chlorophylls. Viola, antheraxanthin, and Zea content was determined after leaves were illuminated for 30 min at 1000 μmol $m^{-2}$ $s^{-1}$. The (Z+1/2A)/(Z+A+V) ratio quantifies the operation of the xanthophyll cycle. Data are mean values of four experiments. Significantly different values with respect to the wild type are marked with an asterisk ($P > 0.05$).

a thylakoid organization similar to the wild type. Chloroplasts from the double mutant koCP24/26 accumulated starch granules normally but had a higher ratio of stroma membranes to grana stacks than wild-type chloroplasts and their grana membranes had fewer partitions.

### Organization and Stoichiometry of Chlorophyll Proteins

The organization of pigment-protein complexes was analyzed by nondenaturing Deriphat-PAGE. In agreement with a previous report (Havaux et al., 2004), seven major green bands were resolved upon solubilization of thylakoid membranes with 0.8% dodecyl-α-D-maltoside (α-DM) (Figure 3). The uppermost band (band 7) contained the supramolecular PSI-LHCI complex. PSII-LHCII dissociated into its components, namely, the PSII core dimer and monomer (bands 6 and 5, respectively) and antenna moieties, including the CP29-CP24-$(LHCII)_3$ supercomplex (band 4; Bassi and Dainese, 1992), LHCII trimer (band 3), and monomeric Lhcbs (band 2). Band 1 was composed of free pigments that dissociated during solubilization. A faint band was

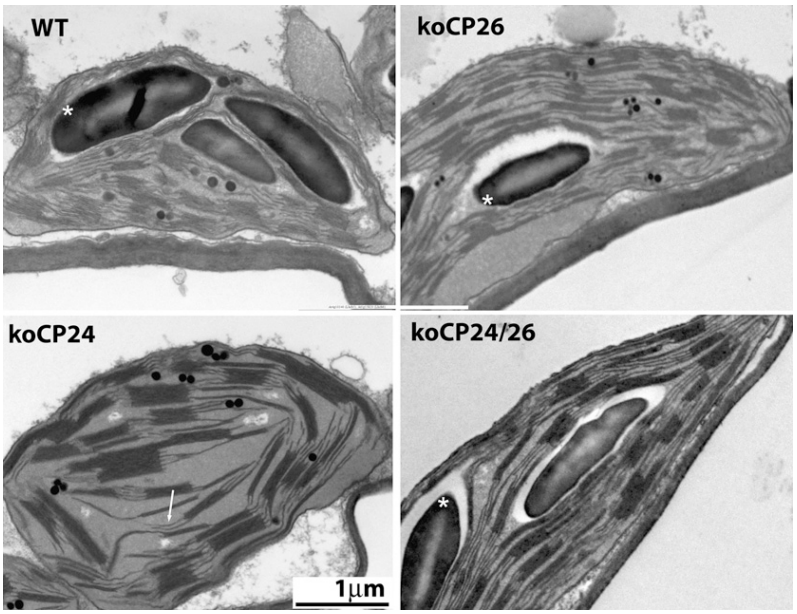


**Figure 2.** Transmission Electron Micrographs of Plastids from Mesophyll Cells of the Wild Type and Mutants.

Leaf samples were harvested at the midpoint of the light period from plants grown in short-day conditions (100 μmol photons $m^{-2}$ $s^{-1}$, 25°C, 8/16 h day/night). Starch granules (marked with asterisks) can be distinguished from plastoglobules (small black dots). Stroma membranes with blunt ends not engaged in grana stacks in koCP24 chloroplasts are indicated by an arrow.

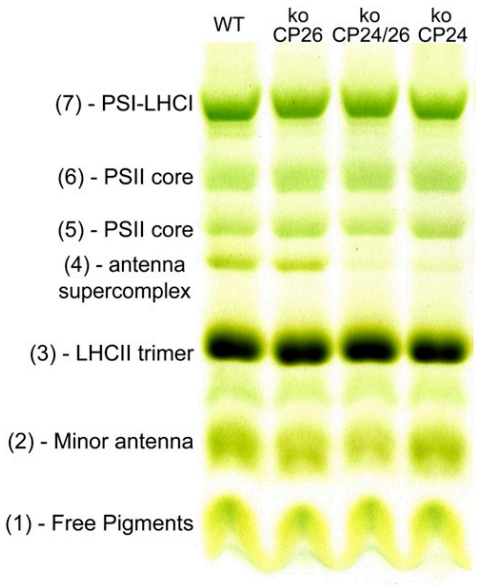


**Figure 3.** Analysis of Pigment-Protein Complexes of the Wild Type and Mutant.

Thylakoid pigmented complexes were separated by nondenaturing Deriphat-PAGE.

also detected between bands 2 and 3, containing the PSII core subunit CP43. Chlorophyll distribution between pigment proteins was not strongly modified in mutant thylakoids compared with the wild type. The major difference was that koCP24 and koCP24/26 had reduced levels of band 4. Also, the relative amount of band 2 was affected, being lowest in the double mutant and highest in the wild type. The ratio between monomeric and dimeric PSII core complexes was constant in all plants tested. Densitometric analysis of the green gels allowed evaluation of the total chlorophyll associated with PSI-LHCI (band 7) versus PSII + Lhcb components (bands 2 to 6). koCP24 showed a slightly higher PSII-core/Lhcb ratio (0.26) and a lower PSI-LHCI/PSII-Lhcb ratio (koCP24 = 1.26) than the wild type (0.22 and 1.84, respectively). koCP26 did not show significant differences with respect to the wild type, while the koCP24/26 had a higher PSII/Lhcb ratio (0.28).

We then verified alterations in Lhc stoichiometry in thylakoids extracted from the different mutants (Figure 4) by quantitative immunoblot analysis using CP47 as an internal standard (Ballottari et al., 2007). In koCP24, besides the complete lack of CP24, the LHCII component Lhcb3 was also strongly decreased, while CP29 and CP26 were increased with respect to the wild type. We also detected a very small increase in Lhcb1 and Lhcb2 but below statistical significance. In koCP26, the only clear difference was the increase in CP29 and in CP24 content, while the remaining Lhcb proteins did not change within the error of the determination. The double mutant koCP24/26 showed a strong decrease in Lhcb3 and, to a lesser extent, of CP29 while Lhcb1 was increased by 60%. Lhcb2 was also increased, although to a lower extent. Remarkably, PsbS subunit content did not show significant differences between all genotypes (Figure 4).

### Photosynthetic Functions: NPQ of Chlorophyll Fluorescence

Since antenna polypeptides have been implicated in energy dissipation (Walters et al., 1996), we evaluated the capacity of different mutants to activate the NPQ (Figure 5). Wild-type and koCP26 plants grown in control conditions had a NPQ of 2.7 after 8 min of illumination at 1200 μmol photons $m^{-2}$ $s^{-1}$, consistent with literature data (Niyogi, 1999). In the same conditions, the NPQ of koCP24 was clearly different: similar to the wild type, it showed a rapid rise to a value of 1.0 in the first minute of illumination at 1200 μmol photons $m^{-2}$ $s^{-1}$ but then reached a plateau that lasted for the remaining 7 min of illumination. The double koCP24/26 mutant also showed a fast rise to a value of 1.0; however, a delay of 1.5 to 2 min was then evident before resuming rise and reaching, after 8 min of illumination, an NPQ value similar to the wild type. The dark recovery of fluorescence was clearly different, with the wild type retaining a quenching level (qI) of 0.65, while koCP26 and koCP24/26 further released quenching to 0.4 and koCP24 to 0.18. Thus, koCP24/26 showed the most complete relaxation of quenching.

### Determination of Light-Induced Proton Gradient by 9-Aminoacridine Quenching

NPQ amplitude has been reported to be dependent on the concentration of PsbS (Li et al., 2002a) and on the lumenal pH

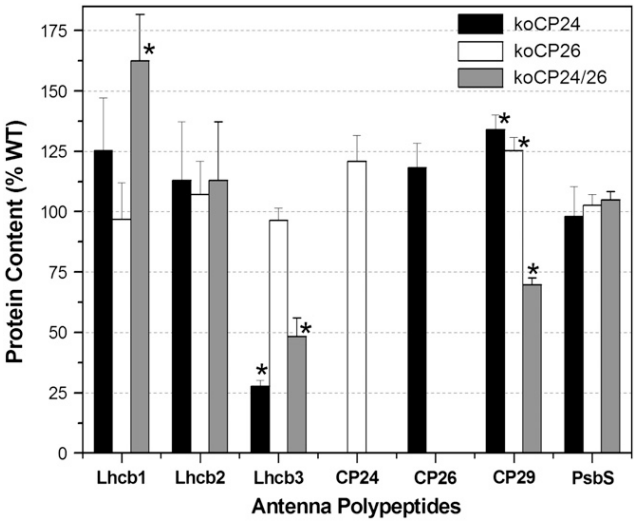


**Figure 4.** Immunological Quantification of Lhc Proteins in Thylakoid Membranes of Wild-Type and Mutant Plants.

Lhc proteins of purified thylakoid membranes were immunodetected with specific antibodies. The mean optical density of bands developed in four lanes (loaded with 1.0, 0.75, 0.50, and 0.25 μg of chlorophyll, respectively) was plotted against amount of chlorophyll loaded to assess the linearity of response and compared with the optical density of reaction bands of an antibody directed to the PSII core subunit CP47. Total amount of each subunit is expressed as a percentage of the corresponding wild-type content. Data are expressed as means ± SD ($n = 4$). Significantly different values from wild-type membranes are marked with an asterisk (according to Student's $t$ test, $P < 0.05$).

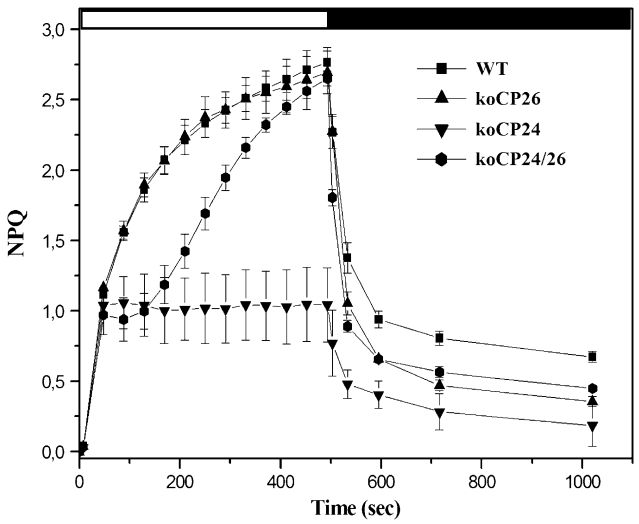


**Figure 5.** NPQ Analysis of Wild-Type and Mutant Genotypes.

Kinetics of NPQ induction and relaxation were recorded with a pulse-amplitude modulated fluorometer. Chlorophyll fluorescence was measured in intact, dark-adapted leaves, during 8 min of illumination at 1260 μmol $m^{-2}$ $s^{-1}$ followed by 9 min of dark relaxation. All NPQ values of mutant plants after 530 s (dark recovery) are significantly lower than the corresponding wild-type values (means ± SD, $n = 4$, Student's $t$ test, $P < 0.05$).

(Horton et al., 1996). Since PsbS content was the same in all genotypes analyzed (Figure 4), we determined the capacity of intact chloroplasts to produce changes in thylakoid pH by following the light-induced quenching of 9-aminoacridine (9-AA) in the presence of methylviologen as the final electron acceptor (Johnson et al., 1994). The only genotype significantly affected in proton pumping into the chloroplast lumen in these conditions was koCP24 (Figure 6A), while the others performed similar to the wild type. Differences between the wild type and koCP24 were confirmed over a wide range of light intensities (Figure 6C). This is consistent with the hypothesis that the limitation in NPQ described above for koCP24 is (at least in part) associated with a reduced acidification of the lumen upon illumination.

Viola deepoxidation is also dependent on low lumenal pH, and it has been reported to be slower in the *pgr1* mutant, which has a reduced proton gradient (Munekage et al., 2001). Deepoxidation rate was slower in koCP24 than in either wild-type or koCP24/26 plants (Figures 6B and 6D), thus providing an independent confirmation that pH generation is affected in the CP24-less genotype. Measurement of NPQ in the isolated chloroplast preparation used for 9-AA quenching yielded similar qE amplitudes in the wild type, koCP26, and koCP24/26 but was two times lower in koCP24, implying that the relation between NPQ and ΔpH was conserved in the conditions used for transmembrane gradient determination (see Supplemental Table 1 online).

## ETR

Differences in transmembrane gradient could be due to changes in electron transport (ET) capacity. To test this hypothesis, ET rate was evaluated in vivo on plants grown in control light conditions by fluorescence analysis at different light intensities under saturating $CO_2$ conditions (1%) (Figure 7). In the wild type, the light-dependent increase in ET approached saturation at 650 μmol photons $m^{-2}$ $s^{-1}$, and after this value no further increase was observed. koCP24 showed significantly lower rates of ETR, also at very low light intensities. By contrast, koCP24/26 and koCP26 plants showed ETR behavior not significantly different with respect to the wild type.

## Fluorescence Transient Analysis

To determine if the mutations affected the capacity of the antenna system to transfer absorbed energy to reaction centers, we measured the functional antenna size of PSII by estimating the rise time of florescence in the presence of 3-(3,4-dichlorophenyl)-1,1-dimethylurea (DCMU). No significant differences were observed between the different genotypes considered in this study (Table 2), suggesting that the light-harvesting capacity is not affected despite the depletion in some antenna subunits.

Further insights into the light-harvesting and ET activity were obtained by analyzing the fluorescence induction in dark-adapted leaves. We determined $F_0$ (a parameter inversely related to the efficiency of energy transfer from antenna pigments to open PSII reaction centers), $F_v/F_m$ (an estimate of the maximum quantum efficiency of PSII photochemistry [Butler and Strasser, 1978]), $t_m$ (the time to reach the maximal fluorescence), and area (the area above the fluorescence transient). The former two parameters ($F_0$ and $F_v/F_m$) refer to the structure and function of PSII only, while the latter two yield information on ET activity after $Q_A^-$, the first electron acceptor of PSII (Strasser et al., 1995). A first observation was that all knockout mutants have a higher $F_0$ value than the wild type. The increase was rather small, although significant, in koCP26 mutants and larger in koCP24 and in the double mutant. This suggests that a larger fraction of absorbed energy is lost as fluorescence in the mutants, implying that the connection between the major LHCII complex and PSII RC is less efficient in the absence of minor antenna proteins (Table 2).

The maximum quantum efficiency of PSII photochemistry ($F_v/F_m$) was similar in the wild type and koCP26, while it was reduced in koCP24 and koCP24/26 plants (Table 2).

When examining later steps of fluorescence induction, it appeared that koCP24 was slower in reaching $F_m$: fluorescence rose till the end of the measurement window, while the other genotypes were already declining toward $F_s$. In koCP24, $t_m$ was significantly longer than in any other genotype (Table 2). Since $F_m$ is reached when the plastoquinone (PQ) pool is fully reduced, these results suggest the existence of restrictions in electron transfer to the PSII acceptor PQ.

For a more detailed analysis of the ET contribution to the fluorescence induction curve, we calculated the integrated area between the measured fluorescence signal and the maximal measured fluorescence $F_m$, given by: $Area = \int_0^{tm} (F_m - F_t)dt$.

This area value has to be normalized by $F_v$ to compare different samples, yielding a parameter called $S_m$. The $S_m$ to $t_m$ ratio expresses the average redox state of $Q_A$ in the time span from 0

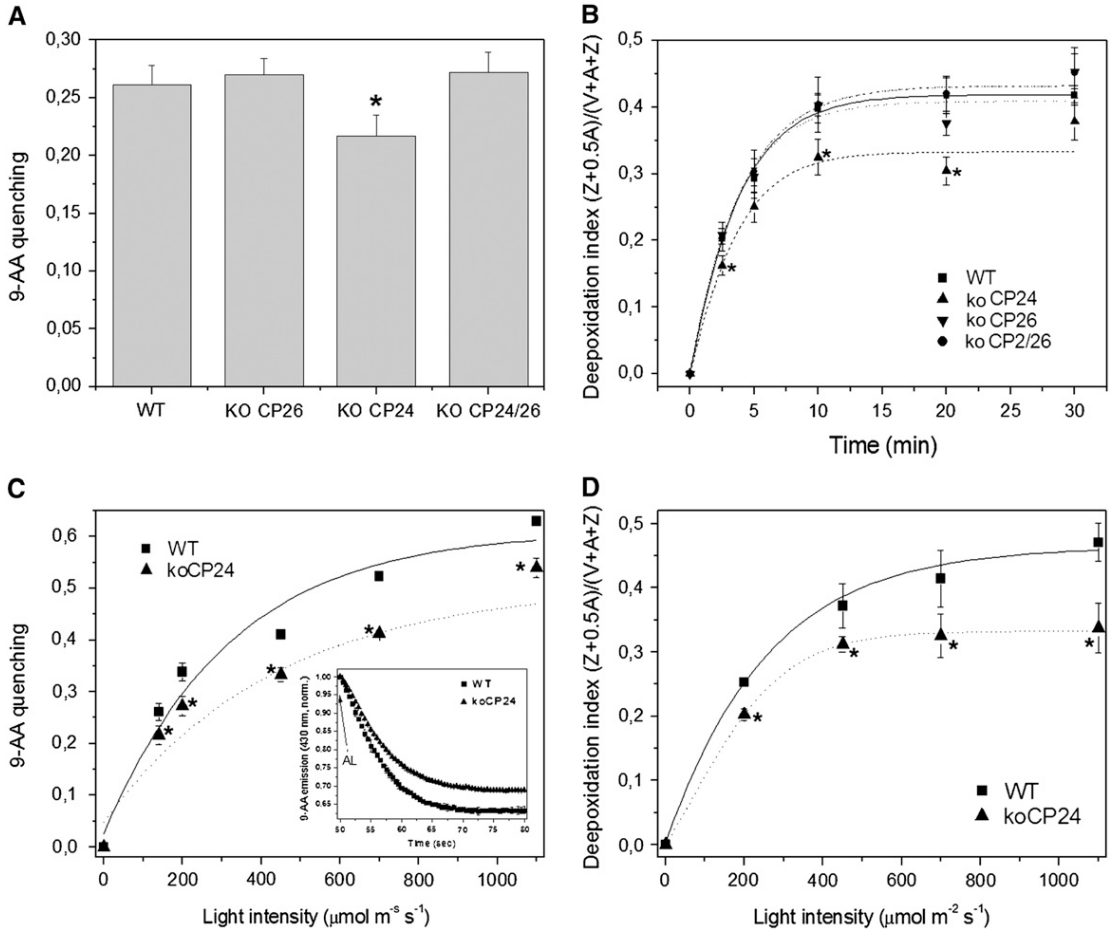


**Figure 6.** Measurement of Trans-Thylakoid ΔpH.

**(A)** The light-dependent quenching of 9-AA fluorescence in intact chloroplasts was quantified as a measure for trans-thylakoid ΔpH.
**(B)** Time course of violaxanthin deepoxidation in wild-type and mutant plants. Leaf discs from dark-adapted leaves were illuminated at 450 μmol $m^{-2}$ $s^{-1}$ (white actinic light). At different times, discs were frozen in liquid nitrogen and total pigment extracted.
**(C)** Amplitude of light-dependent quenching of 9-AA fluorescence measured at different light intensities on wild-type and koCP24 intact chloroplast. Inset: traces of 9-AA fluorescence emission (430 nm) during ΔpH buildup (induced by red actinic light, 450 μmol $m^{-2}$ $s^{-1}$) shows a slower lumen acidification in mutant chloroplasts. AL, red actinic light turned on.
**(D)** Amplitude of violaxanthin deepoxidation was measured on leaf discs from the wild type and koCP24 after illumination (10 min) at different light intensities.
All data are expressed as mean ± SD ($n = 4$). Significantly different values according to Student's $t$ test ($P < 0.05$) are marked with an asterisk.

to $t_m$ and, thus, the average fraction of open reaction centers during the time needed to complete their closure. This parameter therefore allows a quantification of the ET activity (Strasser et al., 1995). koCP24 had a lower $S_m/t_m$ value than the wild type, meaning that it had a higher average fraction of closed reaction centers. This result implies that ET activity was limited after $Q_A^-$. The other genotypes, on the contrary, had a similar $S_m/t_m$ value to the wild type, thus suggesting a similar ET to $Q_A$ (Table 2).

Fluorescence induction curves also yield information on ET downstream of $Q_A$. Curves are characterized by three rapid rises (0-J, J-I, and I-P) divided by plateau phases (Strasser et al., 1995). Differences were observed in koCP24 with respect to the wild type and the other genotypes (Figure 8): the second rise (J-I) was faster, while the third (I-P) was slower. koCP24/26 plants were affected similarly to koCP24 in their O-J phases of the induction curves, while they had similar kinetics to koCP26 and the wild type at longer times (I-P interval), thus rapidly reaching $F_m$ without revealing restrictions in ET between $Q_A$ and $Q_B$.

Fluorescence parameter analysis thus suggests impairment in PQ reduction rates specifically in koCP24. This phenotype is not retained in the koCP24/26 double mutant, which behaves similarly to wild-type and koCP26 plants.

### Partial ET Reactions

ET activity using artificial donor/acceptors was performed to determine the efficiency of different steps of the transport chain and thus to elucidate the nature and location of ETR restriction in koCP24. Whole-chain ETR was measured in isolated thylakoids by following $O_2$ evolution using $NADP^+$ as electron acceptor and

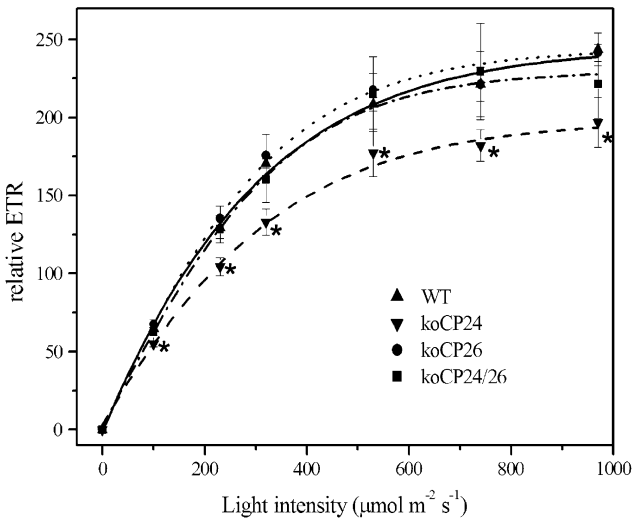


**Figure 7.** ETR Measurements.

Relative ETR as a function of quantum flux density of PAR was measured fluorometrically in light-adapted leaves under saturating $CO_2$ (1%). Data represent an average of five to eight independent measurements and are expressed as mean ± SD. Significantly different values from the wild type ($P < 0.05$, Student's *t* test) are marked with an asterisk.

was expressed as μmol $O_2$ mg $Chl^{-1}$ $h^{-1}$ (Table 3). Wild-type thylakoids exhibited an ETR consistent with previous results (Johnson et al., 1994). koCP26 and koCP24/26 exhibited the same rate of $O_2$ evolution, while koCP24 activity was decreased by 40%, consistent with ETR estimation by fluorescence analysis (Figure 7). ETR from water to PQ was measured using p-benzoquinone (PBQ), which accepts electrons at the $Q_B$ site of PSII. The ETR in this partial electron chain was consistent with results from the whole-chain assay: koCP24 had a lower $O_2$ evolution than the wild type; while koCP26 and koCP24/26 showed a lower rate of ET to PBQ than the wild type, both mutants showed a significantly higher ETR with respect to koCP24. This result suggests that, even if the PBQ was added in excess, $Q_A$ to $Q_B$ $e^-$ transport was lower in the koCP24 mutant with respect to the wild type, possibly by limited diffusion of the electron acceptor to the $Q_B$ site.

ETRs downstream from the plastoquinol ($PQH_2$) and from plastocyanin (PC) to $NADP^+$ (Table 3) have been analyzed spectrophotometrically by following $NADP^+$ reduction. There were not major differences among genotypes, consistent with the hypothesis that the restriction in ET in koCP24 is localized between the $Q_A$ site and the cytochrome $b_6f$ complex. The only significant difference we observed was that koCP26 had a higher rate of $e^-$ transport from $PQH_2$ to PSI than the wild type.

### Kinetics of $Q_A$ Reoxidation

The above suggestion that ET is restricted from $Q_A$ to $Q_B$ in koCP24 plants was verified by a further independent measurement. The PQ diffusion step is accessible to analysis through the evaluation of $Q_A$ reoxidation kinetics by measuring leaf chlorphyll fluorescence decay after a single turn-over flash. In short, when PSII is excited by a very short flash of saturating light, $Q_A$ is fully reduced and fluorescence reaches its maximal value, after which it decreases with a rate dependent on reoxidation of $Q_A$ by PQ diffusing from the surrounding membrane domains. Thus, the kinetics of fluorescence decay depend on the rate of PQ diffusion to the PSII $Q_B$ site (Sane et al., 2003). Fluorescence recovery kinetics were clearly slower in koCP24 than in the wild type and koCP26, implying that the accessibility of the $Q_B$ site to PQ was restricted (Figure 9). Also, koCP24/26 kinetics was somewhat slower than the wild type and koCP26, but the effect was much smaller than in koCP24. To verify that these results were not due to differences in PQ content in different genotypes, we evaluated the total amount of reducible PQ by comparing fluorescence induction in DCMU-infiltrated leaves with dibromothymoquinone-infiltrated leaves (Bennoun, 2001), which did not show significant differences.

### Structural and Functional Analysis of Isolated Grana Membranes

All results presented above support the idea of a restriction of PQ reduction rate in the koCP24 mutant with respect to the other genotypes under study. To find possible explanations for this phenotype, we analyzed the organization of PSII complexes in grana partitions by transmission electron microscopy. Grana membranes were isolated by α-DM fractionation of stacked thylakoid membranes and observed after negative staining as previously described (Morosinotto et al., 2006). The preparation consisted of circular patches of membranes with diameters between 0.7 and 1 μm (see Supplemental Figure 1 online), consistent with derivation from grana partitions (Simpson, 1983).

**Table 2.** Analysis of Room Temperature Chlorophyll Fluorescence

| | Wild Type | koCP24 | koCP26 | koCP24/CP26 |
|---|---|---|---|---|
| $F_0$ | 451 ± 40 | 646 ± 64* | 508 ± 47 | 695 ± 53* |
| $F_v/F_m$ | 0.83 ± 0.02 | 0.71 ± 0.03* | 0.80 ± 0.01 | 0.73 ± 0.03* |
| $t_m$ (ms) | 213.1 ± 25.8 | 1042.3 ± 113.7* | 192.0 ± 24.9 | 218.5 ± 30.7 |
| $S_m/t_m$ | 0.103 ± 0.008 | 0.0328 ± 0.0023* | 0.114 ± 0.015 | 0.112 ± 0.013 |
| $T_{2/3}$ (ms) | 388 ± 68 | 423 ± 71* | 371 ± 42 | 356 ± 43 |

Photosynthetic parameters were provided by analysis of chlorophyll fluorescence measured with green light (7 μmol $m^{-2}$ $s^{-1}$ or 1100 μmol $m^{-2}$ $s^{-1}$; see Methods for details) on leaves of the wild type and mutants. The two-thirds time of the fluorescence rise ($T_{2/3}$) was measured in 3.0 $10^{-5}$ M DCMU infiltrated leaves using a flash of green light (7 μmol $m^{-2}$ $s^{-1}$, 8 s). The $T_{2/3}$ parameter is inversely related to the incident photon flux and is an index of the functional antenna size of PSII. Significantly different values with respect to the wild type are marked with an asterisk ($P > 0.05$).

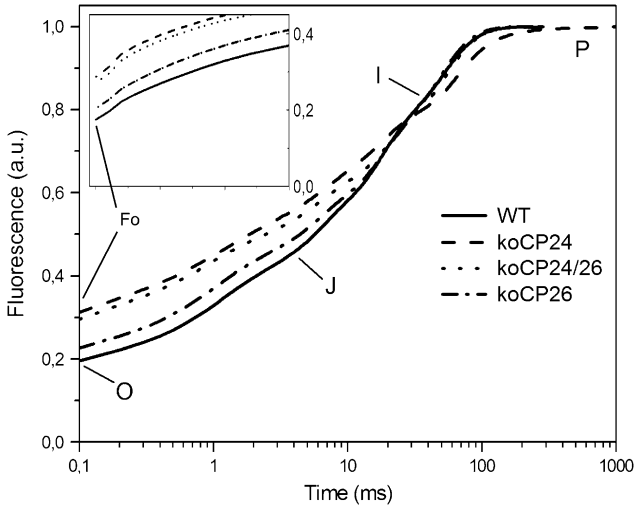


**Figure 8.** PSII Fluorescence Induction Kinetics Normalized to the $F_m$ Value.

Fluorescence rise was induced on dark-adapted leaf, using a saturating flash of green light (1200 μmol $m^{-2}$ $s^{-1}$, 1 s). Inset: the initial rise (sector O-J) of the induction curves. $F_0$ values increase in the order wild type < koCP26 < koCP24 < koCP24/26. Data are expressed as mean values of at least 10 fluorescence curves. A.u., arbitrary units.

SDS-PAGE analysis of the grana preparations from the different genotypes showed large depletion of ATPase and PSI components and enrichment in LHCII and PSII core polypeptides (see Supplemental Figure 2 online). When observed at high resolution (Figure 10A), grana membranes from the wild type are characterized by stain-excluding particles with a tetrameric structure randomly distributed in a negative stain background and identifiable as PSII cores (Simpson, 1979; Tremmel et al., 2003; Morosinotto et al., 2006). Tetrameric particles in wild-type grana occurred at an average density of 3.5 × $10^{-4}$ PSII tetramers $nm^{-2}$, similar to the case of koCP26. The latter showed, however, that membrane patches where particles were loosely organized into rows (Figure 10B). Samples from koCP24 were clearly different, being characterized by highly ordered arrays of tetrameric particles that covered most of the membrane surface and had a repetition size of 170 × 221 Å (Figure 10C). At the periphery of the membrane circles, these tetrameric particles were less ordered and more widely distributed into a negatively stained background (Figure 10F). Grana partitions from the koCP24/26 double mutant were characterized by the presence of particle rows of four to seven tetrameric particles widely spaced, yielding a particle density of 9.9 × $10^{-4}$ $nm^{-2}$ (Figure 10E). We superimposed the array lattice from koCP24 on a background of membranes isolated from the barley (*Hordeum vulgare*) mutant *vir zb63*, chosen as a reference because a high resolution density map is available of this mutant (Morosinotto et al., 2006). This showed that the unit cell of the arrays (16.5 × 25 nm) was the same in the two mutant membranes (Figure 10D). The array in koCP24 thus corresponds to C2S2 supercomplexes as determined at high resolution (Morosinotto et al., 2006).

### State I–State II Transitions

The above results show that both PQ diffusion within grana membranes and the connection between PSII core complexes and outer LHCII are affected in koCP26, koCP24, and koCP24/26 double mutants. The process of state transitions consists in the adjustment of PSI versus PSII antenna size based on the transfer of phosphorylated LHCII from PSII. Since LHCII phosphorylation is induced by overreduction of the PQ pool (Allen, 1992), state transition measurements are a good indicator of the modifications undergone by PQ redox state. According to a well-established procedure, State I to State II transitions were measured from the changes in chlorophyll fluorescence level of leaves when PSI light was overimposed to PSII light, and then PSI light was switched off to induce PQ reduction (Jensen et al., 2000). The amplitude of state transition of the wild type, koCP26, and koCP24/26, measured as decrease in $F_m'$ upon reduction of PQ, is essentially the same (Figure 11). A smaller decrease of $F'_m$ amplitude was instead observed in koCP24. Differences between koCP24 and others were also observed in the amplitude and rate of the stationary fluorescence (Fs), which reflects the redox state of PQ pools, observed upon switching on far-red light, which oxidizes PQ. While the fluorescence decrease was fast in wild-type and koCP26 plants (0.8 s), it was 20-fold slower in koCP24 (18 s) (see Supplemental Figure 3 online). A further difference was observed in the rate of the transition from State II to State I upon switching off far-red light (Figure 11): while the half-time of the transition was similar in the wild type and koCP26

**Table 3.** Effect of Electron Donors and Acceptors on the ETR

| | Wild Type | koCP24 | koCP26 | koCP24/CP26 |
|---|---|---|---|---|
| | μmol $O_2$ $mg^{-1}$ Chlorophyll $h^{-1}$ | | | |
| Whole-chain ET $H_2O \rightarrow NADP^+$ | 15.30 ± 1.02 | 8.96 ± 0.71* | 13.74 ± 0.84 | 13.80 ± 0.93 |
| Partial ET $H_2O \rightarrow$ PBQ (PSII) | 45.33 ± 0.38 | 19.33 ± 0.34* | 40.00 ± 1.50* | 33.51 ± 1.32* |
| Partial ET | μmol NADPH $mg^{-1}$ Chlorophyll $h^{-1}$ | | | |
| $DPIPH_2 \rightarrow NADP^+$ ($PQH_2 \rightarrow$ PSI) | 82.19 ± 6.28 | 86.72 ± 2.86 | 101.93 ± 5.62* | 85.66 ± 1.64 |
| $TMPDH_2 \rightarrow NADP^+$ (PC → PSI) | 143.69 ± 10.04 | 159.74 ± 11.79 | 151.87 ± 12.81 | 149.25 ± 14.41 |

Data are expressed as mean ± SD ($n = 4$). Significantly different values with respect to the wild type are marked with an asterisk (according to Student's $t$ test, $P < 0.05$).

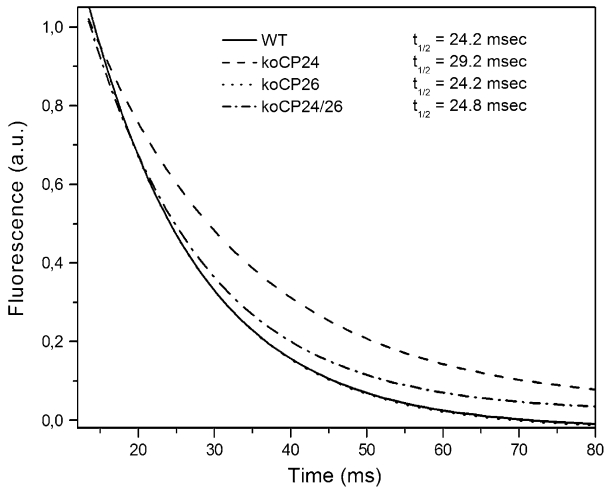


**Figure 9.** $Q_A^-$ Reoxidation Kinetics.

Chlorophyll fluorescence decay kinetics were measured after single-turnover flash illumination in dark-adapted leaves. Drawn lines are fits for the experimental data points. Experimental fluorescence curves were normalized to the corresponding $F_m$ values and represent averages from 12 separate experiments. The experimental data set is shown in Supplemental Figure 6 online.

(88 and 94 s, respectively), it was approximately twice as fast in koCP24 and koCP24/26.

### Functional Characterization of an Independent Allele of koCP24

It is worth noting that the correspondence between the limitation in ETR and the koCP24 mutation was further confirmed by the isolation and characterization of an independent allele of the koCP24 genotype in a different ecotype (Landsberg *erecta* versus Columbia). We show here that this different allele (and ecotype) has the same alteration of photosynthetic parameters described above for koCP24 and that the double koCP24/26 mutant recovers photosynthetic ETR similar to the wild type (see Supplemental Figure 4 online).

## DISCUSSION

Deleting CP24, CP26, or both of these components of the PSII antenna system did not severely affect pigment composition and chloroplast structure. Only koCP24 plants showed a reduction in the rate of Zea synthesis upon exposure to strong light. Nevertheless, this genotype also showed alteration in several photosynthetic parameters and a reduced growth (Figure 1C). All these symptoms were suppressed in the case of the double koCP24/26 mutant, suggesting that phenotypes are not caused merely by the absence of CP24 but rather due to pleiotropic or compensatory effects. This is consistent with the higher reduction in fitness of plants lacking CP24 than of plants lacking CP26 (Ganeteg et al., 2004).

### The Functional Phenotypes Are Caused by Pleiotropic Effects Rather Than by Lack of Function Specifically Associated with Individual Gene Products

The mechanistic reason for the above phenotypes is not obvious. Therefore, we have investigated changes in the composition/function of the antenna system by several methods, including the kinetics of fluorescence rise in the presence of DCMU, the pigment distribution among chlorophyll proteins, and the stoichiometry of Lhcb apoproteins. The kinetics of fluorescence in DCMU yields a functional evaluation of the antenna size (i.e., the flux of photons trapped per reaction center). The photon flux reaching the PSII RC is not significantly different between genotypes (Table 2). Clear differences were, however, detected in the Lhcb polypeptide composition of the different mutants (Figure 4). The effects of deleting a subunit within the PSII-LHCII

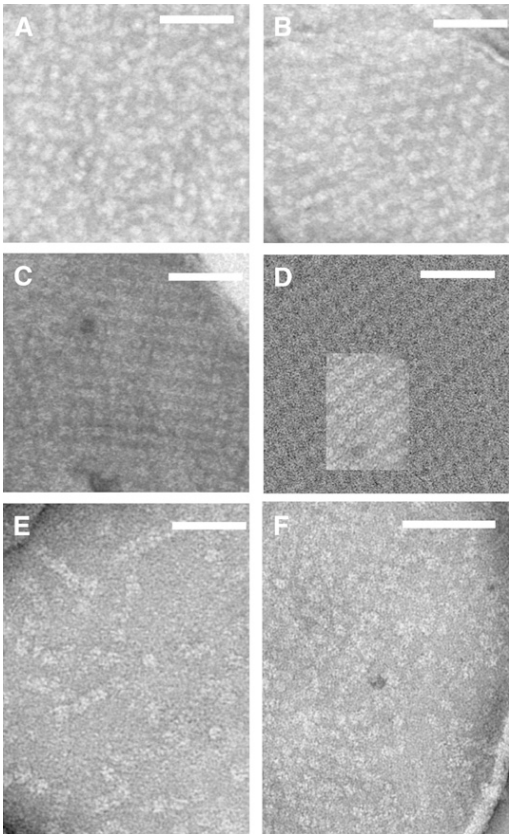


**Figure 10.** EM of Negatively Staining Grana Partition Membranes Obtained by Partial Solubilization with α-DM.

**(A)** to **(C)** and **(E)** High-resolution micrographs show the distribution of stain-excluding tetrameric particles: Wild type **(A)**, koCP26 **(B)**, koCP24 **(C)**, and koCP24/26 **(E)**.

**(D)** A two-dimensional array from koCP24 was superimposed on a larger array from the grana membranes of the barley mutant *vir zb63*, showing that the crystal lattice is identical in the two samples.

**(F)** koCP24 periphery membrane areas in which tetrameric particles were less ordered and more widely distributed into a negatively stained background. The bar is 100 nm long.

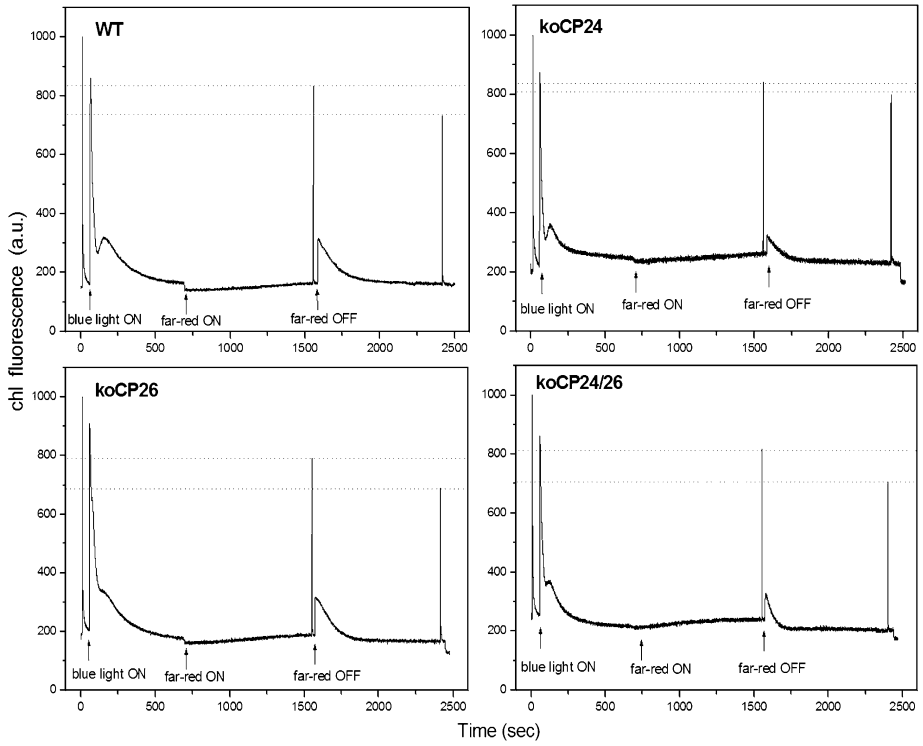


**Figure 11.** Measurement of State 1–State 2 Transitions.

Plants, upon dark adaptation for 1 h, were illuminated with blue light (40 μmol $m^{-2}$ $s^{-1}$, wavelength <500 nm) for 15 min to reach State II. Far-red light source was used to induce transition to State I. Values of $F_m$, $F_m'$, and $F_m''$ were determined by light saturation pulses (4500 μmol $m^{-2}$ $s^{-1}$, 0.6 s).

supercomplex can be various: removal of CP29 was shown to decrease the stability of CP24 (Andersson et al., 2001). Alternatively, the loss of Lhcb1 and Lhcb2 was accompanied by the compensatory overaccumulation of CP26 and Lhcb3 (Ruban et al., 2003). We show that lack of CP26 was accompanied by the increase of CP29 and CP24 and, conversely, lack of CP24 increased CP29 and CP26 (Figure 4), suggesting functional compensation within the group of monomeric Lhcb proteins. An additional effect was observed in both koCP24 and the the koCP24/26 double mutant consisting of a change in the relative abundance of the components of the major LHCII antenna: while Lhcb3 is decreased by 55% (koCP24/26) and 70% (koCP24), Lhcb1 and Lhcb2 are overaccumulated in the double mutant (by 65 and 15%, respectively) and, to a lesser extent, in koCP24 plants. This is likely due to the participation of CP24 in a supramolecular antenna complex that also includes CP29, Lhcb1, Lhcb2, and Lhcb3 polypeptides (Bassi and Dainese, 1992). It is interesting to note that CP24-less plants do not lose CP29, suggesting that this complex is stabilized by direct interaction with the PSII core complex. The compensatory relationship observed within antenna polypeptides in the single mutants is broken in the double mutant (Figure 4): upon genetic deletion of both CP26 and CP24, CP29 is also decreased, yielding a PSII strongly depleted in minor antenna complexes. We suggest that the interaction between the PSII core and minor Lhcbs is cooperative, thus leading to decreased affinity when two of them are lacking.

The efficiency of excitation energy transfer to the PSII RC is affected by depletion of monomeric Lhc, as can be inferred by the analysis of the initial fluorescence level ($F_0$): $F_0$ level is inversely related to the efficiency of energy transfer from LHCII to PSII RC. We observed a steady increase in $F_0$ in the order wild type< koCP26< koCP24 = koCP24/26 (Figure 8, Table 2). This is a clear indication that the connection between the PSII core and the bulk trimeric LHCII was partially impaired in the mutants. Cooperativity between PSII centers has been reported to be affected in koCP24, possibly as the result of the clustering of LHCII and/or PSII RC particles observed by electron microscopy (EM) analysis (Kovacs et al., 2006). This implies that exciton migration between many LHCII trimers decreases the probability that an exciton visiting a closed PSII center is then quenched by a neighboring open reaction center. While functional antenna size of different genotypes was essentially the same in wild-type and knockout plants, $F_0$ increases steadily when monomeric Lhcb proteins are deleted and is maximal in koCP24 and koCP24/26 where organization of LHCII into clusters separated from PSII RC is maximal (Figure 10). This can be reconciled by the hypothesis that exciton transfer is slower in the absence of monomeric Lhcs, which decreases the probability of trapping by PSII RC and thus reduces PSII quantum yield.

State transitions, the mechanism by which photosystems balance their complement of light-harvesting antennas depending on the reduction state of the intermediate electron carrier PQ,

are triggered by changes of the relative affinity of LHCII for either PSI or PSII, which is regulated by a reversible phosphorylation (Jensen et al., 2000). Neither CP24 nor CP26 are phosphorylated in higher plants (Bassi et al., 1988); thus, changes in state transitions are not expected. While this was verified for koCP26, koCP24 was affected in its capacity to activate state transitions (Figure 11). This effect has been attributed to a decreased presence of PSII-connected LHCII-type M trimers (Kovacs et al., 2006). This statement is not consistent with our finding that the LHCII trimer complement is not significantly affected in our genotypes (Figure 3) and appears to be rather efficient in transferring excitation energy to PSII RC (Table 2). Furthermore, the koCP24/26 mutant, although showing increased $F_0$, is fully able to perform state transitions. Rather, we observe that in koCP24 and koCP24/26, the fluorescence changes induced by switching off the far-red light are faster than the wild type, implying that the transiently reduced state of the free PQ pool is more promptly relaxed in koCP24 and koCP24/26 than the wild type by migration of the LHCII to the RC of PSI. However, koCP24 and koCP24/26 differ in their capacity to undergo reduction of the PQ pool and to activate state transitions (Figure 11).

### The Topology of Grana Membranes Is Affected by Mutations

Grana partitions are made up essentially of proteins with very little lipids, which are tightly bound to photosynthetic complexes (Tremolieres et al., 1994). Previous work on negatively stained PSII membranes and cryo-EM analysis of negatively and unstained membranes has shown that tetrameric PSII particles protrude from the membrane plane, while Lhc particles are located in the dark background (Simpson, 1979). In grana membranes from the wild type, the distribution of tetrameric PSII particles is homogeneous through the whole surface. This is not the case for koCP24, where most of the area is occupied by arrays of tetrameric particles and the remaining patches are formed by a stained background with rare stain-excluding particles. The PSII arrays in koCP24 are composed of C2S2 supercomplexes (Figure 10D) since they have the same basic unit as is found in *vir zb63*, a genotype with a strongly reduced Lhc antenna system lacking CP24 and a large fraction of the LHCII trimers (Morosinotto et al., 2006). koCP24, on the other hand, has a full complement of LHCII trimers (Figures 1 and 4). We conclude that grana membranes of koCP24, besides having arrays of C2S2 particles, contain discrete patches of LHCII trimers that are interspersed by a few PSII core complexes (Figure 10F). We conclude that in some discrete areas of koCP24 grana membranes, the LHCII/PSII core ratio is strongly increased: in these grana partitions, LHCII fluorescence is not efficiently quenched photochemically, thus yielding increased $F_0$. When both CP24 and CP26 are missing, the PSII core appears to be randomly distributed within a network of trimeric LHCII, underlining lack of organized interactions between the PSII RC and its antenna. Depletion in CP24 leads to the formation of C2S2 arrays. We can speculate that the array formation is due to the lack of connection between the inner antenna system and the outer LHCII trimer population, which exposes interaction sites between CP26 of one supercomplex and CP26 of the neighboring complex (Morosinotto et al., 2006). This hypothesis is consistent with the report of CP26 forming trimers when overaccumulated in antisense LHCII plants (Ruban et al., 2003), showing that CP26–CP26 interactions might be strong. In the double mutant, lack of CP26 subunits is thus probably responsible for the disruption of arrays.

### How Does the Lack of CP24 Affect Growth and ETR?

The only genotype with a drastically reduced growth rate is koCP24. However, lack of this antenna subunit in itself is unlikely to limit plant growth since PSII quantum yield is only marginally affected (Table 2), while it has been reported that acclimation of wild-type plants to high light yields into 80% decrease in CP24 content without affecting neither plant growth nor the amplitude NPQ (Ballottari et al., 2007). Decreased NPQ, moreover, cannot be considered as the cause for low growth rate in koCP24 since the *npq4* mutant, lacking qE, is affected only in harsh stress conditions (Li et al., 2002b) and even grows better than the wild type in low light (Dall'Osto et al., 2005), a feature not found in koCP24 plants. Reduced growth of koCP24 has been attributed to increased $F_0$ and decreased connectivity with respect to the wild type (Kovacs et al., 2006), but this is in contrast with the observation that $F_0$ is even higher in the double mutant, which shows normal growth and ETR (Figures 1C and 7). An effect of the mutation is a strong depletion in Lhcb3. However, this polypeptide is also depleted in the koCP24/26 mutant, and koLhcb3 plants have a normal ETR phenotype (L. Dall'Osto, unpublished data).

EM analysis of chloroplasts shows that photosynthesis is affected in koCP24 since starch grains, accumulated within the chloroplasts of wild-type, koCP26, and koCP24/26 plants, cannot be detected in koCP24. This effect correlates with a reduced ETR both in leaves (Figure 7) and isolated chloroplasts of koCP24 (Table 3). Partial ET reactions localize the restricted step to between the $Q_A$ site of PSII and the cytochrome $b_6f$ complex, since electron donors to cytochrome $b_6f$ are effective in sustaining $NADP^+$ reduction at similar rates in all genotypes. We conclude that lack of CP24 leads to restriction of $PQH_2$ diffusion from the PSII $Q_B$ site to the cytochrome $b_6f$ complex, which is the limiting step for photosynthetic ET (Joliot and Joliot, 1977). We cannot formally exclude that ET restriction upon CP24 deletion is located between $Q_A$ and $Q_B$ within the PSII core. Nevertheless, this hypothesis seems highly unlikely since it would imply that lack of one Lhcb can have an impact on the PSII core, while lack of two Lhcbs restores full function. Moreover, CP24 subunit, together with all antenna proteins, is lacking in Chlorina *f2* and yet the ETR is higher than in the wild type (Guo et al., 2007).

While koCP24 has most of the membrane partition surface occupied by tightly packed arrays of PSII supercomplexes, this feature is not evident in wild-type, koCP26, and koCP24/26 plants (Figure 10), which have normal rates of ET. We conclude that the restriction in ET is associated with the regular organization of PSII particles into arrays in the koCP24 mutant. Indeed, the restriction in ET was confirmed by fluorescence induction in the isolated grana membrane preparation used in the EM analysis (see Supplemental Figure 5 online).

ET from the PSII $Q_B$ site to cytochrome $b_6f$ is mediated by the small diffusible transporter PQ, whose diffusion in the membrane

bilayer strongly depends on the organization of intrinsic membrane proteins, which are extremely crowded in grana partitions (Tremmel et al., 2003). PSII organized into ordered arrays restricts protein dynamics and limits the PQ diffusion. While the surface occupancy of randomly organized PSII and LHCII particles is 0.72 to 0.77 (Tremmel et al., 2003), ordered C2S2 arrays leave very little space in between particles (Morosinotto et al., 2006), thus allowing PQ diffusion only in boundary lipids tightly bound to membrane complexes (Tremolieres et al., 1994). This is fully consistent with the analysis of fluorescence induction curves (Figure 8; see Supplemental Figure 5 online), where the last phase (J-P), reflecting the reduction of acceptors downstream of PSII, primarily PQ, is delayed by five times in koCP24 with respect to the wild type. Moreover, the $S_m/t_m$ value, expressing the average fraction of open reaction centers during the time needed to complete their closure (Strasser et al., 1995), is three times smaller in koCP24 than in the wild type, implying a higher average fraction of closed reaction centers in the mutants. Together with the observation that ET from cytochrome *b*$_6$*f* to PC is equally efficient in all genotypes, this implies a restricted diffusion of $PQH_2$ between site $Q_B$ and cytochrome *b*$_6$*f* that increases $Q_A^-$ reduction. A final confirmation of the above hypothesis was obtained by the measurement of $Q_A$ reoxidation kinetic, which clearly showed a reduced rate of ET from $Q_A$ to PQ pool (Figure 9).

Alternatively, a longer average diffusion distance between $Q_A$ and cytochrome *b*$_6$*f* could produce the same effect on ET. Such an effect would likely be present in membrane domains organized into C2S2 arrays that would confine cytochrome *b*$_6$*f* complexes, which are normally present in both grana and stroma exposed membranes (Vallon et al., 1991), to grana margins, and/or to stroma membranes. However, our data suggest that neither changes in activity of cytochrome *b*$_6$*f* (Table 3) nor the increased distance between $Q_A$ and cytochrome *b*$_6$*f* (see Supplemental Figure 5 online) are responsible for ET limitations. We observed a reduced ET activity from water to PBQ in koCP24 chloroplasts, while steps downstream were unaffected (Table 3). Since oxidized PBQ is present in excess, this effect cannot be due to a lower activity of cytochrome *b*$_6$*f* but only to a limited accessibility of PQB to PSII. Furthermore, the slower $Q_A$ reoxidation kinetics in koCP24 was not due to a higher average distance between $Q_B$ sites and cytochrome *b*$_6$*f* in this genotype, since fluorescence kinetic differences would be removed by dibromothymoquinone treatments (see Supplemental Figure 5 online).

### Why Does Restriction in PQ Diffusion Affect qE?

qE is triggered by low lumenal pH (Briantais et al., 1980), while the major lumen acidification step is realized by proton pumping concomitant to $PQH_2$ oxidation by the cytochrome *b*$_6$*f* complex. Decreased $PQH_2$ diffusion will thus result in decreased proton pumping. This was confirmed by our observation that the koCP24 mutant had a decreased capacity to generate a pH gradient and synthesized Zea at a slower rate than the wild-type, koCP26, and koCP24/26 plants (Figures 6B and 6D). It is worth noting that koCP24, besides a slower rate of Zea synthesis, also has a lower deepoxidation index at saturating light than the wild type. This can be explained by considering that the release of Viola from outer binding sites of LHCII, which is promoted by lumen acidification, is likely limited in this genotype (Caffarri et al., 2001). We conclude that koCP24 is a proton gradient regulation (*pgr*) mutant. Its NPQ phenotype, similarly to *pgr* mutants (Munekage et al., 2001, 2002), is mainly due to a decreased capacity for proton accumulation at the transition from dark to light. koCP24 generates a pH-dependent quenching similar to wild-type plants in the first minute of illumination (Figure 5), but quenching does not develop further beyond this point. In the first seconds of illumination, lumen pH decreases in the mutant and in the wild type. A further decrease in the mutant, however, is limited by its restricted proton transport, and ΔpH does not reach the same amplitude. In addition, reduced Zea synthesis and limited protonation of DCCD binding sites in CP29, CP26, and PsbS might contribute to limitation of the second part of NPQ development. Previous work with koCP24 has underlined the importance of membrane organization and protein–protein interaction between Lhc subunits for the proper operation and full expression of qE (Kovacs et al., 2006). This is consistent with our finding that the restriction in ET is to be ascribed to changes in the PQ diffusion rate caused by tight interaction between C2S2 modules in regular arrays. The alternative view that disconnection of a trimeric LHCII fraction hosting the quenching site is responsible for decreased qE (Kovacs et al., 2006) is inconsistent with our finding that disconnected LHCII domains are far more extended in koCP24/26 than koCP24 plants, while koCP24/26 have a wild-type level of qE (Figure 5).

### The NPQ Rise Kinetics Are Affected by Lack of Zea-Exchanging Lhc Proteins

A different pattern of NPQ rise kinetics is observed in the double mutant than in the wild type: although reaching the same qE amplitude at 8 min light, there is a clear plateau between 1 and 3 min, after which the kinetics ascend again. This genotype lacks both CP26 and CP24, the two most effective Lhc proteins in Viola>Zea exchange (Morosinotto et al., 2003) and has reduced CP29. Since Zea has been shown to decrease the activation energy required for the transition from unquenched to quenched conformation (Wentworth et al., 2003), we interpret these results as the effect of a slower transduction of conformational change signal, upon protonation of PsbS, to Lhc proteins, where quenching is catalyzed even in the absence of Zea bound (Briantais, 1994; Bonente et al., 2007). The high levels of qE in koCP24/26 mutants, although with slower kinetics than the wild type, suggest that the major LHCII, which is still present with only 50% of CP29 proteins, might play a role in qE. Based on the slower onset of quenching in the double mutant, it can be hypothesized that monomeric Lhcs might transfer conformational information from PsbS to LHCII. The construction of a mutant without minor CPs will allow verification of this hypothesis.

Finally, it has been proposed that CP26 plays a major role in qI, based on its capacity to assume a quenched conformation upon Zea binding that can be isolated from high-light-treated thylakoids (Dall'Osto et al., 2005). Here, we show that koCP26, although having normal levels of qE, has reduced qI (Figure 5), and the double mutant koCP24/26 does not further decrease its

qI level, supporting a specific role of CP26 in catalyzing qI type of quenching. This suggests that although Lhcb proteins might have overlapping functions, they each fulfill specific roles in light harvesting and photoprotection.

### What Is the Function of CP24 and CP26 in the Organization of PSII?

CP26 is a component of the PSII antenna in the most ancient green algae species in which photoprotection is mainly performed through Zea synthesis (Baroli et al., 2003) independently from qE (Ledford et al., 2007), which is strongly decreased in green algae with respect to higher plants (Finazzi et al., 2004). We propose that CP26, here shown to be largely responsible for qI, is specialized in Zea-mediated photoprotection (Dall'Osto et al., 2005). Unlike CP26 and CP29, CP24 is a recent addition to the PSII antenna system of the green lineage, appearing only in land plants (Rensing et al., 2007). Chloroplasts of land plants are characterized by large grana stacks made up of partition domains with larger diameters than those of green algae (Larkum and Vesk, 2003). Thus, higher plants are expected to experience restriction of PQ diffusion (Lavergne and Joliot, 1991) between PSII reaction centers and cytochrome $b_6f$ during linear ET, which has been suggested to occur mainly in grana margins (Joliot and Joliot, 2005). *Chlamydomonas reinhardtii* lacks CP24 (Teramoto et al., 2001) and forms C2S2 particles (Boekema et al., 2000), which are prone to form regular arrays (Dekker and Boekema, 2005) that further restrict PQ diffusion. The increased size of grana discs in land plants was a result of evolution that separated PSI from PSII, which increased the efficiency of light harvesting for PSII and established a fine-tuning between cyclic and linear electron flow (Finazzi et al., 2001). This might have led to the requirement of an additional monomeric complex for interfacing the PSII core with trimeric LHCII during changes in antenna size induced by acclimation at low light intensities (Ballottari et al., 2007). This implies that the organization of photosystems in the wild type allows for the highest rate of PQ diffusion, reminiscent of grana organization in green algae (A. Alboresi, S. Caffarri, F. Nogué, R. Bassi, and T. Morosinotto, unpublished data).

We conclude that minor chlorophyll proteins function in bridging dimeric PSII core complexes to the major trimeric LHCII antenna both structurally and functionally. This is particularly evident in CP24/CP26-less plants in which PSII-rich and LHCII-rich domains are formed within grana partitions. The tight regular arrays formed by C2S2 supercomplexes also affect ETRs, most likely by restricting PQ diffusion to cytochrome $b_6f$ complexes, which yields decreased lumen acidification and reduction of qE. We suggest that CP24, the latest addition to Lhcb proteins during evolution (Rensing et al., 2007), has evolved to overcome limitations in PQ diffusion caused by the increased size of grana stacks in land plants with respect to green algae.

This work showed how a specific antenna protein has, besides a direct involvement in light harvesting, a large effect on ET through its role in thylakoid biogenesis and assembly. This is a clear example of how a complex system like thylakoid membranes functions due to the optimization of all its components and the tuning of their interactions with each other over evolutionary time.

## METHODS

### Plant Material

*Arabidopsis thaliana* T-DNA insertion mutants (Columbia ecotype) SALK_077953, with insertion into the *Lhcb6* gene, and SALK_014869, with insertion into the *Lhcb5* gene, were obtained from NASC collections (Alonso et al., 2003). An additional T-DNA insertion mutant into the *Lhcb6* gene (*Arabidopsis* Gene Trap line GT6248, Landsberg *erecta* ecotype) was obtained form Cold Spring Harbor Laboratory (Sundaresan et al., 1995). This allele is indicated as koCP24*lan*, and the corresponding control genotype as WT*lan*. Homozygous plants were identified by immunoblot analysis. Individual mutants were crossed, and F1 seeds were grown and self-fertilized to obtain the F2 generation. Homozygous double mutant plants were selected in the F2 population by immunoblotting with specific antibodies. Mutants were grown for 4 to 6 weeks at 100 $\mu$mol photons $m^{-2}$ $s^{-1}$, 21°C, 90% humidity, and 8 h of daylight.

### Pigment Analysis

Pigments were extracted from leaf discs, either dark-adapted or light-treated (30 min, 1000 $\mu$mol photons $m^{-2}$ $s^{-1}$) at room temperature (22°C): samples were frozen in liquid nitrogen, ground in 85% acetone buffered with $Na_2CO_3$, and then the supernatant of each sample was recovered after centrifugation (15 min at 15,000*g*, 4°C); separation and quantification of pigments were performed by HPLC (Gilmore and Yamamoto, 1991) and by fitting of the spectrum of the acetone extract with spectra of individual pigments (Croce et al., 2002) and recorded using an Aminco DW-2000 spectrophotometer (SLM Instruments).

### Thylakoid Isolation and Sample Preparation

Unstacked thylakoids were isolated from leaves as previously described (Bassi et al., 1988), while functional chloroplasts for ETR and $\Delta$pH measurements were obtained as described (Casazza et al., 2001).

### Gel Electrophoresis and Immunoblotting

SDS-PAGE analysis was performed with the Tris-Tricine buffer system as previously described (Schägger and von Jagow, 1987). For immunotitration, thylakoid samples corresponding to 0.25, 0.5, 0.75, and 1 $\mu$g of chlorophyll were loaded for each sample and electroblotted on nitrocellulose membranes. Filters were incubated with antibodies raised against Lhcb1, Lhcb2, Lhcb3, CP29 (Lhcb4), CP26 (Lhcb5), CP24 (Lhcb6), PsbS, or CP47 (PsbB) and were detected with alkaline phosphatase–conjugated antibody, according to Towbin et al. (1979). Signal amplitude was quantified ($n = 4$) using the GelPro 3.2 software (Bio-Rad). To avoid any deviation between different immunoblots, samples were compared only when loaded in the same gel.

### Deriphat PAGE Analysis

Nondenaturing Deriphat-PAGE was performed following the method described previously (Peter et al., 1991), but using 3.5% (w/v) acrylamide (38:1 acrylamide/bisacrylamide) in the stacking gel and in the resolving gel and an acrylamide concentration gradient from 4.5 to 11.5% (w/v) stabilized by a glycerol gradient from 8 to 16%. Thylakoids concentrated at 1 mg/mL chlorophyll were solubilized with a final 0.8% $\alpha$-DM, and 30 $\mu$g of chlorophyll were loaded in each lane. The integrated optical density measured in each band was checked to linearly correlate to the chlorophyll amounts present in each complex.

### EM

Intact leaf fragments from wild-type and mutant 3-week-old leaves, grown in control conditions, were fixed, embedded, and observed in thin section as previously described (Sbarbati et al., 2004).

EM on isolated grana membranes was conducted using an FEI Tecnai T12 electron microscope operating at 100 kV accelerating voltage. Samples were applied to glow-discharged carbon-coated grids and stained with 2% uranyl acetate. Images were recorded using a CCD camera (SIS Megaview III).

### In Vivo Fluorescence and NPQ Measurements

NPQ of chlorophyll fluorescence and PSII yield ($\Phi_{PSII}$) were measured on whole leaves at room temperature with a PAM 101 fluorimeter (Heinz-Walz). Minimum fluorescence ($F_0$) was measured with a 0.15 $\mu$mol $m^{-2}$ $s^{-1}$ beam, maximum fluorescence ($F_m$) was determined with a 0.6-s light pulse (4500 $\mu$mol $m^{-2}$ $s^{-1}$), and white continuous light (1200 $\mu$mol $m^{-2}$ $s^{-1}$) was supplied by a KL1500 halogen lamp (Schott). NPQ, $\Phi_{PSII}$, and relative ETR were calculated according to the following equation (Van Kooten and Snel, 1990): $NPQ = (F_m\text{-}F_m')/F_m'$, $\text{rel ETR} = \Phi_{PSII} \cdot \text{PAR}$, where $F_m$ is the maximum chlorophyll fluorescence from dark-adapted leaves, $F_m'$ the maximum chlorophyll fluorescence under actinic light exposure, $F_s$ the stationary fluorescence during illumination, and PAR the photosynthetic active radiations (white light, measured as $\mu$mol $m^{-2}$ $s^{-1}$).

State transition experiments were performed using whole plants according to established protocols (Jensen et al., 2000). Preferential PSII excitation was provided by illumination with blue light at an intensity of 40 $\mu$mol photons $m^{-2}$ $s^{-1}$ provided by a KL1500 lamp equipped with a 650-nm interference filter, and excitation of PSI was achieved using far-red light from an LED light source (Heinz-Walz; 102-FR) applied for 15 min simultaneously with red light. Periods of far-red and blue light conditions were used alternately, and the $F_m$ level in State I ($F_m'$) and State II ($F_m''$) was determined at the end of each cycle by the application of a saturating light pulse as described above.

Fluorescence induction kinetics was measured with a home-built apparatus. Fluorescence was excited using a green LED with a peak emission at 520 nm and detected in the near infrared. For the antenna size determination, leaf discs were infiltrated with 3.0 $10^{-5}$ M DCMU, 150 mM sorbitol, and 10 mM HEPES, pH 7.5. Variable fluorescence was induced with a green light of 7 $\mu$mol $m^{-2}$ $s^{-1}$. The time corresponding to two-thirds of the fluorescence rise ($T_{2/3}$) was taken as a measure of the functional antenna size of PSII (Malkin et al., 1981). In DCMU-treated leaves, rate of fluorescence rise depends on light intensity and functional antenna size of PSII. Thus, keeping the saturating flash intensity constant, PSII with higher functional antenna size will reduce all the available $Q_A$ pool more rapidly and will have a lower $T_{2/3}$ of fluorescence raise. This provides an estimate of the incident photon flux.

The reoxidation kinetics of $Q_A$ were measured as the decay of chlorophyll *a* fluorescence using a pulse-amplitude modulated fluorimeter (Heinz-Walz). Saturating single-turnover flashes obtained from a single turnover flash unit (Heinz Walz; XE-ST) were used to convert all $Q_A$ to $Q_A^-$. The variable fluorescence decay, reflecting the reoxidation of $Q_A^-$, was detected at 20-$\mu$s resolution. Data from 12 recordings were averaged.

### Measure of ΔpH

The kinetics of ΔpH formation across the thylakoid membrane was measured using the method of 9-AA fluorescence quenching, as previously described (Johnson et al., 1994). The reaction buffer composition was as follows: 0.1 M sorbitol, 5 mM $MgCl_2$, 10 mM NaCl, 20 mM KCl, 30 mM Tricine/NaOH, pH 7.8, 100 $\mu$M methylviologen, and 2 $\mu$M 9-aminoacridine. The chlorophyll concentration in the reaction buffer was adjusted to 20 $\mu$g/mL.

### ET with Artificial Donors and Acceptor

Linear ET from artificial donors to $NADP^+$ was measured in a dual-wavelength spectrophotometer (Unicam AA; Thermo scientific), while ET from PSII to PBQ and the whole ETR from water to $NADP^+$ were measured following the oxygen evolution. The $O_2$ production was measured on functional thylakoids at 20°C in a Clark-type oxygen electrode system (Hansatech Instruments) under red light illumination (150 $\mu$mol photons $m^{-2}$ $s^{-1}$). These measurements were performed as described by Casazza et al. (2001). $NADP^+$ reduction rate was measured spectrophotometrically, while oxygen evolution rate was measured with a Clark-type polarographic oxygen electrode system (as described in Casazza et al., 2001) under red light illumination (150 $\mu$mol $m^{-2}$ $s^{-1}$). Concentrations used were as follows: 0.5 mM $NADP^+$, 300 mM PBQ, 50 $\mu$M $DPIPH_2$ (dichlorophenlindophenol), 250 $\mu$M $TMPDH_2$ (*N*, *N*, *N*, *N*-tetramethyl-*p*-phenylene-diamine, reduced form), and thylakoids to a final chlorophyll concentration of 10 $\mu$g/mL.

### Accession Numbers

Sequence data from this article can be found in the Arabidopsis Genome Initiative or GenBank/EMBL databases under accession numbers At4g10340 (*LHCB5*) and At1g15820 (*LHCB6*).

### Supplemental Data

The following materials are available in the online version of this article.

**Supplemental Figure 1.** Micrograph of Negatively Stained Grana Partition Preparation Obtained by Limited $\alpha$-DM Solubilization of Stacked Thylakoids.

**Supplemental Figure 2.** Analysis of Pigment-Protein Complexes of the Wild Type and Mutant.

**Supplemental Figure 3.** Kinetics of Plastoquinol Reoxidation upon Exposure to Far-Red Light.

**Supplemental Figure 4.** Characterization of an Additional Allele for koCP24 (koCP24*lan*) Establishes That This Is the Responsible Mutation for the Observed Phenotype.

**Supplemental Figure 5.** Chlorophyll Fluorescence Induction Curves Measured on Grana Membrane Preparations from the Wild Type and koCP24 Mutant.

**Supplemental Figure 6.** $Q_A^-$ Reoxidation Kinetics.

**Supplemental Table 1.** NPQ Measurements on Intact Chloroplasts of the Wild Type and Mutant Genotypes.

### ACKNOWLEDGMENTS

We thank A. Sbarbati and P. Bernardi for the use of the EM facility at the University of Verona Medical Center. We also thank J. Lavergne (Commissariat à l'Energie Atomique, Cadarache, France) and P. Joliot (Institut de Biologie Physico-Chimique, Paris) for many discussion of PQ diffusion during the early postdoctoral visit of R.B. at Institut de Biologie Physico-Chimique. Financial support for this work was provided by the RBLA0345SF_002 Grant of the Italian Ministry of Research.

Received September 19, 2007; revised February 21, 2008; accepted March 13, 2008; published April 1, 2008.

### REFERENCES

**Allen, J.F.** (1992). Protein phosphorylation in regulation of photosynthesis. Biochim. Biophys. Acta **1098:** 275–335.

**Alonso, J.M., et al.** (2003). Genome-wide insertional mutagenesis of *Arabidopsis thaliana.* Science **301:** 653–657.

**Andersson, J., Walters, R.G., Horton, P., and Jansson, S.** (2001). Antisense inhibition of the photosynthetic antenna proteins CP29 and CP26: Implications for the mechanism of protective energy dissipation. Plant Cell **13:** 1193–1204.

**Andersson, J., Wentworth, M., Walters, R.G., Howard, C.A., Ruban, A.V., Horton, P., and Jansson, S.** (2003). Absence of the Lhcb1 and Lhcb2 proteins of the light-harvesting complex of photosystem II - Effects on photosynthesis, grana stacking and fitness. Plant J. **35:** 350–361.

**Asada, K.** (1999). The water-water cycle in chloroplasts: Scavenging of active oxygens and dissipation of excess photons. Annu. Rev. Plant Physiol. Plant Mol. Biol. **50:** 601–639.

**Ballottari, M., Dall'Osto, L., Morosinotto, T., and Bassi, R.** (2007). Contrasting behavior of higher plant photosystem I and II antenna systems during acclimation. J. Biol. Chem. **282:** 8947–8958.

**Barber, J., and Andersson, B.** (1992). Too much of a good thing - Light can be bad for photosynthesis. Trends Biochem. Sci. **17:** 61–66.

**Baroli, I., Do, A.D., Yamane, T., and Niyogi, K.K.** (2003). Zeaxanthin accumulation in the absence of a functional xanthophyll cycle protects *Chlamydomonas reinhardtii* from photooxidative stress. Plant Cell **15:** 992–1008.

**Bassi, R., and Dainese, P.** (1992). A supramolecular light-harvesting complex from chloroplast Photosystem II membranes. Eur. J. Biochem. **204:** 317–326.

**Bassi, R., Giuffra, E., Croce, R., Dainese, P., and Bergantino, E.** (1996). Biochemistry and molecular biology of pigment binding proteins. In Light an an Energy Source and Information Carrier in Plant Physiology, R.C. Jennings, G. Zucchelli, F. Ghetti, and G. Colombetti, eds (New York: Plenum Press), pp. 41–63.

**Bassi, R., Rigoni, F., Barbato, R., and Giacometti, G.M.** (1988). Light-harvesting chlorophyll a/b proteins (LHCII) populations in phosphorylated membranes. Biochim. Biophys. Acta **936:** 29–38.

**Bennoun, P.** (2001). Chlororespiration and the process of carotenoid biosynthesis. Biochim. Biophys. Acta **1506:** 133–142.

**Boekema, E.J., van Breemen, J.F., van Roon, H., and Dekker, J.P.** (2000). Arrangement of photosystem II supercomplexes in crystalline macrodomains within the thylakoid membrane of green plant chloroplasts. J. Mol. Biol. **301:** 1123–1133.

**Boekema, E.J., van Roon, H., van Breemen, J.F., and Dekker, J.P.** (1999). Supramolecular organization of photosystem II and its light-harvesting antenna in partially solubilized photosystem II membranes. Eur. J. Biochem. **266:** 444–452.

**Bonente, G., Howes, B.D., Caffarri, S., Smulevich, G., and Bassi, R.** (2007). Interactions between the photosystem II subunit psbs and xanthophylls studied in vivo and in vitro. J. Biol. Chem., in press.

**Briantais, J.-M.** (1994). Light-harvesting chlorophyll a-b complex requirement for regulation of Photosystem II photochemistry by non-photochemical quenching. Photosynth. Res. **40:** 287–294.

**Briantais, J.-M., Vernotte, C., Picaud, M., and Krause, G.H.** (1980). Chlorophyll fluorescence as a probe for the determination of the photoinduced proton gradient in isolated chloroplasts. Biochim. Biophys. Acta **591:** 198–202.

**Butler, W.L., and Strasser, R.J.** (1978). Effect of divalent cations on energy coupling between the light harvesting chlorophyll a/b complex and photosystem II. In Proceedings of the 4th International Congress on Photosynthesis, D.O. Hall, J. Coombs, and T. Goodwin, eds (London: Biochemical Society), pp. 9–20.

**Caffarri, S., Croce, R., Breton, J., and Bassi, R.** (2001). The major antenna complex of photosystem II has a xanthophyll binding site not involved in light harvesting. J. Biol. Chem. **276:** 35924–35933.

**Casazza, A.P., Tarantino, D., and Soave, C.** (2001). Preparation and functional characterization of thylakoids from *Arabidopsis thaliana.* Photosynth. Res. **68:** 175–180.

**Crimi, M., Dorra, D., Bosinger, C.S., Giuffra, E., Holzwarth, A.R., and Bassi, R.** (2001). Time-resolved fluorescence analysis of the recombinant photosystem II antenna complex CP29. Effects of zeaxanthin, pH and phosphorylation. Eur. J. Biochem. **268:** 260–267.

**Croce, R., Canino, G., Ros, F., and Bassi, R.** (2002). Chromophore organization in the higher-plant photosystem II antenna protein CP26. Biochemistry **41:** 7334–7343.

**Dall'Osto, L., Caffarri, S., and Bassi, R.** (2005). A mechanism of nonphotochemical energy dissipation, independent from Psbs, revealed by a conformational change in the antenna protein CP26. Plant Cell **17:** 1217–1232.

**Dekker, J.P., and Boekema, E.J.** (2005). Supramolecular organization of thylakoid membrane proteins in green plants. Biochim. Biophys. Acta **1706:** 12–39.

**Di Paolo, M. L., Peruffo dal Belin, A., and Bassi, R.** (1990). Immunological studies on chlorophyll-a/b proteins and their distribution in thylakoid membrane domains. Planta **181:** 275–286.

**Dominici, P., Caffarri, S., Armenante, F., Ceoldo, S., Crimi, M., and Bassi, R.** (2002). Biochemical properties of the PsbS subunit of photosystem II either purified from chloroplast or recombinant. J. Biol. Chem. **277:** 22750–22758.

**Durnford, D.G.** (2003). Structure and regulation of algal light-harvesting complex genes. In Photosynthesis in Algae, A.W.D. Larkum, S.E. Douglas, and J.A. Raven, eds (Dordrecht, The Netherlands: Kluwer Academic Publishers), pp. 63–82.

**Finazzi, G., Barbagallo, R.P., Bergo, E., Barbato, R., and Forti, G.** (2001). Photoinhibition of *Chlamydomonas reinhardtii* in State 1 and State 2: Damages to the photosynthetic apparatus under linear and cyclic electron flow. J. Biol. Chem. **276:** 22251–22257.

**Finazzi, G., Johnson, G.N., Dall'Osto, L., Joliot, P., Wollman, F.A., and Bassi, R.** (2004). A zeaxanthin-independent nonphotochemical quenching mechanism localized in the photosystem II core complex. Proc. Natl. Acad. Sci. USA **101:** 12375–12380.

**Ganeteg, U., Kulheim, C., Andersson, J., and Jansson, S.** (2004). Is each light-harvesting complex protein important for plant fitness? Plant Physiol. **134:** 502–509.

**Gilmore, A.M., and Yamamoto, H.Y.** (1991). Zeaxanthin formation and energy-dependent fluorescence quenching in pea chloroplasts under artificially mediated linear and cyclic electron transport. Plant Physiol. **96:** 635–643.

**Guo, J.W., Guo, J.K., Zhao, Y., and Du, L.F.** (2007). Changes of Photosystem II electron transport in the chlorophyll-deficient oilseed rape mutant studied by chlorophyll fluorescence and thermoluminescence. J. Integr. Plant Biol. **49:** 689–705.

**Harrer, R., Bassi, R., Testi, M.G., and Schäfer, C.** (1998). Nearest-neighbor analysis of a photosystem II complex from *Marchantia polymorpha* L.(liverwort), which contains reaction center and antenna proteins. Eur. J. Biochem. **255:** 196–205.

**Havaux, M., Dall'Osto, L., Cuine, S., Giuliano, G., and Bassi, R.** (2004). The effect of zeaxanthin as the only xanthophyll on the structure and function of the photosynthetic apparatus in *Arabidopsis thaliana.* J. Biol. Chem. **279:** 13878–13888.

**Horton, P., Ruban, A.V., and Walters, R.G.** (1996). Regulation of light harvesting in green plants. Annu. Rev. Plant Physiol. Plant Mol. Biol. **47:** 655–684.

**Jansson, S.** (1999). A guide to the Lhc genes and their relatives in Arabidopsis. Trends Plant Sci. **4:** 236–240.

**Jensen, P.E., Gilpin, M., Knoetzel, J., and Scheller, H.V.** (2000). The PSI-K subunit of photosystem I is involved in the interaction between light-harvesting complex I and the photosystem I reaction center core. J. Biol. Chem. **275:** 24701–24708.

**Johnson, G.N., Young, A.J., and Horton, P.** (1994). Activation of non-photochemical quenching in thylakoids and leaves. Planta **194:** 550–556.

**Joliot, P., and Joliot, A.** (1977). Evidence for a double hit process in photosystem II based on fluorescence studies. Biochim. Biophys. Acta **462:** 559–574.

**Joliot, P., and Joliot, A.** (2005). Quantification of cyclic and linear flows in plants. Proc. Natl. Acad. Sci. USA **102:** 4913–4918.

**Kovacs, L., Damkjaer, J., Kereiche, S., Ilioaia, C., Ruban, A.V., Boekema, E.J., Jansson, S., and Horton, P.** (2006). Lack of the light-harvesting complex CP24 affects the structure and function of the grana membranes of higher plant chloroplasts. Plant Cell **18:** 3106–3120.

**Larkum, A.W.D., and Vesk, M.** (2003). Algal plastids: Their fine structure and properties. In Photosynthesis in Algae, A.W.D. Larkum, S.E. Douglas, and J.A. Raven, eds (Dordrecht, The Netherlands: Kluwer Academic Publishers), pp. 11–28.

**Lavergne, J., and Joliot, P.** (1991). Restricted diffusion in photosynthetic membranes. Trends Biochem. Sci. **16:** 129–134.

**Ledford, H.K., Chin, B.L., and Niyogi, K.K.** (2007). Acclimation to singlet oxygen stress in *Chlamydomonas reinhardtii.* Eukaryot. Cell **6:** 919–930.

**Li, X.P., Bjorkman, O., Shih, C., Grossman, A.R., Rosenquist, M., Jansson, S., and Niyogi, K.K.** (2000). A pigment-binding protein essential for regulation of photosynthetic light harvesting. Nature **403:** 391–395.

**Li, X.P., Gilmore, A.M., Caffarri, S., Bassi, R., Golan, T., Kramer, D., and Niyogi, K.K.** (2004). Regulation of photosynthetic light harvesting involves intrathylakoid lumen pH sensing by the PsbS protein. J. Biol. Chem. **279:** 22866–22874.

**Li, X.P., Gilmore, A.M., and Niyogi, K.K.** (2002a). Molecular and global time-resolved analysis of a psbS gene dosage effect on pH- and xanthophyll cycle-dependent nonphotochemical quenching in photosystem II. J. Biol. Chem. **277:** 33590–33597.

**Li, X.P., Muller-Moule, P., Gilmore, A.M., and Niyogi, K.K.** (2002b). PsbS-dependent enhancement of feedback de-excitation protects photosystem II from photoinhibition. Proc. Natl. Acad. Sci. USA **99:** 15222–15227.

**Malkin, S., Armond, P.A., Mooney, H.A., and Fork, D.C.** (1981). Photosystem II photosynthetic unit sizes from fluorescence induction in leaves. Correlation to photosynthetic capacity. Plant Physiol. **67:** 570–579.

**Morosinotto, T., Baronio, R., and Bassi, R.** (2002). Dynamics of chromophore binding to Lhc proteins in vivo and in vitro during operation of the xanthophyll cycle. J. Biol. Chem. **277:** 36913–36920.

**Morosinotto, T., Bassi, R., Frigerio, S., Finazzi, G., Morris, E., and Barber, J.** (2006). Biochemical and structural analyses of a higher plant photosystem II supercomplex of a photosystem I-less mutant of barley. Consequences of a chronic over-reduction of the plastoquinone pool. FEBS J. **273:** 4616–4630.

**Morosinotto, T., Caffarri, S., Dall'Osto, L., and Bassi, R.** (2003). Mechanistic aspects of the xanthophyll dynamics in higher plant thylakoids. Physiol. Plant. **119:** 347–354.

**Munekage, Y., Hojo, M., Meurer, J., Endo, T., Tasaka, M., and Shikanai, T.** (2002). PGR5 is involved in cyclic electron flow around photosystem I and is essential for photoprotection in Arabidopsis. Cell **110:** 361–371.

**Munekage, Y., Takeda, S., Endo, T., Jahns, P., Hashimoto, T., and Shikanai, T.** (2001). Cytochrome b(6)f mutation specifically affects thermal dissipation of absorbed light energy in Arabidopsis. Plant J. **28:** 351–359.

**Niyogi, K.K.** (1999). Photoprotection revisited: Genetic and molecular approaches. Annu. Rev. Plant Physiol. Plant Mol. Biol. **50:** 333–359.

**Niyogi, K.K.** (2000). Safety valves for photosynthesis. Curr. Opin. Plant Biol. **3:** 455–460.

**Pesaresi, P., Sandona, D., Giuffra, E., and Bassi, R.** (1997). A single point mutation (E166Q) prevents dicyclohexylcarbodiimide binding to the photosystem II subunit CP29. FEBS Lett. **402:** 151–156.

**Peter, G.F., Takeuchi, T., and Thornber, J.P.** (1991). Solubilization and two-dimensional electrophoretic procedures for studying the organization and composition of photosynthetic membrane polypeptides. Methods **3:** 115–124.

**Rensing, S.A., et al.** (2007). The Physcomitrella genome reveals evolutionary insights into the conquest of land by plants. Science **319:** 64–69.

**Ruban, A.V., Walters, R.G., and Horton, P.** (1992). The molecular mechanism of the control of excitation energy dissipation in chloroplast membranes - Inhibition of ΔpH-dependent quenching of chlorophyll fluorescence by dicyclohexylcarbodiimide. FEBS Lett. **309:** 175–179.

**Ruban, A.V., Wentworth, M., Yakushevska, A.E., Andersson, J., Lee, P.J., Keegstra, W., Dekker, J.P., Boekema, E.J., Jansson, S., and Horton, P.** (2003). Plants lacking the main light-harvesting complex retain photosystem II macro-organization. Nature **421:** 648–652.

**Sane, P.V., Ivanov, A.G., Hurry, V., Huner, N.P., and Oquist, G.** (2003). Changes in the redox potential of primary and secondary electron-accepting quinones in photosystem II confer increased resistance to photoinhibition in low-temperature-acclimated Arabidopsis. Plant Physiol. **132:** 2144–2151.

**Sbarbati, A., Merigo, F., Benati, D., Tizzano, M., Bernardi, P., and Osculati, F.** (2004). Laryngeal chemosensory clusters. Chem. Senses **29:** 683–692.

**Schägger, H., and von Jagow, G.** (1987). Tricine-sodium dodecyl sulfate-polyacrylamide gel electrophoresis for the separation of proteins in the range from 1 to 100 kDa. Anal. Biochem. **166:** 368–379.

**Simpson, D.J.** (1979). Freeze-fracture studies on barley plastid membranes. 3. Location of the light-harvesting chlorophyll-protein. Carlsberg Res. Commun. **44:** 305–336.

**Simpson, D.J.** (1983). Freeze-fracture studies on barley plastid membranes. VI. Location of the P700-chlorophyll a-protein 1. Eur. J. Cell Biol. **31:** 305–314.

**Strasser, R.J., Srivastava, A., and Govindjee.** (1995). Polyphasic chlorophyll a fluorescence transient in plants and cyanobacteria. Photochem. Photobiol. **61:** 32–42.

**Sundaresan, V., Springer, P., Volpe, T., Haward, S., Jones, J.D., Dean, C., Ma, H., and Martienssen, R.** (1995). Patterns of gene action in plant development revealed by enhancer trap and gene trap transposable elements. Genes Dev. **9:** 1797–1810.

**Teardo, E., De Laureto, P.P., Bergantino, E., Dalla, V.F., Rigoni, F., Szabo, I., and Giacometti, G.M.** (2007). Evidences for interaction of PsbS with photosynthetic complexes in maize thylakoids. Biochim. Biophys. Acta **1767:** 703–711.

**Teramoto, H., Ono, T., and Minagawa, J.** (2001). Identification of Lhcb gene family encoding the light-harvesting chlorophyll-a/b proteins of photosystem II in *Chlamydomonas reinhardtii.* Plant Cell Physiol. **42:** 849–856.

**Towbin, H., Staehelin, T., and Gordon, J.** (1979). Electrophoretic transfer of proteins from polyacrylamide gels to nitrocellulose sheets: Procedure and some applications. Proc. Natl. Acad. Sci. USA **76:** 4350–4354.

**Tremmel, I.G., Kirchhoff, H., Weis, E., and Farquhar, G.D.** (2003). Dependence of plastoquinol diffusion on the shape, size, and density of integral thylakoid proteins. Biochim. Biophys. Acta **1607:** 97–109.

**Tremolieres, A., Dainese, P., and Bassi, R.** (1994). Heterogenous lipid distribution among chlorophyll-binding proteins of photosystem II in maize mesophyll chloroplasts. Eur. J. Biochem. **221:** 721–730.

**Vallon, O., Bulte, L., Dainese, P., Olive, J., Bassi, R., and Wollman, F.A.** (1991). Lateral redistribution of cytochrome b6/f complexes along thylakoid membranes upon state transitions. Proc. Natl. Acad. Sci. USA **88:** 8262–8266.

**Van Kooten, O., and Snel, J.F.H.** (1990). The use of chlorophyll fluorescence nomenclature in plant stress physiology. Photosynth. Res. **25:** 147–150.

**Walters, R.G., Ruban, A.V., and Horton, P.** (1996). Identification of proton-active residues in a higher plant light-harvesting complex. Proc. Natl. Acad. Sci. USA **93:** 14204–14209.

**Wentworth, M., Ruban, A.V., and Horton, P.** (2003). Thermodynamic investigation into the mechanism of the chlorophyll fluorescence quenching in isolated photosystem II light-harvesting complexes. J. Biol. Chem. **278:** 21845–21850.

**Yakushevska, A.E., Keegstra, W., Boekema, E.J., Dekker, J.P., Andersson, J., Jansson, S., Ruban, A.V., and Horton, P.** (2003). The structure of photosystem II in Arabidopsis: Localization of the CP26 and CP29 antenna complexes. Biochemistry **42:** 608–613.

# Supplementary materials

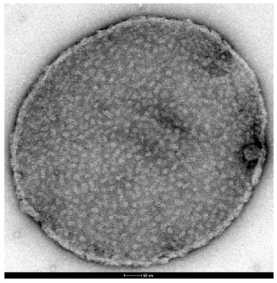

**Figure S1.**

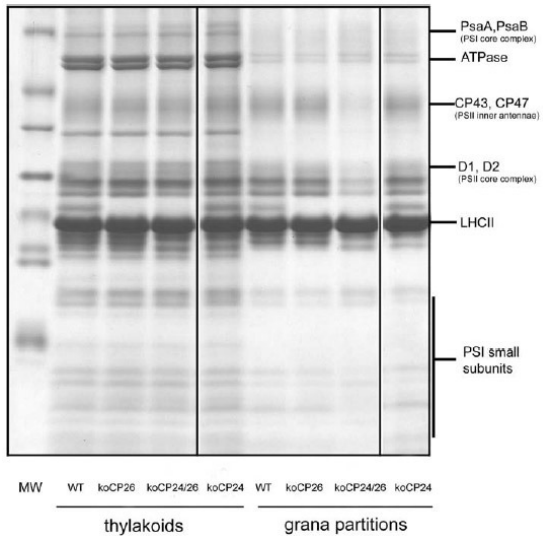


**Figure S2.**

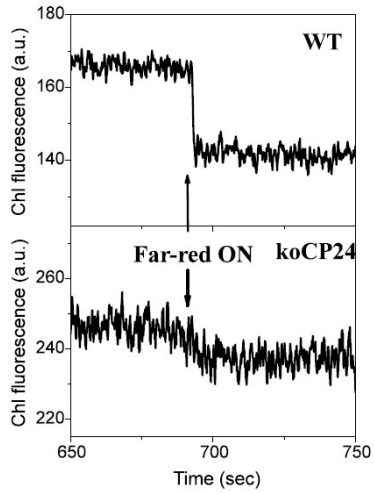


**Figure S3.**

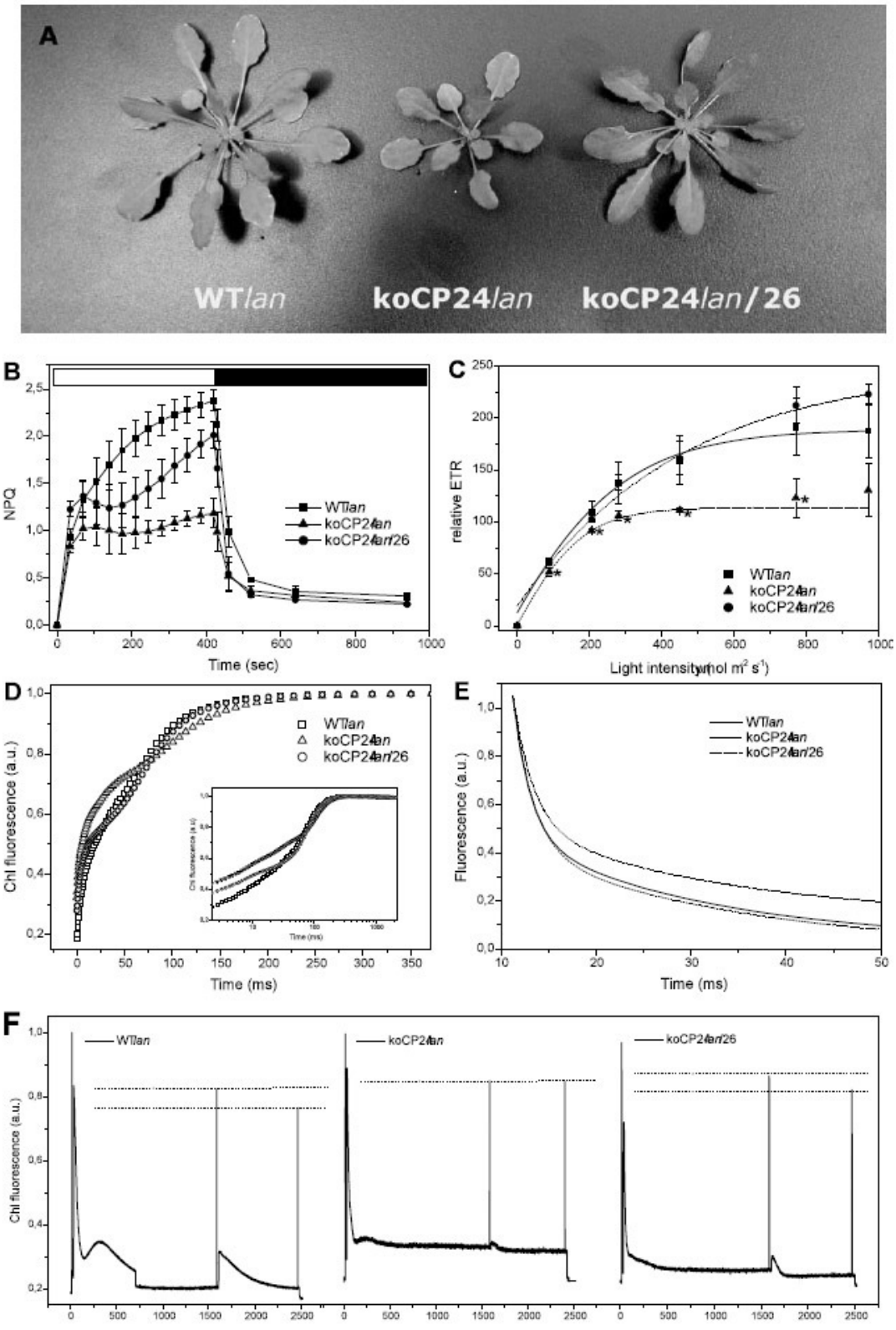
A
WTlan
koCP24lan
koCP24lan/26
B
NPQ
Time (sec)
WTlan
koCP24lan
koCP24lan/26
C
relative ETR
Light intensity (µmol m-2 s-1)
WTlan
koCP24lan
koCP24lan/26
D
Chl fluorescence (a.u.)
Time (ms)
WTlan
koCP24lan
koCP24lan/26
E
Fluorescence (a.u.)
Time (ms)
WTlan
koCP24lan
koCP24lan/26
F
Chl fluorescence (a.u.)
WTlan
koCP24lan
koCP24lan/26

**Figure S4.**

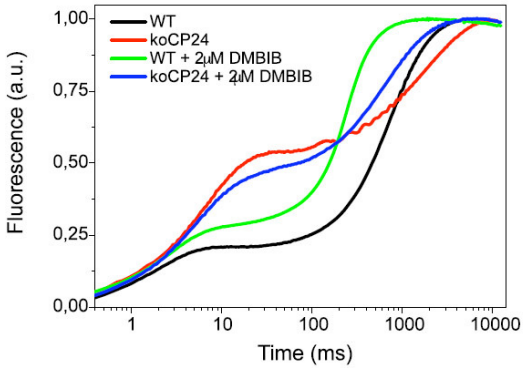


**Figure S5.**

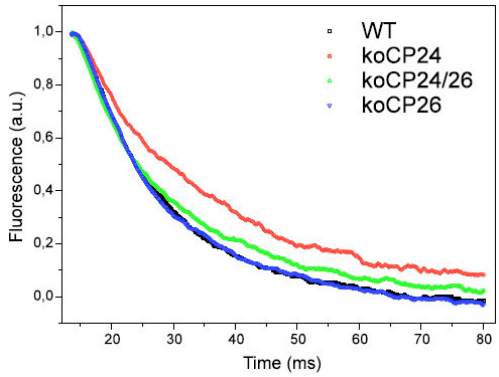


**Figure S6.**

| | WT | koCP24 | koCP26 | koCP24/26 |
|---|---|---|---|---|
| NPQ | 0.76 ± 0.21 | 0.41 ± 0.07 | 0.76 ± 0.07 | 0.68 ± 0.01 |

**Table S1.**

**Supplemental Figure S1**. **Micrograph of negatively stained grana partition preparation obtained by limited α-DM solubilization of stacked thylakoids.** WT and mutants yielded circular membrane patches of similar shape and size consistent with the diameter of grana stacks as observed in figure 2. The bar is 50 nm.

**Supplemental Figure S2. Analysis of pigment-protein complexes of WT and mutant.** Pigmented complexes from thylakoids and BBY were separated by denaturing SDS-PAGE.

**Supplemental Figure S3. Kinetics of plastoquinol re-oxidation upon exposure to far-red light.** Details of Chl fluorescence traces described in Figure 11 shows decrease in stationary fluorescence (Fs) amplitude after oxidation of PQ obtained by turning on far-red light. Kinetics of Fs decrease depend on the rate of activation of kinase by reduced $PQH_2$.

**Supplemental Figure S4. Characterization of an additional allele for koCP24 (koCP24*lan*) establishes that this mutation is the only responsible of the observed phenotype.** (A) Phenotype of wild type and mutant plants, grown in control conditions for four weeks (100 µmol photons $m^{-2}s^{-1}$, 25°C, 8/16 h d/n). (B) Kinetics of non-photochemical quenching (NPQ) induction and relaxation. Chlorophyll fluorescence was measured in intact, dark-adapted leaves, during 8 min of illumination at 1260 µmol $m^{-2}s^{-1}$followed by 9 min of dark relaxation. (C) Relative ETR as a function of quantum flux density of the photosynthetically active radiation (PAR), measured fluorometrically in light-adapted leaves under saturating $CO_2$ (1%). (D) PSII fluorescence induction kinetics normalized to the $F_m$ value. (E) $Q_A^-$ re-oxidation kinetics. Chl fluorescence decay kinetics were measured after single-turnover flash illumination in dark-adapted leaves. Drawn lines are fits for the experimental data points. Experimental fluorescence curves were normalized to the corresponding Fm values and represent averages from 12 separate experiments. (F) Measurement of state 1-state 2 transitions.

**Supplemental Figure S5**. **Chl fluorescence induction curves measured on grana membrane preparations from WT and koCP24 mutant.** The grana membrane preparation was also analyzed for fluorescence induction kinetics in order to verify that the functional features detected in leaves were actually present in the membrane preparation analyzed by electron microscopy. KoCP24 fluorescence rise was faster than WT in the O-I transition while it reached $F_{max}$ at longer times than WT. Also the characteristics of koCP26 and koCP24/26 samples reproduced leaf results. In order to investigate if differences in $Q_A$ re-oxidation kinetics were due to a higher average distance between PSII $Q_B$ sites and cyt *b6f* into the grana stacks, PSII membranes were treated with the cyt *b6f* inhibitor DBMIB. Both WT and koCP24 grana samples exhibited a faster kinetic of fluorescence rise, i.e. $Q_A$ reduction, in the presence of DBMIB with respect to their controls, implying some electron transport component (i.e. cyt b6/f) was blocked by the treatment. However, this effect was similar in both samples, suggesting no important differences in the distribution of this electron carrier were present in WT with respect to koCP24. Transient fluorescence rise was induced with a saturating green light (1100 μmol $m^{-2}$ $s^{-1}$, 10 sec). Measurements were performed either in buffer solution (black, red traces) or in the presence of the Cyt *b6f* inhibitor DBMIB 2 μM + ascorbate 25 mM (green, blue traces).

**Supplemental Figure S6. $Q_A^-$ re-oxidation kinetics.** Chl fluorescence decay kinetics were measured after single-turnover flash illumination in dark-adapted leaves. The variable fluorescence decay, reflecting the re-oxidation of $Q_A$, was detected at 20 μs resolution. Experimental fluorescence curves were normalized to the corresponding Fm values and represent averages from 12 separate experiments.

**Supplemental Table S1. NPQ measurements on intact chloroplasts of WT and mutant genotypes.** Maximum values of non-photochemical quenching (NPQ) were recorded with a PAM fluorometer. Chlorophyll fluorescence was measured in intact, dark-adapted chloroplasts, the same used for 9-AA quenching measurements. NPQ was induced during 6 min of illumination at 1260 μmol $m^{-2}s^{-1}$followed by 6 min of dark relaxation. All data are expressed as mean ± SD, n=3.

## A.2 Lhcb4 depletion affects the stability of PSII supercomplex and impairs photoprotection.

### A.2.1 Introduction

Oxygenic photosynthesis, which exploits light as energy source to fuels ATP and NADPH production, as well as $CO_2$ fixation and synthesis of organic compounds, is accomplished by a series of reactions in the chloroplast. Light harvesting is the primary process in photosynthesis and consists into absorption of light and transfer of excitons to the photosynthetic reaction center (RC). Hundreds of chlorophyll (Chl) molecules are structurally organized into a light-harvesting system and functionally associated with a RC to form a Photosystem (PS)II unit.

PSII catalyzes the water splitting and electron transport to plastoquinone (PQ). Its light-harvesting system consists of two distinct types of pigment-protein complexes, binding chlorophylls and carotenoids: an inner antenna made by the plastid-encoded core subunits PsbB (CP47) and PsbD (CP43), which coordinate Chl *a* and $\beta$-carotene, and the outer antenna consisting into a number of Chl *a*/Chl *b*/xanthophylls binding light-harvesting complexes (Lhcbs) (Jansson, 1994). The most abundant antenna is LHCII (Thornber, 1969), which bind half of the thylakoid Chl molecules and serves as the main solar energy collector. It is organized into heterotrimers of Lhcb1, Lhcb2 and/or Lhcb3 (Jansson, 1994; Bassi et al., 1996; Jackowski and Jansson, 1998). Moreover, three monomeric minor antennae complexes called CP29, CP26 and CP24 (Bassi et al., 1996) are located in between the and the peripheral LHCII antenna, thus participating to the stabilization of the oligomeric PSII structure (Yakushevska et al., 2003). In *Arabidopsis*, single genes encode Lhcb5 (CP26) and Lhcb6 (CP24) subunits, while Lhcb4 (CP29) is encoded by three genes, highly conserved but differently expressed: isoforms lhcb4.1 and lhcb4.2 are found in equimolar amounts in thylakoids and their corresponding genes show similar expression levels, while lhcb4.3 is 20 times less expressed in control condition (Jansson, 1999). The polypeptide encoded by lhcb4.3 has not been detected in thylakoids, so far and is predicted to lack a large part of the C-terminal domain, a peculiar feature of Lhcb4.1 and Lhcb4.2 isoforms as compared to the rest of Lhc proteins; because of these differences it has been renamed as Lhcb8 (Klimmek et al., 2006).

A remarkable feature of antenna complexes is the ability to actively regulate PSII quantum efficiency through control mechanisms that optimize photosynthetic performance thus avoiding the damaging effects of excess light. Indeed, under stable irradiation, the efficiency of photosynthetic machinery is optimal for a given light intensity. Nevertheless, rapidly fluctuating light

intensity, temperature and water availability easily causes over-excitation of photosystems and leads to an increased chlorophyll excited state ($^1$Chl$^*$) lifetime, and an increased probability of Chl *a* triplet formation ($^3$Chl$^*$) by intersystem crossing and single oxygen ($^1O_2$) formation (Melis, 1999). Since $^3$Chl$^*$ production is a constitutive properties of antenna Chls (Mozzo et al. 2008), a plant's ability to activate photoprotection mechanisms and prevent damages is as important to its survival as its ability to harvest light. Safety systems have evolved to either detoxify reactive oxygen species (ROS) produced (Asada, 1999) or prevent their formation (Niyogi, 2000). Lhcbs are involved in a number of photoprotection mechanisms, being active in (i) controlling $^1$Chl$^*$ concentration with a set of inducible mechanisms, namely non-photochemical quenching (NPQ), that allows the harmless thermal dissipation of excess absorbed photons by PSII bulk antenna (Horton, 1996); (ii) quenching of $^3$Chl$^*$ and scavenging of ROS through xanthophylls bound to the complex; (iii) balancing excitation pressure between PSI and PSII by either short-term migration of phosphorylated LHCII between photosystems (Allen, 1992; Haldrup et al., 2001), or long-term reduction of PSII antenna size under prolonged over-excitation (Ballottari et al., 2007). Indeed, *ch1* mutant of *Arabidopsis* reveals that Lhcs are vital for effective photoprotection: in these plants, the lack of Chl *b* leads to degradation of Lhc proteins (Havaux et al., 2007) and mutant exhibits a strongly enhanced photoxidation in high light (HL) (Dall'Osto et al., 2010).

The specific role of individual Lhcs in photosynthesis has been investigated using reverse genetic. Antisense lines of *Arabidopsis* devoid of LHCII (Ruban et al., 2003) showed a reduced fitness for plants grown on field with respect to controlled climate conditions, while only minor differences were observed in growth rate, PSII quantum yield, photosynthetic rate at saturating irradiances and capacity for NPQ (Andersson et al., 2003).

Rather, several evidences suggested that minor antennae have a crucial role in the regulation of $^1$Chl$^*$ concentration and PSII photoprotection: (1) low lumenal pH results in protonation of CP26 and CP29 on specific glutamic acid residues (Pesaresi et al., 1997; Walters et al., 1996); (2) their allosteric L2 site can bind zeaxanthin (Zea) (Morosinotto et al., 2002), synthesized by a two-step deepoxidation of the existing violaxanthin when plants are exposed to excess light conditions (Demmig-Adams et al., 1989); (3) xanthophylls exchange, synergistically with protonation, leads to a conformational change that affect spectroscopic properties of complexes (Dall'Osto et al., 2005; Avenson et al., 2007).

*Arabidopsis* knockout lines that completely lack both CP26 and CP24 has been recently described (de Bianchi et al., 2008): overall electron transport, NPQ maximal amplitude, growth rate and photoprotection capacity of the double mutant were similar to wild type (WT). So far the specific role of

CP29 in light harvesting and energy dissipation was investigated in antisense transgenic lines depleted in the target protein; measurements showed photosynthetic electron transport rate (ETR) and sensitivity to photoxidative stress similar to the wild type, and minor changes in NPQ kinetic and amplitude (Andersson et al., 2001); however, the mild stress conditions tested leave the question open about the role of CP29 in photoprotection.
One additional motif of interest is that role of the three distinct Lhcb4 isoforms in *Arabidopsis* has never been addressed. Several evidence suggest that CP29 has important roles in both light harvesting and photoprotection: CP29 level with respect to PSII RC is maintained even under prolonged photoxidative stress (Ballottari et al., 2007). HL and/or low temperature stress leads to CP29 phosphorylation in both monocots (Testi et al., 1996) and dicots (Hansson and Vener, 2003; Tikkanen et al., 2006); in *Zea mays*, CP29 phosphorylating genotypes are resistant to cold stress (Bergantino et al. 2005, Mauro et al., 1997) and water stress (Liu et al., 2009). Phosphorylation affects spectral properties of CP29 increasing interactions between Chl molecules and decreasing fluorescence yield (Croce et al., 1996). Moreover, in maize thylakoids, CP29 was identified as an interaction partner of PsbS (Teardo et al., 2007), the trigger of qE (Li et al., 2000) which controls the light-dependent dissociation of a pentameric complex which is needed for NPQ (Betterle et al., 2009). In HL CP29 exchanges Viola with Zea upon lumen acidification (Bassi et al., 1997; Morosinotto et al., 2002) and can bind the qE (energy quenching) inhibitor DCCD (Pesaresi et al., 1997). Finally, CP29 has been suggested to host a quenching site catalyzing the formation of xanthophyll radical cation (Holt et al., 2005; Ahn et al., 2008).
In the present work, we have addressed the question of the function of CP29 and its different isoforms in *Arabidopsis thaliana*. To this aim, we have constructed knock-out mutants lacking one, two or three Lhcb4 isoforms and analyzed their performance in photosynthesis and photoprotection. We found that PSII quantum efficiency and capacity for NPQ were affected by lack of CP29. Photoprotection efficiency was lower in koLhcb4 plants with respect to either WT or mutants retaining a single Lhcb4 isoform. Interestingly, while deletion of either isoforms Lhcb4.1 or Lhcb4.2 yields into a compensatory accumulation of the remaining subunit, the double mutant Lhcb4.1/4.2 did not accumulate Lhcb4.3. Instead lacks of CP29 (koLhcb4) did not result in any significant alteration in linear/cyclic electron transport rate and amplitude of state transition.

### A.2.2 Materials and Methods

*Plant material and growth conditions - Arabidopsis thaliana* T-DNA insertion mutants (*Columbia ecotype*) GK Line ID282A07 (insertion into

the *lhcb4.1* gene), SAIL_910_D12 (insertion into the *lhcb4.2* gene) and SALK_032779 (insertion into the *lhcb4.3* gene) were obtained from NASC collections (Alonso et al., 2003). Homozygous plants were identified by PCR analysis using the following primers:
forward 5'-TCACCAGATAACGCAGAGTTTAATAG-3' and reverse
5'-CACATGATAATGATTTTAAGATGAGGAG-3' for *lhcb4.1* sequence,
5'-CCATATTGACCATCATACTCATTGC-3' for the insertion; forward
5'-GCGTTTGTGTTTAGCGTTTCGACATCTGTCTG-3' and reverse
5'-GGTACCCGGGTGGTTTCCGACATTAGC-3' for *lhcb4.2* sequence,
5'-GCCTTTTCAGAAATGGATAAATAGCCTTGCTTCC-3' for the insertion; forward 5'-GTGAGCTGATCCATGGAAGGTGG-3' and reverse
5'-GGCCGGTTTTGAACGATTGATGTGAC-3' for *lhcb4.3* sequence
and 5'-GCGTGGACCGCTTGCTGCAACT-3' for the insertion.
Genotypes koLhcb4, koLhcb4.1/4.2, koLhcb4.2/4.3 and koLhcb4.1/4.3 were obtained by crossing single mutant plants and selecting progeny by PCR analysis. For reverse transcriptase-mediated-PCR, total RNA was isolated from 4-weeks old plants with Trizol protocol for RNA extraction. Reverse transcription was performed using M-MLV reverse transcriptase with oligo-dT primer and 1,5$\mu$g of total RNA from WT and mutant plants. For normalization purposes actin2 (At3g18780) was chosen as an endogenous control. The primers used were as follows:
5'-GTGGCTCCCGGTATCCATCC-3' and
5'-TTGAACCGCGAATCCCAAGAAGG-3' for lhcb4.1 cDNA;
5'-GGTTTCCGACATTAGCTCCAATTC-3' and
5'-CTGAACCGCAAAACCCAAGAATC-3' for lhcb4.2 cDNA;
5'-CCGGTTCGGGTTCAGTTTCGG-3'and
5'-GGCAAGGAAGCTGACAGGGC-3' for lhcb4.3 cDNA;
5'-CCTCATGCCATCCTCCGTCTTG-3'
and 5'-GAGCACAATGTTACCGTACAGATCC-3' for actin2 cDNA.
*Arabidopsis* T-DNA insertion mutant koLhcb3 (SALK_020342) from NASC was obtained by selecting progeny by western-blotting using specific antibody against Lhcb3 subunit; asLHCII (Andersson et al., 2003) was obtained by NASC (N6363). *Arabidopsis* insertion mutants koLhcb6 and koLhcb5/Lhcb6 were isolated as previously described (de Bianchi et al., 2008). Mutants were grown for 5 weeks at 100 $\mu$mol photons $m^{-2}s^{-1}$, 21°C, 70% humidity, and 8 h of daylight.
*Stress conditions* - Short-term HL treatment was performed for 45 min at 1200 $\mu$mol photons $m^{-2}s^{-1}$ at RT (24°C) in order to measure kinetic of zeaxanthin accumulation on detached leaves. Samples for HPLC analysis were rapidly frozen in liquid nitrogen prior to pigment extraction. Longer photo-oxidative stress was induced by exposing whole plants to 500 $\mu$mol photons $m^{-2}s^{-1}$ at 4°C and 900 $\mu$mol photons $m^{-2}s^{-1}$ at 4°C, for 8 and

10 days, and 1600 $\mu$mol photons $m^{-2}s^{-1}$ at 24°C for 10 days. Light was provided by halogen lamps (Focus 3, Prisma, Italy) and filtered through a 2-cm recirculation water layer to remove infrared radiation.

*Pigment analysis* - Pigments were extracted from leaf discs, either dark-adapted or HL-treated, with 85% acetone buffered with $Na_2CO_3$, then separated and quantified by HPLC (Gilmore and Yamamoto, 1991).

*Membrane isolation* - Unstacked thylakoids were isolated from dark-adapted or HL-treated leaves as previously described (Bassi et al., 1988).

*Gel Electrophoresis and Immunoblotting* - SDS-PAGE analysis was performed with the Tris-Tricine buffer system as previously described (Schägger and von Jagow, 1987), with the addition of 7M urea to the running gel in order to separate Lhcb4 isoforms. Non-denaturing Deriphat-PAGE was performed following the method developed by Peter et al., 1991 with modification previously described (Havaux et al., 2004). Thylakoids concentrated at 1 mg/ml chlorophylls were solubilised with a final 0.7% $\alpha$-DM, and 25 $\mu$g of chlorophyll were loaded in each lane. The integrated optical density measured in each band was checked to linearly correlate to the chlorophyll amounts present in each complex. For immunotitration, thylakoid samples corresponding to 0.25, 0.5, 0.75, and 1 $\mu$g of chlorophyll were loaded for each sample and electroblotted on nitrocellulose membranes. Filters were incubated with antibodies raised against Lhcb1, Lhcb2, Lhcb3, CP29 (Lhcb4), CP26 (Lhcb5), CP24 (Lhcb6), or CP47 (PsbB) and were detected with alkaline phosphatase-conjugated antibody, according to Towbin et al., 1979. Signal amplitude was quantified (n = 4) using the GelPro 3.2 software (Bio-Rad). To avoid any deviation between different immunoblots, samples were compared only when loaded in the same gel.

*In Vivo Fluorescence and NPQ Measurements* - NPQ of chlorophyll fluorescence was measured on whole leaves at room temperature with a PAM 101 fluorimeter (Heinz-Walz). Minimum fluorescence ($F_0$) was measured with a 0.15 $\mu$mol photons $m^{-2}s^{-1}$ beam, maximum fluorescence ($F_m$) was determined with a 0.6 s light pulse (4500 $\mu$mol photons $m^{-2}s^{-1}$), and white continuous light (1200 $\mu$mol photons $m^{-2}s^{-1}$) was supplied by a KL1500 halogen lamp (Schott). NPQ, $\phi$PSII, and relative ETR were calculated according to the following equation (Van Kooten and Snel, 1990): NPQ=($F_m$-$F_m$')/$F_m$', $\phi_{PSII}$=($F_m$'-$F_s$)/$F_m$', rel ETR=$\phi_{PSII}$·PAR, qP=($F_m$'-$F_s$)/($F_m$'-$F_0$) where $F_0$ is the fluorescence determined in darkness by a weak measuring beam, $F_m$ is the maximum chlorophyll fluorescence from dark-adapted leaves measured after the application of a saturating flash, $F_m$' the maximum chlorophyll fluorescence under actinic light exposure, $F_s$ the stationary fluorescence during illumination, and PAR the photosynthetic active radiations (white light).

State transition experiments were performed using whole plants according to established protocols (Jensen et al., 2000). Preferential PSII excitation

was provided by illumination with blue light (40 $\mu$mol photons $m^{-2}s^{-1}$) provided by a KL1500 lamp equipped with a short pass filter, and excitation of PSI was achieved using far-red light from a LED light source (Heinz-Walz; 102-FR) applied for 15 min simultaneously with blue light. Periods of far-red and blue light conditions were used alternately, and the $F_m$ level in State I ($F_{m1}$) and State II ($F_{m2}$) was determined at the end of each cycle by the application of a saturating light pulse as described above. The parameter qT (PSII cross section changes) was calculated as ($F_{m1}$-$F_{m2}$)/$F_{m1}$ (where $F_{m1/2}$ is the maximal fluorescence yield in State 1/2).

Fluorescence induction kinetics was recorded with a home-built apparatus in order to measure functional antenna size on leaves. $Sm/t_{F_{max}}$ was calculated from variable fluorescence curves induced with green light (1100 $\mu$mol photons $m^{-2}s^{-1}$) according to Strasser and Strasser 1995. For measurements of PSII functional antenna size, leaves were infiltrated with 30 $\mu$M DCMU and 150 mM sorbitol, and variable fluorescence was induced with a green light of 7 $\mu$mol photons $m^{-2}s^{-1}$. The reciprocal of time corresponding to two-thirds of the fluorescence rise ($T_{2/3}$) was taken as a measure of the functional antenna size of PSII (Malkin et al., 1981). For measurements of the PSII repair process, whole plants were illuminated at 4°C for 5 h to induce photoinhibition of PSII at 850 $\mu$mol photons $m^{-2}s^{-1}$, and restoration of the $F_v/F_m$ ratios was subsequently followed at irradiances of 15 $\mu$mol photons $m^{-2}s^{-1}$ (Aro et al., 1994).

*Analysis of P700 redox state* - Spectrophotometric measurements were performed using a LED spectrophotometer (JTS10, Biologic Science Instruments, France) in which absorption changes are sampled by weak monochromatic flashes (10-nm bandwidth) provided by light emitting diodes (LED). $P700^+$ reduction following a flash was assayed as detailed by Golding et al., 2004. Leaves were infiltrated with 500 $\mu$M DCMU in 150 mM sorbitol. A 200-ms saturating flash of red light ($\lambda_{max}$=630 nm; 3000 $\mu$mol photons $m^{-2}s^{-1}$) was delivered to the leaf, and changes in absorbance at 705 nm were used to measure the kinetic of $P700^+$ reduction. Oxidized P700 ($\Delta$Amax) was recorded during far-red light illumination (1500 $\mu$mol photons $m^{-2}s^{-1}$, $\lambda_{max}$=720 nm). The level of oxidized P700 in the leaf ($\Delta$A) was determined during illumination with red light (from 100 to 980 $\mu$mol photons $m^{-2}s^{-1}$, $\lambda_{max}$=720 nm) as previously described (Zygadlo et al., 2005). Antenna size of PSI was estimated according to Kim et al., 2009.

*Accession Numbers* - Sequence data from this article can be found in the *Arabidopsis* Genome Initiative or GenBank/EMBL databases under accession numbers At5g01530 (Lhcb4.1), At3g08940 (Lhcb4.2), At2g40100 (Lhcb4.3), At5g54270 (Lhcb3), At4g10340 (Lhcb5), At1g15820 (Lhcb6).

### A.2.3 Results

The construction of a plant missing CP29 (*koLhcb4*) complex requires the isolation of knock out mutants at three distinct loci, namely lhcb4.1, lhcb4.2 and lhcb4.3 (Jansson, 1999). We identified koLhcb4.1, koLhcb4.2, and koLhcb4.3 homozygous lines in seed pools obtained from the Nottingham *Arabidopsis* Stock Centre (NASC) by PCR analysis of genomic DNA using isoform-specific primers (Figure A.1A). Triple knock out mutant koLhcb4 was obtained by selection of the progeny from crossing of single mutant. PCR analysis confirmed that all Lhcb4 coding region carried T-DNA insertion in both alleles (Figure A.1A), while reverse-transcriptase-mediated PCR demonstrated that mRNAs of all Lhcb4 isoforms were absent in mutant (Figure A.1B). Moreover, from screening F2 generation it was possible to isolate double mutants expressing single Lhcb4 isoforms, namely koLhcb4.2/4.3 (retaining Lhcb4.1), koLhcb4.1/4.3 (retaining Lhcb4.2) and koLhcb4.1/4.2 (retaining Lhcb4.3). Thylakoid membranes isolated from koLhcb4 were depleted in the corresponding gene product (Figure A.1C). The most abundant isoforms, Lhcb4.1 and Lhcb4.2, were resolved by 7$\mu$M urea containing SDS-PAGE (see Additional Figure A.7). *koLhcb4* mutant did show significant reduction in growth with respect to the WT in control light lighting (100 $\mu$mol photons $m^{-2}s^{-1}$, 24°C, 8/16 day/night), and did not differ in either Chl content per leaf area or Chl/Car ratio. Instead, koLhcb4 plants showed a small but significant decrease in Chl *a*/Chl *b* ratio with respect to WT (Table I).

To determine if the mutations affected the capacity of the antenna system to transfer absorbed energy to reaction centers, we measured the functional antenna size of PSII on leaves by estimating the rise time of Chl florescence in the presence of DCMU. No significant differences were observed between koLhcb4 and WT (Table I), suggesting that the light-harvesting capacity was not affected despite the depletion in CP29. Analysis of the fluorescence induction in dark-adapted leaves (Butler and Strasser, 1978) revealed a higher $F_0$ value, and a significant decrease of maximum quantum efficiency of PSII ($F_v/F_m$) in koLhcb4 than the wild type. Thus, a larger fraction of absorbed energy is lost as fluorescence in the mutant, implying that the connection between the major LHCII complex and PSII RC is less efficient in the absence of CP29 minor antenna protein (Table I). Nevertheless parameter $S_m/t_{Fmax}$, that is used for quantification of PSII electron transport activity, was essentially the same in koLhcb4 than WT, thus implying that electron transport was not limited downstream of $Q_A^-$ in mutant leaves.

**Table I:** *Chl content and fluorescence induction parameters determined for leaves of wild-type and koLhcb4 plants.*

| | **Chl a/b** | **Chl/Car** | **$\mu$g Chl/cm$^2$** | **$F_0$** | **$F_v/F_m$** | **$t_{2/3F_{max}}$ (ms)** | **$Sm/t_{F_{max}}$ (ms$^{-1}$)** |
|---|---|---|---|---|---|---|---|
| **WT** | 3.06 ± 0.07 | 3.63 ± 0.08 | 20.7 ± 3.0 | 0.261 ± 0.012 | 0.790 ± 0.007 | 172 ± 13 | 1.12 ± 0.04 |
| **koLhcb4** | 2.83 ± 0.06 * | 3.58 ± 0.03 | 19.0 ± 1.1 | 0.195 ± 0.002 * | 0.747 ± 0.021 * | 164 ± 16 | 1.27 ± 0.06 |

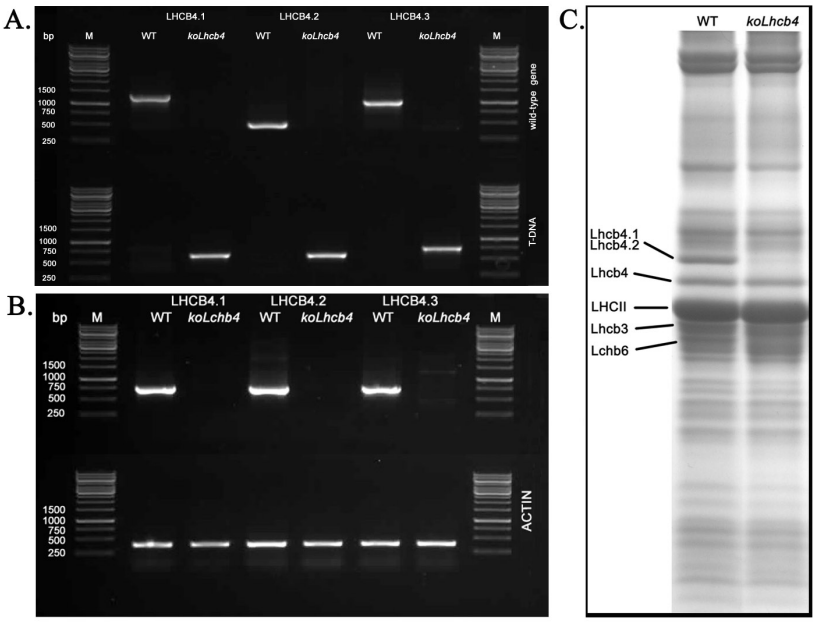


**Figure A.1:** *Genetic and biochemical characterization of koLhcb4 mutant.*
***A.****Amplification of lhcb4.1, lhcb4.2, lhcb4.3 loci with allele specific primer PCR. At the top the amplification using gene specific primer: 1378 bp, 520 bp, 1046 bp for the amplification respectively of lhcb4.1, lhcb4.2, lhcb4.3 locus. At the bottom amplification using a gene specific primer and the T-DNA specific primer: 697 bp, 661 bp, 773 bp for the amplification respectively of lhcb4.1, lhcb4.2, lhcb4.3 knock out locus . Details of primer sequence are reported in materials and methods.*
***B.****RT-PCR measurement of gene-specific transcripts. Sequences of the oligonucleotides used are reported in Materials and Methods. Top panel: for each gene, RNA extracted from WT and the corresponding mutant was subjected to reverse transcription, followed by 30 cycles of PCR amplification. Bottom panel: amplification of the actin2 control transcript from the same RNAs. M: molecular weight marker. The expected sizes of the PCR products are: lhcb4.1: 724 bp; lhcb4.2: 715 bp; lhcb4.3: 730 bp; ACTIN: 384 bp.*
***C.****SDS/PAGE analysis performed with the Tris-Tricine buffer system as previously described (Schägger and von Jagow, 1987), with the addition of 7M urea to the running gel in order to separate Lhcb4 isoforms. Selected apoprotein bands are marked. Fifteen micrograms of chlorophylls were loaded in each lane.*

## Organization and Stoichiometry of Pigment-Protein complexes

The organization of pigment-binding complexes was analyzed by non-denaturing Deriphat-PAGE. Upon solubilization of thylakoid membranes with 0.7% dodecyl-$\alpha$D-maltoside (DM) seven major green bands were resolved (Figure A.2C). In WT, the PSI-LHCI complex was found as a major band (B7) in the upper part of the gel while the components of the

PSII-LHCII migrated as multiple green band with different apparent mass, namely the PSII core dimer and monomer (B6 and B5, respectively) and the antenna moieties, including the CP29-CP24-(LHCII-M trimer) supercomplex (B4) (Bassi, 1992), LHCII trimer (B3), and monomeric Lhcbs (B2). Four faint green bands with high apparent molecular mass were detected in the upper part of the gel (B8) containing un-dissociated PSII supercomplexes with different LHCII composition. The major differences detected in koCP29 with respect to WT consisted into the lack of band 4 and a reduced level of PSII supercomplexes in koLhcb4 with respect to WT. Densitometric analysis of the green gels showed an higher PSI/PSII ratio in koLhcb4 mutant (1.38 ± 0.11) with respect to WT (1.04 ± 0.03). In order to detect possible alterations in the relative amount of pigment-protein subunits, we proceeded to determine the stoichiometry of photosynthetic subunits by immunoblotting tritation using CP47 (PsbB) as internal standard (Ballottari et al., 2007). The mutant koLhcb4 showed the complete absence of both Lhcb4 (CP29) and Lhcb6 (CP24) proteins (Figure A.2A), while there was a 60% increase in Lhcb5 (CP26) and Lhcb1 content (Figure A.2B) with respect to WT levels. Differences on PSI/PSII ratio between WT and koLhcb4, previously determined by densitometric analysis on green gel, were confirmed by quantitative immunoblot using PsaA and PsbB specific antibodies (Figure A.2B).

### Photosynthetic functions: electron transport rate and state transition.

Since pigment-protein complexes participate in modulating electron transport between photosystems, PSII and PSI function during photosynthesis was further analyzed by chlorophyll fluorometry. koLhcb4 showed no significant differences vs WT neither in the extent of PSII oxidized state (qP) nor in the ETR through PSII, measured on leaves at different light intensities in the presence of saturating $CO_2$ (Figure A.3 A,B). The capacity to adjust photosystems antenna size through reversible association of LHCII with either PSII and PSI, a process known as state transitions (Allen, 1992), was measured in koLhcb4 plants. According to a well established procedure, State I to State II transitions were measured from the changes in chlorophyll fluorescence level on leaves when PSI light was over-imposed to PSII light, and then PSI light was switched off to induce reduction of PQ pool (Jensen et al., 2000). The final extent of the state transitions observed after a 15 min illumination was the same in both genotypes, being qT not significantly different in WT and koLhcb4 (0.091 ± 0.002 and 0.091 ± 0.006, respectively) (Figure A.3 C,D); nevertheless, the rate of the transition from State I to State II upon switching off far-red light was considerably three times faster

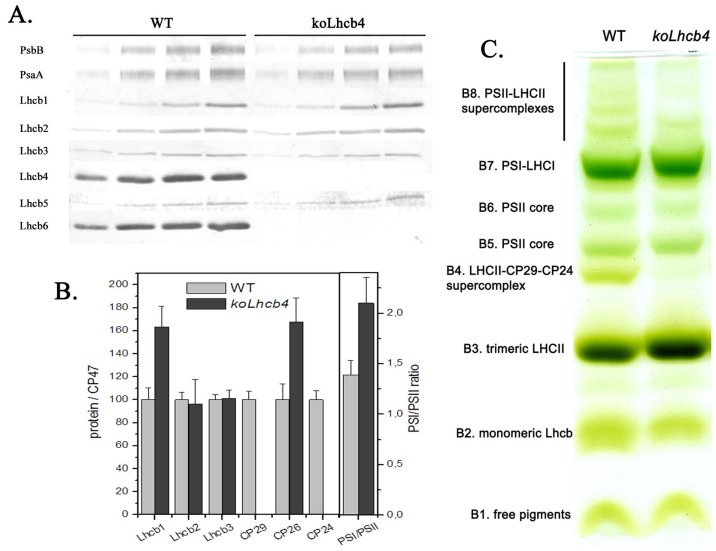


**Figure A.2:** *Polypeptide Composition of Thylakoid Membranes from Wild-Type and koLhcb4.*
***A.*** *Immunoblot analysis of thylakoid membranes with antibodies directed against individual gene products: minor antenna proteins, LHCII subunit, PSII core subunit PsbB (CP47) and PSI core subunit PsaA. Thylakoid samples corresponding to 0.25, 0.5, 0.75, and 1 μg of chlorophyll were loaded for each sample.*
***B.*** *Results from the immunotritation of thylakoids' proteins. PSII antenna subunits were normalized to the core amount, PsbB content (Ballottari et al., 2007). We also determined the ratio between the amount of the two photosystems as PsaA/PsbB ratio.*
***C.*** *Thylakoid pigmented complexes were separated by nondenaturing Deriphat-PAGE. 25 μg of chlorophyll were loaded in each lane.*

in koLhcb4 ($t_{1/2}$=71 ± 5 sec) with respect to WT ($t_{1/2}$=204 ± 17 sec). Fluorescence induction analysis on intact leaves showed an higher $F_0$ value, thus a less efficient connection between LHCII and PSII reaction center in the absence of Lhcb4 proteins (Table I); this finding is similar to results previously described for koCP24 mutants (Kovacs et al., 2006; de Bianchi et al., 2008) and was attributed to a looser association of M-trimers to PSII supercomplex and hence more easily moving towards stromal lamellae. If indeed lacks of Lhcb4 would affect the kinetic of LHCII distribution between photosystems, one might expect an effect on the oxidation state of PSI and/or an altered cyclic electron transport. Cyclic electron flow was determined by following the re-reduction of $P700^+$ using absorbance changes at 705 nm, upon far-red saturating flashes, on leaves infiltrated with DCMU (Figure A.4A). The fast decay component of $P700^+$, that has been attributed to CEF, showed no differences between WT and koLhcb4. In order to measure the photosynthetic electron flow through PSI during steady state photosynthesis *in vivo*, we measured the dependence of the P700 oxidation ratio ($\Delta A/\Delta A_{max}$) vs light intensity (Figure A.4B). The oxidation ratio of P700 in koLhcb4 approaches saturation around 600 $\mu$E, thus significantly faster than in WT. In contrast the PSI functional antenna size, measured by the rate coefficient of oxidation of P700 by steady far-red light after a saturating

flash, was the same in both genotypes (Figure A.4C). Therefore, the differential kinetics of P700 oxidation ratio can reasonably be attributed to the higher PSI/PSII ratio of koLhcb4 with respect to WT, as shown in Figure A.2.

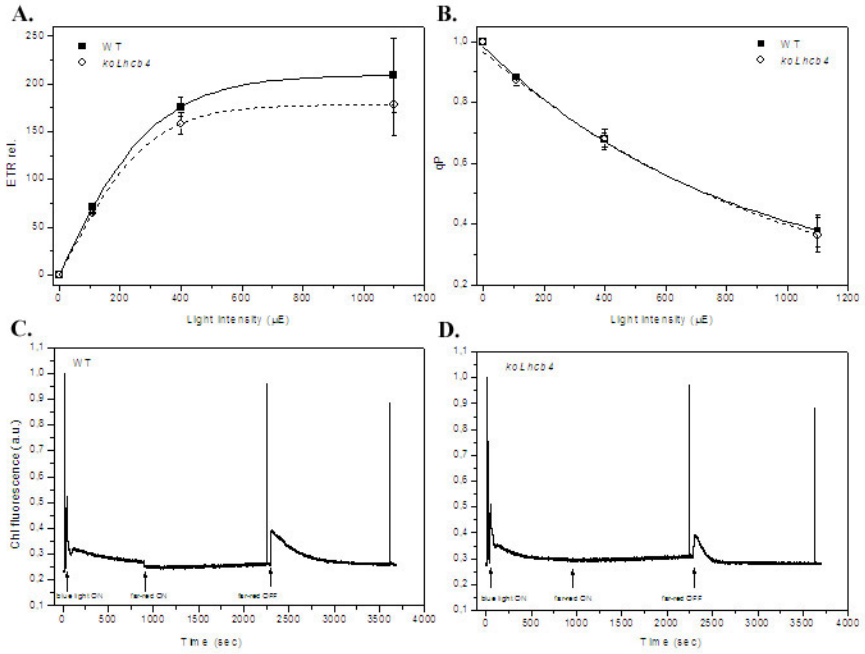


**Figure A.3:** *ETR, qP, state transitions of WT and koLhcb4.*
***A.*** *Dependence of the relative electron transport rate (ETR) on light intensity on wild-type and koCP29 leaves. RelETR is calculated as relETR=$\phi$PSII·PAR, where $\phi$PSII is the quantum yield of electron transfer at PSII and is a measure of the overall efficiency of PSII reaction centers in the light.*
***B.*** *Amplitude of photochemical quenching (qP) at different light intensities on wild-type and koCP29 leaves. qP reflects the redox state of the primary electron acceptor of PSII, $Q_A$.*
***C.*** *Measurement of State 1-State 2 Transition of WT and koCP29. Plants, upon dark adaptation for 1 h, were illuminated with blue light (40 µmol photons $m^{-2}s^{-1}$, wavelength <500 nm) for 15 min to reach State II. Far-red light source was used to induce transition to State I. Values of $F_m$, $F_m$', and $F_m$" were determined by light saturation pulses (4500 µmol photons $m^{-2}s^{-1}$, 0.6 s).*

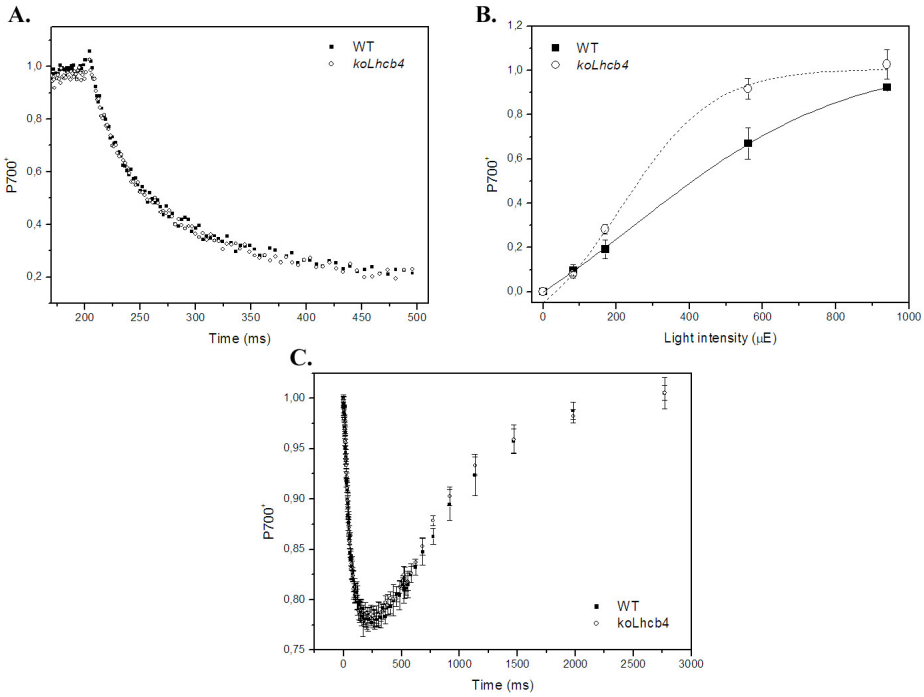


**Figure A.4:** *P700 measurements: cyclic ET, redox state P700, antenna size PSI.*
*A. The reduction of P700+ following a 200-ms flash of saturating red light (3000 µmol photons $m^{-2}s^{-1}$) in leaves of WT and koLhcb4 infiltrated with 500 µM DCMU. Leaves were infiltrated in the presence of 150 mM sorbitol, to avoid osmotic effects. The decay followed a complex curve, as described previously (Johnson, 2007). The fast component in this decay has previously been attributed to CEF and the slower reduction phases are thought to indicate the slower processes of redox equilibration occurring in the chloroplast (Johnson, 2007; Golding, 2003).*
*B. Dependence of the P700 oxidation ratio ($\Delta A/\Delta Amax$) on light intensity.*
*C. P700 oxidation of leaves illuminated with a far red background light (1400 µmol photons $m^{-2}s^{-1}$) after the application of a saturating flash of red light (3000 µmol photons $m^{-2}s^{-1}$).*

## Non-photochemical quenching of Chl fluorescence.

Antenna proteins have been implicated in thermal energy dissipation (Walters et al., 1996; Avenson et al., 2008), although the capacity of these complexes to activate NPQ is still under debate (Andersson et al., 2001; Ruban et al., 2007; de Bianchi et al., 2008; Barros et al., 2009). Therefore, we evaluated the capacity of koLhcb4 plants to induce thermal dissipation. WT had a NPQ of 2.5 after 8 min of illumination at 1200 $\mu$mol photons $m^{-2}s^{-1}$, according to literature data (Niyogi, 1999). koLhcb4 leaves, although showing a fast rise to a value of 1.0 in the first minute of illumination, where then delayed in further rise by 2-3 minutes vs WT reaching a value of 1.6 at 8 minutes; recovery in the dark was faster and more complete than in WT (Figure A.5A). Kinetics of formation and relaxation of NPQ were also analyzed during two successive 25 minutes of illumination, with 20 min of darkness in between (Figure A.5B). The kinetics of quenching formation confirmed that the extent of the rapid phase of NPQ was reduced koLhcb4

with respect to WT; furthermore, the slow phase was delayed in the first light period in koLhcb4 plants, while it exhibited a faster induction during the second light period, almost reaching WT level (Figure A.5B). In order to exclude that differences in NPQ induction kinetic were due to an impaired capacity for Zea synthesis at the onset of HL, we measured the time-course of Zea accumulation on both WT and koLhcb4 leaf discs, upon illumination at 1200 $\mu$mol photons $m^{-2}s^{-1}$ (Figure A.5C): de-epoxidation rate was the same in both genotypes at each time point, thus the reduction of NPQ amplitude in the first phase of illumination did not appear to be due to altered xanthophyll cycle activity, rather it is affected by loss of Lhcb4. In order to elucidate the contribution of the three CP29 isoforms to the early phases of energy quenching, we further analyzed the NPQ kinetics of *Arabidopsis* mutants expressing individual isoforms and results are reported on Figure A.5D. The mutant retaining Lhcb4.1 as the only CP29 isoform (koLhcb4.2/4.3) had an NPQ kinetic similar to the WT, thus showing that accumulation of Lhcb4.1 alone can fully restore NPQ to WT values. Instead the expression of the Lhcb4.2 isoform (koLhcb4.1/4.3) only partially recovered the quenching activity. Finally Lhcb4.3-only plants (koLhcb4.1/4.2) showed kinetic of NPQ similar to the koLhcb4, implying the presence of the Lhcb4.3 did not contribute to NPQ activity.

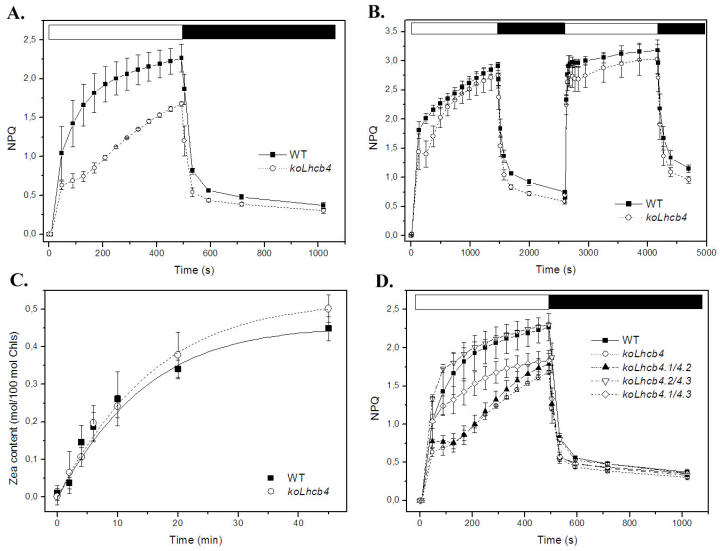


**Figure A.5:** *NPQ WTvsCP29, NPQ with Zea, Kinetic Zea formation at 1000 $\mu$mol photons $m^{-2}s^{-1}$, NPQ all isoforms.*
*A) NPQ kinetics of WT and koLhcb4 illuminated with 1200 $\mu$mol photons $m^{-2}s^{-1}$.*
*B) Kinetics of the formation and relaxation of photoprotective energy dissipation. Fluorescence was monitored in leaves of WT and koCP29 plants during two periods of illumination with white light ($\mu$mol photons $m^{-2}s^{-1}$) with a 20 min period of darkness in between, as indicated by the white and black bars.*
*C) Time course of violaxanthin deepoxidation in wild-type and koCP29 plants. Leaf discs from dark-adapted leaves were illuminated at 1200 $\mu$mol photons $m^{-2}s^{-1}$ (white actinic light). At different times, discs were frozen in liquid nitrogen and total pigments extracted.*
*D) NPQ kinetics of WT, koLhcb4 and the other mutants having only one of the three Lhcb4 isoform. The expression of the isoform Lhcb4.1 lead to complete compensation of the koLhcb4 NPQ phenotype, with a NPQ kinetic similar to WT one; instead the expression of the second isoform partially recovered the quenching ability, particularly in the first minutes of induction, but without reaching the WT final value in 8 minute of illumination.*

## Photosensitivity under short- and long-term stress conditions

Treatment of plants with strong light produces photoxidative stress, whose amplitude is enhanced in low temperature condition (Zhang and Scheller, 2004). In this conditions, enhanced release of $^1O_2$ produces bleaching of pigments, extensive lipid oxidation and PSII photoinhibition. Therefore photodamages can be measured as a decrease in the PSII photochemical efficiency ($F_v/F_m$ ratio). The sensitivity to photoxidative stress was assessed on whole plants, upon transfer from control conditions to high light at low temperature (500 $\mu$mol photons $m^{-2}s^{-1}$, 4°C) and stress was followed for 2 days monitoring the level of photoinhibition, assayed by chlorophyll fluorometry ($F_v/F_m$). Results are summarized in Figure A.6: HL treatment caused a decrease of $F_v/F_m$ from 0.8 to 0.4 in WT plants, while koLhcb4 showed a stronger photoinhibition. In order to evaluate the contribution of different Lhcb on photoprotection, we compared photoinhibition kinetics of different antenna mutants, namely koCP24/26, koLhcb3 and LHCII antisense plants (AsLHCII). Interestingly, mutants either lacking both minor

antennae CP24 and CP26 or LHCII or Lhcb3 did not show higher photodamage than WT when challenged in the same conditions (Figure A.6A). These results showed that koLhcb4 plants were the most sensitive to photoxidative stress among Lhcb mutants. Indeed the effects of Lhcb4 depletion were not compensated by over-accumulation of other Lhcbs subunits. Measurements of $F_v/F_m$ recovery after a photoinhibitory treatment clearly showed that WT and koLhcb4 leaves had the same kinetic of PSII quantum efficiency recovery (Additional Figure A.8), implying that the photosensitivity of mutant plants is due to a less effective photoprotection rather than to impaired PSII repair mechanism at low temperature (Aro et al., 1994).

In order to understand if different Lhcb4 isoforms had a specific role in chloroplast photoprotection, we measured the level of PSII photoinhibition on ko mutants expressing individual Lhcb4 isoforms. The accumulation of either Lhcb4.1 or Lhcb4.2 led to a recover in resistance to WT level, while the only expression of isoform Lhcb4.3 (koLhcb4.1/4.2 mutant) did no enhance photoprotection capacity with respect to koLhcb4 (Figure A.6). More detailed analysis were performed after 3 and 8 days of treatment with higher stress (900 $\mu$mol photons $m^{-2}s^{-1}$) by determining the leaf content of chlorophylls, molecules that are target of photoxidative stress. Mutants koLhcb4 and koLhcb4.1/4.2 underwent a significant reduction of leaf chlorophyll content upon stress treatment (Table II), while mutants lacking Lhcb4.3 only or retaining either Lhcb4.1 or Lhcb4.2 did not show this effect, thus confirming that compensatory accumulation of either Lhcb4.1 or Lhcb4.2 isoforms can restore photoprotection to WT level. Interestingly, the presence of wild type alleles of Lhcb4.3 as the only Lhcb4 isoform did not restore photoprotection to WT levels. To get further insights on the Lhcb4.3 expression and function, we tried to verify if this antenna protein isoform was accumulated upon several stress conditions: a) 500 $\mu$mol photons $m^{-2}s^{-1}$, 4°C for 2 days; b) 900 $\mu$mol photons $m^{-2}s^{-1}$, 4°C for 10 days; c) 1600 $\mu$mol photons $m^{-2}s^{-1}$, 24°C for 10 days. Thylakoids were isolated from WT, koLhcb4 and koLhcb4.1/4.2 at the end of stress, and protein content was analyzed by immunoblotting using an antibody that recognize all Lhcb4 apoproteins (Additional Figure A.9). Since no Lhcb4 polypeptides were detected in koLhcb4.1/4.2 for all conditions tested, we conclude that plants retaining the lhcb4.3 gene-only were unable to accumulating the gene product to a detectable level.

**Table II:** *Chl content of leaves illuminated at 900 $\mu$mol photons $m^{-2}s^{-1}$ for 8 days of wild-type and koLhcb4 plants.*

| | | $\mu$g Chl/cm$^2$ | | | | |
|---|---|---|---|---|---|---|
| | | **WT** | **koLhcb4** | **koLhcb4.2/4.3** | **koLhcb4.1/4.3** | **koLhcb4.1/4.2** |
| Days of stress | **0** | 21.7 ± 2.86 | 19.5 ± 0.16 | 23.5 ± 1.2 | 21.5 ± 2.1 | 22.2 ± 2.6 |
| | **3** | 19.1 ± 0.7 | 16.5 ± 1.6 * | 18.9 ± 2.6 | 17.7 ± 0.9 | 17.0 ± 1.4 * |
| | **8** | 20.3 ± 2.2 | 13.7 ± 1.7 * | 19.7 ± 2.0 | 18.1 ± 2.3 | 15.8 ± 1.8 * |

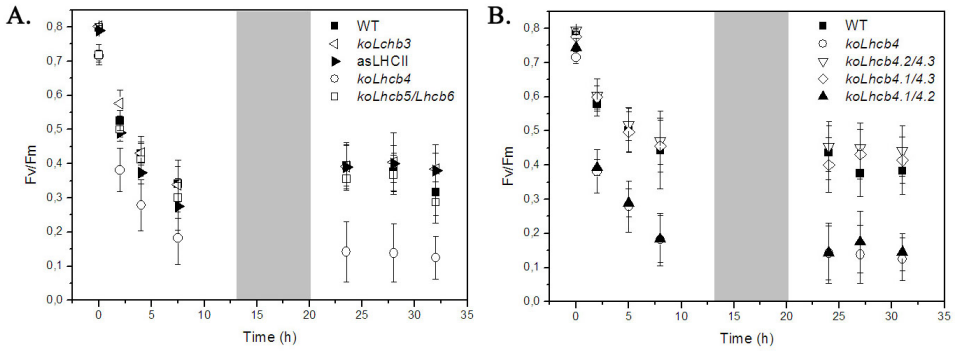


**Figure A.6:** *Photoinhibition WT vs koLhcb4 vs mutants of antenna.*
*Whole plants were treated at 500 µmol photons $m^{-2}s^{-1}$ and 4˚C for 30 hours with a 6-hour period of low light (20 µmol photons $m^{-2}s^{-1}$) between the 12 hours of HL stress. Low light interval permitted the PSII efficiency recovery. Panel A, WT versus koCP29, koCP26CP24, koLhcb3 and LHCII antisense. Panel B. WT, ko CP29 and isoform mutants.*

**Table III:** *Chl content and fluorescence induction parameters determined for leaves of WT, koLhcb4 and mutants lacking two Lhcb4 isoforms.*

| | **Chl a/b** | **Chl/Car** | **µg Chl/cm$^2$** | **$F_0$** | **$F_v/F_m$** | **$t_{2/3}$ (ms)** |
|---|---|---|---|---|---|---|
| **WT** | 3.06 ± 0.07 | 3.63 ± 0.08 | 20.7 ± 3.0 | 0.195 ± 0.002 | 0.790 ± 0.007 | 172 ± 13 |
| **koLhcb4** | 2.83 ± 0.06* | 3.58 ± 0.03 | 19.0 ± 1.1 | 0.253 ± 0.021 * | 0.747 ± 0.021* | 164 ± 16 |
| **koLhcb4.2/4.3** | 2,97 ± 0,03 | 3,70 ± 0,13 | 22,5 ± 1,2 | 0.213 ± 0.012 | 0.796 ± 0.004 | 172 ± 10 |
| **koLhcb4.1/4.3** | 2,97 ± 0,03 | 3,61 ± 0,09 | 22,6 ± 4,5 | 0.231 ± 0.012* | 0.777 ± 0.007* | 163 ± 21 |
| **koLhcb4.1/4.2** | 2,83 ± 0,09* | 3,63 ± 0,08 | 22,9 ± 2,5 | 0.266 ± 0.004* | 0.745± 0.007* | 178 ± 13 |

### A.2.4 Discussion

The loss of Lhcb4 in *A. thaliana* does not strongly affect growth rate, pigment compositions and photosynthetic performance of plants under control light conditions. Indeed, linear and cyclic electron transport rate are similar to wild-type plants as well as the functional antenna size (Figure A.3, Table I). Nevertheless, CP29-less plants showed a reduced photoprotection capacity when exposed to high irradiance at low temperature. The highest sensitivity to photoxidative stress of koLhcb4, amongst all other Lhcb knock-out mutants, is consistent with the higher reduction in fitness of plants lacking CP29 with respect to other PSII antenna mutants (Ganeteg et al., 2004; Andersson et al., 2001). This result confirms the importance of this gene product for plants performance both in artificial stress conditions and in the natural environment.

### Lack of Lhcb4 in *Arabidopsis* results in a compensatory modulation of the photosynthetic apparatus.

In order to investigate the role of Lhcb4 on light harvesting function, we first analyzed changes in the antenna systems upon Lhcb4 depletion. The kinetics of chlorophyll fluorescence, measured on leaves in the presence of DCMU, showed that the flux of photons trapped per reaction center, i.e. the PSII functional antenna size, is the same for both genotypes. Furthermore,

the parameter $S_m/t_{Fmax}$, expressing the average fraction of open reaction center during the time needed to complete their closure, is even higher in koLhcb4 with respect to WT plants, thus ruling out the possibility of an electron transport restriction in PSII due to lack of CP29 (Table I). We then proceeded to titrate the different Lhcb proteins with respect to PSII RC in WT and koLhcb4. We found that CP26 and Lhcb1 are over-accumulated by about 60%, thus suggesting compensation, at least for the light harvesting function, among Lhcb proteins according to previous reports (Ruban et al., 2003; de Bianchi et al., 2008). CP24 complex is completely missing (Figure A.2B), implying that removal of CP29 decreases its stability, consistent with CP29 being the docking site of CP24 (Andersson et al., 2001; Caffarri et al., 2009), both participating to a pentameric complex, called B4 complex, which connects inner and outer antenna system (Bassi et al. 1992, Betterle et al. 2009). Increased $F_0$ (Table I) clearly showed that the efficiency of excitation energy transfer from the antenna to the PSII reaction center is decreased. This is consistent with the results obtained in others ko mutants for monomeric Lhcbs (Kovacs et al., 2006; de Bianchi et al., 2008) while not such an effect was observed in AsLhcb1/Lhcb2 (Andersson et al., 2003). According to previous evidences (de Bianchi et al., 2008) this is due to the presence of disconnected LHCII domains. We can speculate that lack of CP29 and CP24 weakens the interactions of LHCII-M, which is directly interacting with CP29 through CP24, as well as of LHCII-L, consistent with the decreased molecular mass and relative abundance of PSII supercomplexes (Figure A.2C). Finally, an additional effect was observed in koLhcb4, consisting of an increase in the PSI/PSII ratio: both densitometric analysis of Deriphat-PAGE and immunotitration with specific antibodies, revealed that, while the mutant has a full complement of LHCII and PSI-LHCI (PsaA), PSII (PsbB) content is decreased by 25% in CP29-less plants (Figure A.2B, A.2C).

### Lack of Lhcb4 does not affect both the rate and regulation of photosynthetic electron transport.

State transition is the mechanism by which photosystems balance, by a reversible phosphorylation (Jensen et al., 2000; Allen and Nilsson, 1997), their complement of light-harvesting antennas (LHCII) depending on the reduction state of the intermediate electron carrier PQ. CP29 can be phosphorylated in *Arabidopsis* (Hansson and Vener, 2003) and phosphorylated Lhcb4 was associated in *C. reinhardtii* to PSI-LHCI supercomplexes only in state II (Takahashi et al., 2006); therefore, changes in state transitions could be expected in Lhcb4-less plants. Results displayed on Figures A.3 C-D show that koLhcb4 was not affected in its capacity to activate state

transition, being qT the same in both genotypes; indeed, WT and mutant do not differ in their capacity to undergo reduction of the plastoquinone pool and to activate Lhcb phosphorylation (Bellafiore et al., 2005), since the reduction state of PQ (qP value) is the same in both genotypes at all light intensities tested (Figure A.3B). Rather, we observe that in koCP29 the fluorescence changes induced by switching off the far-red light are faster than the wild type, implying that the transiently reduced state of the free PQ pool is more promptly relaxed with respect to wild type by migration of the LHCII to the RC of PSI. The same state transition phenotype has been described for koCP24 and koCP24/26 plants (de Bianchi et al., 2008) and it is a clear indication that the connection between PSII core and the bulk trimeric LHCII are partially impaired in these mutants as demonstrated by the increased $F_0$ value. In *C. reinhardtii*, state transitions do not only fulfil the role of balancing light absorption between photosystems, they also increase PSI electron flow at the expenses of that of PSII; thus it has been proposed that they allows a switch between linear and cyclic electron flow around PSI (Vallon et al., 1991). We investigated if this evidence is true also in *Arabidopsis*. Although lacks of Lhcb4 was shown to modulate state transitions kinetic, it does not affect neither linear (Figure A.3A) nor cyclic electron transport rate (Figure A.4). A final confirmation of the above results was obtained by the measurements of electron flow through PSI during steady state photosynthesis *in vivo*: indeed, the oxidation ratio of P700 in koLhcb4 approaches saturation much faster than in WT, thus showing an opposite phenotype than expected for a mutant blocked on cyclic electron transport (Munekage et al., 2004) (Figure A.4B). Since PSI functional antenna size was the same in both genotypes (Kim et al., 2009), differential kinetics of P700 oxidation ratio can reasonably be attributed to the higher PSI/PSII ratio of koLhcb4 with respect to WT (Figure A.2C).

### NPQ rise kinetic is affected by lack of Lhcb4.

A different pattern of NPQ rise kinetics is observed in koCP29 with respect to the wild type: the mutant reaches a lower qE amplitude at 8 min light and there is a clear plateau between 1 and 3 min, after which the kinetics rises up again (Figure A.5A), likewise to that measured on koCP24/26 double mutant (de Bianchi et al., 2008). This behavior could be ascribe to Zea synthesis. In fact, minor antenna proteins were shown to be effective in exchanging Viola with Zea (Morosinotto et al., 2003); Zea has been implicated in decreasing the activation energy required to the transition from unquenched to quenched conformation (Wentworth et al., 2003) upon perception of lumenal over-acidification signal, mediated by PsbS protonation (Li et al., 2004). Thus, lack of Lhcb4, while does not affect ETR and $\Delta$pH

build-up (Figure A.3A), seems to yields into a slower transduction of conformational change signal to Lhcb. KoLhcb4 lacks two of the three Zea-binding minor complexes (CP24 and CP29) and retains only CP26. Evidences for charge transfer quenching were recently described in all three of the individual minor antennae complexes of PSII (Ahn et al., 2008). The high level of qE in koLhcb4 (Figure A.5A) suggests that Lhcb5, that show a 60% compensatory increase in the mutant with respect to WT level and is the most effective in xanthophyll exchange (Dall'Osto et al., 2006; Morosinotto et al., 2003), might be able to counterbalance the missing CP29 and CP24. Alternatively, the major LHCII might play a role in qE as well: based on the slower onset of quenching in the mutant, it can be hypothesized that minor antennae mediate PsbS-dependent conformational changes on LHCII. The hypothesis that altered qE kinetic should be attributable to changes in the trans-thylakoid $\Delta$pH gradient, is unlikely since de-epoxidation kinetic of violaxanthin is the same in both WT and the mutant (Figure A.5C). It is worth noting that measurements of NPQ formation during a second, longer period of illumination reveals that both amplitude and kinetic of qE were barely indistinguishable from that of wild-type (Figure A.5D). The slower qE rise during the onset of first illumination suggest that lack of Lhcb4 slowed down the Zea-dependent transition to a quenching conformation of PSII, maybe due to a lower rate of xanthophyll exchange on remaining monomeric Lhcbs, while it appears unlikely that binding of Zea to V1 site of LHCII is differentially affected in WT and mutant plants. Indeed, longer light periods, that allows saturation of Zea binding to PSII, leads to a full qE expression, thus showing that residual Lhcb subunits can compensate, although with a lower rate, for the missing ones. Finally, we can look at the qI component of NPQ. Previous results supported a specific role of CP26 in catalyzing qI type of quenching (Dall'Osto et al., 2005) since koCP26 (koLhcb5) plants have reduced long-term fluorescence quenching (de Bianchi et al., 2008); instead, removal of Lhcb6 has negligible effect on qI amplitude, since double mutant koCP24/26 does not further decrease its qI level with respect to koLhcb5 (de Bianchi et al., 2008). Present results show that removal of Lhcb4 reduces the extent of qI as well (Figure A.5A), even upon prolonged illumination (Figure A.5B), thus suggesting that although Lhcb proteins might have overlapping functions, they each fulfil specific roles in light harvesting and photoprotection.

### Resistance to photoxidative stress is decreased in koLhcb4 plants with respect to wild-type.

PSII structural integrity is essential for the protection of the chloroplast from photoxidative stress (Bergantino et al., 2003; Horton and Ruban, 2005).

The koLhcb4 mutant specifically lacks CP29 and are more sensitive to stress caused by high-light treatment at low temperature. This effect cannot be ascribed to a pleiotropic effect of Lhcb4 depletion on photosynthetic electron transport efficiency, since lack of Lhcb4 does not affect either amplitude or the regulation of photosynthetic electron transport. Possible mechanisms underlying the increased photoinhibition *in vivo* are (1) the thermal dissipation of $^1Chl^*$ (qE and qI) (Johnson et al., 2007); (2) changes on PSII structural integrity (Ruan et al., 2001; Krieger et al., 1998). Depletion of Lhcb4 only affects qE at the onset of illumination, while NPQ bring its maximal amplitude near WT level on a longer timescale. Thus, we conclude that the differential resistance of WT vs koLhcb4 plants to HL stress is not due to differences on qE. We observed a steady increase in $F_0$ in koLhcb4 plants with respect to wild type, being a clear indication that the connection between PSII core complex and outer LHCII was partially impaired. Although we cannot exclude that higher sensitivity to HL of koLhcb4 could be due to LHCII disconnection, we notice that the koCP24/26 double mutant was clearly as resistant as wild-type plant, despite a $F_v/F_m$ reduction comparable to that of Lhcb4-less plants (de Bianchi et al., 2008). We conclude that the increased photosensitivity is a specific effect of the lack on CP29 (Lhcb4), which implies that CP29 has the highest importance in providing photoprotection with respect to all others Lhcb proteins. We can hypothesize that occupancy of Lhcb4 binding site into PSII might form a protective shield surrounding the PSII reaction center, thus subtracting core complexes from radical chain reactions of peroxy-lipids during photooxidative stress. Unlikely CP24 and CP26, Lhcb4 (CP29) is required for the binging of trimeric LHCII at any of the three binding positions inside PSII, thus allowing structural integrity of PSII (Boekema et al., 1999). Therefore, despite compensatory increase of CP26, Lhcb4 (CP29) depletion on thylakoids may get into a less stable PSII supercomplex: indeed the extreme photosensitivity of *Arabidopsis* mutants such as *ch1* (Dall'Osto et al., 2010) can be ascribed to lacks of a proper organization of light-harvesting complexes surrounding the PSII reaction center. Thus, among light-harvesting complexes of PSII, Lhcb4 appears to be the most critical in optimizing PSII photoprotection: it appears to be the most ancient among proteins conserved during evolution and associated with PSII (Koziol et al., 2007), it maintains its stoichiometry with respect to the reaction centre even under stressing growth conditions which lead to depletion of others Lhcbs (Ballottari et al., 2007) and upon mutations that strongly modify xanthophyll composition of chloroplast (Havaux et al., 2004). Previous reports described rapidly induced phosphorylation of Lhcb4 in barley under water stress (Liu et al., 2009); furthermore, in monocots, full protection of reaction center under cold stress was achieved only in lines that were able to phosphorylate

CP29 (Mauro et al., 1997) through a mechanism that modulates spectral properties of the subunit and provides a mechanism for the regulation of PSII (Croce et al., 1996). Since phosphorylation of Lhcb4 was identified in thylakoid membranes of *Arabidopsis* as well (Hansson and Vener, 2003), we cannot exclude that higher photoinhibition of *Arabidopsis* koLhcb4 mutant in low temperature might be due to the absence of phosphorylated CP29.

### Effect of the accumulation of the individual isoforms on koLhcb4 phenotype

The koLhcb4 $F_0$ and NPQ phenotypes are differentially compensated when single Lhcb4 isoforms are expressed in double koLhcb4 mutants, yielding into a range of phenotypes. The Lhcb4.1 accumulation restores $F_v/F_m$ to WT levels, while Lhcb4.2 are only partially effective in this function (intermediate $F_v/F_m$ value between WT and koLhcb4) and Lhcb4.3 is completely inefficient, its decrease in $F_v/F_m$ is similar to the triple koLhcb4 (Table III). This last mutant expressing Lhcb4.3 as the only CP29 isoform also showed the same reduction in Chl $a/b$ ratio as measured in triple koLhcb4, thus being a first evidence that removal of the most abundant isoforms of CP29 (Lhcb4.1 and Lhcb4.2) in *Arabidopsi*s (Jansson, 1999) does not result in the compensatory accumulation of Lhcb4.3 (Table III). The analysis of NPQ kinetic on mutants expressing single Lhcb4 isoforms reveals that only accumulation of subunit Lhcb4.1 can restore the quenching capacity to WT level, while Lhcb4.2 expression gets into a partial recovery of wild-type pattern of NPQ rise (Figure A.5D); differential behavior between Lhcb4.1 and Lhcb4.2 isoforms in modulating NPQ might be due to specific functional features of subunits, although it cannot be excluded it arises by differences in Lhcb4 content (Additional Figure A.7): the total Lhcb4 content is higher when only the first isoform (Lhcb4.1) is expressed than in the mutant with only the second (Lhcb4.2). *Arabidopsis* expressing Lhcb4.3 as the only CP29 isoform showed NPQ kinetics indistinguishable from that of koLhcb4 plants: this is consistent with the $F_0$ value and with the evidence that no Lhcb4 subunits can be detected by western blot in double mutant koLhcb4.1/4.2 (Additional Figure A.9). The compensating behavior of this isoform in stressed condition is quite different: Lhcb4.1 and Lhcb4.2 showed the same compensatory phenotype consisting into an increase of the photoprotection of mutant with a single isoforms expressed. Mutants koLhcb4.1/4.2, instead, showed the same stressed phenotype of koLhcb4 giving another evidence that the third isoform seems not to be expressed. In fact although Lhcb4.3 is transcribed under stress conditions (Dall'Osto et al 2010 unpubblished), we were unable to detect the corresponding protein even by keeping plants under a variety of stress conditions. It should

be noted that our antibody is effective in detecting recombinant Lhcb4.3 expressed in *E. coli* (Additional Figure A.9). This raises the question of what lhcb4.3 sequence actually represents. This gene appeared recently in plant genome: its sequence is not present in algal genomes and no orthologous were found in the moss *Physcomitrella patens*, thus appearing only at later stages in the evolution of the green lineage (Alboresi et al., 2008). In agreement with these evolutionary considerations, it seems unlikely that a new gene conserved in higher plants has no function or is not translate at all. EST data from *Arabidopsis* show that lhcb4.3 is expressed at very low level (Jansson, 1999), and its expression seem confined to dicots (Yu 2002, Goff 2002); furthermore, clustering analysis of Lhc superfamily expression data (Klimmek et al., 2006) confirmed the rarely expressed gene lhcb4.3 has a regulation pattern in *Arabidopsis* that clearly differs from that of the abundantly expressed Lhc proteins. Lhcb4.3 protein is shorter than other Lhcb4 isoforms and its sequence considerably differs from both Lhcb4.1 and Lhcb4.2 isoforms. It has been proposed (Klimmek et al., 2006) that protein subtypes branching at distance higher than the distance between Lhcb1/2 and Lhcb3 groups might have different functions: this is the case among Lhcb4.3 and Lhcb4.1/4.2 isoforms, the former appear as a unique Lhcb subtype that might fulfill a specific function. The Lhcbs expression profile in different tissue (https://www.genevestigator.com/gv/index.jsp; Sawchuk et al., 2008) shows that Lhcb4.3 mRNA is present preferentially in developed rosette and flowers, as in bolting and young flowers. Nevertheless, we cannot exclude that Lhcb4.3 is accumulated in special and still unexplored environmental/developmental conditions. Thus, so far, the role of this isoform remains elusive.

### A.2.5 Conclusions

In conclusion, we have shown a specific effect for Lhcb4 in protecting PSII from photoinhibition, which could account for the koLhcb4 higher sensitivity to high-light stress. Thus, we propose that the binding of Lhcb4, located in between LHCII trimers and RC of PSII supercomplexes, is particularly effective in protecting PSII from ROS produced during photosynthetic process. Similarly to other monomeric Lhcb, Lhcb4 functions in bridging dimeric PSII core complexes to the major trimeric LHCII antenna both structurally and functionally. The present work showed how the absence of a specific antenna protein, although does not restrict light harvesting and photosynthetic electron transport rate, produces a large effect on PSII photoprotection through its role in supercomplexes assembly. It is in accordance with evidences that the core antenna system was developed prior to green algal diversification (Koziol et al., 2007) and comprised Lhcb4 protein associated

with PSII. This is a clear example of how a complex system like thylakoid membranes functions due to the optimization of all its components and the tuning of their interactions with each other over evolution time.

## Additional data

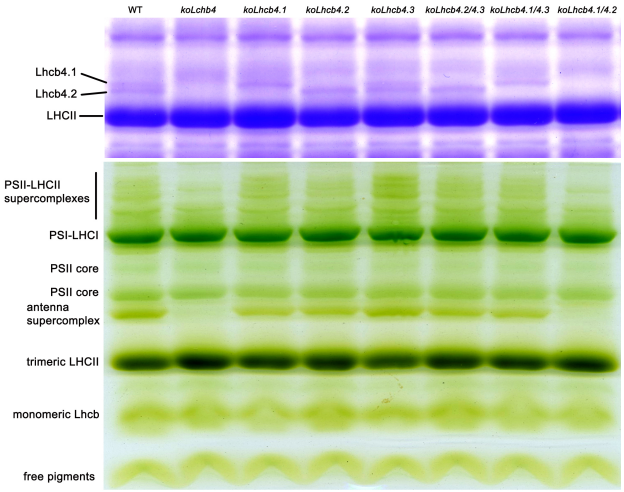


**Figure A.7:** *Polypeptide Composition of Thylakoid Membranes from Wild-Type and koLhcb4 isoform mutant.*
*Upper part. SDS/PAGE analysis performed with the Tris-Tricine buffer system as previously described (Schägger and von Jagow, 1987), with the addition of 7M urea to the running gel in order to separate Lhcb4 isoforms. Selected apoprotein bands are marked. Fifteen micrograms of chlorophylls were loaded in each lane.*
*Lower part. Thylakoid pigmented complexes were separated by nondenaturing Deriphat-PAGE. 25 µg of chlorophyll were loaded in each lane.*

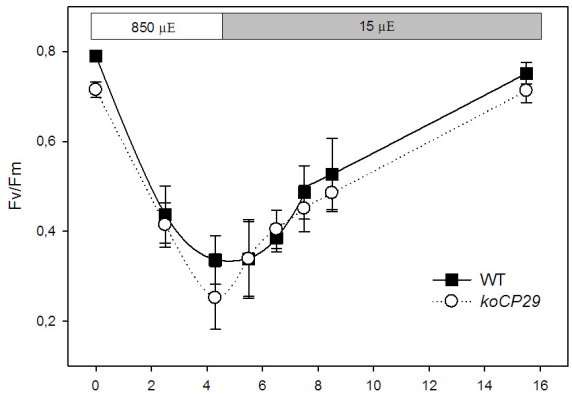


**Figure A.8:** *PSII repair efficiency in WT and koLhcb4.*
*PSII repair efficiency was quantified by measuring $F_v/F_m$ recovery on whole plants in low light (15 µmol photons $m^{-2}s^{-1}$) after photoinhibitory treatment (850 µmol photons $m^{-2}s^{-1}$) for WT and koLhcb4 plants.*

## Abbreviations

Chl, chlorophyll; $^1$Chl*, chlorophyll excited state; $^3$Chl*, Chl triplet; DCCD, N,N'-dicyclohexylcarbodiimide; DCMU, 3-(3,4-diclorophenyl)-1,1-dimethyl

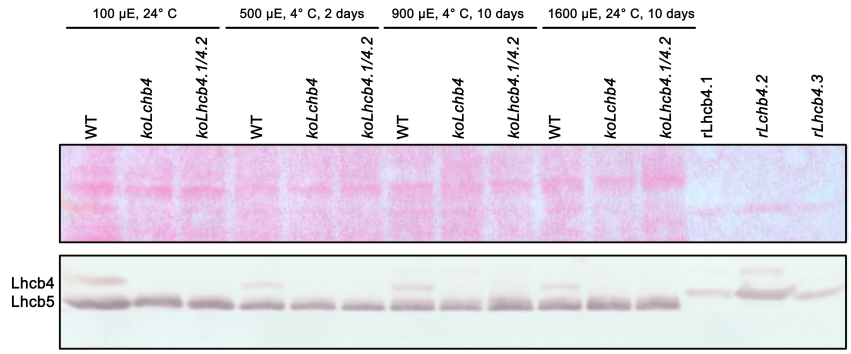


**Figure A.9:** *Immunoblot analysis of thylakoid membranes.*
*Upper part. Ponceau of the blotting: thylakoids' lanes were equally loaded.*
*Lower part. Immunoblot analysis of thylakoids from WT, koLhcb4 and koLhcb4.1/4.2 in control and stressed condition. A polyclonal antibody directed against Lhcb4 isoform and Lhcb5 was used.*
*In the last three lanes the recombinant isoforms (rLhcb) were loaded.*

urea; DM, dodecyl-$\alpha$ D-maltoside; ETR, electron transport rate; HL, high light; Lhc, light harvesting complex; NPQ, non-photochemical quenching; $^1O_2$, single oxygen; PQ, plastoquinone; PS, Photosystem; qE, energy quenching; qI, inhibitory quenching; qP, photochemical quenching; RC, reaction center; ROS, reactive oxygen species; WT, wild type; Zea, zeaxanthin.

## Reference List

**Ahn,T.K.,** Avenson,T.J., Ballottari,M., Cheng,Y.C., Niyogi,K.K., Bassi,R., and Fleming,G.R. (2008). Architecture of a charge-transfer state regulating light harvesting in a plant antenna protein. Science 320, 794-797.

**Alboresi,A.,** Caffarri,S., Nogue,F., Bassi,R., and Morosinotto,T. (2008). In silico and biochemical analysis of Physcomitrella patens photosynthetic antenna: identification of subunits which evolved upon land adaptation. PLoS. One. 3, e2033.

**Allen,J.F.** (1992). Protein phosphorylation in regulation of photosynthesis. Biochim. Biophys. Acta 1098, 275-335.

**Allen,J.F.** and Nilsson,A. (1997). Redox signalling and the structural basis of regulation of photosynthesis by protein phosphorylation. Physiol. Plant. 100, 863-868.

**Alonso,J.M.,** Stepanova,A.N., Leisse,T.J., Kim,C.J., Chen,H., Shinn,P., Stevenson,D.K., Zimmerman,J., Barajas,P., Cheuk,R., Gadrinab,C., Heller,C., Jeske,A., Koesema,E., Meyers,C.C., Parker,H., Prednis,L., Ansari,Y., Choy,N., Deen,H., Geralt,M., Hazari,N., Hom,E., Karnes,M., Mulholland,C., Ndubaku,R., Schmidt,I., Guzman,P., Aguilar-Henonin,L., Schmid,M., Weigel,D., Carter,D.E., Marchand,T., Risseeuw,E., Brogden,D., Zeko,A., Crosby,W.L., Berry,C.C., and Ecker,J.R. (2003). Genome-wide insertional mutagenesis of Arabidopsis thaliana. Science 301, 653-657.

**Andersson,J.,** Walters,R.G., Horton,P., and Jansson,S. (2001). Antisense inhibition of the photosynthetic antenna proteins CP29 and CP26: Implications for the mechanism of protective energy dissipation. Plant Cell 13, 1193-1204.

**Andersson,J.,** Wentworth,M., Walters,R.G., Howard,C.A., Ruban,A.V., Horton,P., and Jansson,S. (2003). Absence of the Lhcb1 and Lhcb2 proteins of the light-harvesting complex of photosystem II - effects on photosynthesis, grana stacking and fitness. Plant J. 35, 350-361.

**Aro,E.M.,** McCaffery,S., and Anderson,J.M. (1994). Recovery from Photoinhibition in Peas (Pisum sativum L.) Acclimated to Varying Growth Irradiances (Role of D1 Protein Turnover). Plant Physiol 104, 1033-1041.

**Asada,K.** (1999). THE WATER-WATER CYCLE IN CHLOROPLASTS: Scavenging of Active Oxygens and Dissipation of Excess Photons. Annu. Rev. Plant Physiol Plant Mol. Biol. 50, 601-639.

**Avenson,T.J.,** Ahn,T.K., Zigmantas,D., Niyogi,K.K., Li,Z., Ballottari,M., Bassi,R., and Fleming,G.R. (2007). Zeaxanthin radical cation formation in minor light-harvesting complexes of higher plant antenna. J. Biol Chem.

**Ballottari,M.,** Dall'Osto,L., Morosinotto,T., and Bassi,R. (2007). Contrasting behavior of higher plant photosystem I and II antenna systems during acclimation. Journal of Biological Chemistry 282, 8947-8958.

**Barros,T.,** Royant,A., Standfuss,J., Dreuw,A., and Kuhlbrandt,W. (2009). Crystal structure of plant light-harvesting complex shows the active, energy-transmitting state. Embo Journal 28, 298-306.

**Bassi,R.** and Dainese,P. (1992). A Supramolecular Light-Harvesting Complex from Chloroplast Photosystem-II Membranes. Eur. J. Biochem. 204, 317-326.

**Bassi, R.,** Giuffra, E., Croce, R., Dainese, P., and Bergantino, E. Biochemistry and molecular biology of pigment binding proteins. Jennings, R. C., Zucchelli, G., Ghetti, F., and Colombetti, G. NATO ASI series[287], 41-63. 1996. New York, Plenum Press. Life Science. Ref Type: Serial (Book,Monograph)

**Bassi,R.,** Rigoni,F., Barbato,R., and Giacometti,G.M. (1988). Light-harvesting chlorophyll a/b proteins (LHCII) populations in phosphorylated membranes. Biochim. Biophys. Acta 936, 29-38.

**Bassi,R.,** Sandona,D., and Croce,R. (1997). Novel aspects of chlorophyll a/b-binding proteins. Physiol. Plant. 100, 769-779.

**Bellafiore,S.,** Bameche,F., Peltier,G., and Rochaix,J.D. (2005). State transitions and light adaptation require chloroplast thylakoid protein kinase STN7. Nature 433, 892-895.

**Bergantino,E.,** Dainese,P., Cerovic,Z., Sechi,S., and Bassi,R. (1995). A post-translational modification of the photosystem II subunit CP29 protects maize from cold stress. J. Biol. Chem. 270, 8474-8481.

**Bergantino,E.,** Segalla,A., Brunetta,A., Teardo,E., Rigoni,F., Giacometti,G.M., and Szabo,I. (2003). Light- and pH-dependent structural changes in the PsbS subunit of photosystem II. Proc. Natl. Acad. Sci. U. S. A 100, 15265-15270.

**Betterle,N.,** Ballottari,M., Zorzan,S., de Bianchi,S., Cazzaniga,S., Dall'Osto,L., Morosinotto,T., and Bassi,R. (2009). Light-induced dissociation of an antenna hetero-oligomer is needed for non-photochemical quenching induction. J. Biol. Chem. 284, 15255-15266.

**Boekema,E.J.,** van Roon,H., van Breemen,J.F., and Dekker,J.P. (1999). Supramolecular organization of photosystem II and its light-harvesting antenna in partially solubilized photosystem II membranes. Eur. J. Biochem. 266, 444-452.

**Butler,W.L.** and Strasser,R.J. (1978). Effect of divalent cations on energy coupling between the light- harvesting chlorophyll a/b complex and photosystem II., pp. 11-20.

**Caffarri,S.,** Kouril,R., Kereiche,S., Boekema,E.J., and Croce,R. (2009). Functional architecture of higher plant photosystem II supercomplexes. Embo Journal 28, 3052-3063.

**Croce,R.,** Breton,J., and Bassi,R. (1996). Conformational Changes Induced by Phosphorylation in the CP29 Subunit of Photosystem II. Biochemistry 35, 11142-11148.

**Dall'Osto,L.,** Caffarri,S., and Bassi,R. (2005). A mechanism of nonphotochemical energy dissipation, independent from Psbs, revealed by a conformational change in the antenna protein CP26. Plant Cell 17, 1217-1232.

**Dall'Osto,L.,** Cazzaniga,S., Havaux,M., and Bassi,R. (2010). Enhanced Photoprotection by Protein-Bound vs Free Xanthophyll Pools: A Comparative Analysis of Chlorophyll b and Xanthophyll Biosynthesis Mutants. Mol. Plant.

**Damkjaer,J.T.,** Kereiche,S., Johnson,M.P., Kovacs,L., Kiss,A.Z., Boekema,E.J., Ruban,A.V., Horton,P., and Jansson,S. (2009). The Photosystem II Light-Harvesting Protein Lhcb3 Affects the Macrostructure of Photosystem II and the Rate of State Transitions in Arabidopsis. Plant Cell.

**Dall'Osto,L.**, Lico,C., Alric,J., Giuliano,G., Havaux,M., and Bassi,R. (2006). Lutein is needed for efficient chlorophyll triplet quenching in the major LHCII antenna complex of higher plants and effective photoprotection in vivo under strong light. Bmc Plant Biology 6, 32.

**de Bianchi,S.,** Dall'Osto,L., Tognon,G., Morosinotto,T., and Bassi,R. (2008). Minor antenna proteins CP24 and CP26 affect the interactions between photosystem II subunits and the electron transport rate in grana membranes of Arabidopsis. Plant Cell 20, 1012-1028.

**Demmig-Adams,B.,** Winter,K., Kruger,A., and Czygan,F.-C. (1989). Light stress and photoprotection related to the carotenoid zeaxanthin in higher plants. In Photosynthesis. Plant Biology Vol.8, W.R.Briggs, ed. (New York: Alan R. Liss), pp. 375-391.

**Ganeteg,U.,** Kulheim,C., Andersson,J., and Jansson,S. (2004). Is each light-harvesting complex protein important for plant fitness? Plant Physiol 134, 502-509.

**Gilmore,A.M.** and Yamamoto,H.Y. (1991). Zeaxanthin Formation and Energy-Dependent Fluorescence Quenching in Pea Chloroplasts Under Artificially Mediated Linear and Cyclic Electron Transport. Plant Physiol. 96, 635-643.

**Goff,S.A.,** Ricke,D., Lan,T.H., Presting,G., Wang,R., Dunn,M., Glazebrook,J., Sessions,A., Oeller,P., Varma,H., Hadley,D., Hutchison,D., Martin,C., Katagiri,F., Lange,B.M., Moughamer,T., Xia,Y., Budworth,P., Zhong,J., Miguel,T., Paszkowski,U., Zhang,S., Colbert,M., Sun,W.L., Chen,L., Cooper,B., Park,S., Wood,T.C., Mao,L., Quail,P., Wing,R., Dean,R., Yu,Y., Zharkikh,A., Shen,R., Sahasrabudhe,S., Thomas,A., Cannings,R., Gutin,A., Pruss,D., Reid,J., Tavtigian,S., Mitchell,J., Eldredge,G., Scholl,T., Miller,R.M., Bhatnagar,S., Adey,N., Rubano,T., Tusneem,N., Robinson,R., Feldhaus,J., Macalma,T., Oliphant,A., and Briggs,S. (2002). A draft sequence of the rice genome (Oryza sativa L. ssp. japonica). Science 296, 92-100.

**Golding,A.J.,** Finazzi,G., and Johnson,G.N. (2004). Reduction of the thylakoid electron transport chain by stromal reductants–evidence for activation of cyclic electron transport upon dark adaptation or under drought. Planta 220, 356-363.

**Haldrup,A.,** Jensen,P.E., Lunde,C., and Scheller,H.V. (2001). Balance of power: a view of the mechanism of photosynthetic state transitions. Trends Plant Sci. 6, 301-305.

**Hansson,M.** and Vener,A.V. (2003). Identification of three previously unknown in vivo protein phosphorylation sites in thylakoid membranes of Arabidopsis thaliana. Mol. Cell Proteomics. 2, 550-559.

**Havaux,M.,** Dall'Osto,L., and Bassi,R. (2007). Zeaxanthin has Enhanced Antioxidant Capacity with Respect to All Other Xanthophylls in Arabidopsis Leaves and functions independent of binding to PSII antennae. Plant Physiol.

**Havaux,M.,** Dall'Osto,L., Cuine,S., Giuliano,G., and Bassi,R. (2004). The effect of zeaxanthin as the only xanthophyll on the structure and function of the photosynthetic apparatus in Arabidopsis thaliana. J. Biol. Chem. 279, 13878-13888.

**Havaux,M.,** Eymery,F., Porfirova,S., Rey,P., and Dormann,P. (2005). Vitamin E Protects against Photoinhibition and Photooxidative Stress in Arabidopsis thaliana. Plant Cell 17, 3451-3469.

**Holt,N.E.,** Zigmantas,D., Valkunas,L., Li,X.P., Niyogi,K.K., and Fleming,G.R. (2005).

Carotenoid cation formation and the regulation of photosynthetic light harvesting. Science 307, 433-436.

**Horton,P.** (1996). Nonphotochemical quenching of chlorophyll fluorescence. In Light as an Energy Source and Information Carrier in Plant Physiology, R.C.Jennings, ed. (Plenum Press: New York), pp. 99-111.

**Horton,P.** and Ruban,A. (2005). Molecular design of the photosystem II light-harvesting antenna: photosynthesis and photoprotection. J. Exp. Bot. 56, 365-373.

**Jackowski,G.** and Jansson,S. (1998). Characterization of photosystem II antenna complexes separated by non-denaturing isoelectric focusing. Z. Naturforsch. C 53, 841-848.

**Jansson,S.** (1994). The light-harvesting chlorophyll a/b-binding proteins. Biochim. Biophys. Acta 1184, 1-19.

**Jansson,S.** (1999). A guide to the Lhc genes and their relatives in Arabidopsis. Trends Plant Sci. 4, 236-240.

**Jensen,P.E.,** Gilpin,M., Knoetzel,J., and Scheller,H.V. (2000). The PSI-K subunit of photosystem I is involved in the interaction between light-harvesting complex I and the photosystem I reaction center core. J. Biol. Chem. 275, 24701-24708.

**Johnson,M.P.,** Havaux,M., Triantaphylides,C., Ksas,B., Pascal,A.A., Robert,B., Davison,P.A., Ruban,A.V., and Horton,P. (2007). Elevated zeaxanthin bound to oligomeric LHCII enhances the resistance of Arabidopsis to photooxidative stress by a lipid-protective, antioxidant mechanism. J. Biol. Chem. 282, 22605-22618.

**Kim,E.H.,** Li,X.P., Razeghifard,R., Anderson,J.M., Niyogi,K.K., Pogson,B.J., and Chow,W.S. (2009). The multiple roles of light-harvesting chlorophyll a/b-protein complexes define structure and optimize function of Arabidopsis chloroplasts: a study using two chlorophyll b-less mutants. Biochim. Biophys. Acta 1787, 973-984.

**Klimmek,F.,** Sjodin,A., Noutsos,C., Leister,D., and Jansson,S. (2006). Abundantly and rarely expressed Lhc protein genes exhibit distinct regulation patterns in plants. Plant Physiol 140, 793-804.

**Kovacs,L.,** Damkjaer,J., Kereiche,S., Ilioaia,C., Ruban,A.V., Boekema,E.J., Jansson,S., and Horton,P. (2006). Lack of the light-harvesting complex CP24 affects the structure and function of the grana membranes of higher plant chloroplasts. Plant Cell 18, 3106-3120.

**Koziol,A.G.,** Borza,T., Ishida,K., Keeling,P., Lee,R.W., and Durnford,D.G. (2007). Tracing the evolution of the light-harvesting antennae in chlorophyll a/b-containing organisms. Plant Physiol 143, 1802-1816.

**Krieger,A.,** Rutherford,A.W., Vass,I., and Hideg,E. (1998). Relationship between activity, D1 loss, and Mn binding in photoinhibition of photosystem II. Biochemistry 37, 16262-16269.

**Li,X.P.,** Bjorkman,O., Shih,C., Grossman,A.R., Rosenquist,M., Jansson,S., and Niyogi,K.K. (2000). A pigment-binding protein essential for regulation of photosynthetic light harvesting. Nature 403, 391-395.

**Li,X.P.,** Gilmore,A.M., Caffarri,S., Bassi,R., Golan,T., Kramer,D., and Niyogi,K.K. (2004). Regulation of photosynthetic light harvesting involves intrathylakoid lumen pH sensing by the PsbS protein. J. Biol. Chem. 279, 22866-22874.

**Liu,W.J.,** Chen,Y.E., Tian,W.J., Du,J.B., Zhang,Z.W., Xu,F., Zhang,F., Yuan,S., and Lin,H.H. (2009). Dephosphorylation of photosystem II proteins and phosphorylation of CP29 in barley photosynthetic membranes as a response to water stress. Biochim. Biophys. Acta 1787, 1238-1245.

**Malkin,S.,** Armond,P.A., Mooney,H.A., and Fork,D.C. (1981). Photosystem II photosynthetic unit sizes from fluorescence induction in leaves. Correlation to photosynthetic capacity. Plant Physiol. 67, 570-579.

**Mauro,S.,** Dainese,P., Lannoye,R., and Bassi,R. (1997). Cold-resistant and cold-sensitive

maize lines differ in the phosphorylation of the photosystem II subunit, CP29. Plant Physiol. 115, 171-180.

**Melis,A.** (1999). Photosystem-II damage and repair cycle in chloroplasts: what modulates the rate of photodamage ? Trends Plant Sci. 4, 130-135.

**Morosinotto,T.,** Baronio,R., and Bassi,R. (2002). Dynamics of Chromophore Binding to Lhc Proteins in Vivo and in Vitro during Operation of the Xanthophyll Cycle. J. Biol. Chem. 277, 36913-36920.

**Morosinotto,T.,** Caffarri,S., Dall'Osto,L., and Bassi,R. (2003). Mechanistic aspects of the xanthophyll dynamics in higher plant thylakoids. Physiologia Plantarum 119, 347-354.

**Mozzo,M.,** Dall'Osto,L., Hienerwadel,R., Bassi,R., and Croce,R. (2008). Photoprotection in the antenna complexes of photosystem II: role of individual xanthophylls in chlorophyll triplet quenching. J. Biol. Chem. 283, 6184-6192.

**Munekage,Y.,** Hashimoto,M., Miyake,C., Tomizawa,K., Endo,T., Tasaka,M., and Shikanai,T. (2004). Cyclic electron flow around photosystem I is essential for photosynthesis. Nature 429, 579-582.

**Niyogi,K.K.** (1999). Photoprotection revisited: Genetic and molecular approaches. Annu. Rev. Plant Physiol. Plant Mol. Biol. 50, 333-359. Niyogi,K.K. (2000). Safety valves for photosynthesis. Curr. Opin. Plant Biol. 3, 455-460.

**Niyogi,K.K.** (2000). Safety valves for photosynthesis. Curr. Opin. Plant Biol. 3, 455-460.

**Pesaresi,P.,** Sandona,D., Giuffra,E., and Bassi,R. (1997). A single point mutation (E166Q) prevents dicyclohexylcarbodiimide binding to the photosystem II subunit CP29. FEBS Lett. 402, 151-156.

**Peter,G.F.,** Takeuchi,T., and Thornber,J.P. (1991). Solubilization and two-dimensional electrophoretic procedures for studying the organization and composition of photosynthetic membrane polypeptides. Methods: A Companion to Methods in Enzymology 3, 115-124.

**Ruan,X.,** Xu,Q., Mao,H.B., Li,G.F., Wei,J., Gong,Y.D., Kuang,T.Y., and Zhao,N.M. (2001). Strong-light photoinhibition treatment accelerates the changes of protein secondary structures in triton-treated photosystem I and photosystem II complexes. J. Protein Chem. 20, 247-254.

**Ruban,A.V.,** Berera,R., Ilioaia,C., van Stokkum,I.H., Kennis,J.T., Pascal,A.A., Van Amerongen,H., Robert,B., Horton,P., and van Grondelle,R. (2007). Identification of a mechanism of photoprotective energy dissipation in higher plants. Nature 450, 575-578.

**Ruban,A.V.,** Wentworth,M., Yakushevska,A.E., Andersson,J., Lee,P.J., Keegstra,W., Dekker,J.P., Boekema,E.J., Jansson,S., and Horton,P. (2003). Plants lacking the main light-harvesting complex retain photosystem II macro-organization. Nature 421, 648-652.

**Sawchuk,M.G.,** Donner,T.J., Head,P., and Scarpella,E. (2008). Unique and overlapping expression patterns among members of photosynthesis-associated nuclear gene families in Arabidopsis. Plant Physiol 148, 1908-1924.

**Schägger,H.** and von Jagow,G. (1987). Tricine-sodium dodecyl sulfate-polyacrylamide gel electrophoresis for the separation of proteins in the range from 1 to 100 kDa. Anal. Biochem. 166, 368-379.

**Takahashi,H.,** Iwai,M., Takahashi,Y., and Minagawa,J. (2006). Identification of the mobile light-harvesting complex II polypeptides for state transitions in Chlamydomonas reinhardtii. Proc. Natl. Acad. Sci. U. S. A 103, 477-482.

**Teardo,E.,** De Laureto,P.P., Bergantino,E., Dalla,V.F., Rigoni,F., Szabo,I., and Giacometti,G.M. (2007). Evidences for interaction of PsbS with photosynthetic complexes in maize thylakoids. Biochim. Biophys. Acta 1767, 703-711.

**Testi,M.G.,** Croce,R., Polverino-De Laureto,P., and Bassi,R. (1996). A CK2 site is re-

versibly phosphorylated in the photosystem II subunit CP29. FEBS Lett. 399, 245-250.

**Thornber,J.P.** (1969). Comparison of a chlorophyll a-protein complex isolated from a blue-green alga with chlorophyll-protein complexes obtained from green bacteria and higher plants. Biochim. Biophys. Acta 172, 230-241.

**Tikkanen,M.,** Piippo,M., Suorsa,M., Sirpio,S., Mulo,P., Vainonen,J., Vener,A.V., Allahverdiyeva,Y., and Aro,E.M. (2006). State transitions revisited-a buffering system for dynamic low light acclimation of Arabidopsis. Plant Mol. Biol. 62, 779-793.

**Towbin,H.,** Staehelin,T., and Gordon,J. (1979). Electrophoretic transfer of proteins from polyacrylamide gels to nitrocellulose sheets: Procedure and some applications. Proc. Natl. Acad. Sci. USA 76, 4350-4354.

**Vallon,O.,** Bulte,L., Dainese,P., Olive,J., Bassi,R., and Wollman,F.A. (1991). Lateral redistribution of cytochrome b6/f complexes along thylakoid membranes upon state transitions. Proc. Natl. Acad. Sci. U. S. A 88, 8262-8266.

**Van Kooten,O.** and Snel,J.F.H. (1990). The use of chlorophyll fluorescence nomenclature in plant stress physiology. Photosynt. Res. 25, 147-150.

**Walters,R.G.,** Ruban,A.V., and Horton,P. (1996). Identification of proton-active residues in a higher plant light- harvesting complex. Proc. Natl. Acad. Sci. USA 93, 14204-14209.

**Wentworth,M.,** Ruban,A.V., and Horton,P. (2003). Thermodynamic investigation into the mechanism of the chlorophyll fluorescence quenching in isolated photosystem II light-harvesting complexes. Journal of Biological Chemistry 278, 21845-21850.

**Yakushevska,A.E.,** Keegstra,W., Boekema,E.J., Dekker,J.P., Andersson,J., Jansson,S., Ruban,A.V., and Horton,P. (2003). The structure of photosystem II in Arabidopsis: localization of the CP26 and CP29 antenna complexes. Biochemistry 42, 608-613.

**Yu,J.,** Hu,S., Wang,J., Wong,G.K., Li,S., Liu,B., Deng,Y., Dai,L., Zhou,Y., Zhang,X., Cao,M., Liu,J., Sun,J., Tang,J., Chen,Y., Huang,X., Lin,W., Ye,C., Tong,W., Cong,L., Geng,J., Han,Y., Li,L., Li,W., Hu,G., Huang,X., Li,W., Li,J., Liu,Z., Li,L., Liu,J., Qi,Q., Liu,J., Li,L., Li,T., Wang,X., Lu,H., Wu,T., Zhu,M., Ni,P., Han,H., Dong,W., Ren,X., Feng,X., Cui,P., Li,X., Wang,H., Xu,X., Zhai,W., Xu,Z., Zhang,J., He,S., Zhang,J., Xu,J., Zhang,K., Zheng,X., Dong,J., Zeng,W., Tao,L., Ye,J., Tan,J., Ren,X., Chen,X., He,J., Liu,D., Tian,W., Tian,C., Xia,H., Bao,Q., Li,G., Gao,H., Cao,T., Wang,J., Zhao,W., Li,P., Chen,W., Wang,X., Zhang,Y., Hu,J., Wang,J., Liu,S., Yang,J., Zhang,G., Xiong,Y., Li,Z., Mao,L., Zhou,C., Zhu,Z., Chen,R., Hao,B., Zheng,W., Chen,S., Guo,W., Li,G., Liu,S., Tao,M., Wang,J., Zhu,L., Yuan,L., and Yang,H. (2002). A draft sequence of the rice genome (Oryza sativa L. ssp. indica). Science 296, 79-92.

**Zhang,S.** and Scheller,H.V. (2004). Photoinhibition of Photosystem I at chilling temperature and subsequernt recovery in Arabidopsis thaliana. Plant Cell Physiol. 45, 1595-1602.

**Zygadlo,A.,** Jensen,P.E., Leister,D., and Scheller,H.V. (2005). Photosystem I lacking the PSI-G subunit has a higher affinity for plastocyanin and is sensitive to photodamage. Biochim. Biophys. Acta 1708, 154-163.

# Section B

# Membrane dynamics and re-organization for the quenching events: B4 dissociation and identification of two distinct quenching sites.

## B.1 PsbS controls protein segregation in chloroplast thylakoid membranes.

N. Betterle, M. Ballottari, S. Zorzan, S. de Bianchi, S. Cazzaniga, L. Dall'Osto, T. Morosinotto and R. Bassi.

For the experiments done in this article I provided the monomeric Lhcb ko mutants and I contributed with the other authors with suggestions in the discussion of the experimental design and results. Some indication for the experimental drawn came from observation on NPQ phenotype that I measured. This article has been selected by Alexey Amunts and Nathan Nelson for "Faculty of 1000" as new finding and interested hypothesis.

THE JOURNAL OF BIOLOGICAL CHEMISTRY VOL. 284, NO. 22, pp. 15255–15266, MAY 29, 2009


# Light-induced Dissociation of an Antenna Hetero-oligomer Is Needed for Non-photochemical Quenching Induction[S]

Received for publication, November 13, 2008, and in revised form, March 19, 2009 Published, JBC Papers in Press, March 23, 2009, DOI 10.1074/jbc.M808625200

**Nico Betterle[‡1], Matteo Ballottari[‡1], Simone Zorzan[‡], Silvia de Bianchi[‡], Stefano Cazzaniga[‡], Luca Dall'Osto[‡], Tomas Morosinotto[§2], and Roberto Bassi[‡3]**

*From the [‡]Dipartimento Scientifico e Tecnologico, Università di Verona, Strada Le Grazie 15, I-37134 Verona, Italy and the [§]Dipartimento di Biologia, Università di Padova, Via Ugo Bassi 58, 35131 Padova, Italy*

**PsbS plays a major role in activating the photoprotection mechanism known as "non-photochemical quenching," which dissipates chlorophyll excited states exceeding the capacity for photosynthetic electron transport. PsbS activity is known to be triggered by low lumenal pH. However, the molecular mechanism by which this subunit regulates light harvesting efficiency is still unknown. Here we show that PsbS controls the association/dissociation of a five-subunit membrane complex, composed of two monomeric Lhcb proteins (CP29 and CP24) and the trimeric LHCII-M. Dissociation of this supercomplex is indispensable for the onset of non-photochemical fluorescence quenching in high light, strongly suggesting that protein subunits catalyzing the reaction of heat dissipation are buried into the complex and thus not available for interaction with PsbS. Consistently, we showed that knock-out mutants on two subunits participating to the B4C complex were strongly affected in heat dissipation. Direct observation by electron microscopy and image analysis showed that B4C dissociation leads to the redistribution of PSII within grana membranes. We interpreted these results to mean that the dissociation of B4C makes quenching sites, possibly CP29 and CP24, available for the switch to an energy-quenching conformation. These changes are reversible and do not require protein synthesis/degradation, thus allowing for changes in PSII antenna size and adaptation to rapidly changing environmental conditions.**

Photosynthetic reaction centers exploit solar energy to drive electrons from water to $NADP^+$. This transport is coupled to $H^+$ transfer from chloroplast stroma to thylakoids lumen, building a proton gradient for ATP synthesis (1). The capacity for light absorption is increased by pigment-binding proteins that compose the antenna system. In higher plants, the antenna is composed of the nuclear-encoded Chl[4] *a*/*b*-binding light-harvesting complexes (Lhc). The major constituent of the photosystem II (PSII) outer antenna is LHCII, a heterotrimer composed by different combinations of Lhcb1, Lhcb2, and Lhcb3 gene products (2). Three additional monomeric antenna complexes (CP29, CP26, and CP24) encoded by the *lhcb4*, *lhcb5*, and *lhcb6* genes, respectively, are localized in between the core complex and LHCII (3). Similarly, PSI has four Lhca antenna proteins, yielding a total of 10 distinct Lhc isoforms (2). Differences between the mentioned isoforms have been largely conserved in all higher plants during at the last 350 million years of evolution, strongly indicating that each pigment-protein complex has a specific function (4), although the specific role of each gene product in light harvesting and/or photoprotection is still under debate (5). Their topological organization into the supercomplex has been analyzed by electron microscopy and biochemical methods (3, 6–8) showing that Lhcb subunits are organized into two layers around the PSII core. The inner layer is composed of CP29, CP26, and the S-type LHCII trimer, forming, together with the PSII core, the so-called $C_2S_2$ particle (9, 10). The outer layer is made of LHCII trimers and CP24, to build up the larger $C_2S_2M_2L_x$ complexes (9) in which the number of LHCII-L trimers depends on the light intensity during growth (11, 12).

This structural organization responds to the requirements of light harvesting regulation; in high light, when absorbed energy does not limit growth, the PSII antenna loses the components of the external antenna layer, namely CP24, LHCII-M, and LHCII-L (12), whereas the internal antenna components, CP26, CP29, and LHCII-S, are always retained in a 1:1 stoichiometry with the PSII core complex. This is consistent with the composition of a mutant exhibiting chronic plastoquinone reduction, mimicking overexcitation (10). Such an acclimation to contrasting light conditions, however, requires days to weeks (12, 13), whereas plants are often exposed to rapid changes in light intensity, temperature, and water availability. In these conditions, incomplete photochemical quenching leads to an increased Chl excited state ($^1Chl^*$) lifetime and increased probability of Chl *a* triplet formation ($^3Chl^*$) by intersystem crossing. Chl triplets react with oxygen ($^3O_2$) and form harmful reactive oxygen species, responsible for photoinhibition and oxidative stress (14). These harmful events are counteracted by photoprotection mechanisms consisting either in the scavenging of generated reactive oxygen species (15) or in prevention of

[S] The on-line version of this article (available at http://www.jbc.org) contains supplemental Figs. S1–S4.

[1] Both authors contributed equally to this work.

[2] Supported by Grant PRIN 20073YHRLE.

[3] Supported by Grants FIRB RBLA0345SF002 (Solanacee) and FISR IDROBIO. from the Italian Ministry of Research Special Fund for Basic Research. To whom correspondence should be addressed: Dipartimento Scientifico e Tecnologico, Università di Verona, Strada Le Grazie 15, I-37134 Verona, Italy. Tel.: 39-045-802-7915; Fax: 39-045-802-7929; E-mail: bassi@sci.univr.it.

[4] The abbreviations used are: Chl, chlorophyll; PSI and PSII, photosystem I and II, respectively; LHCII, light-harvesting complex II; NPQ, non-photochemical quenching; WT, wild type; IOD, integrated optical density; EM, electron microscopy; μE, microeinstein; HPLC, high pressure liquid chromatography; α-DM, *n*-dodecyl-α-D-maltoside.

**TABLE 1**

**Pigment-binding properties of light-treated leaves and isolated grana membranes**

The pigment composition of leaves during light treatment was analyzed by HPLC. Values (bold numbers) are reported as normalized to 100 total Chl molecules. S.D. is also indicated.

| | Chl *a*/*b* | Neoxanthin | Violaxanthin | Anteraxanthin | Lutein | Zeaxanthin | β-Carotene |
|---|---|---|---|---|---|---|---|
| **Grana** | | | | | | | |
| WT dark | **2.19** | **4.9** | **3.1** | **0.0** | **12.1** | **0.0** | **6.5** |
| S.D. | 0.04 | 0.4 | 0.2 | | 0.3 | | 0.4 |
| WT light (30 min) | **2.16** | **5.3** | **1.6** | **0.5** | **12.0** | **0.9** | **6.0** |
| S.D. | 0.03 | 0.5 | 0.2 | 0.1 | 0.3 | 0.1 | 0.6 |
| WT light (90 min) | **2.33** | **4.8** | **1.4** | **0.4** | **11.2** | **1.1** | **5.9** |
| S.D. | 0.03 | 0.3 | 0.1 | 0.1 | 0.2 | 0.1 | 0.2 |
| WT recovery (90 min) | **2.42** | **4.8** | **1.9** | **0.8** | **10.9** | **0.7** | **6.2** |
| S.D. | 0.07 | 0.4 | 0.1 | 0.1 | 0.5 | 0.1 | 0.1 |
| N4 dark | **2.37** | **5.2** | **2.4** | **0.0** | **12.0** | **0.0** | **6.6** |
| S.D. | 0.02 | 0.7 | 0.1 | | 0.1 | | 0.1 |
| N4 light (30 min) | **2.31** | **5.7** | **1.5** | **0.3** | **12.2** | **0.6** | **6.1** |
| S.D. | 0.04 | 1.1 | 0.2 | 0.1 | 0.1 | 0.1 | 0.3 |
| N4 light (90 min) | **2.22** | **6.2** | **1.5** | **0.3** | **12.5** | **0.8** | **5.5** |
| S.D. | 0.04 | 1.3 | 0.2 | 0.1 | 0.4 | 0.1 | 0.3 |
| **Leaves** | | | | | | | |
| WT dark | **3.12** | **4.5** | **4.3** | **0.0** | **12.7** | **0.0** | **7.1** |
| S.D. | 0.26 | 0.4 | 0.3 | | 1.1 | | 0.1 |
| WT light (30 min) | **3.31** | **4.9** | **1.5** | **0.9** | **11.5** | **2.3** | **7.6** |
| S.D. | 0.02 | 0.4 | 0.1 | 0.1 | 0.1 | 0.1 | 0.3 |
| WT light (90 min) | **3.20** | **4.3** | **1.2** | **0.6** | **12.3** | **2.4** | **6.5** |
| S.D. | 0.07 | 0.3 | 0.1 | 0.1 | 1.0 | 0.2 | 1.5 |
| WT recovery (90 min) | **3.20** | **4.3** | **2.9** | **1.4** | **12.5** | **1.1** | **6.7** |
| S.D. | 0.03 | 0.1 | 0.4 | 0.3 | 1.1 | 0.1 | 0.3 |

their production through dissipation of the $^1$Chl* in excess (16, 17). This latter process is known as non-photochemical quenching (NPQ) and is observed as light-dependent quenching of Chl fluorescence. NPQ has been shown to be composed by at least two components with different activation time scales. The first, feedback de-excitation quenching ($q_E$), is rapidly activated upon increasing light intensity, whereas a second component ($q_I$) is slower. Full NPQ activation requires zeaxanthin synthesis (18, 19) and the PsbS protein (20) that senses low lumenal pH through two lumen-exposed protonatable residues (21, 22). Mutants lacking Chl *b*, and thus lacking Lhc proteins, or exhibiting alterations in the topological organization of PSII antenna also undergo a strong reduction in NPQ, demonstrating the involvement of antenna proteins in its activation (23–25).

In this work we analyzed the changes in the organization of the PSII antenna during exposure to strong light and NPQ development. We found that a supramolecular complex, named B4C, composed of CP29, CP24, and LHCII-M, connects the inner and outer antenna moieties, dissociates during light exposure, and reassociates during subsequent dark recovery. Dissociation of the B4C complex appears necessary for the establishment of non-photochemical fluorescence quenching. Upon illumination, PSII distribution within grana membranes was also affected, and we observed a shorter distance between PSII reaction centers, implying enrichment in $C_2S_2$ complexes and depletion in the outer LHCII components. These results suggest that the NPQ process includes a rapid and reversible change in the organization of grana membranes with disconnection of a subset of Lhcb proteins from the PSII reaction center.

## EXPERIMENTAL PROCEDURES

*Plant Growth, Light Treatment, and Thylakoid Isolation*—WT plants of *Arabidopsis thaliana* ecotype Columbia and mutants *npq1, npq2, npq4, koLhcb3, koCP24*, and *koCP26* were obtained from the *Arabidopsis* Biological Resource Center; the complemented *npq4* mutant with PsbS WT and E122Q, E226Q, and double E122Q/E226Q mutants were obtained as described previously (21); the *npq2*/*npq4* double mutant was obtained by crossing *npq2* and *npq4* mutants; the koCP29 triple mutant was obtained by crossing the single mutants *Lhcb4.1*, *Lhcb4.2*, and *Lhcb4.3* obtained from the *Arabidopsis* Biological Resource Center. WT plants and mutants were grown for 4–6 weeks at 100 μmol of photons $m^{-2}$ $s^{-1}$, 21 °C, 90% humidity, and 8 h of daylight. Leaves detached from plants grown for 3 weeks were adapted to 1 h in the dark and eventually treated for 30 min at 1500 μmol of photons $m^{-2}$ $s^{-1}$ or for different times as indicated under "Results." Unstacked thylakoids were isolated from dark-adapted or light-treated leaves as described previously (26). Membranes corresponding to 150 mg of chlorophyll were washed with 5 mM EDTA and then solubilized with 0.6% α-DM. Solubilized samples were then fractionated by ultracentrifugation in a 0.1–1 M sucrose gradient containing 0.03% α-DM and 20 mM HEPES, pH 7.5 (SW60ti rotor, 5 h 30 min at 60,000 rpm, 4 °C).

*Grana Membrane Isolation*—Grana membranes were isolated from dark- and light-adapted samples using α-DM solubilization of stacked thylakoids as described elsewhere (10).

*Quantification of B4C Dissociation*—The image of each sucrose gradient fractionation was analyzed by using Gel-Pro Analyzer© software to determine the integrated optical density (IOD) of the different bands. B4C was quantified as the ratio between the IOD of the corresponding band and the sum of all bands corresponding to antenna proteins (band 2, 3, and 4).

*Pigment Analyses*—Pigments were extracted from leaf discs or grana membranes (see below and Table 1) with 80% acetone (v/v) and then separated and quantified by HPLC (27).

*In Vivo Fluorescence Analysis*—Non-photochemical quenching of Chl fluorescence was measured on whole leaves at room

temperature with a PAM 101 fluorimeter (Walz, Effeltrich, Germany). Minimum fluorescence ($F_0$) was measured with a 0.15 $\mu$mol $m^{-2}$ $s^{-1}$ beam, and maximum fluorescence ($F_m$) was determined with a 0.6-s light pulse (4500 $\mu$mol $m^{-2}$ $s^{-1}$). White continuous light (100–2000 $\mu$mol $m^{-2}$ $s^{-1}$) was supplied by a KL1500 halogen lamp (Schott, Mainz, Germany). NPQ was calculated according to the following equation (28): $NPQ = (F_m - F'_m)/F'_m$, where $F_m$ is the maximum Chl fluorescence from dark-adapted leaves and $F'_m$ the maximum Chl fluorescence under actinic light exposition. For photoinhibition analyses, $F_v/F_m$ was determined after 5 or 15 h of dark incubation following light treatment with equivalent results.

*Electron Microscopy and Image Analysis*—Electron microscopy (EM) on isolated grana membranes was conducted using an FEI Tecnai T12 electron microscope operating at 100 kV accelerating voltage. Samples were applied to glow-discharged carbon-coated grids and stained with 2% uranyl acetate. Images were recorded using a charge-coupled device camera. Best stained grana patches were analyzed and PSII core positions were identified using Boxer software, manually edited in case of uncertain attributions. Distribution of PSII cores within the image distribution was analyzed by a homemade procedure written in MATLAB© (available upon request), which determines the distance between each core and the closest (or *n* closest) neighbor. In total around 1000 points, resulting from at least three independent biological replications, were considered for the analysis for each sample.

## RESULTS

*A Pentameric Lhcb Complex (B4C) Is Dissociated upon Light Treatment*—PSII antenna organization has been shown to be fundamental for the full establishment of NPQ, which, in fact, is significantly impaired in plants depleted of antenna proteins or where the antenna organization is affected (23–25). To test whether a reorganization of grana membranes is involved in NPQ, we analyzed the interactions between the PSII-LHCII supercomplex subunits using sucrose gradient ultracentrifugation upon mild solubilization of thylakoid membranes. To this aim, *Arabidopsis* plants were either dark-adapted or illuminated with saturating light for 30 min. Upon illumination, leaves were cooled in ice water slurry, and thylakoids were isolated, solubilized with $\alpha$-DM, and fractionated by ultracentrifugation. Different pigment-protein complexes migrated as green bands depending on their sizes, as shown in Fig. 1*A*. Light treatment affected the band pattern, and sucrose band 4 (B4) disappeared. This band is made of a Lhc supercomplex composed of monomeric CP24, CP29, and a LHCII trimer (6). Hereafter we will refer to this pentameric Lhc complex as B4C. The distribution of individual Lhcb proteins among different green bands was analyzed in detail by using specific antibodies. As shown in Fig. 1*B*, a large fraction of the CP24 and CP29 subunits is present in the B4C from the dark-adapted sample, whereas the rest, in monomeric form, is found in fraction 2 (B2). After light treatment, CP24 and CP29 were barely detectable in the gradient fraction corresponding to B4C, whereas they increased in the B2 fraction. These results show that the reduction of B4C in the gradients is indeed due to the dissociation of this oligomeric antenna complex. Among the other polypeptides analyzed, it was very interesting to observe that Lhcb3 is an enriched component of B4C in the dark. Upon light treatment, Lhcb3 was instead found in the monomeric fraction, confirming that this subunit participates in light-dependent dissociation of the B4C supercomplex. Lhcb1–2, the major components of LHCII trimers, are found mostly in B3, as expected, and in the monomeric B2 fraction. A fraction of Lhcb1–2 is also detected in B4C; their relative abundance appears to be rather low. However, this is only because of their high enrichment in B2 and B3 fractions. In fact, by loading equal Chl amounts of B2, B3, and B4 in a Coomassie-stained gel (Fig. 1*C*), it is clear that Lhcb1–2 are indeed present in significant amounts in B4C, in agreement with to a previous report (6). To further confirm that Lhcb1–2 are genuine B4C components, we observed that their content in B4C was reduced upon light treatment, just as all of the other previously mentioned compo-

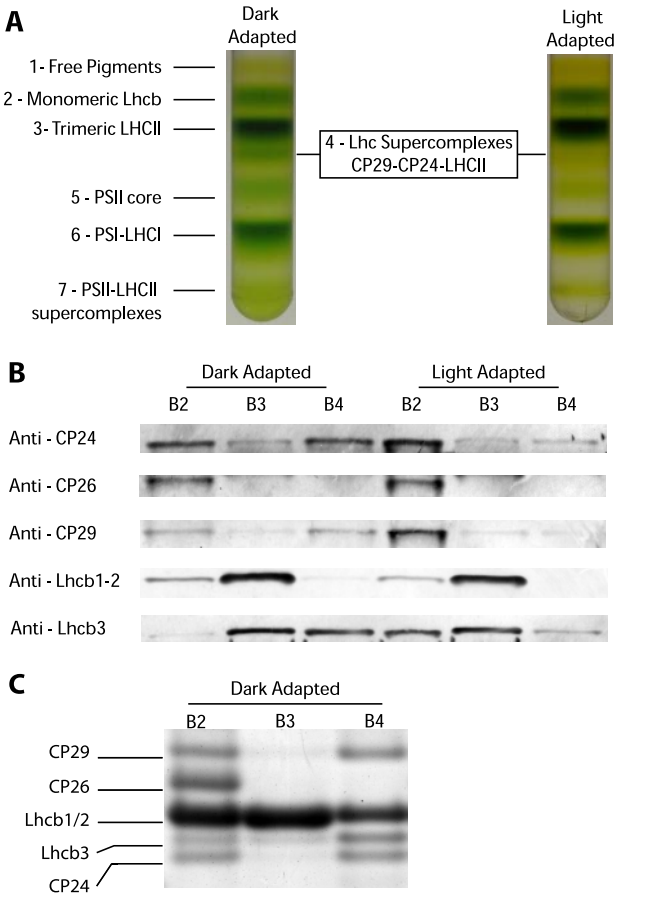


FIGURE 1. **Light-dependent dissociation of B4C protein complex in *A. thaliana*.** *A*, sucrose gradient fractionations of mildly solubilized thylakoids membranes purified from dark- and light-adapted (30 min at 1500 $\mu$E) leaves. In the dark thylakoid pigment-binding complexes separate into seven distinct bands, the fourth one (B4C) being depleted in light-treated sample. *B*, distribution of monomeric antenna proteins in sucrose gradients between bands 2, 3, and 4 from dark- and light-adapted samples. Western blotting analysis was carried out using specific antibodies against CP24, CP26, CP29, Lhcb1–2, and Lhcb3, respectively. Samples from different bands were loaded in amounts proportional to their abundance in the sucrose gradient. In Lhcb1–2 blotting, each band was loaded with five times less protein to avoid antibody signal saturation. *C*, Coomassie-stained SDS-PAGE loading of equal Chl amounts (2 $\mu$g) from sucrose gradient bands 2, 3, and 4 from dark-adapted samples. Bands corresponding to CP29, CP26, Lhcb1/2, Lhcb3, and CP24, as identified by Western blotting, are indicated. Only the gel region where antenna polypeptides are migrating is shown.

nents of this complex (Fig. 1*B*). CP26, instead, is not involved in B4C formation, as shown by the fact that it is found in B2, in a monomeric state, irrespective of the treatment.

Thereafter we analyzed the dependence of B4C dissociation on light intensities; dissociation increased with the level of illumination, reaching saturation above 1500 $\mu$E (Fig. 2*A*). State transitions are known to involve dissociation of LHCII subunits from PSII reaction centers (29) and cannot be excluded as the cause of B4C complex dissociation. However, state transitions are saturated at low light (200 $\mu$E) and are inhibited by high light, in agreement with their role in balancing PSI *versus* PSII photon trapping under limiting light conditions (30, 31) and thus are unlikely to be correlated with B4C dissociation.

Also, we did not observe any increase in phosphorylated CP29 in light-treated samples, consistent with previous results (30). This is an indication that this phenomenon is also unrelated to B4C dissociation.

At least two processes can be active under high light conditions leading to B4C dissociation: one is photoinhibition, meaning light-induced damages in PSII, and the other is non-photochemical quenching. To test whether one of these processes (or both) is involved in B4C dissociation, we measured the recovery of variable fluorescence, a marker of photoinhibition, upon illumination with different intensities (1500 $\mu$E; Fig. 2*A*). It clearly appears that $F_v/F_m$ is significantly affected only with the highest light intensity, whereas B4C dissociation, instead, occurs with weaker levels of illumination, suggesting that the two phenomena are not correlated. Instead, the level of B4C dissociation at different light intensities closely matches the amplitude of NPQ obtained under the same light conditions (Fig. 2*A*); in fact, both NPQ and B4C show activation with increasing illumination. This correlation is evidenced in Fig. 2*B*, where it can be appreciated how B4C dissociation and NPQ have a similar dependence on light intensity, different from $F_v/F_m$ (Fig. 2*C*). We thus tentatively concluded that B4C dissociation correlates with NPQ rather than with photoinhibition.

We analyzed the time dependence on light of B4C dissociation; as shown in Fig. 3*A*, dissociation increases with time. This process is reversible, and following dark incubation, B4C slowly reassociates. Upon a lag phase of 15 min, B4C can be detected again at 30 min, and the dark control level is reached upon 45 min of dark adaptation (Fig. 3*B*). We also verified that these results were not due to the thylakoid fractionation technique used, by analyzing the kinetics of B4C dissociation by nondenaturing Deriphat-PAGE. We obtained results fully consistent with sucrose gradient analysis (data not shown).

*Pharmacologic and Genetic Analysis of B4 Complex Dissociation*—To investigate in more detail the correlation between NPQ and B4C dissociation, light treatment was performed on leaves treated with nigericin, a NPQ inhibitor through its uncoupling effect on the trans-membrane pH gradient (Fig. S1*A*). As shown in Fig. 4*A*, in nigericin-treated leaves, the B4C complex is stable, implying that its light-dependent dissociation requires the presence of a trans-membrane pH gradient.

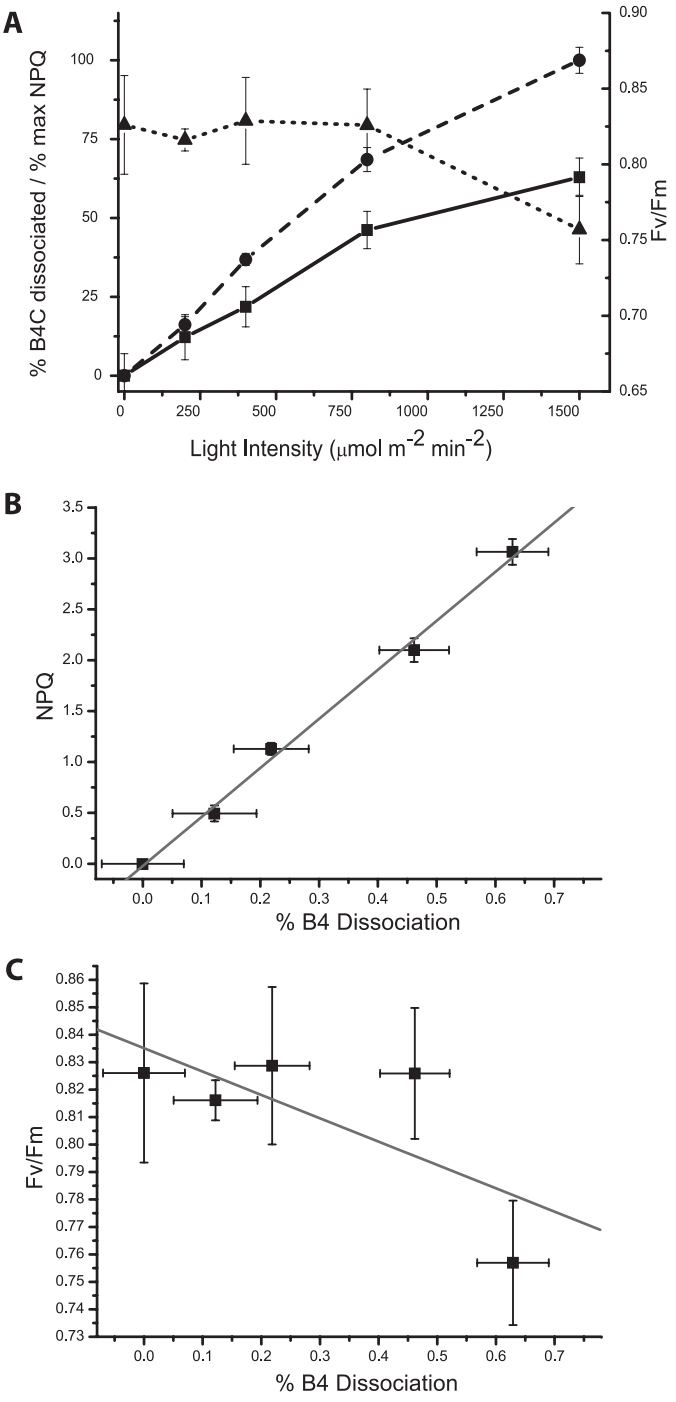


FIGURE 2. *A*, comparison of B4C dissociation (*solid line*, *squares*), NPQ (*dashed line*, *circles*), and PSII yield ($F_v/F_m$, *dotted line*, *triangles*). All parameters were evaluated after 30 min of light treatment at the indicated intensity. B4C is quantified as the ratio of the band with respect to the sum of all bands containing antenna upon separation of pigment-binding complexes in sucrose gradient or nondenaturing gel. NPQ values, in order to have a scale comparable with B4C dissociation, are expressed as a fraction of the maximal value (3.1). $F_v/F_m$ values where measured after 15 min of dark incubation following light treatment to allow for PSII reduction and NPQ relaxation but not recovery from photoinhibition. *B*, correlation between B4C dissociation and NPQ measured with different light intensities is analyzed in more detail. Line shows the linear fitting of reported points (*R*-value is 0.997). *C*, correlation analysis of $F_v/F_m$ and B4C dissociation determined using different illumination intensities. Line shows the best linear fitting of reported points (*R*-value is 0.71).

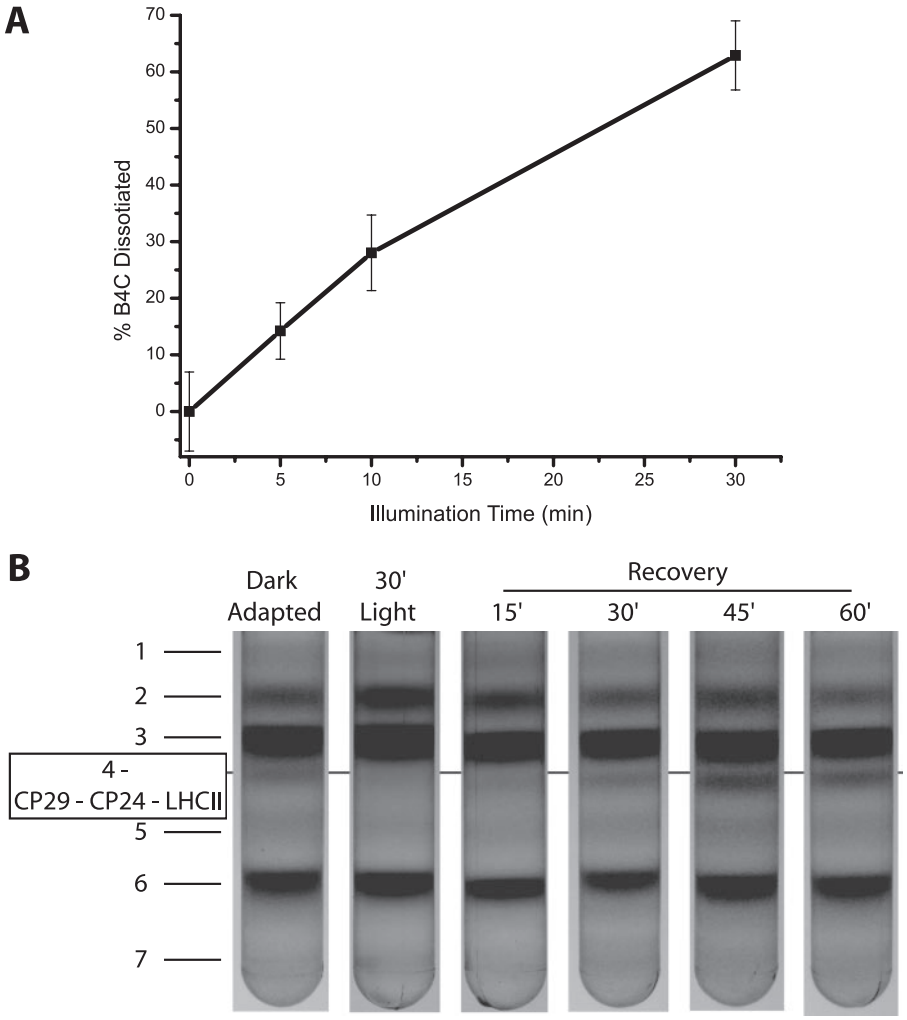


FIGURE 3. **Time dependence of B4C dissociation and reassociation in *A. thaliana*.** *A*, B4C dissociation was determined from sucrose gradients after different durations of 1500 $\mu$E illumination. B4C is quantified as described under "Experimental Procedures." *B*, reassociation of B4C complex in samples left in the dark for 15, 30, 45, and 60 min after a 30-min-long illumination at 1500 $\mu$E.

To dissect the components of the relation between B4C and NPQ, we analyzed a series of mutants that are affected in NPQ at different levels, namely *npq4* impaired in $q_E$, the fastest NPQ component due to the absence of PsbS (20); *npq1* (no zeaxanthin and reduced NPQ (32)); and *npq2* with constitutive zeaxanthin and accelerated NPQ (32); as well as the double *npq2*/*npq4* mutant. The NPQ kinetics of these genotypes have been reported in earlier work and are shown here in supplemental Fig. S1 (20, 32, 33). The results from Fig. 4, *A* and *B*, show that the *npq4* mutation completely abolishes the light-dependent B4C dissociation, even in the presence of constitutive zeaxanthin, implying a key role for the PsbS protein in the process. Zeaxanthin is also a factor in B4C dissociation; in fact, in its absence, the *npq1* mutant undergoes only 30% dissociation of B4C upon illumination, whereas, when present constitutively, as in the *npq2* mutant, B4C is dissociated faster than in the WT (not shown).

PsbS activity in NPQ has been reported to be dependent on the protonation of two lumen-exposed glutamate residues (21, 22). The analysis of B4C dissociation in mutants at these Glu residues thus allows verification of the hypothesis that PsbS activity in B4C dissociation and in NPQ is mediated by the same mechanism, *i.e.* the protonation of Glu-122 and Glu-226 residues. To this aim, we analyzed *npq4* mutants complemented with PsbS-encoding sequences carrying either WT, E122Q, E226Q or the double E122Q/E226Q mutant sequence (21, 22). The data in Fig. 4*C* show that the double mutant is unable to dissociate B4C, whereas each of the single glutamate mutants undergoes ~40% B4C dissociation. The complementation with the WT PsbS sequence instead fully restored the capacity for light-dependent B4C dissociation. Thus, the extent of B4C dissociation was completely correlated with the NPQ activity of each genotype (all kinetics are shown in supplemental Fig. S1). It is worth mentioning that PsbS protein was detected in sucrose gradients in several of the pigmented fractions, as reported previously (34, 35), and that this distribution did not change upon light treatment.

*Specific Lhcb Mutants Show Constitutive B4C Dissociation*—The crucial role of PsbS in NPQ has been known for several years (20). After intense debate, it is now widely recognized that its role is to sense the low lumenal pH, thus inducing a quenching conformation of specific antenna complexes where the quenching reaction(s) occur (36–38). Because antenna polypeptides are involved both in structurally building the B4C and in catalyzing the quenching reactions, we investigated the effect of knocking out individual components of the PSII antenna system on the levels and kinetics of NPQ and on the structural stability of B4C. In Fig. 5*A*, sucrose gradient fractionation patterns of thylakoids purified from dark-adapted plants depleted in CP24, CP26 (25), Lhcb1 and -2 (39), CP29, and Lhcb3 (this work) are shown. We observed that knock-out mutants for some B4C components, namely CP29, CP24, and Lhcb3, do actually miss B4C. Instead, depletion of Lhcb1 and -2 does not affect B4C abundance in the sucrose gradient, implying that Lhcb3 is not equivalent to the other LHCII components as far as its contribution to the building of B4C. On this basis, we propose that B4C complex formation requires the direct interaction of Lhcb3, CP29, and CP24. On the contrary, Lhcb1 and Lhcb2, although participating in the trimeric LHCII M component, are not indispensable for B4C formation. Consistently, B4 is present in koCP26 plants.

Analysis of the above genotypes by pulse fluorometry during light treatment showed that the mutants on B4C components

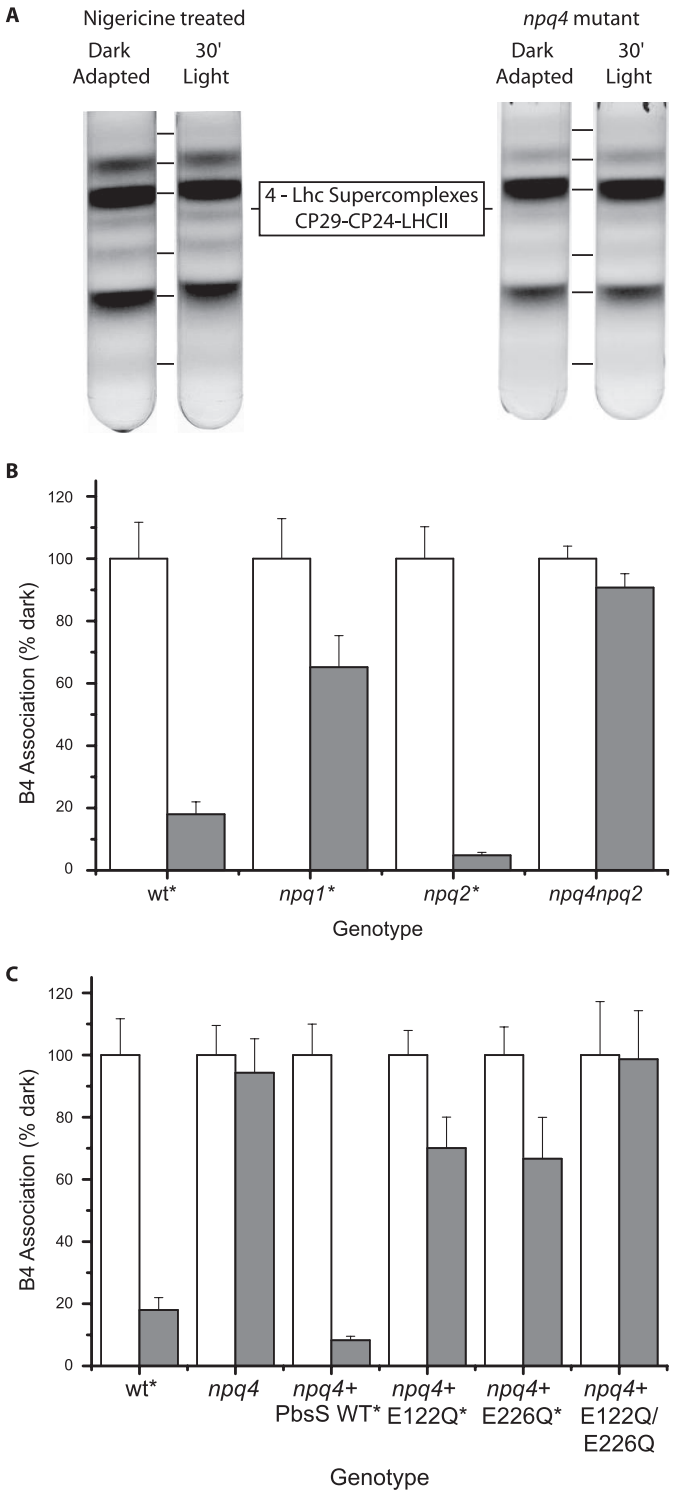


FIGURE 4. **Dependence of B4C dissociation on ΔpH, PsbS, and zeaxanthin.** *A*, light dependent B4C dissociation in nigericin-treated leaves (*left*) and PsbS-depleted mutant (*npq4*, *right*); *B*, quantification of B4C in leaves that are either dark-adapted (*white*) or treated with 1500 μE for 30 min (*gray*). WT is compared with mutants affected by zeaxanthin biosynthesis (*npq1*) or constitutively accumulating zeaxanthin (*npq2*) and in an *npq2/npq4* dark-adapted double mutant in (*white*). *C*, quantification of B4C in leaves that are either dark-adapted (*white*) or treated with 1500 μE for 30 min (*gray*). WT is compared with *npq4*, also complemented with PsbS WT or mutated E122Q and/or E226Q. Quantifications in *B* and *C* were performed as described in the legend for Fig. 2. All genotypes where dark- and light-treated samples are significantly different ($p > 0.05$, $n = 3$) are indicated by an *asterisk*. NPQ measurements for all genotypes are reported in supplemental Fig. S1.

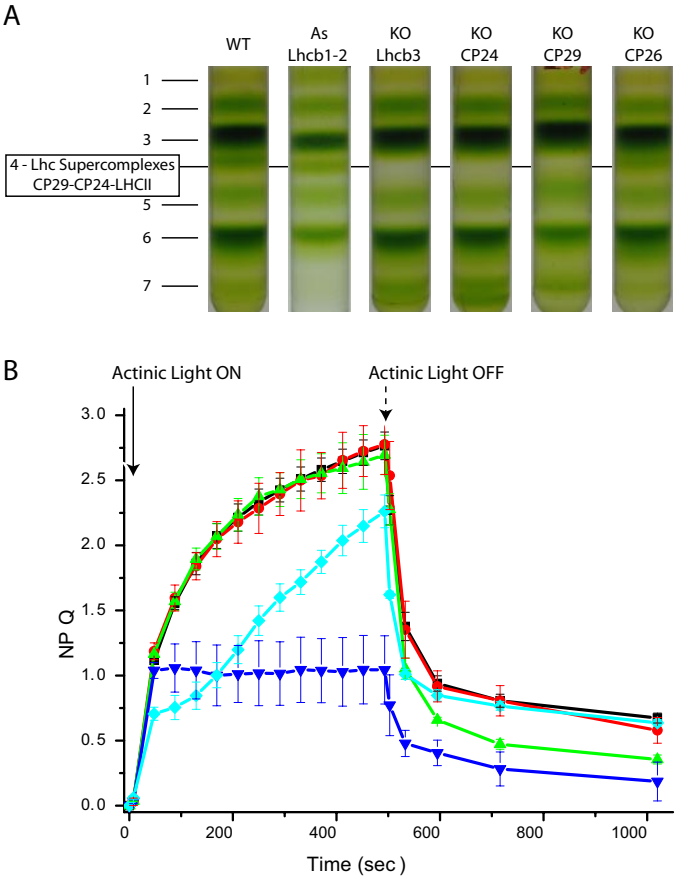


FIGURE 5. **Dependence of B4C and NPQ on the presence of individual Lhc proteins.** *A*, the capacity of B4C formation was analyzed in plants depleted of individual Lhcb proteins by separating different pigment-binding complexes from dark-adapted thylakoid membranes. Genotypes analyzed were WT, koLhcb3, koCP24, koCP29 (which is a triple knock-out in all CP29 *Arabidopsis* isoforms, Lhcb4.1, Lhcb4.2, and Lhcb4.3) and koCP26. *B*, NPQ dependence on antenna composition, analyzed by comparing WT (*black*) with plants depleted of CP26 (*green*), CP24 (*blue*), CP29 (knock-out in Lhcb4.1, Lhcb4.2, and Lhcb4.3 (*cyan*)), and Lhcb3 (*red*).

were not equivalent as far as their NPQ behavior; ko-Lhcb3 did not show any effect, whereas CP29 and CP24 were deeply affected, showing a significant decrease in NPQ amplitude and slower induction kinetics. Although the effect of CP24 depletion on the NPQ process has recently been well described (24, 25), the NPQ kinetics of koCP29 reveals that also this subunit has a relevant role in NPQ induction, different from previous suggestions coming from the study of antisense plants (42). Lhcb1 and -2-depleted plants showed very similar kinetics but a slightly lower amplitude of NPQ with respect to WT (not shown), in agreement with previous reports (39). CP26 is the only Lhcb complex not involved directly in B4C assembly, in agreement with its location in a different domain of the PSII supercomplex (3). The NPQ kinetic of koCP26 plants is unaffected in the onset during light treatment but has a faster recovery of fluorescence in the dark, implying an effect on the $q_I$ component (Fig. 5*B*). We concluded that the presence of a stable B4C complex is not a prerequisite for NPQ and that the NPQ properties of the mutants depend on the residual composition in Lhcb complexes of the different genotypes. However, when B4C complex is present, its dissociation is needed for NPQ expression.

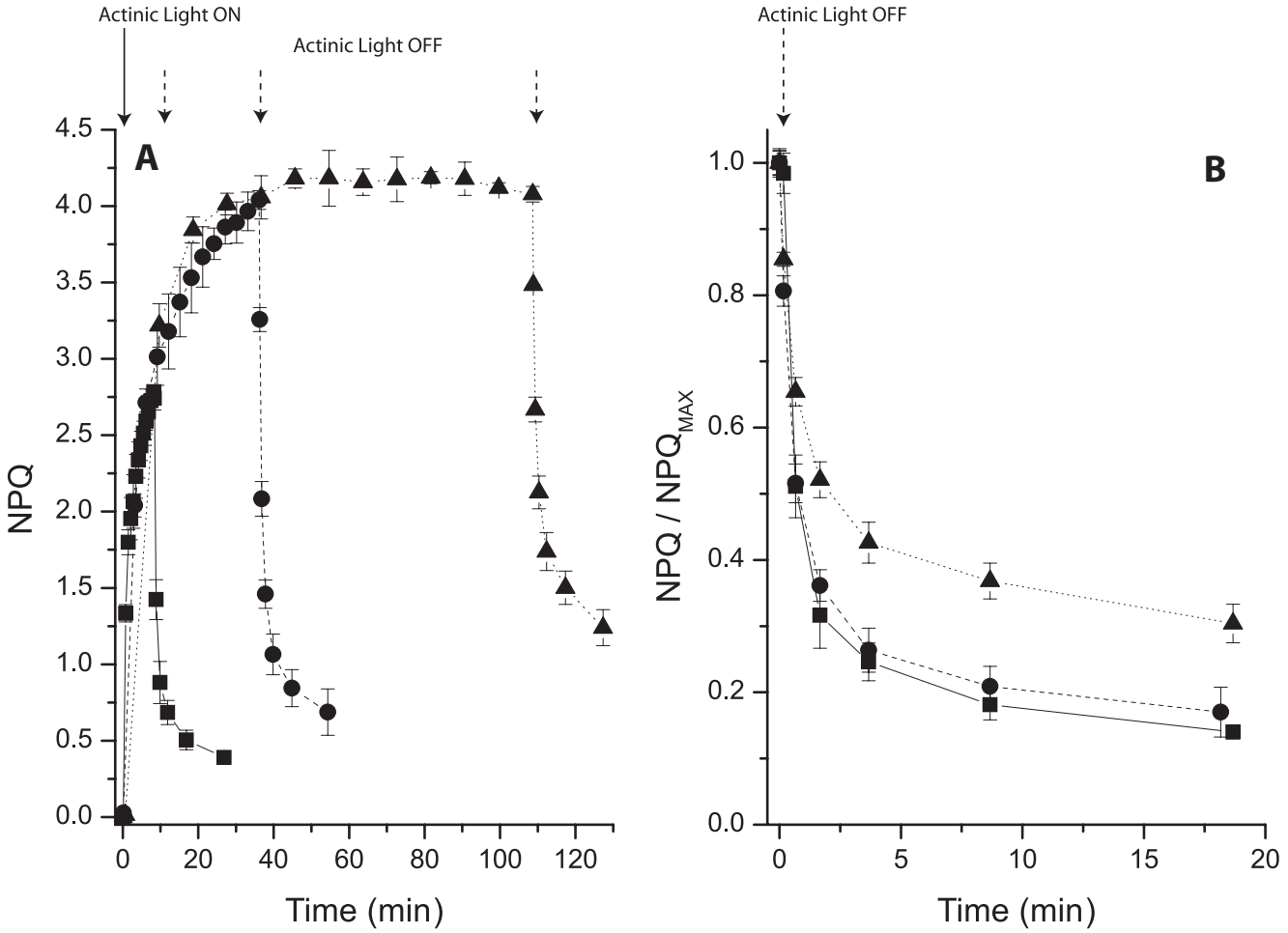


FIGURE 6. **Long term NPQ induction and recovery.** *A*, NPQ kinetics in WT leaves was recorded using different durations of actinic light. For all samples NPQ was recorded at 12 points during illumination. Curves with 8, 36, and 108 min of actinic light are shown, respectively, as a *solid line* with *squares*, a *dashed line* with *circles*, and a *dotted line* with *triangles*. In all samples, six points were recorded at the same time intervals during dark recovery. *B*, enlargement of recovery kinetics shown in *A* after normalization to maximal NPQ.

*NPQ upon Prolonged Illumination*—NPQ and B4C dissociation have in common a dependence on light intensity and the presence of PsbS. These phenomena, however, are activated in different time scales. The literature shows that the onset of NPQ requires only a few minutes, whereas B4C dissociation needs a longer period of illumination. In order to compare the two processes over the same time span, we measured NPQ kinetics using a longer exposure to actinic light than what is usually reported in the literature. In Fig. 6 we show the NPQ kinetics in WT *Arabidopsis* plants upon illumination for 8, 30, and 90 min. These kinetics show that the largest part of NPQ is activated within a few minutes of illumination ($t_{½}$ is 3 min) but continues to rise for up to 30 min. After 90 min of illumination NPQ amplitude is stable at its saturated level. However, the kinetics of dark relaxation was slower upon 90 min of illumination than what observed after 8 or 30 min of light. This is evidenced in Fig. 6*B*, where the NPQ decay curves are normalized to the maximal NPQ value. Although relaxation kinetics are similar upon 8 or 30 min of illumination, they are slower upon 90 min of treatment. We can exclude the suggestion that this effect is due to the normalization procedure, because the level of quenching is very similar following 30 and 90 min of illumination.

The possibility that photoinhibition could be a reason for the slowdown of fluoresce recovery was assayed by measuring dark recovery of PSII quantum yield after light treatment. As this was essentially the same in plants that were treated with light for 30 or 90 min, we concluded that differential photoinhibition is not the cause of the different kinetics of fluorescence recovery after NPQ (supplemental Fig. S2). Alternatively, sustained quenching could be due to zeaxanthin accumulation (33). However, no difference was observed in the *Zea* content of leaves treated with 30 or 90 min of actinic light, and the recovery of violaxanthin content was very similar (supplemental Fig. S2).

We concluded that, in addition to the two well known phases of NPQ consisting of a rapidly developing step dominated by $q_E$ and a slower phase depending on zeaxanthin synthesis (19), we could distinguish a later phase with sustained quenching. During this later phase the properties of the photosynthetic apparatus undergo changes that cannot be explained in terms of photoinhibition or zeaxanthin quenching, and yet they significantly affect the recovery of fluorescence.

*The Organization of Grana Membranes Is Modified upon PsbS-dependent Dissociation of the B4C Complex*—In order to test the hypothesis that the slowly developing changes of the slowest NPQ phase described above involve a reorganization of

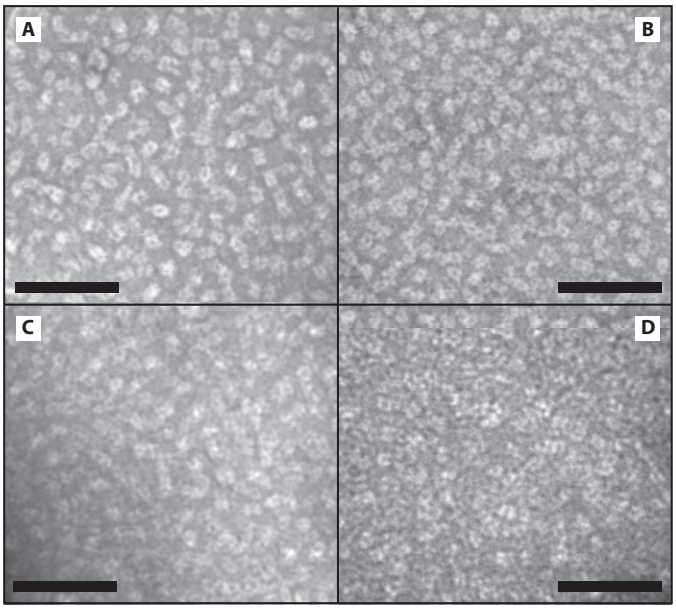


FIGURE 7. **EM of grana membranes isolated upon light treatment.** EM of grana membranes isolated from WT leaves that were dark-adapted (*A*) or treated with 30 min of light (*B*), 90 min of light (*C*), or 90 min of light and 90 min of dark (*D*). *Space bar* represents 100 nm.

the thylakoid membrane, we studied the organization of the PSII components in grana membranes through direct observation by electron microscopy. In grana partitions, the PSII complex forms $C_2S_2$ particles (3), which constitute the inner antenna system and are maintained even in high light-adapted plants (12) and include a subset of the B4C complex, namely CP29. The rest of the B4C components are part of the outer antenna, which is assembled under low light conditions, leading to the formation of larger $C_2S_2M_2L_X$ particles (3). This suggests that the integrity of B4C is required for the formation of large supercomplexes and its dissociation could lead to a reorganization of the antenna system with a consequent reduction of antenna size. To test this hypothesis, we analyzed the organization of grana membranes in WT and selected mutants upon treatment with light. To this aim we isolated grana membranes from plants illuminated for different periods, using a mild solubilization with $\alpha$-DM, which preserves the interaction between PSII components and the overall mutual organization of PSII units (10). Photosystem II forms tightly packed domains in grana partition membranes with very little lipid interspersed between protein complexes (43). When observed by transmission electron microscopy upon negative staining, PSII membranes were characterized by stain-excluding particles with a tetrameric structure that could be readily identified as PSII cores (Fig. 7). Lhc protrude less from the membrane plane than PSII reaction centers and are thus covered by an electron-dense stain. The observation of grana membranes isolated from leaves treated with different light intensities did not show any eye-catching difference (Fig. 7).

Searching for more subtle differences, we identified in each image the position of the PSII cores and calculated the distance of the closest neighbor. The distribution of the distances is reported in supplemental Fig. S3. In most cases, the closest PSII core is located at 16–17 nm. Two shoulders in the distribution are also visible, one at 14 nm and a second at 20–21 nm. This distribution, with one main peak and two symmetric shoulders, is close to that obtained previously using different microscopic methods, AFM and freeze fracture (44, 45). This allowed us to conclude that, despite our using a different approach, the results obtained for the dark-adapted sample were quite consistent with published data, strongly supporting the reliability of grana isolation and image analysis procedures.

To reduce the dependence of the results on the possible imprecise assignment of PSII cores, we repeated the analysis by calculating for each core the average distance from the four closest PSII cores rather than from the closest neighbor only. As shown in Fig. 8, data deviations in this case were smaller, because the error in PSII core location is partially compensated for by the larger sampling. This method was thus employed to analyze grana membranes isolated from light-treated leaves (data considering only the closest neighbor are shown in the supplemental material). As shown in Fig. 8*B*, upon 30 min of illumination the PSII distribution shows a decrease in the population with an average distance of 22 nm and a compensating increase of the 18–19 nm population. The difference is significantly greater in the sample illuminated for 90 min; in that case, there is a far lesser abundance of PSII cores, with an average distance of 22 nm and the highest frequency found at 18 nm.

We also verified the reversibility of the phenomenon by analyzing samples that, after 90 min of illumination, were further incubated in the dark for 90 min before grana isolation. In this case (Fig. 8*C*), we observed that the average distance between PSII increased, showing a decrease in the content of PSII cores of $<17$ nm and an increase in abundance for all points of $>19$ nm. Thus, although the recovery was partial and likely required a longer time to complete, these data strongly suggest the phenomenon is reversible. As a control, it is interesting to observe the phenotype of PsbS-less mutant *npq4*. Data from mutant grana isolated before and after 90 min of light treatment are shown in Fig. 8*D*. Remarkably, the distribution is substantially unaffected by light treatment. These results thus allowed us to conclude that light induces a redistribution of PSII cores within grana membranes but only in the presence of PsbS protein.

## DISCUSSION

*B4C Complex Has a Key Role in Building the PSII Supercomplex*—CP29 and CP26 are located in direct contact with the PSII core complex (9, 46, 47) and interact with the LHCII-S trimer to form the so-called $C_2S_2$ particles (9). This PSII complex organization is found in plants grown under any conditions, even very intense light, and in mutants with constitutively reduced plastoquinone where PSII is constantly over-excited (10). $C_2S_2$ particles thus represent the minimal PSII supercomplex.

Growth in low or moderate light leads to the accumulation of additional antenna complexes, CP24, LHCII-M, and LHCII-L trimers (12, 48), and the formation of an outer antenna system in $C_2S_2M_2$ particles or higher mass supercomplexes (9). PSII-LHCII supramolecular complexes thus appear to include two layers of Lhc proteins: the inner layer, composed by CP26, CP29, and the LHCII-S trimer, and the outer layer, including CP24 and at least two LHCII trimers (M and L).

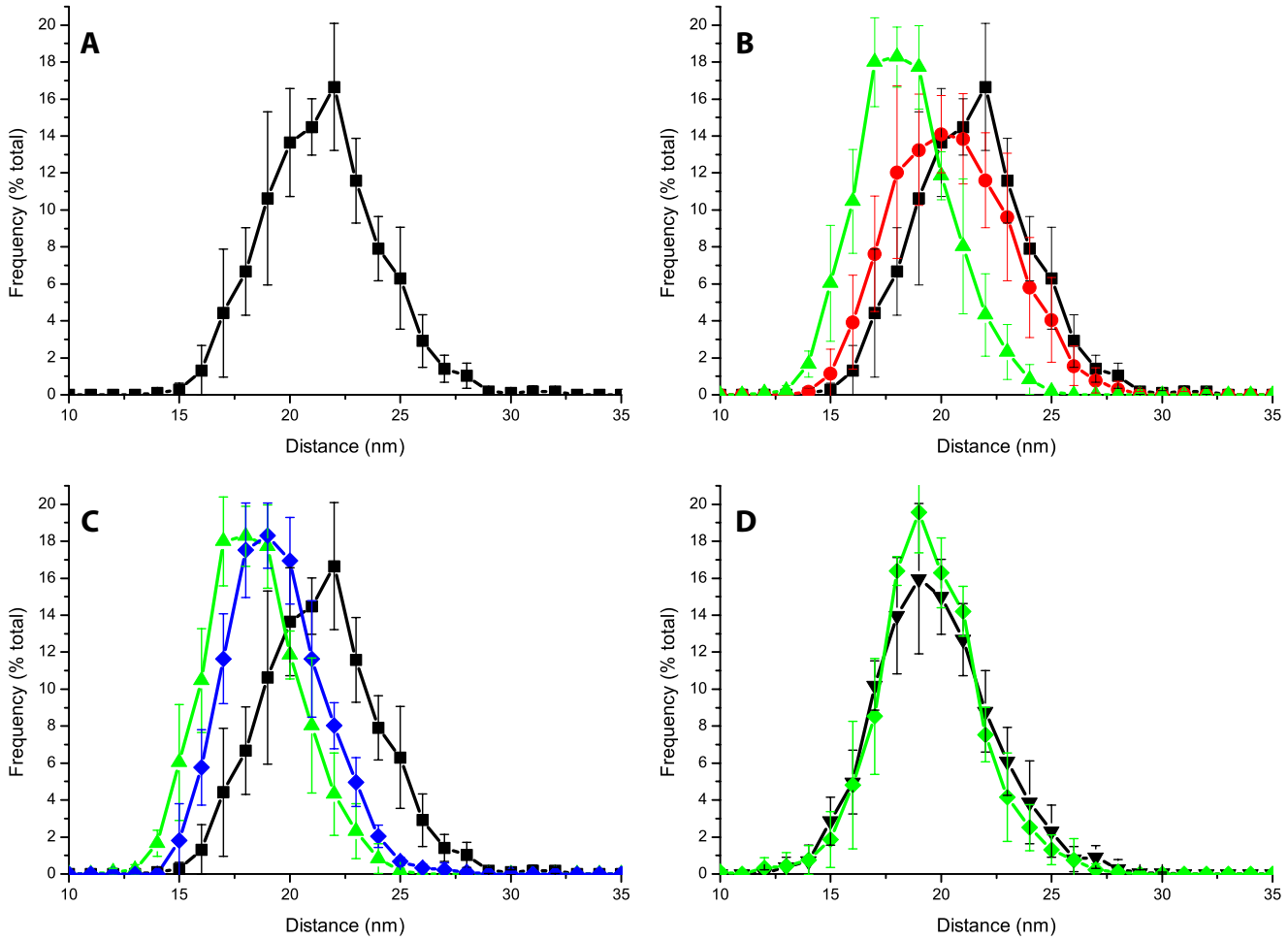


FIGURE 8. **Analysis of PSII distribution in grana isolated from dark/light-treated leaves.** *A*, distribution of PSII complexes in grana membranes from dark-adapted leaves expressed as the average distance from the four nearest PSII core complexes. *B*, comparison of PSII distribution in dark-adapted samples (*black squares*) or those treated with 30 min (*red circles*) and 90 min (*green triangles*) of light before grana isolation. *C*, comparison of light-adapted samples (*green triangles*) with samples treated successively with 90 min of dark following light treatment (*blue diamonds*). *D*, effect of light treatment on PSII distribution in *npq4* grana membranes. Dark-adapted sample is shown as *black triangles* and 90-min light-treated sample as *green diamonds*. S.D. in the case of the *x* axes is the maximum 1.5 nm.

B4C is a Lhc supercomplex composed of CP29 (inner layer), CP24, and LHCII-M (outer) (46). B4C has been described (6) as a product of incomplete solubilization of PSII membranes with mild detergents. It was later understood to represent a structural brick of the PSII-LHCII supercomplexes as shown by electron microscopy and cross-linking studies of the interactions of these subunits (3, 9, 49). Its presence is fundamental for the structure of PSII supercomplexes with larger antenna sizes. A further confirmation of this view comes from the observation that green algae, which do not have CP24 and Lhcb3 subunits, are not able to form B4C complex. In fact, green algae show the presence of $C_2S_2$ particles only (47). It can be asked whether all CP29 and CP24 subunits are organized into a B4 supercomplex with a LHCII trimer. Fig. 1 shows that a non-negligible amount CP29 and CP24 is found as monomers. However, in a previous report from *Zea mays*, 100% of the CP29 and CP24 was found in the B4C (6). These considerations suggest that monomerization of CP24 and CP29 is most likely because of partial destabilization of the B4C supercomplex due to detergent treatment during thylakoids solubilization.

*Dissociation of the B4C Complex Is Correlated to Non-photochemical Quenching*—In this work we have reported on the light-dependent dissociation of the supramolecular pentameric complex composed of CP29, CP24, and the LHCII-M trimer (6), which connects the inner and outer moieties of the light-harvesting system. We noticed that the fractionation pattern of PSII subunits in sucrose gradients or nondenaturing PAGE was modified upon strong illumination; an oligomeric green band, B4C, present in dark-adapted leaves, dissociated from its monomeric and trimeric components (Fig. 1).

Pharmacologic and genetic analysis showed that B4C dissociation correlates fully with NPQ. In fact, we observed that this event was sensitive to the uncoupler nigericin and was up-modulated by zeaxanthin, as shown by the *npq1* mutant, which cannot synthesize *Zea* and is inefficient in both B4C dissociation and NPQ. The most striking evidence of this correlation, however, comes from the phenotype of PsbS-depleted plants, which are unable to activate NPQ and do not show the light-dependent dissociation of B4C (Fig. 4). Furthermore, the mutation of each of two lumen-exposed glutamate residues in PsbS, essen-

tial for NPQ activation (20, 21), leads to an NPQ decrease of ~50% (21). Here, we show that the same mutation impairs the dissociation of B4C to approximately the same extent (Fig. 4), making it very unlikely that these two phenomena are independent but occur simultaneously upon illumination.

*Functional Role of B4C Dissociation in Non-photochemical Quenching*—The above results suggest a tight relationship between B4C dissociation and NPQ. It is, however, unclear whether dissociation of B4C is sufficient for feedback de-excitation or if additional operations are involved in the process that might well be fulfilled by PsbS. One way to address this question is to compare the WT with mutants in which B4C is constitutively dissociated, such as koCP24 (Fig. 5). In this mutant, dark-adapted plants have a higher fluorescence level than the WT, implying that the disconnected LHCII is not efficiently quenched (24, 25). Furthermore, koCP24 plants are able, despite the complete absence of B4C, to activate NPQ, although at a reduced level with respect to WT. By analyzing different mutants depleted in antenna proteins, koLhcb3 and koCP29 in Fig. 5, we noticed that the absence of B4C in a number of these mutants did not completely abolish NPQ, although the kinetics were differently affected depending on the residual complement of Lhcb proteins in each mutant.

B4C dissociation by itself is thus not sufficient for NPQ. However, in all cases where B4C was present in the dark, we never observed NPQ without B4C dissociation. This suggests that B4C stabilizes an unquenched state and that its dissociation is required for quenching activation. On these bases, we hypothesized that the quenching activity is performed by one or more B4C components. The integrity of B4C prevents quenching, which can be triggered only when this supercomplex is dissociated. It is not clear at present whether the role of PsbS is limited to the dissociation of B4C or if it extends to establishing an interaction with the resulting dissociated Lhcb subunits. We favor the latter hypothesis because in koCP24 the disconnected LHCII-M + L are clearly detectable; however, they are not quenched (24). Indeed, the koCP24 genotype mimics the constitutive dissociation of B4C, and EM analysis of its grana membranes clearly shows that in the absence of B4C, PSII core is nonhomogeneously distributed in grana membrane disks with PSII-rich areas and LHCII-enriched stain-depleted domains (supplemental Fig. S4).

It might be asked which of the different subunits are the "quenching sites." Considering the similarity between antenna proteins it is unlikely that quenching occurs in only one subunit, and they may well all contribute. Nevertheless, recent reports are helpful in identifying some preferential quenching sites based on the *in vivo* effect of knocking out individual gene products on NPQ amplitude/kinetics and on the capacity of catalyzing the transient formation of carotenoid radical cation, a chemical species proposed to be responsible for excess energy quenching (50) by isolated pigment-protein complexes. Thus, depletion of Lhcb1 and -2 (39) or Lhcb3 (Fig. 5) has little effect on NPQ *in vivo*, and these antenna subunits cannot produce any carotenoid radical cation *in vitro* (51).

Monomeric Lhcb4, -5, and -6 do indeed perform charge transfer quenching *in vitro* (37, 51), whereas *in vivo* depletion strongly affects NPQ components: $q_E$ in the case of CP24 and CP29 (25) (Fig. 5) and $q_I$ in the case of CP26. The involvement of two components of B4C complex in $q_E$, together with the NPQ depletion in all mutants/conditions where B4C complex cannot be dissociated, is strong evidence for the direct interaction of a PsbS-minor Lhc complex in triggering NPQ.

*An NPQ Model Based on the Rearrangement of PSII Supercomplex Antenna*—A possible discrepancy between B4C dissociation and NPQ can be found in their activation time scales. In fact, a large fraction of NPQ is activated within a few minutes after the dark to light transition ($t_{½}$ ~ 3 min; Fig. 6), whereas we observed that B4C dissociation is developed with a $t_{½}$ of 12–15 min (Fig. 3). This phenomenon thus appears to have the same time scale of the slow phase of NPQ activation. However, the method we used for biochemical detection of B4C dissociation, *i.e.* sucrose gradient ultracentrifugation, is all but rapid and sensitive. It is likely that dissociated B4C need to be accumulated in order to be detected by biochemical fractionation and/or that unstable B4C dissociation is involved in the fastest phase of NPQ. In fact, after light treatment, thylakoid isolation and solubilization requires about 60 min. Thus, despite the fact that all operations were performed in ice water, we cannot exclude the possibility that early changes were reverted to before thylakoid solubilization and gradient loading. On the contrary, the physiological effects that elicit NPQ might be activated in a few seconds by a partial and unstable B4C dissociation, which, if the high light conditions are maintained, is increased by a complete B4C dissociation and stabilized by the structural redistribution of complexes within the grana membrane.

Our results provide experimental support of previous suggestions that (i) PsbS functions by interacting with other antenna proteins; (ii) PsbS controls the grana membrane organization; and (iii) structural modification in photosystems are implied in NPQ (35, 38, 52, 53). Such an extensive PSII reorganization might appear surprising. Nevertheless, recently reported data are consistent with such a model; FRAP measurements show that the greater part of complexes (75%) within grana membranes is substantially immobile. However, the remaining complexes, likely identified as antenna complexes, have instead a high diffusion coefficient. According to this hypothesis, an antenna complex might travel from the center to the limit of the grana membrane in about 2 s (54). These results thus suggest that a rearrangement of antenna complexes, also implying protein displacement, would be compatible with NPQ kinetics. Furthermore, the latter study suggests that this movement is not only diffusion-driven but is likely to be "oriented"; in this respect, a role could be played by PsbS activity, which might help in creating the so-defined diffusion channels (54). Concerning the role of PsbS, it interesting that we observed a small but significant difference between WT and *npq4* in PSII core distribution in the dark. This is consistent with the observation that *npq4* mutants grow better in low light conditions than do WT (33), suggesting that PsbS activity is not fully restricted to excess light conditions.

*B4C Dissociation Induces a Rapid Decrease in the Antenna Size of PSII Supercomplex*—Structural analysis of grana membranes clearly showed that light treatment induces a decrease in the distance between PSII reaction centers. This effect was reversible upon dark recovery, in parallel with the dissociation

and reassociation of B4C. Grana membranes are densely packed with PSII components and contain little free lipids (43, 55). Thus, the distance between PSII core complex is determined mainly by the Lhcb protein complement of photosystems (10, 24, 44, 47). We concluded that light treatment, with the involvement of PsbS activity, leads to a reversible dissociation of the outer layer of the PSII antenna system from the reaction center complex, thus reducing the size of the antenna system , which feeds excitation energy to PSII reaction centers.

We observed that such a PSII redistribution requires more than 30 min (Fig. 8). Thus, it correlates with the stabilization of NPQ occurring in the 30–90-min interval (Fig. 6), suggesting that NPQ stabilization occurs by rearranging PSII complexes and their antenna.

The advantage of such a regulatory mechanism is clear if we consider that overexcitation of PSII is the major source of photoinhibition (14). Long term acclimation to high light is well known to lead to a reduction of peripheral antenna size (11, 12). However, the acclimatory process requires protein degradation and takes several days, and it is not useful or energetically affordable when light intensity varies within minutes. NPQ, which is instead the major regulatory mechanism acting within these time scales (17), could thus work by functionally dissociating part of the antenna from the core complex while avoiding degradation and resynthesis.

*The Fate of Lhcb upon Disconnection from PSII Reaction Centers*—It might be asked where antenna complexes travel to upon disconnection from the PSII core particles. Possible destinations are the grana periphery and the stroma lamellae. The former hypothesis is likely for at least a fraction of the antenna, as the PSII distribution was shown to be reversible. In the case of koCP24 it was also observed that regions with lower PSII core density were generally found in the grana periphery (supplemental Fig. S4). On a longer time scale (hours or even days), it is also possible that antenna complexes may migrate even further. Early work in fact showed that in light-treated leaves, LHCII isoforms disappear from grana membranes and are found in stroma membranes (56). Because proteolysis is particularly active in stroma membranes, antenna migrating here might be degraded, leading to a stable downsizing of PSII antenna size. This hypothesis suggests the idea that the domain segregation process described here under prolonged illumination contributes to the acclimatory modulation of the PSII antenna size.

*Evolution of NPQ Mechanisms in Viridiplantae*—It is interesting to point out that CP24 and Lhcb3, two of the three components of the B4C complex, are late additions to the PSII antenna system, being present only in land plants (4) and never detected in algae. *Arabidopsis* mutants that are missing any of these polypeptides are also missing B4C (Fig. 5), demonstrating that they are fundamental for the formation of the supercomplexes. Algae and plants also differ as to their PsbS content. In fact, although the gene is present in several algal genomes, the corresponding polypeptide is not accumulated in any algal species analyzed thus far (40, 41). Furthermore, in algae, only $C_2S_2$ supercomplexes have been found, while larger supercomplexes, such as those of land plants, have never been observed (47). This suggests the hypothesis that the regulatory mechanism we described in this work might have evolved upon land colonization in order to defend plants from the highly variable conditions found in the land environment (17). On the contrary, algal water environment is more stable in temperature, light, and $CO_2$ supply, thus making a fast quenching mechanism less important in algae with than in plants (29).

*Conclusion*—We have described herein new experimental evidence on the function of PsbS, consisting of the reorganization of the protein domains in grana membranes as suggested recently (53). This reorganization is obtained by controlling the assembly of a pentameric complex, called B4C, which includes components of both the inner (CP29) and outer (CP24, LHCII-M) moieties of PSII antenna system. In low light the complex is assembled and PSII antenna size is maximal; in high light the complex dissociates, and we proposed that $C_2S_2$ particles dissociates from CP24/LHCII-M/LHCII-L complexes that migrates to the periphery or the grana. Upon dissociation of PSII supercomplexes the formation of quenching sites in PSII antenna, which we propose to be CP24 and CP29, is allowed by the dissociation of B4C and accessibility of these minor Lhc to the interaction with PsbS. We also suggest that this regulation of PSII supercomplex assembly is part of a control cycle connecting short term energy dissipation to long term regulation of PSII antenna size upon acclimation.

*Acknowledgments—We thank G. Tognon for technical assistance with EM and Prof. Niyogi for the kind gift of npq4 mutants.*

**REFERENCES**

1. Nelson, N., and Ben Shem, A. (2004) *Nat. Rev. Mol. Cell Biol.* **5,** 971–982
2. Caffarri, S., Croce, R., Cattivelli, L., and Bassi, R. (2004) *Biochemistry* **43,** 9467–9476
3. Boekema, E. J., van Roon, H., Calkoen, F., Bassi, R., and Dekker, J. P. (1999) *Biochemistry* **38,** 2233–2239
4. Alboresi, A., Caffarri, S., Nogue, F., Bassi, R., and Morosinotto, T. (2008) *PLoS ONE* **3,** e2033
5. Horton, P., and Ruban, A. (2005) *J. Exp. Bot.* **56,** 365–373
6. Bassi, R., and Dainese, P. (1992) *Eur. J. Biochem.* **204,** 317–326
7. Boekema, E. J., Hankamer, B., Bald, D., Kruip, J., Nield, J., Boonstra, A. F., Barber, J., and Rögner, M. (1995) *Proc. Natl. Acad. Sci. U. S. A.* **92,** 175–179
8. Nield, J., Orlova, E. V., Morris, E. P., Gowen, B., van Heel, M., and Barber, J. (2000) *Nat. Struct. Biol.* **7,** 44–47
9. Boekema, E. J., van Roon, H., van Breemen, J. F., and Dekker, J. P. (1999) *Eur. J. Biochem.* **266,** 444–452
10. Morosinotto, T., Bassi, R., Frigerio, S., Finazzi, G., Morris, E., and Barber, J. (2006) *FEBS J.* **273,** 4616–4630
11. Bailey, S., Walters, R. G., Jansson, S., and Horton, P. (2001) *Planta* **213,** 794–801
12. Ballottari, M., Dall'Osto, L., Morosinotto, T., and Bassi, R. (2007) *J. Biol. Chem.* **282,** 8947–8958
13. Lindahl, M., Yang, D. H., and Andersson, B. (1995) *Eur. J. Biochem.* **231,** 503–509
14. Barber, J., and Andersson, B. (1992) *Trends Biochem. Sci.* **17,** 61–66
15. Asada, K. (1999) *Annu. Rev. Plant Physiol. Plant Mol. Biol.* **50,** 601–639
16. Niyogi, K. K. (2000) *Curr. Opin. Plant Biol.* **3,** 455–460
17. Kulheim, C., Agren, J., and Jansson, S. (2002) *Science* **297,** 91–93
18. Niyogi, K. K., Björkman, O., and Grossman, A. R. (1997) *Plant Cell* **9,** 1369–1380
19. Demmig-Adams, B. (1990) *Biochim. Biophys. Acta* **1020,** 1–24
20. Li, X. P., Bjorkman, O., Shih, C., Grossman, A. R., Rosenquist, M., Jansson, S., and Niyogi, K. K. (2000) *Nature* **403,** 391–395
21. Li, X. P., Phippard, A., Pasari, J., and Niyogi, K. K. (2002) *Funct. Plant Biol.* **29,** 1131–1139

22. Li, X. P., Gilmore, A. M., Caffarri, S., Bassi, R., Golan, T., Kramer, D., and Niyogi, K. K. (2004) *J. Biol. Chem.* **279,** 22866–22874
23. Briantais, J.-M. (1994) *Photosynth. Res.* **40,** 287–294
24. Kovacs, L., Damkjaer, J., Kereiche, S., Ilioaia, C., Ruban, A. V., Boekema, E. J., Jansson, S., and Horton, P. (2006) *Plant Cell* **18,** 3106–3120
25. de Bianchi, S., Dall'Osto, L., Tognon, G., Morosinotto, T., and Bassi, R. (2008) *Plant Cell* **20,** 1012–1028
26. Bassi, R., Rigoni, F., Barbato, R., and Giacometti, G. M. (1988) *Biochim. Biophys. Acta* **936,** 29–38
27. Gilmore, A. M., and Yamamoto, H. Y. (1991) *Plant Physiol.* **96,** 635–643
28. Van Kooten, O., and Snel, J. F. H. (1990) *Photosynth. Res.* **25,** 147–150
29. Wollman, F. A. (2001) *EMBO J.* **20,** 3623–3630
30. Tikkanen, M., Piippo, M., Suorsa, M., Sirpio, S., Mulo, P., Vainonen, J., Vener, A. V., Allahverdiyeva, Y., and Aro, E. M. (2006) *Plant Mol. Biol.* **62,** 779–793
31. Bellafiore, S., Barneche, F., Peltier, G., and Rochaix, J. D. (2005) *Nature* **433,** 892–895
32. Niyogi, K. K., Grossman, A. R., and Björkman, O. (1998) *Plant Cell* **10,** 1121–1134
33. Dall'Osto, L., Caffarri, S., and Bassi, R. (2005) *Plant Cell* **17,** 1217–1232
34. Dominici, P., Caffarri, S., Armenante, F., Ceoldo, S., Crimi, M., and Bassi, R. (2002) *J. Biol. Chem.* **277,** 22750–22758
35. Teardo, E., De Laureto, P. P., Bergantino, E., Dalla, V. F., Rigoni, F., Szabo, I., and Giacometti, G. M. (2007) *Biochim. Biophys. Acta* **1767,** 703–711
36. Ruban, A. V., Berera, R., Ilioaia, C., van Stokkum, I. H., Kennis, J. T., Pascal, A. A., Van Amerongen, H., Robert, B., Horton, P., and van Grondelle, R. (2007) *Nature* **450,** 575–578
37. Ahn, T. K., Avenson, T. J., Ballottari, M., Cheng, Y. C., Niyogi, K. K., Bassi, R., and Fleming, G. R. (2008) *Science* **320,** 794–797
38. Bonente, G., Howes, B. D., Caffarri, S., Smulevich, G., and Bassi, R. (2008) *J. Biol. Chem.* **283,** 8434–8445
39. Andersson, J., Wentworth, M., Walters, R. G., Howard, C. A., Ruban, A. V., Horton, P., and Jansson, S. (2003) *Plant J.* **35,** 350–361
40. Finazzi, G., Johnson, G. N., Dall'Osto, L., Zito, F., Bonente, G., Bassi, R., and Wollman, F. A. (2006) *Biochemistry* **45,** 1490–1498
41. Bonente, G., Passarini, F., Cazzaniga, S., Mancone, C., Buia, M. C., Tripodi, M., Bassi, R., and Caffarri, S. (2008) *Photochem. Photobiol.* **84,** 1359–1370
42. Andersson, J., Walters, R. G., Horton, P., and Jansson, S. (2001) *Plant Cell* **13,** 1193–1204
43. Tremolieres, A., Dainese, P., and Bassi, R. (1994) *Eur. J. Biochem.* **221,** 721–730
44. Kirchhoff, H. (2008) *Trends Plant Sci.* **13,** 201–207
45. Kirchhoff, H., Lenhert, S., Buchel, C., Chi, L., and Nield, J. (2008) *Biochemistry* **47,** 431–440
46. Yakushevska, A. E., Keegstra, W., Boekema, E. J., Dekker, J. P., Andersson, J., Jansson, S., Ruban, A. V., and Horton, P. (2003) *Biochemistry* **42,** 608–613
47. Dekker, J. P., and Boekema, E. J. (2005) *Biochim. Biophys. Acta* **1706,** 12–39
48. Frigerio, S., Campoli, C., Zorzan, S., Fantoni, L. I., Crosatti, C., Drepper, F., Haehnel, W., Cattivelli, L., Morosinotto, T., and Bassi, R. (2007) *J. Biol. Chem.* **282,** 29457–29469
49. Harrer, R., Bassi, R., Testi, M. G., and Schäfer, C. (1998) *Eur. J. Biochem.* **255,** 196–205
50. Holt, N. E., Zigmantas, D., Valkunas, L., Li, X. P., Niyogi, K. K., and Fleming, G. R. (2005) *Science* **307,** 433–436
51. Avenson, T. J., Ahn, T. K., Zigmantas, D., Niyogi, K. K., Li, Z., Ballottari, M., Bassi, R., and Fleming, G. R. (2008) *J. Biol. Chem.* **283,** 3550–3558
52. Horton, P., Johnson, M. P., Perez-Bueno, M. L., Kiss, A. Z., and Ruban, A. V. (2008) *FEBS J.* **275,** 1069–1079
53. Kiss, A. Z., Ruban, A. V., and Horton, P. (2008) *J. Biol. Chem.* **283,** 3972–3978
54. Kirchhoff, H., Haferkamp, S., Allen, J. F., Epstein, D. B., and Mullineaux, C. W. (2008) *Plant Physiol.* **146,** 1571–1578
55. Tremmel, I. G., Kirchhoff, H., Weis, E., and Farquhar, G. D. (2003) *Biochim. Biophys. Acta* **1607,** 97–109
56. Kyle, D. J., Staehelin, L. A., and Arntzen, C. J. (1983) *Arch. Biochem. Biophys.* **222,** 527–541

# Supplementary materials

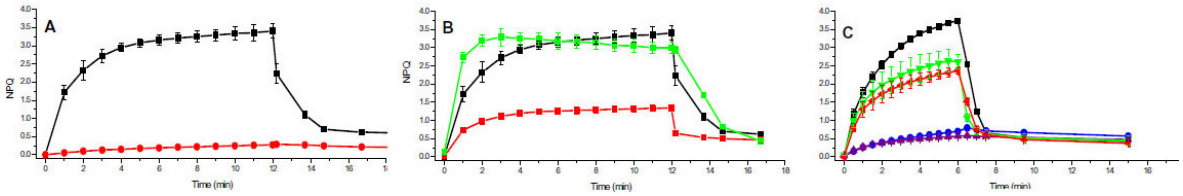


**Figure S1.**

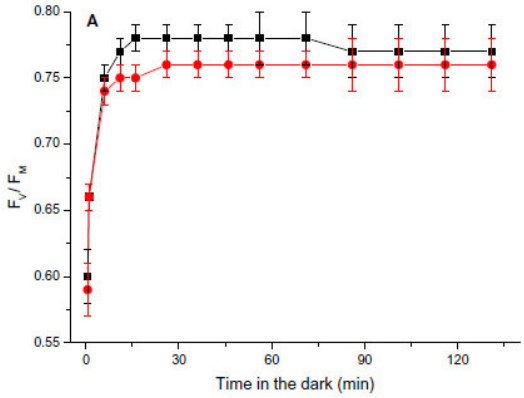


**B**

| | 30 minutes light | 90 minutes light |
|---|---|---|
| **Dark** | n.d | n.d. |
| **End light treatment** | 2.29± 0.10 | 2.43±0.23 |
| **15' recovery** | 1.50±0.13 | 1.72±0.30 |
| **90' recovery** | 1.03±0.04 | 1.06±0.05 |

**Figure S2.**

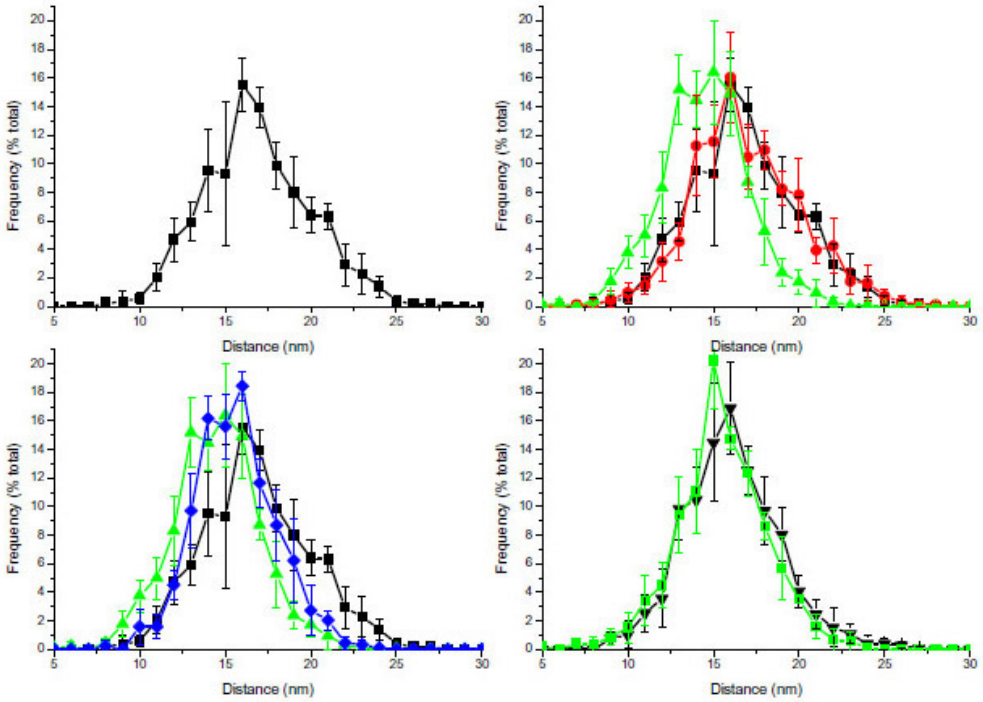


**Figure S3.**

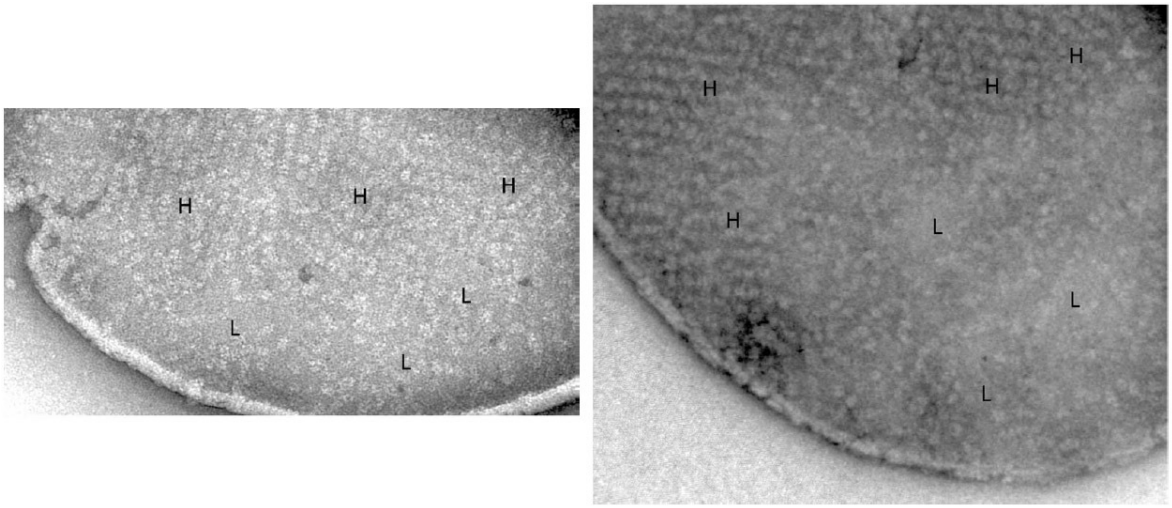


**Figure S4.**

**Supplementary Figure S1. NPQ kinetics dependence from nigericine and genotype.** A) NPQ measured in leaves infiltrated with nigericine (red), an uncoupler dissipating ΔpH across the thylakoids membranes, as compared with control leaves infiltrated with buffer only (black). B) NPQ Dependence on carotenoid composition, analyzed by comparing plants depleted (*npq1*, red) or accumulating constitutively zeaxanthin (*npq2*, green). C) NPQ dependence on PsbS is analyzed by comparing PsbS-less plants (*npq4*, blue) with *npq4* plants complemented with PsbS in the WT form (*npq4*+PsbS, black) and PsbS where either one or both lumen exposed glutamate residues binding DCCD were mutated into glutamine (E122Q, E226Q and E122Q/E226Q, respectively green and red and purple).

**Supplementary Figure S2. PSII recovery and zeaxanthin content in leaves after prolonged NPQ measurements.** A) PSII yield (Fv/Fm) in dark adapted conditions was measured in leaves treated with 30 (black squares) and 90 minutes (red circles) of high light following light treatment leaves were incubated in the dark for 60 minutes before measurement. B) Zeaxanthin content in leaves was also analyzed during the prolonged NPQ measurements. Values for samples treated for 30 and 90 minutes of actinic light are shown.

**Supplementary Figure S3. Analysis of PSII core distribution, considering only the closest neighbor.** Distribution of PSII complexes in grana membranes was analyzed as shown in figure 4 of the main text, but considering only the distance of the closest PSII core rather than the average of the closest four. A) Distribution in dark adapted sample. B) Comparison of PSII distribution in samples dark adapted (black squares) or treated with 30 (red circles) and 90 minutes (green triangles) of light before grana isolation. C) Comparison of sample either light adapted (green triangles) or incubated in the dark for 90 minutes following light treatment (blue diamonds). D) effect of light treatment in PSII distribution in *npq4* grana. Dark adapted sample is shown in black triangles, sample light treated for 90 minutes in green diamonds.

**Supplemental Figure S4. EM images from KoCP24.** EM pictures of negatively stained grana membranes purified from KOCP24 plants. Regions with high or low density of PSII core complexes are indicated with H and L respectively.

## B.2 Quenching in *Arabidopsis thaliana* mutants lacking monomeric antenna proteins of photosystem II.

Y. Miloslavina*[1], S. de Bianchi*[2], L. Dall'Osto[2], R. Bassi and A. R. Holzwarth[1]

[1]Max-Planck-Institut für Bioanorganische Chemie, Stiftstraße 34-36, D-45470 Mülheim a.d.Ruhr, Germany;

[2]Dipartimento di Biotecnologie, Università di Verona, I-37134 Verona, Italy

The ultra-fast chlorophyll fluorescence measurements were done with accurate spectroscopic instruments in the Max-Planck-Institut in Mulheim (Germany) as also the analysis of fluorescence decays by global target analysis. I provided the biochemical and functional characterization of the mutants which is essential for the interpretation of the results. Particularly the stoichiometry between individual chlorophyll-proteins.

### B.2.1 Introduction

Plants use light as the energy source for their metabolism. During the early steps of photosynthesis, solar energy is efficiently absorbed, and excitons are transferred to the photosynthetic reaction centers (RC) by a complex array of pigment-binding proteins, the light-harvesting antenna complexes (Lhc), localized at the periphery of each photosystem (Ben Shem et al., 2003; Caffarri et al., 2009). Lhc proteins are not only involved in light harvesting: they are also acting in photoprotection by multiple mechanisms, including chlorophyll (Chl) singlet energy dissipation ($^1$Chl$^*$), Chl triplet quenching and scavenging of reactive oxygen species (ROS). The antenna system thus, has a dual function: on one hand, it harvests photons and extends the cross section for light absorption in light limiting conditions; on the other hand, it limits damages to the photosynthetic apparatus when light is in excess. Among the photoprotective mechanisms catalysed in the antenna system of higher plants PSII, the energy-dependent quenching of Chl singlet excited states (NPQ) is an essential one which protect plants from sever photodamage under variable light condition (Horton, 1996; Barber and Andersson, 1992) dissipating the excess of energy as heat. Triggering of NPQ is due to the fall of the thylakoid lumen pH (Horton, 1996; Niyogi, 1999) in condition when ATPase cannot fully use the proton gradient created through the thylakoid membrane by photosynthetic electron transport. Low lumenal pH induces the conversion of violaxanthin (Vx) to zeaxanthin (Zx) via the xanthophyll cycle (Gilmore and Yamamoto, 1992; Yamamoto and Kamite, 1972) and activates the PsbS protein (Li et al., 2002; Li et al., 2004): two events essential to full establishment of quenching. Although early proposals

have indicated PsbS as the quenching site for $^1Chl^*$, it is now widely accepted that the primary quenching event(s) are located within the antenna system of PSII (Bonente et al., 2008) owing to the strong down-regulation of NPQ in Chl *b*-less mutants (Briantais, 1994; Espineda et al., 1999; Havaux et al., 2007). The Chl *b* containing antenna consists into one copy each of three monomeric proteins called CP29 (Lhcb4), CP26 (Lhcb5), and CP24 (Lhcb6) and two-four copies, depending on light conditions during growth, of the major antenna complex, called LHCII. The latter is an heterotrimer of the Lhcb1, Lhcb2 and Lhcb3 subunits in different combinations (Jansson, 1994; Jackowski and Jansson, 1998). Proposed mechanism for NPQ point either to a major role the trimeric LHCII which would undergo an aggregation-induced conformational change, allowing for energy transfer quenching by a lutein (Ruban et al., 2007) or to the direct involvement of monomeric Lhcb proteins CP29, CP26 and CP24 (Holt et al., 2005; Ahn et al., 2008; Cheng et al., 2008; Avenson et al., 2008a). According to this proposal, qE (energy quenching) involves Zx, located in the monomeric antenna complexes of PSII, acting as a direct quencher due to transient formation of a $Zx^+$ radical cation and a $Chl^-$ radical anion, followed by recombination to the ground state. Lutein was also shown to participate in the catalysis of qE (Avenson et al., 2009; Li et al., 2009) bound to the minor antenna complexes *Lhcb*. Elucidation of the functional role of individual *Lhcb* proteins has been approached using antisense and knockout (ko) approaches (Andersson et al., 2001; Kovacs et al., 2006). In a recent work koCP24, koCP26 and the double mutant koCP24/26 were analysed showing a major role for CP24 in NPQ (de Bianchi et al., 2008; Kovacs et al., 2006). Further biochemical analysis coupled with electron microscopy of grana membranes has highlighted the role of membrane protein dynamics, showing that during NPQ, the PSII-supercomplex undergoes dissociation and segregation into two domains containing respectively $C_2S_2$ particles, including PSII core, CP29, CP26 and LHCII-S, and a disconnected antenna system composed of CP24 together with LHCII-M and LHCII-L (Betterle et al., 2009).

On the functional side, quenching was followed on intact leaf by ultra-fast Chl fluorescence after the establishment of the steady state NPQ, under physiological conditions. This spectroscopic approach allows to clearly distinguish between the two very different quenching situations: (i) the development of a quenching site(s) in the PSII antenna without a decrease of the physical antenna size, and/or (ii) the decrease of the antenna size due to a functional detachment of parts of the PSII antenna. In the case (i) specifically increases the non-radiative deactivation rate $k_D$ in the antenna and thus decreases the (average) lifetime of the PSII fluorescence without a change in the total PSII amplitude; case (ii) leads to a decrease in the total amplitude of the PSII fluorescence and the appearance of a new ad-

ditional fluorescence component from the functionally detached antenna. What has been proposed basing on fluorescence lifetime analysis *in vivo* is that two independent quenching sites, Q1 and Q2, are activated during NPQ (Holzwarth et al., 2009). Q1 is located in the major LHCII complexes, which are functionally detached from the PSII/RC supercomplex with a mechanism that strictly requires PsbS, but not Zx. Q2 is located in and connected to the PSII complex and it is dependent on the Zx formation (thus absent in *npq1* plants) (Miloslavina et al., 2008). These two quenching events could well originate in each of the two physical domains of grana revealed by electron microscopy analysis (Betterle et al., 2009).
In the present paper we studied the role of individual monomeric Lhcb proteins in the high light (HL) induced quenching. To this aim, we have integrated the set of ko mutants, including koCP26, koCP24 and koCP24/26 with a triple mutant koCP29 (koLhcb4.1/Lhcb4.2/koLhcb4.3) which completely lacks CP29 and is affected in the kinetic of NPQ (Section A.2). We then proceeded to investigate quenching in ko mutants by comparing the fluorescence kinetics under quenched and unquenched conditions in intact leaves. The results are consistent with the two quenching sites being located, respectively, in the $C_2S_2$ domain and in the LHCII-enriched domain. Q1 site is released in the CP24 mutant while Q2 is attenuated in the koCP29 mutant. On these bases we conclude that during the establishment of NPQ *in vivo* the PSII supercomplex dissociates into two moieties, which segregates into distinct domain of the grana membrane and are each protected from over-excitation by the activity of quenching sites identified as CP24 and CP29.

### B.2.2 Materials and Methods

#### Plant material and growth conditions.

*Arabidopsis thaliana* T-DNA insertion mutants (*Columbia* ecotype) SALK_077953, with insertion in the Lhcb6 gene, SALK_014869, with insertion in the Lhcb5 gene and the double mutant koLhcb5/Lhcb6 were previously selected (de Bianchi et al., 2008; Dall'Osto et al., 2005). Triple mutant koCP29 (koLhcb4.1/Lhcb4.2/Lhcb4.3) was isolated as reported in Section A.2. Fully developed leaves of ∼4-5 week-old plants were used for the experiments. Pigment-protein analysis, transition electron microscopy and other detailed study of these knockout mutants (except koCP29) has been recently published (de Bianchi et al., 2008).

#### *In vivo* fluorescence and NPQ measurements.

NPQ of Chl fluorescence and PSII yield ($\Phi_{PSII}$) were measured on whole leaves at room temperature with a PAM 101 fluorimeter (Heinz-Walz). Min-

imum fluorescence ($F_0$) was measured with a 0.15 $\mu$mol photons $m^{-2}s^{-1}$ beam, maximum fluorescence ($F_{max}$) was determined with a 0.6-s light pulse (4500 $\mu$mol photons $m^{-2}s^{-1}$), and white continuous light (600 $\mu$mol photons $m^{-2}s^{-1}$) was supplied by a KL1500 halogen lamp (Schott). NPQ, $\Phi_{PSII}$, and relative ETR were calculated according to the following equation (Van Kooten and Snel, 1990): NPQ=($F_{max}$-$F_{max}$')/$F_{max}$', relETR = $\Phi_{PSII}$ · PAR, where $F_{max}$ is the maximum Chl fluorescence from dark-adapted leaves, $F_{max}$' the maximum Chl fluorescence under actinic light exposure, $F_s$ the stationary fluorescence during illumination, and PAR the photosynthetic active radiations (white light, measured as $\mu$mol photons $m^{-2}s^{-1}$).

### Time-resolved fluorescence measurements.

Fluorescence decays were measured by single photon timing to high S/N ratio in the 678-734 nm wavelength region, excited at 663 nm. For excitation a synchronously pumped cavity-dumped dye laser system with a modelocked argon ion laser (Spectra Physics) as a pumping source was used (Müller et al., 1992; Holzwarth et al., 2005). The fluorescence decays were analyzed by global target analysis (Holzwarth, 1996). Detached plant leaves were placed in a rotation cuvette - consisting of two glass plates (diameter of 10 cm) separated by a 1.5 mm spacer - which was also oscillated sideways. Fluorescence was measured in a front face arrangement from the upper side of the leaves. The cuvette was filled with a sucrose solution (0.3 $\mu$M).
The measurements were performed at three different conditions:

1. Unquenched $\mathbf{F}_0$ state was measured in complete darkness after dark-adaptation overnight. The laser frequency was 800 kHz, the rotation speed 1800 rpm with 78 side movements per minute (mpm). Preliminary checks were done to ensure that the PSII RCs are indeed open.

2. For measurements at unquenched maximal fluorescence $\mathbf{F}_{max}$ conditions, leaves were cut at the stem and dipped immediately in a 45 $\mu$M DCMU solution with the main part of the leaf that was later used for measurement exposed to air. The detached leaves were incubated for 14 hours in the DCMU solution in complete darkness (Toth et al., 2005). For achieving full closure of the PSII RCs during the measurement an additional blue LED light-spot of very low intensity (∼50 $\mu$mol photons $m^{-2}s^{-1}$) was applied immediately before detection of the signal. The laser frequency was 4 MHz and the cuvette speed 1300 rpm/78 mpm.

3. Light-adaptation for the quenched $\mathbf{F}_{NPQ}$ state was carried out using a mixed array plate of red and amber high intensity light-emitting diodes

providing 550-600 $\mu$mol photons $m^{-2}s^{-1}$. Measurements were started after 45 minutes of illumination after stabilization of the quenching. For closing all PSII RCs under quenched $F_{NPQ}$ conditions before entering the measuring light an additional blue high intensity LED ($\sim$2000 $\mu$mol photons $m^{-2}s^{-1}$) was focused on a 1 cm diameter spot right above the fluorescence excitation laser light pulses (1.5 mm diameter). 4 MHz laser frequency was used, the cuvette was rotating at 1800 rpm, which is fast enough to keep the PSII RCs closed.

To measure DAS at one condition 1-2 hours were needed. The measurement of every wavelength was limited maximally to 15 minutes, to avoid stress in the leaves due to prolonged incubation in the rotating cuvette. For every condition freshly prepared leaves from the same batch were used.

### B.2.3 Results

#### NPQ of Chl fluorescence.

The analysis of quenching by fluorescence lifetime characterization can be performed *in vivo*. However, the data collection requires about one-two hour (as reported in materials and methods) for each condition: unquenched $F_0$, maximum fluorescence $F_{max}$ and quenched $F_{NPQ}$. As a reference for the quenching state condition of the sample used in the analysis we measured by pulse fluorometry the NPQ kinetic in the long term for the genotypes analyzed in this work. We obtained $F_0$ and $F_{max}$ value, respectively in absence of actinic light and in presence of a saturating flash, and we determined the $F_{NPQ}$ value after the stabilization of the quenching (1 hour) (Figure B.1). It can be observed that ko mutants show important differences in kinetics of NPQ in the short term as previously reported (Kovacs et al., 2006; de Bianchi et al., 2008; Betterle et al., 2009 Section A.2), however, in the long term the different genotypes all reach a similar level (about 2.0) of fluorescence quenching after one hour of exposure to actinic light except koCP24 that reached the value of 1.5. The quenching state was rapidly reversible in all genotypes upon switching off the light.

#### Fluorescence decay.

Figure B.2 shows fluorescence decays measured by single photon counting at 686 nm as detected on intact leaves of the knockout mutants: koCP24, koCP26, koCP24/CP26 and koCP29. For each genotype two decays are presented, respectively, for the unquenched dark-adapted state ($F_{max}$) and quenched light-adapted ($F_{NPQ}$) states. While the unquenched decays were very similar, the quenched ones showed substantial differences. Table I combines the average lifetimes for each decay and the NPQ values calculated.

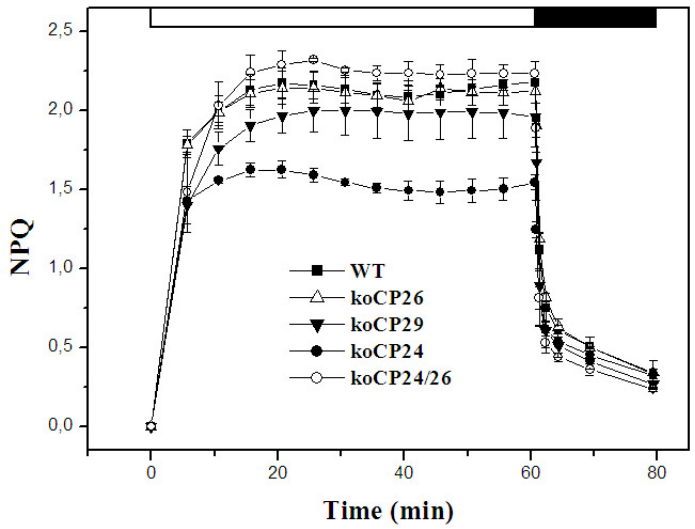


**Figure B.1:** *Long term NPQ analysis of wild-type and antenna mutants. Kinetics of NPQ induction and relaxation were recorded with a pulse amplitude modulated fluorometer in WT and koCP26, koCP24, koCP29 and koCP24/CP26 mutants. Chl fluorescence was measured in intact, dark-adapted leaves, during 60 min of illumination at 600 µmol photons $m^{-2}s^{-1}$ followed by 20 min of dark relaxation.*

While most genotypes showed a ∼3 fold shortening of the average lifetime under quenching conditions, the figure for koCP24 mutant was shortened by only 2 folds and while the NPQ value for all mutants and WT was rather similar (1.7-2.0), the NPQ value for koCP24 was only 1.2. From these data it appears that the role of CP24 antenna complex is the most influential for the quenching, whereas CP29 and CP26 are less critical. However, when CP24 and CP26 were both missing, NPQ resumed its efficiency. This behavior closely match the NPQ kinetics in the long term (Figure B.1).

**Table I:** *Average lifetime $\tau_{av}$, ps of the fluorescence decays measured under the indicated conditions at 686 nm emission wavelength, $\lambda_{exc}$= 663 nm. The illumination conditions for achieving NPQ were the same as used previously, i.e. 550-600 µmol photons $m^{-2}s^{-1}$ of a mixture of amber and red LEDs (Holzwarth et al., 2009).*
**) This value corresponds to the NPQ-value determined from steady state fluorescence intensity at 686 nm. $F_{NPQ}$ corresponds to the maximal value of $F_m$' measured under the conditions of the lifetime measurements.*

| $\tau_{av}$ **at 686 nm, ps** | **WT** | **koCP26** | **koCP24/26** | **koCP29** | **koCP24** |
|---|---|---|---|---|---|
| $\mathbf{F}_0$ | 210 | 193 | 394 | 315 | 398 |
| $\mathbf{F}_{NPQ}$ | 410 | 302 | 336 | 460 | 505 |
| $\mathbf{F}_m$ | 1230 | 917 | 991 | 1376 | 1094 |
| **NPQ**($\tau_{av}$)*=($\mathbf{F}_m$/$\mathbf{F}_{NPQ}$)-1 | 2.0 | 2.0 | 1.9 | 2.0 | 1.2 |

## Target compartment modelling.

For a deeper insight, fluorescence decays were submitted to global target analysis. The experimental data were fit to the kinetic scheme shown in Figure B.3, which allows for dissection of PSII and PSI kinetics from the overall fluorescence decay. The scheme results in a number of rate constants

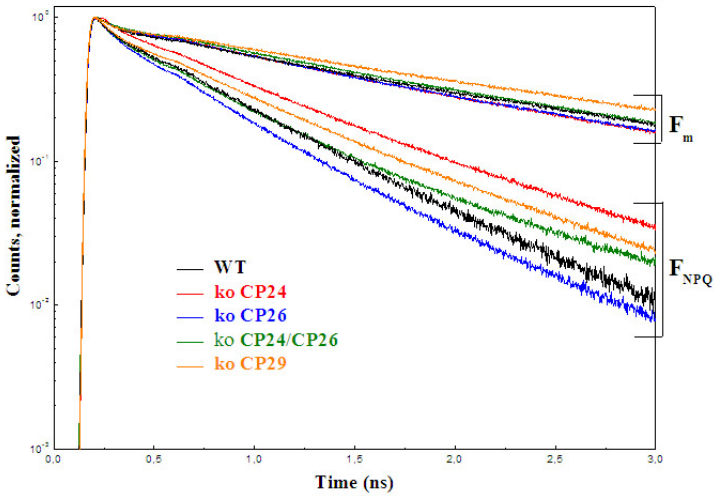


**Figure B.2:** *Fluorescence decay.*
*Normalized fluorescence decays (on a semilogarithmic scale) at 686 nm for WT and knockout mutated intact leaves of Arabidopsis thaliana: koCP24, koCP26, koCP29 and koCP24/26 in the quenched (light-adapted) $F_{NPQ}$ and unquenched (dark-adapted) $F_m$ conditions with closed PSII RCs.*

reflecting energy and electron transfer processes. The kinetic models for PSI and PSII are based on previous results from time-resolved measurements and fluorescence lifetime analysis of isolated PSI (Slavov et al., 2008) and PSII particles (Miloslavina et al., 2006; Szczepaniak et al., 2008) of vascular plants and cyanobacteria. The kinetic schemes with three PSII and four PSI compartments resulted in a very good fit of the kinetics of dark-adapted WT and knockout mutants across the whole wavelength range. The PSII kinetic scheme has one excited state compartment of antenna and RC and two radical pairs (RPs), which account for reduction of pheophytin (RP1) and plastoquinone $Q_A$ (RP2). PSI is described by one excited state compartment of antenna and RC, one RP and two "red" compartments assigned to red-shifted long-wave Chls (Slavov et al., 2008).

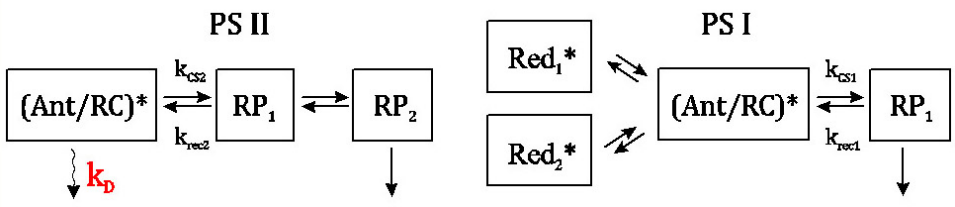


**Figure B.3:** *Kinetic schemes for PSI and PSII used in the global target analysis of the fluorescence decays from A. thaliana leaves.*

Where necessary additional single lifetime components were allowed in the analysis (see e.g. Figure B.5) to represent newly appearing components that could not be fitted within the pure PSI and PSII schemes. Such component(s) are needed to describe the functionally detached LHCII. $k_{CS}$ - rate constant of charge separation reaction, $k_{rec}$ - rate constant of charge recom-

bination, $k_D$ - rate constant for energy dissipation by non-photochemical quenching.

### Detached antenna component.

The compartment model in Figure B.3 was tested for both $F_{max}$ and $F_{NPQ}$ conditions. The resulting decay associated spectra (DAS) are shown in Figure B.4 and Figure B.5, respectively. In general, the model provided excellent fits for $F_{max}$ (Figure B.4). The largest differences between the dark-adapted and the high-light-adapted conditions were two: (i) the average lifetime under NPQ conditions was two-three times shorter than in $F_{max}$ conditions, in particular koCP24 and koCP29 had two times shorter lifetime in quenching conditions; (ii) the appearance of an additional fluorescent antenna compartment marked in red in Figure B.5. This new antenna compartment is functionally disconnected from either PSI or PSII as was clearly revealed by the kinetic and spectral data reported in Figure B.5. The shape of the fluorescence spectrum (DAS) of this additional component was different from both PSI and PSII. The peak of its emission spectrum was slightly red-shifted as compared to the normal PSII emission and had enhanced emission in the long-wavelength range, appearing in a broad plateau above 700 nm.

The relative peak amplitudes of the additional component at 686 nm to the sum of the three PSII amplitudes were 30-39% for WT and koCP24, 52-59% for koCP29 and koCP26, and only 15% for koCP24/26 (Table II - % of detached LHCII). Concomitant with the appearance of the "unconnected antenna" component, the relative DAS amplitudes of the PSII compartment decreased. Thus, this fluorescence decay component appears to derive from an antenna compartment kinetically unconnected from PSII. Hence, we tentatively assign it to a part of LHCII which becomes detached from PSII during the onset of NPQ (Miloslavina et al., 2008). The lifetime of the "detached antenna" component varied between 300 and 600 ps, implying it was significantly quenched as compared to the PSII antenna of dark-adapted leaves. We will refer to this lifetime, which is short with respect to that of unquenched LHCII, as to Q1 quenching site.

Since the DAS amplitude is proportional to the absorption cross-section of the excited pigments, i.e. Chl *a*, the relative amount of the "detached antenna" can be expressed as the number of Chl *a* molecules or LHCII trimers (24 Chl *a*'s) detached per PSII supercomplex (Table II). However, we use the term "trimer" in this case very approximately, not including certain amount of LHCII monomers that can also be detached or present instead of trimers. For this calculation we assume that PSII in the dark-adapted state is organized as $C_2S_2M_2L$ supercomplexes in WT containing

248 molecules Chl *a* (2 cores + 2 copies of CP24, CP26, CP29 + 5 LHCII trimers). In the ko mutants, the missing complexes are compensated by the over-accumulation of others Lhc subunits (de Bianchi et al., 2008) as shown by the measurements of functional antenna size which yield values are not statistically distinguishable from WT. For koCP24 and koCP24/26 we assume a $C_2S_2$ organization, on the basis of direct electron microscopy analysis (Morosinotto et al., 2006; de Bianchi et al., 2008).
In the quenched condition ($F_{NPQ}$), the mutations affected the lifetime of the additional "unconnected antenna" compartment (Q1 site) i.e. detached LHCII, as well as its relative amplitude. This indicates that the antenna complexes which were detached from the PSII cores underwent a different degree of quenching depending on the presence/absence of specific monomeric antenna complexes and that their number was different. For a quantitative comparison the amplitude of the detached LHCII component at its fluorescence maximum (686 nm) was calculated relative to the sum of amplitudes of all PSII plus LHCII components. This figure is given in percentage in Table II (Detached LHCII trimers). In the koCP24/26 mutant one more additional compartment not connected to either PSI or PSII, was necessary to fit the data (Figure B.5D - free LHCII). Its lifetime is very long (3 ns) and the amplitude of its emission spectrum was very low. We assign it hence to a small number of free LHCII trimers which are energetically disconnected from the photosystems and do not undergo quenching in the $F_{NPQ}$ conditions (Figure B.5D).

**Table II:** *Parameters of detached antenna components. Lifetime of the additional compartment assigned to quenched LHCII oligomers, percentage of detached LHCII, the average number of associated Chl* a *molecules, and the corresponding number of detached LHCII trimers.*
* *Calculated from the amplitude of the detached PSII antenna component component in the DAS at its fluorescence maximum (686 nm) relatively to total (amplitude of PS II components + amplitude of detached antenna component).*
** *The number of Chl* a *molecules corresponding to the percentage of detached LHCII. This value was calculated relative to the total Chl* a *per PSII supercomplex, that was assumed to be $C_2S_2M_2$ in WT and koCP26; and $C_2S_2$ in koCP29, koCP24 and koCP24/26 in the darkness (see text).*
*** *The number of LHCII trimers that corresponds to the calculated number of Chl* a *in detached antenna. Based on this number we prepared the detached antenna compartment composition shown in Figure B.6.*

| | **WT** | **koCP26** | **koCP24/26** | **koCP29** | **koCP24** |
|---|---|---|---|---|---|
| **$\tau$[ps] of detached LHCII/CPxx compartment, ps** | 430 | 424 | 390 | 468 | 604 |
| **% of detached** * | 30 | 59 | 15 | 52 | 39 |
| **Chl *a* molecules in detached antenna**** | 60 | 118 | 20 | 76 | 55 |
| **Detached LHCII trimers***** | 2.5 | 5 | <1 | 3 | 2 |

### Non-photochemical deactivation rate constant $k_D$.

Within the PSII model (Figure B.3) the most important rate constant, which directly characterizes the quenching in the PSII-connected antenna is $k_D$. It represents the effective total non-photochemical deactivation rate of the PSII antenna. Table III compares the $k_D$ values for quenched and unquenched plants ($k_D$, $F_{NPQ}$; $k_D$, $F_{max}$). From these values we can calculate the NPQ part in PSII-attached antenna, according to the Stern-Volmer equation calculated from the overall fluorescence (Krause and Jahns, 2003). We will refer to the PSII-connected antenna quenching as to Q2 quenching site. The NPQ is denoted as $NPQ^{(Q2)}$ to avoid confusion with the NPQ parameter. The $NPQ^{(Q2)}$ part for WT and all knockout mutants, except koCP24, was between 3-4. Only koCP24 had a $NPQ^{(Q2)}$ decreased by 60%, suggesting that CP24 is required for the activation of the Q2 site quenching. It was, however, surprising that in the double mutant koCP24/26 the Q2 quenching was not impaired.
It can be seen that, concomitantly with the suppression of the Q2 site of quenching, the absence of CP24 leads to an increased amount of detached LHCII and/or to an increase of its lifetime. In the double mutant koCP24/26, however, this number was reduced by 50% as compared to the WT.

**Table III:** *Average lifetimes $\tau_{av}$ of the pure PSII compartment, the value of NPQ in the Q2 site as calculated from the $\tau_{av}$ of the pure PSII components, the non-photochemical deactivation rates $k_D$, $ns^{-1}$ of the PSII antenna under dark-adapted ($F_m$) and NPQ conditions, and the NPQ-value calculated from the PSII antenna deactivation rates $k_D$.*

| **$\tau_{av}$ of PSII at 686 nm [ps]** | **WT** | **koCP26** | **koCP24/26** | **koCP29** | **koCP24** |
|---|---|---|---|---|---|
| **$\tau_{av}$ [ps] , $F_{NPQ}$** | 560 | 528 | 525 | 852 | 791 |
| **$\tau_{av}$ [ps] , $F_{max}$** | 1280 | 1409 | 1422 | 1544 | 1274 |
| **$NPQ^{(Q2)}$ from $\tau_{av}$** | 1.3 | 1.7 | 1.7 | 0.8 | 0.6 |
| **$k_D$, $ns^{-1}$ , $F_{NPQ}$** | 1.7 | 1.7 | 1.7 | 1.1 | 0.8 |
| **$k_D$, $ns^{-1}$, $F_{max}$** | 0.4 | 0.3 | 0.3 | 0.3 | 0.4 |
| **$NPQ^{(Q2)} = (k_D{}^{(NPQ)}/k_D{}^{(F_m)})$-1** | 3.3 | 4.1 | 4.0 | 2.8 | 1.3 |

## B.2.4 Discussion

### Two quenching sites.

Based on the presented results, we have clear evidence to the occurrence of two different non-photochemical quenching sites under HL adaptation: a) Q1, the functional detachment of an antenna part from PSII, and b) Q2, the PSII core or closely attached to PSII antenna quenching. a) The functional antenna detachment follows from the concomitant decrease of the PSII amplitude and appearance of detached antenna compartment upon HL adaptation. The lifetime of the detached antenna parts *in vivo* in the range of 400-600 ps is much shorter than the lifetime of isolated LHCII antenna

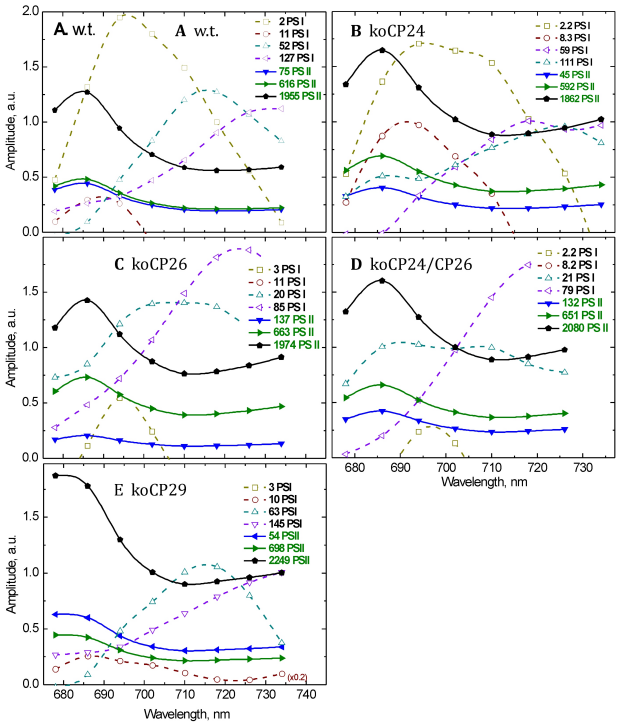


**Figure B.4:** *Fluorescence lifetime components of dark-adapted plants. DAS as obtained from global target analysis of the fluorescence decays of leaves from dark-adapted WT (A) and knockout mutants koCP24 (B), koCP26 (C), koCP24/26 (D) and koCP29 (E) of Arabidopsis thaliana plants under $F_{max}$ conditions (closed RCs).*

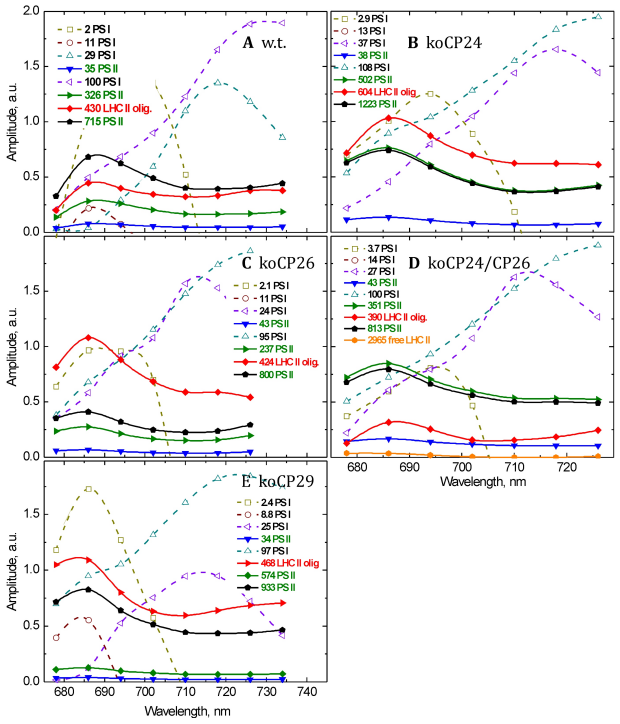


**Figure B.5:** *Fluorescence lifetime components of high-light-adapted plants. DAS (Holzwarth, 1996) are obtained from global target analysis of the fluorescence decays of leaves from WT (A) and knockout mutants koCP24 (B), CP26 (C), CP24/26 (D), and CP29 (E) under high-light-adapted ($F_{NPQ}$) conditions.*

complexes (∼3-4 ns, (Miloslavina et al., 2008) or the average PSII lifetime in dark-adapted leaves with closed RC (1.3-1.4 ns). b) The mechanism of quenching of the PSII-attached antenna (Q2) increases the deactivation rate $k_D$, which is a direct fitting parameter of the model. The occurrence of two quenching sites in WT and the knock-out mutants is in agreement with the recent findings of two quenching sites in diatoms, i.e. *Phaeodactylum tricornutum* and *Cyclotella meneghiniana* (Miloslavina et al., 2009).

In the following we want to understand the details and the mechanisms of NPQ at these two quenching sites. From our previous work we know that the Q1 site is activated only in the presence of PsbS. In PsbS-lacking mutant there was no formation of a new compartment with spectral and kinetic properties of a LHCII antenna disconnected from the PSII RC. These spectroscopic evidences are consistent with the finding that PsbS, upon protonation by low lumenal pH, acts in dissociating the B4 complex, composed by CP29, CP24 and LHCII-M, thus leading to the segregation of PSII supercomplex into a domain, including PSII core, CP29 and CP26 ($C_2S_2$ complex) and a second domain containing CP24 together with LHCII-M and LHCII-L (Betterle et al., 2009). We assume that LHCII trimers are detached since they represent the peripheral antenna and furthermore that M-LHCII trimers are easier detach than S-LHCII trimers because they are less strongly connected to PSII (Yakushevska et al., 2001; Dekker and Boekema, 2005). Since the level of PsbS is not affected in ko mutants for monomeric Lhcbs (de Bianchi et al., 2008), we expect activation of the Q1 site under HL unless the quencher is the knocked out monomeric Lhcb complex targeted by the mutation or undergoes quenching by alternative mechanisms. This is actually evident in koCP24 (Table II) showing that lifetime of the "detached antenna" component is longer than in WT.

Since the Q2 mechanism quenches the antenna functionally attached to PSII, it should be located in the minor antenna complexes and the PSII core. We have found that this type of quenching is strongly dependent on the amount of Zx. According to Bassi et al. (Bassi et al., 1993) 80% of the xanthophyll-cycle active carotenoids is situated in minor antenna complexes. Hence, by knocking-out these complexes one by one, we expected to find out more details on the quenching mechanism at Q2 site. A decrease of the $k_D$ constant of Q2 is observed in koCP29, consistent with its localization in the $C_2S_2$ particles upon segregation of PSII antenna in quenched conditions (Betterle et al., 2009). Significantly, koCP26 does not show a reduction in Q2 efficiency, implying CP29 is the major site for Q2 quenching. Rather, $k_D$ Q2 is increased in koCP26, which can be understood based on the compensatory increase in CP29 (de Bianchi et al., 2008). A second mutant with decreased $k_D$ Q2 is koCP24 which seems contradictory with its partitioning with detached LHCII. However, koCP24 is limited in Zx synthesis because of its

decreased capacity for lumen acidification (de Bianchi et al., 2008) while Q2 is strongly dependent on Zx (Miloslavina et al., 2008; Holzwarth et al., 2009). We thus attribute reduced Q2 quenching in koCP24 to limitation in Zx availability.
From the data analysis of the fluorescence kinetics, we can construct a tentative model describing the parallel action of Q1 and Q2 and the HL-induced reorganizations of PSII in the thylakoid membranes of the WT and knock-out mutants.

### The NPQ quenching model.

In the model we assume that *Arabidopsis* WT, as well as koCP26, have a $C_2S_2M_2$ type of PSII supercomplex organization in the darkness (Yakushevska et al., 2001; Dekker and Boekema, 2005), while other mutants, lacking CP24 protein have $C_2S_2$ organization, namely koCP24, koCP24/26 and koCP29 (Kovacs et al., 2006; de Bianchi et al., 2008).
In the WT both quenching sites, Q1 and Q2, are active. The fraction of LHCII oligomers detached under light conditions is 30%, corresponding on average to two-three trimers per PSII supercomplex, based on the Chl *a* content (Table II). Since loosely (L-) and moderately (M-) bound LHCII complexes are supposed to detach easier than strongly bound ones (S-LHCII), we propose that the prevailing part of PSII supercomplexes in WT is organized as $C_2S_2$ type under HL conditions (Figure B.6).
The koCP26 mutant also possesses two quenching sites as WT. Twice more LHCII trimers detach from PSII forming the Q1 quenching site under HL. Taking the Chl *a* content into consideration, this corresponds to a ratio of five detached LHCII trimers per PSII supercomplex. It means that all major LHCII and even more (some other L-trimer) should be detached from PSII under HL. Since the $NPQ^{(Q2)}$ at Q2 site of koCP26 is slightly more efficient than in WT (4.1 and 3.3, correspondently), and its Q1 site is more active in detaching the LHCIIs too, the CP26 complex is not critically required for the generation of NPQ. We suggest that it rather plays a major role in organizing the antenna subunits of the supercomplex together. We suggest that in its absence, the cooperativity of LHCII binding to the PSII core is disturbed and the dissociation of B4 complex induces the detachment not only of LHCII-M and L but LHCII-S as well (in accordance with Caffarri et al., 2009).
The koCP24/26 mutant is able to generate quenching in the Q2 site as much as the single knock-out mutant koCP26, even though they have a different PSII supercomplex structure in the dark-adapted state ($C_2S_2$ *vs.* $C_2S_2M_2$). The effect of knocking the CP24 additionally out seems to be that a smaller amount of LHCII can detach from PSII. The difference in target

analysis of koCP24/26 was in the appearance in HL of small amount of one more additional compartment that is functionally disconnected from all other compartments. Its lifetime is 3 ns and we assign it to a small amount of free, LHCIIs disconnected from PSII. Free LHCII clusters might exist in this mutant already in the darkness as was revealed by electron microscopy measurements (de Bianchi et al., 2008) showing large fields of LHCIIs with a low density of PSII cores in grana membrane disks. This organization implies a large average distance between LHCII antennas and PSII RC with higher probability of fluorescence emission from unquenched LHCII, consistent with the observed increase in $F_0$ (Table I). The large membrane surfaces crowded by LHCII reproduces the situation described in liposomes reconstituted with purified LHCII which undergoes quenching through the establishment of cooperative interaction between protein subunits (Moya et al., 2001). Interestingly, apart from the absence of CP24 and CP26, this mutant has ∼25% decreased amount of CP29 and ∼50% decreased amount of Lhcb3 protein (de Bianchi et al., 2008). It is compensated by the increased amounts of Lhcb1 (60%) and Lhcb2 (10%). Hence we hypothesize that the sites of CP24 and CP29 can be occupied by some Lhcb1 or Lhcb2 complexes that get involved in the Q2 site of quenching via Lhcb-Lhcb or Lhcb-CP29 interaction, for example and the interactions with the PSII core (Figure B.6).

The koCP29 mutant is lacking not only CP29 but also CP24 thus being actually a phenocopy of CP29/24 (Section A.2). This lack is compensated by an increase of the CP26 and Lhcb1 amounts, both by 60%. Surprisingly, this mutant activates quite well both quenching sites under HL but it has a $k_D$ slightly lower than the WT indicating a specific role of CP29 in Q2 quenching (Table III). It is therefore evident that neither CP24 nor CP29 are be critical for the quenching in the presence of an excess stoikiometric amounts of CP26. Within the monomeric Lhcb sub-family, CP26 occupies an intermediate position between CP29 and CP24 for many biochemical and spectroscopic characteristics (Dainese et al., 1992; Croce et al., 2002) and is active in radical cation quenching (Ahn et al., 2008). We propose that CP26 can in part substitute for CP29 in Q2 quenching, participating to the formation of $C_2S_2$ supercomplexes together with Lhcb1 (also compensatorily increased) (Figure B.6). However, direct evidence for the organization of PSII in koCP29 is still lacking. According to our results (Table II), the equivalent of three LHCII trimers per supercomplex is detached under HL in koCP29, which is more than the number of LHCII bound to the supercomplex in darkness. This might be due to the low stability of $C_2S_2$ supercomplexes due to ectopic binding of Lhcb1 at CP29 sites leading to detachment of minor complexes upon the onset of NPQ. As for the Q1 quenching, the lifetime of "detached antenna" compartment is only slightly longer than in

WT (468 vs 430 ps) implying that lack of CP24 is functionally compensated by another subunit. We hypothesize that the role of CP24 in Q1 quenching is fulfilled by CP26 in excess with respect to the 1:1 stoikiometry with PSII. This hypothesis is consistent with the activity of CP26 in CT quenching (Avenson et al., 2009), with the ability of CP26 of interacting with LHCII-S (Caffarri et al., 2009) even forming trimeric structures in the absence of LHCII (Ruban et al., 2003).

The koCP24 mutant was the only mutant that had a reduced Q2 activity. We have shown that the formation of $\Delta$pH and the de-epoxidation of Vx to Zx under HL are significantly reduced in koCP24. This is likely a consequence of the altered supramolecular organization of the PSII supercomplexes which limits plastoquinone diffusion and lumen acidification thus preventing full activation of violaxanthin de-epoxidase (Section A.1). Since zeaxanthin epoxidase is always active, this is likely to prevent accumulation of Zx at levels similar to WT (de Bianchi et al., 2008). The quenching at the Q2 site may be then suppressed indirectly because of the insufficient amounts of Zx present and not because of the lack of CP24 per se. This fully supports the recent finding that the Q2 quenching site is strongly dependent on the presence of Zx (Holzwarth et al., 2009). The koCP24 mutant has a 70% decrease in Lhcb3 content, which is compensated by an increase in CP29 (by 30%) (de Bianchi et al., 2008). We suggest that the CP29 complexes partially compensate for missing CP24 (de Bianchi et al., 2008, Figure B.6) as for the Q1 quenching activity of the two LHCII trimers detached (Table II); however, the lifetime of the "detached antenna" compartment is longer than in WT (604 vs 430 ps) implying that lack of CP24 limits the capacity of quenching in the outer antenna at least in part. Since the binding of Zx to LHCII is limited to site V1 which has no influence on quenching, low de-epoxidation cannot be the reason for reduced lifetime quenching in Q1. We conclude that CP24, when detaching from PSII-LHCII supercomplex during the onset of NPQ (Betterle et al., 2009) undergoes compartmentation at the periphery of grana discs where contributes to quenching disconnected LHCII L+M, in agreement with its activity in forming radical cations (Avenson et al., 2008b). This is consistent with the lower level of overall quenching measured for koCP24 (Table I) and consistent with the results of pulse fluorometry (Figure B.1).

Why is it that only the koCP24 mutant forms less Zx and hence NPQ, whereas the double mutants that also lack CP24 have a normal NPQ and Zx content? If the reason for the impairment of koCP24 lies in the peculiar supramolecular arrangement of LHCII-PSII in the membrane then it must be assumed that in the double mutants the membrane is organized differently so that the coincidental limitation of electron transport does not occur. One possibility is that when only CP24 is lacking, it is not substi-

tuted by another subunit at its position in $C_2S_2M_2$ supercomplexes, and that vacancy causes the more packed structure that prevents free diffusion of plastoquinone. In the case when not only CP24 is missing but other minor subunits too, their places near the core are substituted by other Lhcb 1 or 2 isoforms (Ruban et al., 2003).
Interestingly it was not possible to obtain koCP29/26 as the double mutation prevented the assembly of a functional PSII and was thus lethal (see also Section D). In this mutant all three minor antenna complexes are probably lacking and a stable supercomplex structure cannot be assembled

### B.2.5 Conclusions

We have found two quenching sites and mechanisms active in *Arabidopsis* leaves under HL. One is a detachment of peripheral antenna from PSII and the other occurs in the PSII core and PSII-attached antenna and depends on Zx. Although the monomeric Lhcb complexes must be involved into the second mechanism, none of the three is indispensable required for the Q2 mechanism to take place because CP26 and CP29 can functionally compensate for each-other, Zx activating non-radiative dissipation processes in both (Ahn et al. 2008, Avenson et al. 2008). CP24 appears to be responsible for Q1 quenching in WT but excess CP26 can compensate for its lack. There is no strict specificity among the complexes with respect to the NPQ mechanism but there is a specificity regarding the functional assembly and organization of the PSII supercomplex and the arrangement of PSII in the membrane, which can affect the energy and electron transport processes and hence, indirectly, NPQ. Thus, the location of the LHCII subunits and the interactions with the neighbouring complexes is at least as important for NPQ as the intrinsic properties of the subunits themselves. If one antenna type is missing, others can probably take the place of the absent Lhcb, showing how flexible the photosynthetic apparatus is concerning its ability to reorganize and maintain a functional and photoprotected structure of PSII.

### Abbreviations

Chl, chlorophyll; $^1$Chl*, Chl excited state; DCMU, 3-(3´,4´-dichlorphenyl)-1,1-dimethylurea; HL, high light; ko, knock out; Lhc, light harvesting complex; NPQ, non-photochemical quenching; ΔpH, transthylakoid proton gradient; PS, photosystem; qE, energy quenching; RC, reaction centre; ROS, reactive oxygen species; XC, xanthophyll cycle; Vx, violaxanthin; Zx, zeaxanthin.

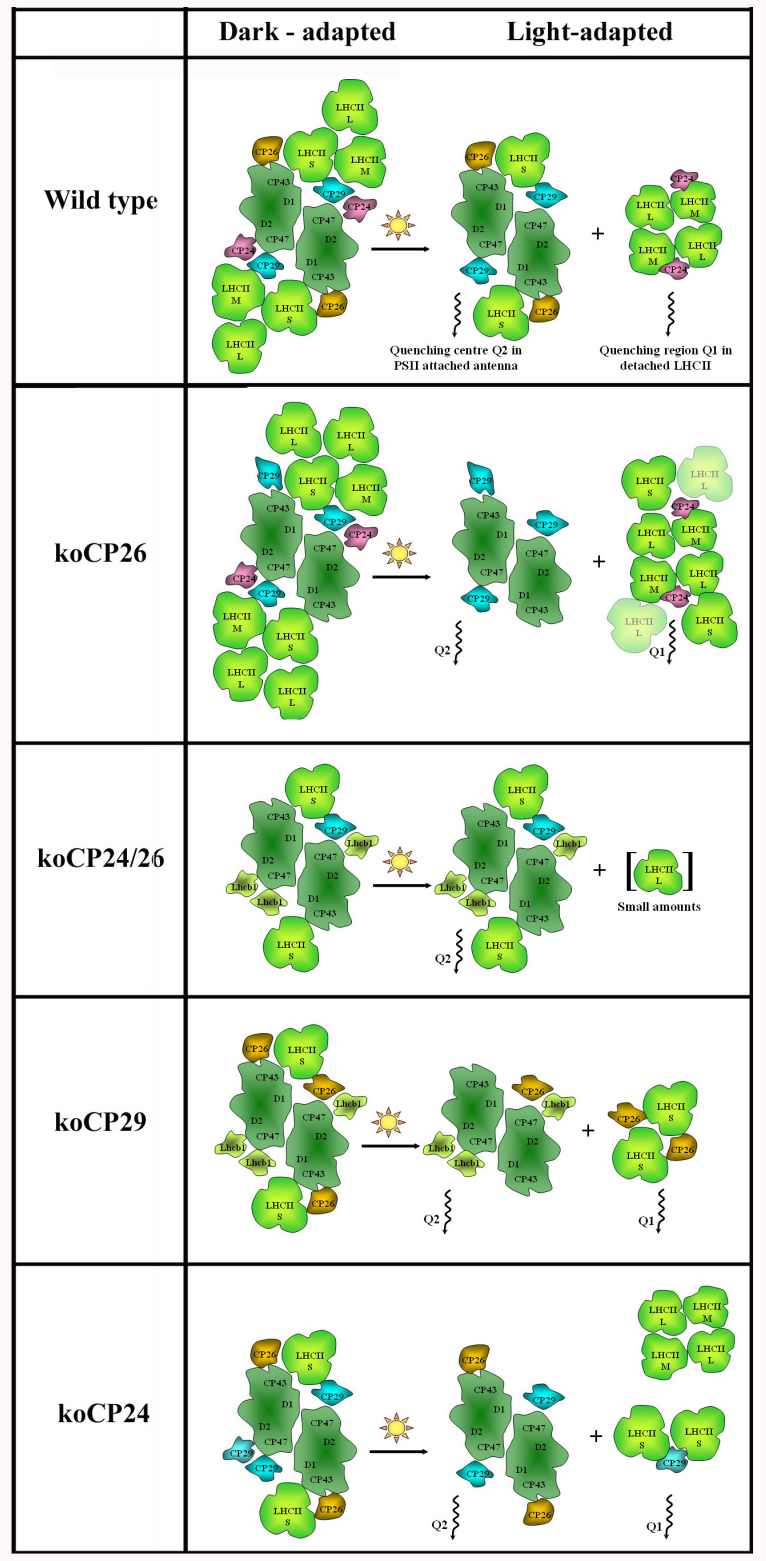


**Figure B.6:** *Model of the PSII supercomplex reorganization under high light adaptation. S, M and L denote strongly, moderately and loosely bound LHCII, respectively. The composition of the dark-adapted antenna refers to the electron microscopy works (Dekker and Boekema, 2005; Yakushevska et al., 2001; Morosinotto et al., 2006; de Bianchi et al., 2008).*

## Reference List

**Ahn,T.K.,** Avenson,T.J., Ballottari,M., Cheng,Y.C., Niyogi,K.K., Bassi,R., and Fleming,G.R. (2008). Architecture of a charge-transfer state regulating light harvesting in a plant antenna protein. Science 320, 794-797.

**Andersson,J.,** Walters,R.G., Horton,P., and Jansson,S. (2001). Antisense inhibition of the photosynthetic antenna proteins CP29 and CP26: Implications for the mechanism of protective energy dissipation. Plant Cell 13, 1193-1204.

**Avenson,T.J.,** Ahn,T.K., Niyogi,K.K., Ballottari,M., Bassi,R., and Fleming,G.R. (2009). Lutein can act as a switchable charge transfer quencher in the CP26 light-harvesting complex. J. Biol. Chem. 284, 2830-2835.

**Avenson,T.J.,** Ahn,T.K., Zigmantas,D., Niyogi,K.K., Li,Z., Ballottari,M., Bassi,R., and Fleming,G.R. (2008a). Zeaxanthin radical cation formation in minor light-harvesting complexes of higher plant antenna. Journal of Biological Chemistry 283, 3550-3558.

**Avenson,T.J.,** Ahn,T.K., Zigmantas,D., Niyogi,K.K., Li,Z., Ballottari,M., Bassi,R., and Fleming,G.R. (2008b). Zeaxanthin radical cation formation in minor light-harvesting complexes of higher plant antenna. J. Biol. Chem. 283, 3550-3558.

**Barber,J.** and Andersson,B. (1992). Too Much of a Good Thing - Light Can Be Bad for Photosynthesis. Trends Biochem. Sci. 17, 61-66.

**Bassi,R.,** Pineau,B., Dainese,P., and Marquardt,J. (1993). Carotenoid-Binding Proteins of Photosystem-II. Eur. J. Biochem. 212, 297-303.

**Ben Shem,A.,** Frolow,F., and Nelson,N. (2003). Crystal structure of plant photosystem I. Nature 426, 630-635.

**Betterle,N.,** Ballottari,M., Zorzan,S., de Bianchi,S., Cazzaniga,S., Dall'Osto,L., Morosinotto,T., and Bassi,R. (2009). Light-induced dissociation of an antenna hetero-oligomer is needed for non-photochemical quenching induction. J. Biol. Chem. 284, 15255-15266.

**Bonente,G.,** Howes,B.D., Caffarri,S., Smulevich,G., and Bassi,R. (2008). Interactions between the photosystem II subunit PsbS and xanthophylls studied in vivo and in vitro. Journal of Biological Chemistry 283, 8434-8445.

**Briantais,J.-M.** (1994). Light-harvesting chlorophyll a-b complex requirement for regulation of Photosystem II photochemistry by non-photochemical quenching. Photosynth. Res. 40, 287-294.

**Caffarri,S.,** Kouril,R., Kereiche,S., Boekema,E.J., and Croce,R. (2009). Functional architecture of higher plant photosystem II supercomplexes. Embo Journal 28, 3052-3063.

**Cheng,Y.C.,** Ahn,T.K., Avenson,T.J., Zigmantas,D., Niyogi,K.K., Ballottari,M., Bassi,R., and Fleming,G.R. (2008). Kinetic modeling of charge-transfer quenching in the CP29 minor complex. J. Phys. Chem. B 112, 13418-13423.

**Croce,R.,** Canino,g., Ros,F., and Bassi,R. (2002). Chromophore organization in the higher-plant photosystem II antenna protein CP26. Biochemistry 41, 7334-7343.

**Dainese,P.,** Santini,C., Ghiretti-Magaldi,A., Marquardt,J., Tidu,V., Mauro,S., Bergantino,E., and Bassi,R. (1992). The organization of pigment-proteins within photosystem II. In Research in Photosynthesis Vol.II, N.Murata, ed. (Dordrecht: Kluwer Academic Publishers), pp. 13-20.

**Dall'Osto,L.,** Caffarri,S., and Bassi,R. (2005). A mechanism of nonphotochemical energy dissipation, independent from Psbs, revealed by a conformational change in the antenna protein CP26. Plant Cell 17, 1217-1232.

**de Bianchi,S.,** Dall'Osto,L., Tognon,G., Morosinotto,T., and Bassi,R. (2008). Minor antenna proteins CP24 and CP26 affect the interactions between photosystem II subunits and the electron transport rate in grana membranes of Arabidopsis. Plant Cell 20, 1012-

1028.

**Dekker,J.P.** and Boekema,E.J. (2005). Supramolecular organization of thylakoid membrane proteins in green plants. Biochim. Biophys. Acta 1706, 12-39.

**Espineda,C.E.,** Linford,A.S., Devine,D., and Brusslan,J.A. (1999). The AtCAO gene, encoding chlorophyll a oxygenase, is required for chlorophyll b synthesis in Arabidopsis thaliana. Proc. Natl. Acad. Sci. U. S. A 96, 10507-10511.

**Gilmore,A.M.** and Yamamoto,H.Y. (1992). Dark induction of zeaxanthin-dependent nonphotochemical fluorescence quenching mediated by ATP. Proc. Natl. Acad. Sci. USA 89, 1899-1903.

**Havaux,M.,** Dall'Osto,L., and Bassi,R. (2007). Zeaxanthin has Enhanced Antioxidant Capacity with Respect to All Other Xanthophylls in Arabidopsis Leaves and functions independent of binding to PSII antennae. Plant Physiol.

**Holt,N.E.,** Zigmantas,D., Valkunas,L., Li,X.P., Niyogi,K.K., and Fleming,G.R. (2005). Carotenoid cation formation and the regulation of photosynthetic light harvesting. Science 307, 433-436.

**Holzwarth,A.R.** (1996). Data analysis of time-resolved measurements. In Biophysical Techniques in Photosynthesis. Advances in Photosynthesis Research, J.Amesz and A.J.Hoff, eds. (Dordrecht: Kluwer Academic Publishers), pp. 75-92.

**Holzwarth,A.R.,** Miloslavina,Y., Nilkens,M., and Jahns,P. (2009). Identification of two quenching sites active in the regulation of photosynthetic light-harvesting studied by time-resolved fluorescence. Chemical Physics Letters 483, 262-267.

**Holzwarth,A.R.,** Muller,M.G., Niklas,J., and Lubitz,W. (2005). Charge recombination fluorescence in photosystem I reaction centers from Chlamydomonas reinhardtii. J. Phys. Chem. B 109, 5903-5911.

**Horton,P.** (1996). Nonphotochemical quenching of chlorophyll fluorescence. In Light as an Energy Source and Information Carrier in Plant Physiology, R.C.Jennings, ed. (Plenum Press: New York), pp. 99-111.

**Jackowski,G.** and Jansson,S. (1998). Characterization of photosystem II antenna complexes separated by non-denaturing isoelectric focusing. Z. Naturforsch. C 53, 841-848.

**Jansson,S.** (1994). The light-harvesting chlorophyll a/b-binding proteins. Biochim. Biophys. Acta 1184, 1-19.

**Kovacs,L.,** Damkjaer,J., Kereiche,S., Ilioaia,C., Ruban,A.V., Boekema,E.J., Jansson,S., and Horton,P. (2006). Lack of the light-harvesting complex CP24 affects the structure and function of the grana membranes of higher plant chloroplasts. Plant Cell 18, 3106-3120.

**Krause,G.H.** and Jahns,P. (2003). Pulse amplitude modulated fluorometry and its application in plant science. In Light Harvesting Antennas in Photosynthesis, B.R.Green and W.Parson, eds. (Dordrecht: Kluwer Academic Publishers), pp. 373-399.

**Li,X.P.,** Gilmore,A.M., Caffarri,S., Bassi,R., Golan,T., Kramer,D., and Niyogi,K.K. (2004). Regulation of photosynthetic light harvesting involves intrathylakoid lumen pH sensing by the PsbS protein. J. Biol. Chem. 279, 22866-22874.

**Li,X.P.,** Gilmore,A.M., and Niyogi,K.K. (2002). Molecular and global time-resolved analysis of a psbS gene dosage effect on pH- and xanthophyll cycle-dependent nonphotochemical quenching in photosystem II. J. Biol. Chem. 277, 33590-33597.

**Li,Z.,** Ahn,T.K., Avenson,T.J., Ballottari,M., Cruz,J.A., Kramer,D.M., Bassi,R., Fleming,G.R., Keasling,J.D., and Niyogi,K.K. (2009). Lutein accumulation in the absence of zeaxanthin restores nonphotochemical quenching in the Arabidopsis thaliana npq1 mutant. Plant Cell 21, 1798-1812.

**Miloslavina Y.,** Grouneva I., Lambrev P.H., Lepetit B., Goss R., Wilhelm C. and Holzwarth A.R. (2009). Ultrafast fluorescence study on the location and mechanism of non-photochemical quenching in diatoms. Biochim. Biophys. Acta 1787, 1189-1197.

**Miloslavina,Y.,** Szczepaniak,M., Muller,M.G., Sander,J., Nowaczyk,M., Rogner,M., and Holzwarth,A.R. (2006). Charge separation kinetics in intact photosystem II core particles is trap-limited. A picosecond fluorescence study. Biochemistry 45, 2436-2442.

**Miloslavina,Y.,** Wehner,A., Lambrev,P.H., Wientjes,E., Reus,M., Garab,G., Croce,R., and Holzwarth,A.R. (2008). Far-red fluorescence: A direct spectroscopic marker for LHCII oligomer formation in non-photochemical quenching. FEBS Letters 582, 3625-3631.

**Morosinotto,T.,** Bassi,R., Frigerio,S., Finazzi,G., Morris,E., and Barber,J. (2006). Biochemical and structural analyses of a higher plant photosystem II supercomplex of a photosystem I-less mutant of barley. Consequences of a chronic over-reduction of the plastoquinone pool. FEBS J. 273, 4616-4630.

**Moya,I.,** Silvestri,M., Vallon,O., Cinque,G., and Bassi,R. (2001). Time-Resolved Fluorescence Analysis of the Photosystem II Antenna Proteins in Detergent Micelles and Liposomes. Biochemistry 40, 12552-12561.

**Müller,M.G.,** Griebenow,K., and Holzwarth,A.R. (1992). Primary processes in isolated bacterial reaction centers from Rhodobacter sphaeroides studied by picosecond fluorescence kinetics. Chem. Phys. Lett. 199, 465-469.

**Niyogi,K.K.** (1999). Photoprotection revisited: Genetic and molecular approaches. Annu. Rev. Plant Physiol. Plant Mol. Biol. 50, 333-359. Ruban,A.V., Berera,R., Ilioaia,C., van Stokkum,I.H., Kennis,J.T., Pascal,A.A., Van Amerongen,H., Robert,B., Horton,P., and van Grondelle,R. (2007). Identification of a mechanism of photoprotective energy dissipation in higher plants. Nature 450, 575-578.

**Ruban,A.V.,** Wentworth,M., Yakushevska,A.E., Andersson,J., Lee,P.J., Keegstra,W., Dekker,J.P., Boekema,E.J., Jansson,S., and Horton,P. (2003). Plants lacking the main light-harvesting complex retain photosystem II macro-organization. Nature 421, 648-652.

**Slavov,C.,** Ballottari,M., Morosinotto,T., Bassi,R., and Holzwarth,A.R. (2008). Trap-limited charge separation kinetics in higher plant photosystem I complexes. Biophys. J. 94, 3601-3612.

**Szczepaniak,M.,** Sugiura,M., and Holzwarth,A.R. (2008). The role of TyrD in the electron transfer kinetics in Photosystem II. Biochim. Biophys. Acta 1777, 1510-1517. Toth,S.Z., Schansker,G., and Strasser,R.J. (2005). In intact leaves, the maximum fluorescence level (F(M)) is independent of the redox state of the plastoquinone pool: a DCMU-inhibition study. Biochim. Biophys. Acta 1708, 275-282.

**Van Kooten,O.** and Snel,J.F.H. (1990). The use of chlorophyll fluorescence nomenclature in plant stress physiology. Photosynt. Res. 25, 147-150.

**Yakushevska,A.E.,** Jensen,P.E., Keegstra,W., van Roon,H., Scheller,H.V., Boekema,E.J., and Dekker,J.P. (2001). Supermolecular organization of photosystem II and its associated light-harvesting antenna in Arabidopsis thaliana. Eur. J. Biochem. 268, 6020-6028.

**Yamamoto,H.Y.** and Kamite,L. (1972). The effects of dithiothreitol on violaxanthin deepoxidation and absorbance changes in the 500nm region. Biochim. Biophys. Acta 267, 538-543.

# Section C

# Excitation energy transfer and membrane organization: role of PSII antenna subunit.

## C.1 Effect of antenna-depletion in Photosystem II on excitation energy transfer in *Arabidopsis thaliana*.

B. van Oort, M. Alberts, S. de Bianchi, L. Dall'Osto, R. Bassi, G. Trinkunas, R. Croce, H. van Amerongen.

For this work I contribute by obtaining knock out mutants and with the biochemical characterization of them regarding the establishing of the PSI/PSII ratio and the protein composition. All the time-resolved spectroscopic measurements were done in Wageningen University by the others authors. We collaborated in the discussion of the experimental results.

# Effect of Antenna-Depletion in Photosystem II on Excitation Energy Transfer in *Arabidopsis thaliana*

Bart van Oort,[†] Marieke Alberts,[†] Silvia de Bianchi,[‡] Luca Dall'Osto,[‡] Roberto Bassi,[‡] Gediminas Trinkunas,[§] Roberta Croce,[¶] and Herbert van Amerongen[†‖]*

[†]Wageningen University, Laboratory of Biophysics, Wageningen, The Netherlands; [‡]Dipartimento di Biotecnologie, Facoltà di Scienze MM.FF.NN, Università di Verona, Verona, Italy; [§]Institute of Physics, Vilnius, Lithuania; [¶]University of Groningen, Groningen Biomolecular Sciences and Biotechnology Institute, Department of Biophysical Chemistry, Groningen, The Netherlands; and [‖]MicroSpectroscopy Centre, Wageningen University, Wageningen, The Netherlands

ABSTRACT The role of individual photosynthetic antenna complexes of Photosystem II (PSII) both in membrane organization and excitation energy transfer have been investigated. Thylakoid membranes from wild-type *Arabidopsis thaliana*, and three mutants lacking light-harvesting complexes CP24, CP26, or CP29, respectively, were studied by picosecond-fluorescence spectroscopy. By using different excitation/detection wavelength combinations it was possible for the first time, to our knowledge, to separate PSI and PSII fluorescence kinetics. The sub-100 ps component, previously ascribed entirely to PSI, turns out to be due partly to PSII. Moreover, the migration time of excitations from antenna to PSII reaction center (RC) was determined for the first time, to our knowledge, for thylakoid membranes. It is four times longer than for PSII-only membranes, due to additional antenna complexes, which are less well connected to the RC. The results in the absence of CP26 are very similar to those of wild-type, demonstrating that the PSII organization is not disturbed. However, the kinetics in the absence of CP29 and, especially, of CP24 show that a large fraction of the light-harvesting complexes becomes badly connected to the RCs. Interestingly, the excited-state lifetimes of the disconnected light-harvesting complexes seem to be substantially quenched.

## INTRODUCTION

In the process of photosynthesis in plants, photosystems work together to transform sunlight energy into chemical energy. The early events in this process: light absorption, excitation energy transfer (EET), and electron transfer occur in Photosystems I and II (PSI and PSII, see the Supporting Material for a schematic view of the macrostructure of the thylakoid membrane). Stable charge separation (CS) occurs within a few hundreds of picoseconds but differs for PSI and PSII. Elaborate research in the past has provided a general picture of these processes and the first kinetic steps could be studied for entire chloroplasts with the use of time-resolved fluorescence. However, agreement was never reached about the assignment and interpretation of all the obtained lifetime components, that moreover differed considerably in many different experiments (for an overview see van Amerongen and Dekker (1)). A great challenge in studies (1–4) on photosynthetic membranes and chloroplasts was that the thylakoid membranes contain both PSI and PSII with their spectra heavily overlapping and reaction kinetics occurring on similar timescales, making it difficult to distinguish between various processes. In more recent years, research has concentrated on the performance of the individual pigment-protein complexes that constitute PSI and PSII. The determination of the crystal structures of PSI (5), the core of PSII (6) and the major light-harvesting complex II of PSII (LHCII) (7) helped to understand the primary events at the molecular level and although many details are still under discussion, a rather detailed picture has emerged (8–10).

Based on the knowledge acquired in vitro it should now be possible to deepen our understanding of the in vivo system with the ultimate goal to apply time-resolved spectroscopy to study chloroplasts in vivo under different conditions and to link the spectroscopic features resolved to the different processes taking place, with special reference to the response of the chloroplast to varying environmental conditions. Here, we study thylakoid membranes from *Arabidopsis thaliana*, which contain both PSI and PSII but we focus on the kinetics of PSII, presenting a way to extract the PSII contribution to the fluorescence.

Photosystem II (PSII) is a large supramolecular pigment-protein complex embedded in the thylakoid membranes of green plants, algae, and cyanobacteria. It uses sunlight to split water into molecular oxygen, protons, and electrons. PSII in higher plants is composed of i), a core complex, consisting of the reaction center (RC) and the Chl *a* binding light-harvesting complexes CP43 and CP47; and ii), the outer, Chl *a*/*b* binding monomeric antenna complexes CP24, CP26, CP29, and trimeric light-harvesting complex II (LHCII) (11) (Fig. 1). In the RC excitations are used to create a primary CS. Primary CS is a reversible reaction, which is followed by further spatial separation of the charges (secondary CS) and transport of an electron to quinone A ($Q_A$) and then further along the electron transfer pathway.

The outer antennae are not only important for harvesting light, but also play essential roles in photoprotective and regulative mechanisms such as Chl *a* triplet quenching (12,13), reactive oxygen species scavenging (14), and non-photochemical quenching (15–17). The quantum efficiency

*Submitted October 1, 2009, and accepted for publication November 9, 2009.*

*Correspondence: herbert.vanamerongen@wur.nl

Editor: Leonid S. Brown.



0006-3495/10/03/0922/10 $2.00

doi: 10.1016/j.bpj.2009.11.012

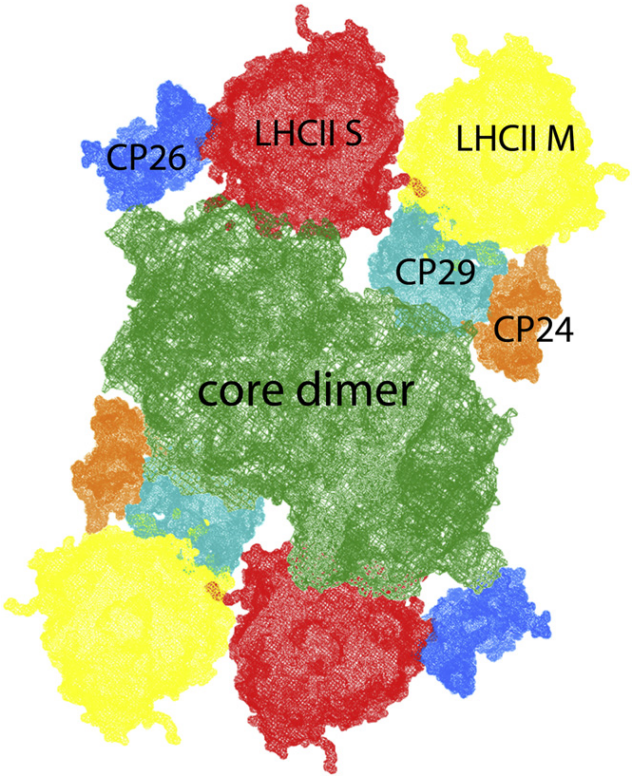


FIGURE 1 Organization of the PSII supercomplex, based on Caffarri et al. (50). The monomeric minor antenna complexes (CP24, CP26, CP29) are located in between the dimeric core and the trimeric major antenna complex LHCII, at positions S and M.

of CS depends on the rate constants of various processes: 1), EET from antenna to RC; 2), CS and charge recombination; 3), stabilization of CS by secondary electron transfer; and 4), relaxation or loss processes: intersystem crossing, internal conversion, and fluorescence.

Recently, a coarse-grained method was developed to correlate these processes to the fluorescence kinetics of PSII membranes (BBY preparations) with open RCs, i.e., with the secondary electron acceptor $Q_A$ being oxidized (18,19). The dimeric supercomplex of PSII (Fig. 1) forms the basic unit for this coarse-grained model. A hopping rate $k_{hop}$ was defined for EET between neighboring monomeric antenna complex (sub)units. The other parameters of the coarse-grained model are the rates of primary and secondary CS and the drop in free energy on primary charge separation. Using this model, and comparing the fluorescence kinetics obtained on 412 nm (relatively more excitations in the core) and 484 nm excitation (relatively more excitations in the outer antenna), it was concluded that the average migration time of an excitation toward the RC contributes 20–25% to the overall average trapping time. Within the context of the coarse-grained model it was calculated that the rate of primary CS in the RC is $(5.5 \pm 0.4 \text{ ps})^{-1}$, the rate of secondary CS is $(137 \pm 5 \text{ ps})^{-1}$ and the drop in free energy on primary CS is $(826 \pm 30)$ cm$^{-1}$. It should be noted that the number of LHCII trimers in these BBY preparations was relatively low (2.45 trimers per RC), i.e., far lower than the number of trimers that is generally believed to be present per RC in thylakoid preparations, namely four (11) (see also below). This might partly explain why the average fluorescence lifetime (~150 ps) found for BBY preparations (18,19) is significantly shorter than the (average) lifetime generally ascribed to PSII for measurements on thylakoid membranes and chloroplasts (many hundreds of picoseconds; for an overview see van Amerongen and Dekker (1) and Dekker and Van Grondelle (9). Another part of the explanation consists of the fact that lifetimes of ~100 ps that are usually observed for thylakoids/chloroplasts have been fully ascribed to PSI in the past (20) whereas PSII membranes also show a similar lifetime (18,19).

In this work, thylakoid membranes of *A. thaliana* are studied with time-resolved fluorescence spectroscopy using different combinations of excitation and detection wavelengths to separate PSI and PSII kinetics. In addition, the mutants *CP24ko*, *CP26ko*, and *CP29as* are studied (lacking minor antenna complexes CP24, CP26, and CP29, respectively) to investigate their role in the structural and functional organization of PSII. These monomeric minor complexes are located in between the PSII core (containing PSII reaction center(s), CP43, and CP47), and LHCII (Fig. 1) (21). Biochemical and physiological analyses have shown that the absence of each of these minor complexes has an effect on the packing of the supercomplexes in the membrane (22,23). In the absence of CP24, only $C_2S_2$ supercomplexes (consisting of a dimeric core (C) complexes and two strongly(S)-bound LHCII trimers) were observed in the membrane, and no supercomplexes containing the so-called LHCII M-trimers (24). CP24 also seems to be required for proper macroorganization of PSII complexes: in its absence, the packing of PSII leads to limitation of plastoquinone diffusion (23). In contrast, the absence of CP26 does not influence the presence of the other complexes within the PSII supercomplexes, but it changes their packing, somewhat shortening the distance between adjacent cores (22). The most drastic effect was observed in the absence of CP29: even on very mild solubilization, it was impossible to observe any microcrystalline arrays of membranes (present in wild-type (WT)), and no PSII supercomplexes were observed (22). This suggests that CP29 is a key component for the stability of the supercomplexes.

The main goal of this study is to unveil the relation between PSII composition and PSII fluorescence decay kinetics, which reflect both EET and CS.

## MATERIALS AND METHODS

### Sample preparation

*A. thaliana* T-DNA insertion mutants (*Columbia* ecotype) SALK_077953 with insertion into the Lhcb6 gene (At1g15820) and SALK_014869 into the Lhcb5 gene (At4g10340) were obtained from the NASC collections

**TABLE 1 Composition of thylakoid membranes from WT and mutants of *A. thaliana***

| Sample | Chl *a*/*b* | PSI/PSII | LHCII/PSII* |
|---|---|---|---|
| WT | 2.69 | 0.69 ± 0.12 | 4.0 |
| *CP29as* | 2.67 | 0.65 ± 0.09 | 3.9 |
| *CP26ko* | 2.62 | 0.64 ± 0.15 | 4.1 |
| *CP24ko* | 2.71 | 0.68 ± 0.11 | 4.1 |

Chl *a*/*b* ratio was determined by fitting of the spectrum of the acetone extract with the spectra of the individual pigments (28), PSI/PSII ratio was calculated using a $\mu$s resolution pump-and-probe spectrometer (30). LHCII trimers/monomeric PSII core ratio was calculated from the PSI/PSII ratio and subunit pigment composition.
*LHCII trimers/monomeric PSII core.

(25). The antisense line for CP29 (26) was a kind gift of S. Jansson (Umea, Sweden). Plants were grown for 6 weeks at 120 $\mu$mol photons $m^{-2}$ $s^{-1}$, 22°C, 70% humidity, and 8 h of daylight.

Thylakoids were isolated from leaves as described before (27). Pigments analysis was carried out by high performance liquid chromatography and by fitting of the spectrum of the acetone extract with the spectra of the individual pigments (28). The Chl *a*/*b* ratio of the thylakoids of different plants was quite similar in all cases (Table 1).

SDS-PAGE analysis was carried out with the Tris-Tricine buffer system as described previously (29).

The PSI/PSII ratio was measured using a JTS-10 spectrophotometer (Bio-Logic Science Instruments, Grenoble, France) in which absorption changes are sampled by monochromatic flashes provided by LED; changes in the amplitude of the electrochromic shift signal were recorded on excitation in the presence or absence of the PSII inhibitors DCMU (50 $\mu$M) and hydroxylamine (1 mM) as described in Cardol et al. (30).

## Fluorescence

Steady-state fluorescence emission spectra, which are necessary to calibrate decay-associated spectra (DAS), were measured after excitation at 412 nm or 484 nm on a Spex Fluorolog 3.2.2 (HORIBA Jobin-Yvon, Edison, NJ).

Time-resolved fluorescence was measured by time-correlated single photon counting, using a home-built setup (31). In brief: excitation was carried out by ~0.2 ps vertically polarized excitation pulses (wavelength 412 nm or 484 nm) at a repetition rate of 3.8 MHz. Fluorescence was collected at right angle to the excitation beam, under magic-angle polarization through interference filters (Schott, Mainz, Germany) that were slightly tilted to avoid reflections. Under the tilt angle, maximal transmission was at 680 nm, 700 nm, or 720 nm (15 nm width). The excitation power was reduced with neutral density filters, to keep RCs in an open state, and to keep the detection rate under 30,000 photons/s, to avoid pile-up distortion. Care was taken to avoid further data distortion, as described in detail in by van Hoek and Visser (32). Photon arrival times were stored in a multichannel analyzer (4096 channels at 2.0 ps time spacing).

The sample was kept at 287 K in a flow cuvette. Under the experimental conditions, with 0.5–4 $\mu$W excitation almost all PSII RCs remain open. More details are provided in the Supporting Material.

## Data analysis

Fluorescence decay curves were analyzed using home-built software (33), using the instrument response function (55 ps full width at half-maximum) measured from the 6 ps decay of pinacyanol iodide in methanol (34). The data were fitted to multi-exponential decay functions ($\sum_i p_i{}^* e^{-t/\tau_i}$) with amplitudes $p_i$ and fluorescence decay times $\tau_i$. During analysis the decay times were forced to be equal for all measurements of a sample. The fit quality was judged from the Poissonian maximum likelihood estimator, the residuals, and the autocorrelation of the residuals.

## Extraction of PSII kinetics

Fit results were interpreted in terms of the average fluorescence lifetime ($\tau_{avg}$) of PSII calculated from the three sub-ns lifetimes that were needed for good fits: $\tau_{avg} = \sum_{i=1}^{3} p_i{}^* \tau_i$, with $\sum_{i=1}^{3} p_i \equiv 1$. However, the decay components are partly due to PSI and partly to PSII. Calculation the PSII average lifetime therefore requires removal of the PSI contribution from the fit results, by unmixing the amplitudes, using the DAS of PSI (35–37), and of PSII and thylakoid membranes (both from this work).

Unmixing requires the calculation of the relative contributions of PSI ($q^{I}_{680}$) and PSII ($q^{II}_{680}$) to the DAS of the fastest decay component for thylakoid membranes measured at 680 nm (with $q^{I}_{680} + q^{II}_{680} = 1$). The DAS of thylakoid membranes at 680 nm ($Thyl_{680}$) is the sum of a PSI part ($PSI_{680}$) and a PSII part ($PSII_{680}$), according to Eq. 1:

$$PSI_{680} + PSII_{680} = Thyl_{680}, \tag{1}$$

and for 720 nm:

$$PSI_{720} + PSII_{720} = Thyl_{720}. \tag{2}$$

$q^{I}_{680}$ and $q^{II}_{680}$ follow from Eq. 1:

$$q^{I}_{680} = \frac{PSI_{680}}{Thyl_{680}} = \frac{PSI_{680}}{PSI_{680} + PSII_{680}}, \tag{3}$$

$$q^{II}_{680} = \frac{PSII_{680}}{Thyl_{680}} = \frac{PSII_{680}}{PSI_{680} + PSII_{680}}. \tag{4}$$

Equations 1 and 2 can be rewritten as Eq. 5 and Eq. 6:

$$-\frac{PSII_{720}}{PSII_{680}} * PSI_{680} - \frac{PSII_{720}}{PSII_{680}} * PSII_{680} = -\frac{PSII_{720}}{PSII_{680}} * Thyl_{680}, \tag{5}$$

$$\frac{PSI_{720}}{PSI_{680}} * PSI_{680} + \frac{PSII_{720}}{PSII_{680}} * PSII_{680} = Thyl_{720}. \tag{6}$$

Adding Eq. 5 and Eq. 6 gives Eq. 7:

$$\left(\frac{PSI_{720}}{PSI_{680}} - \frac{PSII_{720}}{PSII_{680}}\right) * PSI_{680} = Thyl_{720} - \frac{PSII_{720}}{PSII_{680}} * Thyl_{680}. \tag{7}$$

Combining Eq. 7 with Eq. 3 gives

$$q^{I}_{680} = \frac{\frac{Thyl_{720}}{Thyl_{680}} - \frac{PSII_{720}}{PSII_{680}}}{\frac{PSI_{720}}{PSI_{680}} - \frac{PSII_{720}}{PSII_{680}}}. \tag{8}$$

Likewise, it follows from Eq. 1, Eq. 2, and Eq. 4 that

$$q^{II}_{680} = \frac{\frac{Thyl_{720}}{Thyl_{680}} - \frac{PSI_{720}}{PSI_{680}}}{\frac{PSII_{720}}{PSII_{680}} - \frac{PSI_{720}}{PSI_{680}}}. \tag{9}$$

The amplitude of the fastest DAS of PSII equals $PSII^{1}_{680} = q^{II}_{680} * Thyl^{1}_{680}$. The other two thylakoid DAS are fully attributed to PSII, so $PSII^{2,3}_{680} = Thyl^{2,3}_{680}$. The total amplitude of the PSII DAS at 680 nm therefore equals $q^{II}_{680} * Thyl^{1}_{680} + Thyl^{2}_{680} + Thyl^{3}_{680}$. Normalizing the total amplitude gives the relative amplitudes of PSII ($p^{i}_{PSII}$) (Eq. 10), which can be used to calculate the average fluorescence lifetime of PSII ($\tau_{avg}$) (Eq. 11):

$$p^{i}_{PSII} = \begin{cases} \dfrac{q^{II}_{680} * Thyl^{i}_{680}}{q^{II}_{680} * Thyl^{1}_{680} + Thyl^{2}_{680} + Thyl^{3}_{680}} \text{ for } i = 1 \\ \dfrac{Thyl^{i}_{680}}{q^{II}_{680} * Thyl^{1}_{680} + Thyl^{2}_{680} + Thyl^{3}_{680}} \text{ for } i = 2 \text{ or } 3 \end{cases}, \quad (10)$$

$$\tau_{avg} = \sum_{i} p^{i}_{PSII} * \tau_{i}. \quad (11)$$

## Theory and modeling of the fluorescence kinetics

The overall average charge separation time $\tau_{avg}$ can be considered as the sum of two times $\tau_{avg} = \tau_{mig} + \tau_{trap}$. $\tau_{mig}$ is the first passage time or migration time, representing the average time that it takes for an excitation created somewhere in PSII to reach the RC (primary electron donor), and $\tau_{trap}$ is the trapping time. $\tau_{trap}$ is the CS time $\tau_{CS}$ divided by the probability that the excitation is located on the RC (18,38): $\tau_{trap} = N_{eff}\tau_{C}$, with $N_{eff} = N_{PSII}/N_{RC}$, where $N_{PSII}$ and $N_{RC}$ are the numbers of Chl *a* molecules in PSII and the RC, respectively. In the case that the total number of (isoenergetic) pigments for instance doubles, the probability for an excitation to be on the primary donor decreases by a factor of 2 and $\tau_{trap}$ doubles. In case CS is reversible then $\tau_{trap}$ should be replaced by $\tau_{trap} = N_{eff}[\tau_{CS} + \tau_{RP}\exp(-\Delta G/kT)]$ (derivation in Supporting Material) where $\tau_{RP}$ is the secondary CS time and $\Delta G$ is the drop in free energy on primary CS. When excited state decay processes in the antenna are taken into account, the equations change into $\tau_{trap} = \left\{\frac{1}{N_{eff}\tau_{CS}} + \frac{1}{\tau_0}\right\}^{-1}$ for irreversible CS and $\tau_{trap} = \left\{\frac{1}{N_{eff}[\tau_{CS}+\tau_{RP}\exp(-\Delta G/kT)]} + \frac{1}{\tau_0}\right\}^{-1}$ for reversible CS, where $\tau_0$ is the excited antenna complex lifetime (taken as 4 ns; see van Oort et al. (39)). For $\tau_0 \gg \tau_{trap}$ the trapping timescales linearly with the total number of (isoenergetic) pigments.

In Broess et al. (19) the parameters $\tau_{CS}$, $\Delta G$, and $\tau_{RP}$ were determined for PSII membranes from spinach (BBY particles). Assuming that these numbers remain unaltered in the thylakoid membranes, $\tau_{trap}$ can be calculated (19) and the value increases, on increasing the size of the antenna. It was also pointed out in (19) that excitation at 412 and 484 nm lead to different values of $\tau_{avg}$, because excitation at 484 nm leads to relatively more excitations in the outer antenna. Due to invariance of $\tau_{trap}$ with initial excitation conditions, the difference ($\Delta\tau_{avg}$) between the two values characterize solely the change of migration time.

## RESULTS

The thylakoid membranes of the WT and the three mutants were analyzed in terms of pigment and protein composition. The PSI/PSII ratio was calculated using a $\mu$s resolution pump-and-probe spectrometer (30). The obtained ratio was 0.69 for the WT and it was very similar for all the mutants (Table 1), indicating that the absence of one of the minor antennae does not affect the PSI/PSII ratio. The Chl *a*/*b* ratio of the thylakoid preparations from WT and mutants (Table 1) was also very similar in all cases, indicating that, also at the level of PSII, the absence of one of the antennae does not strongly influence the expression of other Lhcb complexes. Indeed, by using the pigment composition of the individual subunits (40) and the measured PSI/PSII value, it can be calculated that in the case of the WT 4 LHCII trimers are present per monomeric PSII core. The data were very similar for the mutants, ranging from 3.9 trimers per PSII in *CP29as* to 4.1 trimers of *CP26ko* and *CP24ko*, identical within experimental errors (Table 1). This is in agreement with the analysis of the protein content on fractionation by SDS PAGE, which showed very similar values for the LHCII/core ratio in all samples (results not shown). It is worth noting that the same method used here to calculate the ratio LHCII/PSII core gave a value of 2.45 trimers of LHCII per monomeric core for the BBY membranes (19), indicating that during the preparation of the grana membranes part of the LHCII trimers is lost.

Fluorescence decay curves were measured for thylakoid membranes of all four samples. The excitation wavelength was either 412 nm or 484 nm, and fluorescence was detected at 680 nm, 700 nm, or 720 nm. Different combinations of excitation and detection wavelength lead to different fractional contributions of PSI and PSII to the fluorescence decay kinetics. This was used to extract the fluorescence kinetics of PSII. The combination 484 nm/680 nm leads to the highest contribution of PSII. The corresponding decay curves are presented in Fig. 2. The combination 412 nm/720 nm leads to the lowest contribution of PSII. The curves with highest/lowest PSII contribution are presented in Fig. 3, for WT, *CP24ko*, and *CP29as*.

The decay curves of WT and *CP26ko* were very similar, whereas those of *CP29as* and *CP24ko* were considerably slower (Figs. 2 and 3). Each sample was measured six times, with different combinations of excitation and detection wavelength. The decay curves were globally fitted to a sum of exponential decay functions. For each sample, four decay components were needed to obtain a satisfactory fit for all wavelength combinations, as was judged from the Poissonian maximum likelihood estimator, and from the residuals and the autocorrelation of the residuals. The fitting results of the WT curves are given in Table 2. Note that the decay times and amplitudes do not necessarily correspond to real physical processes but they provide an accurate description of the data that will be used later.

On moving the detection wavelength to the red, the relative contribution of PSI increases (20), which is reflected by an increase of the amplitude of the 73 ps component (Table 2). Although both PSI and PSII contribute to the 73 ps component, the contribution of PSI is dominant whereas the 251 ps and 532 ps components are due mainly to PSII (see also below). The amplitude of the slowest (several ns) component, which should be ascribed to either closed PSII, free Chl or disconnected light-harvesting complexes is very small and it was omitted in the analysis. Excitation at 412 nm creates relatively higher excitation densities on PSI than excitation at 484 nm (because PSII contains relatively more Chl *b*, which dominates the absorption at 484 nm) causing an increased contribution of the 73 ps component at 412 nm.

In a recent study on dissolved PSI-LHCI crystals, lifetimes of 24 ps, 61 ps, and 143 ps were found with relative amplitudes 0.55, 0.33, and 0.10, respectively, on excitation at

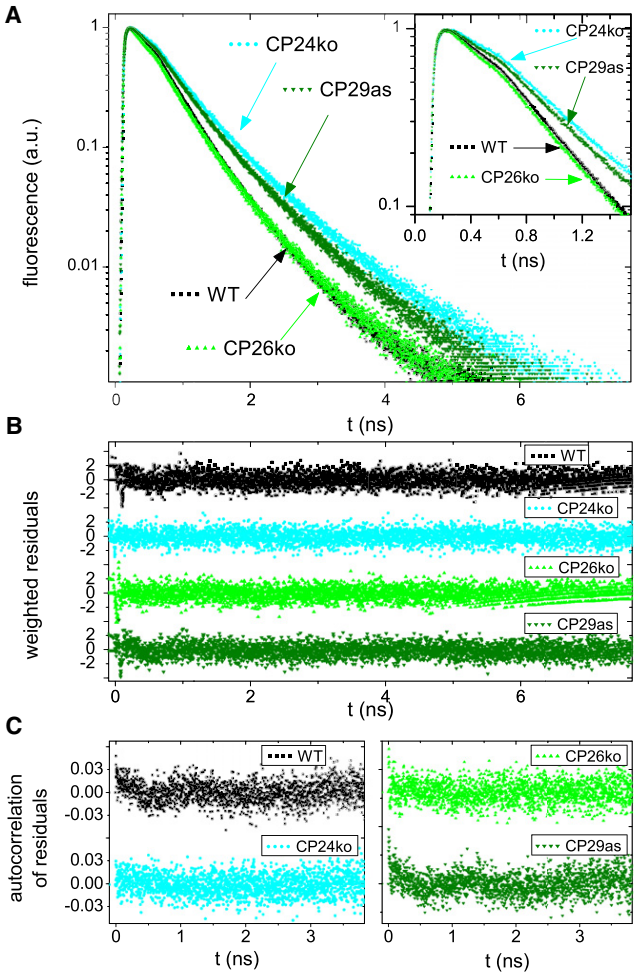


FIGURE 2 Time resolved fluorescence of thylakoid membranes from WT and mutants of *A. thaliana*. (*A*) Normalized fluorescence decay curves. *Inset*: Initial part of the decay curves. (*B*) Weighted residuals of the fits of the decay curves in *A*. (*C*) Autocorrelation of the weighted residuals. (*B* and *C*) Used to evaluate fit quality. The excitation wavelength is 484 nm and the detection wavelength is 680 nm.

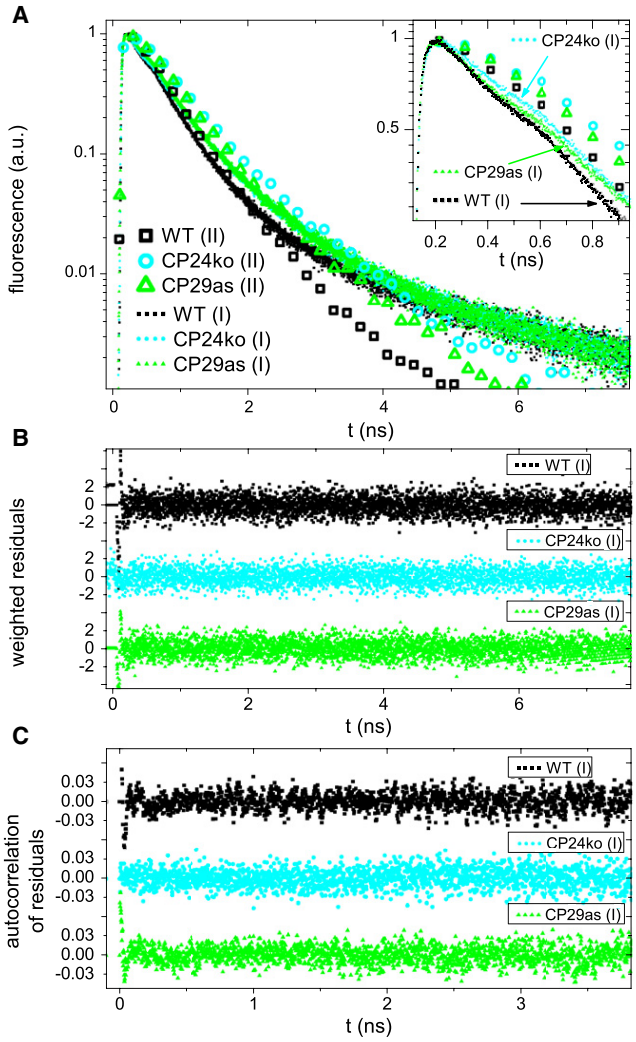


FIGURE 3 Time resolved fluorescence of thylakoid membranes from WT and mutants of *A. thaliana*, for two combinations of excitation/detection wavelengths: 412 nm/720 nm (*dots* labeled (I)) and 484/680 nm (*open symbols* labeled (II)). For (I) relatively more excitations are created in PSI and PSII core and relatively more PSI emission is detected; For (II) relatively more excitations are created in the PSII outer antenna. (*A*) Normalized fluorescence decay curves (symbols for every 200th data point). *Inset*: initial part of the decay curves (symbols for every 100th data point). (*B*) Weighted residuals of the fits of the decay curves in *A*. (*C*) Autocorrelation of the weighted residuals. (*B* and *C*) Used to evaluate fit quality. The complete curves for 484 nm/680 nm are presented in Fig. 2. The data of *CP26ko* are omitted for readability.

410 nm and detection above 710 nm (34). The 24 ps component is not resolved here because of the limited time resolution and the decrease in relative contribution. The 61 ps lifetime is similar to the 73 ps lifetime. The 143 ps component is not detected separately, because its amplitude is relatively small and it contributes to some extent to the 73 and 251 ps components in the fit. PSII also contributes to the 73 ps component as indicated by the analysis of membranes enriched in PSII, which also showed a short component (18,19). It should be noted that it is not possible to discriminate between lifetimes that are close together and they will be lumped into one lifetime in the fitting procedure.

When single traces measured at a particular combination of excitation and detection wavelength are fitted, the obtained lifetimes are somewhat different from the lifetimes obtained with a global fit. However, the calculated average lifetimes are identical and these will be used for further analysis.

The main goal of this study is to understand the relation between the PSII composition and the PSII decay kinetics, which reflect both EET and CS. Therefore, the measured overall kinetics have to be corrected for the contribution of PSI. As already stated above, PSI mainly contributes to the 73 ps component and much less to the other ones. Here, the relative contributions of PSI and PSII to the 73 ps component will be called $q^{\mathrm{I}}$ and $q^{\mathrm{II}}$, with $q^{\mathrm{I}} + q^{\mathrm{II}} = 1$. At 680 nm, $q^{\mathrm{II}}$

**TABLE 2 Results of global fitting of the fluorescence decay curves of WT *A. thaliana***

| | Excitation | | | | | |
|---|---|---|---|---|---|---|
| | 412 nm | | | 484 nm | | |
| Detection | 680 nm | 700 nm | 720 nm | 680 nm | 700 nm | 720 nm |
| $\tau$ (ps)* | *p* | *p* | *p* | *p* | *p* | *p* |
| 73 | 0.250 | 0.366 | 0.501 | 0.150 | 0.221 | 0.281 |
| 251 | 0.390 | 0.349 | 0.279 | 0.468 | 0.442 | 0.394 |
| 532 | 0.351 | 0.276 | 0.210 | 0.376 | 0.332 | 0.317 |
| 1.8–2.6 ns | 0.009 | 0.009 | 0.011 | 0.006 | 0.005 | 0.008 |

The longest lifetime was not fitted globally. Confidence intervals of fluorescence lifetimes ($\tau$) as calculated by exhaustive search were <5%, standard errors of amplitudes, as calculated from 2–5 repeats, were generally <3%, except for the amplitude of the longest lifetime (10–20%). *p*, relative amplitudes.

*Except for the fourth component.

is defined as $q^{II}{}_{680}$ and can be estimated using Eq. 1 (see Materials and Methods for a derivation).

$$q^{II}_{680} = \frac{\frac{Thyl_{720}}{Thyl_{680}} - \frac{PSI_{720}}{PSI_{680}}}{\frac{PSII_{720}}{PSII_{680}} - \frac{PSI_{720}}{PSI_{680}}}, \tag{12}$$

In this equation $Thyl_{720}/Thyl_{680}$ is the ratio of the normalized values of the 73 ps decay associated spectrum (DAS) of thylakoid membranes at 720 nm and 680 nm (see Materials and Methods for more explanation). The DAS are calculated from the fit results in Table 2 and the steady-state fluorescence emission spectra (Supplementary Material), as described in Materials and Methods. The ratio $PSI_{720}/PSI_{680}$ is defined analogously to $Thyl_{720}/Thyl_{680}$. Because spectral equilibration in PSI occurs within the first 10 ps after excitation (34), the ratio $PSI_{720}/PSI_{680}$ is constant for longer-lived DAS and it was taken from literature: at 412 nm excitation $PSI_{720}/PSI_{680} = 1.44$ (average from values in Ihalainen et al. (36,37)), at 484 nm 1.57 (35). The ratio $PSI_{720}/PSI_{680}$ was calculated from the 251 ps DAS of thylakoids, which is thought to arise mainly from PSII although there might be a small contribution from PSI. However, using the 532 ps DAS for calculating $q^{II}{}_{680}$ leads to very similar results, confirming that the contribution of PSI to the 251 ps DAS is minor (Table 3).

After obtaining $q^{II}{}_{680}$, the relative amplitudes ($p^i_{PSII}$) and the average fluorescence lifetime ($\tau_{avg}$) of PSII were calculated using Eq. 13 and Eq. 14 (see Materials and Methods).

$$p^i_{PSII} = \begin{cases} \dfrac{q^{II}_{680} * Thyl^i_{680}}{q^{II}_{680} * Thyl^1_{680} + Thyl^2_{680} + Thyl^3_{680}} \; for\; i = 1 \\ \dfrac{Thyl^i_{680}}{q^{II}_{680} * Thyl^1_{680} + Thyl^2_{680} + Thyl^3_{680}} \; for\; i = 2\; or\; 3 \end{cases} \tag{13}$$

$$\tau_{avg} = \sum_i p^i_{PSII} * \tau_i \tag{14}$$

The same calculations were also done using the DAS at 700 and 680 nm instead of 720 and 680 nm. The results for WT are shown in Table 3.

Excitation at 412 nm leads to average lifetimes that are nearly identical in all cases: 323, 326, 326, and 328 ps i.e., 326 ± 2 ps on average. Excitation at 484 nm leads to the values 339, 338, 340, and 338 ps, i.e., 339 ± 1 ps on average. The latter lifetime is 13 ps longer than the one obtained on exciting at 412 nm and this is due to the fact that on 484 nm excitation a larger fraction of the initial excitations are localized on the outer antenna, whereas 412 nm leads to a relatively larger fraction of PSII core excitation (19).

The same measurements and procedures were repeated for thylakoid preparations from *CP24ko*, *CP26ko* and *CP29as*. For each of these three mutants the average PSII fluorescence lifetime ($\tau_{avg}$) was calculated in the same four ways as described for WT. The resulting values of $\tau_{avg}$ were averaged, giving $\overline{\tau}_{avg}$, and used to calculate standard errors of $\overline{\tau}_{avg}$. The results for excitation at 412 nm and 484 nm are in Table 4.

The results for *CP26ko* are similar to those for WT in the sense that the difference between the average lifetimes on 412 and 484 nm is similar (15 vs. 13 ps). For *CP29as* and *CP24ko* this difference is larger, namely 30 and 83 ps,

**TABLE 3 Fluorescence kinetics at 680 nm of PSII in thylakoids of WT *A. thaliana***

| | PSII ratios from 251 ps DAS | | | | PSII ratios from 532 ps DAS | | | |
|---|---|---|---|---|---|---|---|---|
| Wavelengths used for PSI removal | 700/680 nm | | 720/680 nm | | 700/680 nm | | 720/680 nm | |
| Excitation | 412 nm | 484 nm | 412 nm | 484 nm | 412 nm | 484 nm | 412 nm | 484 nm |
| $\tau$ (ps) | $p^i_{PSII}$ | $p^i_{PSII}$ | $p^i_{PSII}$ | $p^i_{PSII}$ | $p^i_{PSII}$ | $p^i_{PSII}$ | $p^i_{PSII}$ | $p^i_{PSII}$ |
| 73 | 0.195 | 0.122 | 0.185 | 0.125 | 0.187 | 0.119 | 0.181 | 0.125 |
| 251 | 0.424 | 0.487 | 0.429 | 0.485 | 0.428 | 0.489 | 0.431 | 0.485 |
| 532 | 0.381 | 0.391 | 0.386 | 0.390 | 0.385 | 0.392 | 0.388 | 0.390 |
| $\tau_{avg}$ (ps) | 323 | 339 | 326 | 338 | 326 | 340 | 328 | 338 |

The kinetics were derived from the kinetics of thylakoid membranes by removing the PSI contribution, using the ratios of the PSI and PSII DAS at 700/680 nm or 720/680 nm. The PSI ratios were taken from literature (35–37), and the PSII ratios were obtained from the PSII DAS of either 251 ps or 532 ps. For details, see text. Confidence intervals of fluorescence lifetimes ($\tau$) were <5% (calculated by exhaustive search), standard errors of amplitudes ($p^i_{PSII}$) were generally <5% (calculated from 2–5 repeats). Confidence intervals of average lifetimes ($\tau_{avg}$) were <1%. This is smaller than the uncertainties of the fit parameters due to correlations between fit parameters.

**TABLE 4 Average fluorescence lifetimes at 680 nm of PSII in thylakoids of WT *A. thaliana* and mutants**

| | $\overline{\tau}_{avg}$(ps) | | |
|---|---|---|---|
| Excitation | 412 nm | 484 nm | Difference (ps) |
| WT | 326 (0.9) | 339 (0.5) | 13 (1.3) |
| *CP24ko* | 329 (2.5) | 413 (1.0) | 83 (2.6) |
| *CP26ko* | 303 (0.1) | 318 (1.0) | 15 (1.0) |
| *CP29as* | 391 (2.0) | 420 (0.8) | 30 (2.7) |

The values were calculated from fluorescence kinetics of thylakoid membranes by removing the PSI contribution in four ways: using the ratios of the DAS at 700/680 nm or 720/680 nm, and using the PSII DAS of either 251 ps or 532 ps (for WT the results of each of these four calculations are shown in Table 3). From the four calculations the average fluorescence lifetime ($\overline{\tau}_{avg}$) and standard errors of the mean (in brackets) were calculated. See text for details.

whereas in these mutants the average lifetime on 484 nm excitation is substantially longer than for WT and *CP26ko*.

## DISCUSSION

The average lifetime of PSII is twice as long in thylakoid membranes as in PSII membranes. This difference is ascribed to the fact that the number of LHCII trimers per PSII RC in the PSII membranes was 2.45, whereas for the thylakoid preparations that are used in this study, the value is ~4. The overall average trapping time $\tau_{avg}$ can be considered as the sum of the migration time or first passage time $\tau_{mig}$ and the trapping time $\tau_{trap}$, i.e., $\tau_{avg} = \tau_{mig} + \tau_{trap}$ (38). Although this is strictly speaking only correct for a regular lattice, it is a good approximation in the case of less regular structures like for instance the PSII membrane (18).

To estimate the contribution of both $\tau_{mig}$ and $\tau_{trap}$ to the overall trapping time it was assumed that the parameters for charge separation for the PSII RCs in the current preparations are the same as for the RC in the BBY preparations (19). This is reasonable because the core complexes are probably almost identical in both preparations. By using the fact that there are 4 LHCII trimers per RC, the value of $\tau_{trap}$ was calculated to be 181 ps (See Materials and Methods, taking into account a 4 ns excited state lifetime of the antenna). Note that $\tau_{trap}$ does not depend on the organization of the pigments with respect to each other (38). This value of $\tau_{trap}$ is larger than the 120 ps for the BBY preparations (19) ($\tau_{trap}$ is 124 ps in those preparations when a 4 ns decay in the antenna is taken into account). This difference between PSII in thylakoid and BBY membranes is entirely caused by the additional ~1.5 trimers of LHCII per RC, which increase the antenna size, and thereby reduce the equilibrium population of excited states in the RC.

The migration time $\tau_{mig}$ is thus ~150 ps for WT PSII (i.e., $\tau_{mig} = \tau_{avg} - \tau_{trap} = 330$ ps $-$ 181 ps). This is substantially slower than observed for the BBY preparations, where it was found to be ~35 ps (19). This can be interpreted in terms of connectivity between LHCII and RC. In supercomplexes of *A. thaliana* each PSII RC is in very close association with 2 LHCII trimers (41,42). The BBY preparation contained 2.45 LHCII trimers per RC, suggesting that most of the LHCII trimers are arranged in this type of supercomplexes ($C_2S_2M_2$) in the grana region of the membrane (as also directly observed by electron microscopy (EM) analysis (43)). This agrees with recent time-resolved fluorescence results on isolated supercomplexes (44) that show only slightly faster decay times than the BBY complexes. That means that the overall organization and composition of isolated supercomplexes is very similar to that in BBY preparations. However, in thylakoid membranes $\tau_{mig}$ is ~4 times slower (150 ps vs. 35 ps). This implies that in the thylakoid membranes the migration time from the additional trimers is substantially longer than from the trimers in the supercomplexes. This increase of the migration time is also responsible for the fact that the difference in average lifetime on 412 and 484 nm excitation is 13 ps, i.e., a factor of 3 larger than for the BBY particles (where it was 4.3 ps (19)). As was also pointed out in Materials and Methods, the difference in the average lifetime for the two excitation wavelengths is approximately proportional to the migration time.

The average lifetimes for *CP26ko* are only somewhat faster than for WT, and the difference in lifetimes on exciting at 412 and 484 nm is very similar to the difference observed for WT, indicating that the migration time is also very similar in both cases. This suggests that the difference in the overall lifetime is primarily due to the smaller number of pigments per RC in the mutant, but that the absence of CP26 does not influence the overall performance of the supercomplexes, in agreement with the EM analysis of mildly solubilized membranes of this mutant (22). This indicates that PSII supercomplexes are still in the $C_2S_2M_2$ form, when CP26 is absent. It can be concluded that the absence of CP26 does not have any direct or indirect effect on the energy transfer and trapping processes.

The situation is different for *CP29as*. The absence of CP29 should lead to a value for $\tau_{trap}$ that is similar to the value in the absence of CP26 or even smaller due to the additional loss of CP24 in the *CP29as* mutant (26). Because the average fluorescence lifetime is longer than for *CP26ko* and also WT, this means that $\tau_{mig}$ must have increased. This agrees with the fact that the difference in average lifetime on 412 and 484 nm excitation is 30 ps, i.e., more or less double the value as for *CP26ko* and WT, indicating that $\tau_{mig}$ should be ~300 ps. The value of $\tau_{trap}$ is calculated (in the same way as for WT) to be ~174 ps, similar to what is expected for WT (181 ps) and *CP26ko* (174 ps). Together, these numbers would thus predict an average lifetime of ~300 + 174 = 474 ps, somewhat longer than the observed lifetime of ~400 ps. This difference might be due to faster charge separation kinetics in the RC for this mutant but, more likely, it can also be due to a fast decay rate of the excited state for light-harvesting complexes or a subset of them.

The difference between measured and calculated average lifetime is even more pronounced for *CP24ko*: The difference in average lifetime on 412 and 484 nm excitation is 80 ps that implies an increase of the migration time with a factor of 5–6 as compared to the WT, meaning that the migration time by itself would already be 800–1000 ps, much longer than the observed lifetimes of 300–400 ps. The most straightforward way to explain the large difference in average lifetime on 412 and 484 nm excitation, as well as the faster-than-WT average lifetime on 412 nm excitation, is heterogeneity: the coexistence of regions of PSII characterized by a short trapping time and regions that contain badly connected or disconnected light-harvesting complexes that are quenched substantially.

The fact that for *CP29as* the difference of the excited-state lifetimes for the two excitation wavelengths is smaller than for *CP24ko*, whereas the average lifetime is larger is surprising, considering that in both mutants the amount of LHCII is identical to that of the WT. This suggests that the absence of CP29 slows down the transfer from LHCII to the core, but does not completely block it. By contrast, in the case of *CP24ko*, a large part of the LHCII trimers is apparently completely disconnected from the core. This result thus indicates a different organization of the subunits in the membranes of the two mutants.

Indeed, in the case of *CP24ko*, two different regions could be identified in the membrane by EM: i), microcrystalline arrays composed of highly ordered $C_2S_2$ supercomplexes; and ii), regions strongly enriched in LHCII (23). Thus, in *CP24ko* fast energy transfer is expected for the $C_2S_2$ supercomplexes that are present in high amounts in the membrane, whereas a slower lifetime should be associated to the regions enriched in LHCII, thus explaining the large difference in lifetime observed on exciting at different wavelengths.

To test this hypothesis we assumed that the different regions are not interconnected, in the sense that excitations cannot move from one region to the other. With the use of the absorption of the individual subunits we calculated the relative probabilities to excite the $C_2S_2$ supercomplexes and the LHCII-only region (considering that three out of the four LHCII present per core are located in this region). We could thus solve a system of equations in which the two unknowns are the average lifetime of $C_2S_2$ and that of disconnected LHCII in the membrane (Eq. 15). The excitation vectors $a_j^i$ in Engelmann et al. (4) were calculated using the absorption spectra of core and antennas normalized to the number of Chls:

$$\begin{cases} a_{412}^{C2S2} * \tau_{C2S2} + a_{412}^{LHCII} * \tau_{LHCII} = \tau_{avg,412} \\ a_{484}^{C2S2} * \tau_{C2S2} + a_{484}^{LHCII} * \tau_{LHCII} = \tau_{avg,484} \end{cases}. \quad (15)$$

This leads to an average lifetime of 110 ps for $C_2S_2$, whereas it is 560 ps for the disconnected antenna. This result is in excellent agreement with the measurements on the BBY membrane where a lifetime of 150–165 ps was observed for complexes containing 2.5 LHCII per monomeric core (19), in which case the difference in lifetime is simply due to the smaller number of Chls associated with the $C_2S_2$ complexes as compared to $C_2S_2M_2$ + 0.5 LHCII trimer in the BBY preparations. From the average lifetime for the BBY membrane one would expect an average lifetime of 95–105 ps for $C_2S_2$, very close to the obtained value of 110 ps. Moreover, it is close to the average lifetime of 115 ps that was obtained for a mixture of $C_2S_2$ and $C_2SM$ (44).

It is striking that the excited-state lifetime of the disconnected LHCIIs is much shorter than the lifetime of ~4 ns for LHCII in detergent and liposomes (45,46). Interestingly a shortening of LHCII excited-state lifetime requires only a small change of volume and free energy (47). Indeed, a shorter lifetime occurs under many conditions: when LHCII is tightly packed in liposomes (45), or when it is aggregated (39), or crystallized (48), suggesting that interactions between the complexes in the membrane cause a shortening of excited-state lifetime. It is interesting to note that recently in LHCII preparations that were argued to be in a similar state as in the thylakoid membrane the excited-state lifetime turned out to be ~600 ps (49).

In the case of the membranes of *CP29as* no microcrystalline arrays could be detected on mild solubilization (22). Moreover, not even individual supercomplexes could be observed in these conditions indicating that CP29 is a key subunit for the stability of the supercomplex. Furthermore, CP29 is positioned in between the outer LHCII and the core and as such forms part of the energy transfer pathway from LHCII to the reaction center, thus suggesting that in its absence the transfer from LHCII to the RC might be slower. It is concluded that in the membrane of *CP29as*, each core is surrounded by several LHCII complexes that are still able to transfer energy to the RC, but less efficiently than in the WT.

## CONCLUSIONS

It proved possible to extract the time-resolved fluorescence kinetics of PSII from the kinetics of thylakoid preparations, by correcting for the PSI contribution. From the results the following is concluded:

PSII contributes significantly to the short (<100 ps) fluorescence component, which is usually ascribed to PSI only.

LHCII trimers that are not part of the $C_2S_2M_2$ PSII supercomplexes are responsible for migration times of the excitations to the RCs that are much longer than those for the trimers within the supercomplexes (hundreds instead of tens of ps). In the WT membranes, there are approximately two trimers present per core in the supercomplex and two are present in a different region. This explains why the average fluorescence lifetimes are substantially longer for PSII in intact thylakoid membranes than in grana preparations.

The absence of CP26 leaves the PSII organization nearly unaltered as evidenced by very similar migration times in the presence and absence of CP26. In contrast, the absence of CP29 and especially CP24 lead to substantial changes in the PSII organization as evidenced by a significant increase of the apparent migration time, demonstrating a bad connection between a significant part of the antennae and the RCs.

Antenna complexes that are badly connected or unconnected to an RC are strongly quenched: a fluorescence lifetime of ~560 ps implies a fluorescence quantum yield of <4%, indicating extensive decay of Chl excited states by heat dissipation.

Applying the same analysis on thylakoid membranes of different composition, and under various environmental stress conditions will provide substantial new knowledge on the variability of excitation migration. Such experiments are in progress currently.

## SUPPORTING MATERIAL

Details about the experimental conditions, fluorescence emission spectra, $\tau_{trap} = N_{eff}[\tau_{CS} + \tau_{RP} \exp(-G/kT)]$ derivation of and calculation of decay associated spectra are available at http://www.biophysj.org/biophysj/supplemental/S0006-3495(09)01739-1.

Stefan Jansson, Umea University, is thanked for the kind gift of Lhcb4 antisense plants.

This work is was supported by the Stichting voor Fundamenteel onderzoek der Materie, which is financially supported by the Netherlands Organization for Scientific Research (B.v.O.). Fondo Integrativo per la Ricerca di Base (RBLA0345SF_002 and RBIP06CTBR_006 to R.B.), the Netherlands Organization for Scientific Research-Earth and Life Sciences (VIDI grant to R.C.), and the Lithuanian State Science and Studies Foundation (G.T.).

## REFERENCES

1. van Amerongen, H., and J. P. Dekker. 2003. Light-harvesting in Photosystem II. *In* Light-Harvesting Antennas in Photosynthesis. B. R. Green and W. W. Parson, editors. Kluwer Academic Publishers, Dordrecht. 219–251.
2. van Grondelle, R., J. P. Dekker, …, V. Sundstrom. 1994. Energy transfer and trapping in photosynthesis. *Biochim. Biophys. Acta.* 1187:1–65.
3. Veerman, J., M. D. McConnell, …, D. Bruce. 2007. Functional heterogeneity of photosystem II in domain specific regions of the thylakoid membrane of spinach (*Spinacia oleracea L.*). *Biochemistry.* 46:3443–3453.
4. Engelmann, E. C. M., G. Zucchelli, …, R. C. Jennings. 2005. The effect of outer antenna complexes on the photochemical trapping rate in barley thylakoid Photosystem II. *Biochim. Biophys. Acta.* 1706:276–286.
5. Amunts, A., O. Drory, and N. Nelson. 2007. The structure of a plant photosystem I supercomplex at 3.4 A resolution. *Nature.* 447:58–63.
6. Loll, B., J. Kern, …, J. Biesiadka. 2005. Towards complete cofactor arrangement in the 3.0 A resolution structure of photosystem II. *Nature.* 438:1040–1044.
7. Liu, Z. F., H. Yan, …, W. Chang. 2004. Crystal structure of spinach major light-harvesting complex at 2.72 A resolution. *Nature.* 428:287–292.
8. Novoderezhkin, V. I., M. A. Palacios, …, R. van Grondelle. 2005. Excitation dynamics in the LHCII complex of higher plants: modeling based on the 2.72 Angstrom crystal structure. *J. Phys. Chem. B.* 109:10493–10504.
9. Dekker, J. P., and R. Van Grondelle. 2000. Primary charge separation in Photosystem II. *Photosynth. Res.* 63:195–208.
10. Şener, M. K., C. Jolley, …, K. Schulten. 2005. Comparison of the light-harvesting networks of plant and cyanobacterial photosystem I. *Biophys. J.* 89:1630–1642.
11. Dekker, J. P., and E. J. Boekema. 2005. Supramolecular organization of thylakoid membrane proteins in green plants. *Biochim. Biophys. Acta.* 1706:12–39.
12. Barzda, V., E. J. G. Peterman, …, H. van Amerongen. 1998. The influence of aggregation on triplet formation in light-harvesting chlorophyll *a*/*b* pigment-protein complex II of green plants. *Biochemistry.* 37:546–551.
13. Mozzo, M., L. Dall'Osto, …, R. Croce. 2008. Photoprotection in the antenna complexes of photosystem II: role of individual xanthophylls in chlorophyll triplet quenching. *J. Biol. Chem.* 283:6184–6192.
14. Dall'Osto, L., S. Cazzaniga, …, R. Bassi. 2007. The Arabidopsis aba4-1 mutant reveals a specific function for neoxanthin in protection against photooxidative stress. *Plant Cell.* 19:1048–1064.
15. Ahn, T. K., T. J. Avenson, …, G. R. Fleming. 2008. Architecture of a charge-transfer state regulating light harvesting in a plant antenna protein. *Science.* 320:794–797.
16. Ruban, A. V., R. Berera, …, R. van Grondelle. 2007. Identification of a mechanism of photoprotective energy dissipation in higher plants. *Nature.* 450:575–578.
17. Horton, P., A. V. Ruban, and R. G. Walters. 1996. Regulation of light harvesting in green plants. *Annu. Rev. Plant Physiol. Plant Mol. Biol.* 47:655–684.
18. Broess, K., G. Trinkunas, …, H. van Amerongen. 2006. Excitation energy transfer and charge separation in photosystem II membranes revisited. *Biophys. J.* 91:3776–3786.
19. Broess, K., G. Trinkunas, …, H. van Amerongen. 2008. Determination of the excitation migration time in Photosystem II consequences for the membrane organization and charge separation parameters. *Biochim. Biophys. Acta.* 1777:404–409.
20. Roelofs, T. A., C.-H. Lee, and A. R. Holzwarth. 1992. Global target analysis of picosecond chlorophyll fluorescence kinetics from pea chloroplasts: a new approach to the characterization of the primary processes in photosystem II α- and β-units. *Biophys. J.* 61:1147–1163.
21. Harrer, R., R. Bassi, …, C. Schäfer. 1998. Nearest-neighbor analysis of a photosystem II complex from *Marchantia polymorpha L.* (liverwort), which contains reaction center and antenna proteins. *Eur. J. Biochem.* 255:196–205.
22. Yakushevska, A. E., W. Keegstra, …, P. Horton. 2003. The structure of photosystem II in *Arabidopsis*: localization of the CP26 and CP29 antenna complexes. *Biochemistry.* 42:608–613.
23. de Bianchi, S., L. Dall'Osto, …, R. Bassi. 2008. Minor antenna proteins CP24 and CP26 affect the interactions between photosystem II subunits and the electron transport rate in grana membranes of Arabidopsis. *Plant Cell.* 20:1012–1028.
24. Kovács, L., J. Damkjaer, …, P. Horton. 2006. Lack of the light-harvesting complex CP24 affects the structure and function of the grana membranes of higher plant chloroplasts. *Plant Cell.* 18:3106–3120.
25. Alonso, J. M., A. N. Stepanova, …, J. R. Ecker. 2003. Genome-wide insertional mutagenesis of *Arabidopsis thaliana*. *Science.* 301:653–657.
26. Andersson, J., R. G. Walters, …, S. Jansson. 2001. Antisense inhibition of the photosynthetic antenna proteins CP29 and CP26: implications for the mechanism of protective energy dissipation. *Plant Cell.* 13:1193–1204.
27. Casazza, A. P., D. Tarantino, and C. Soave. 2001. Preparation and functional characterization of thylakoids from *Arabidopsis thaliana*. *Photosynth. Res.* 68:175–180.
28. Croce, R., G. Canino, …, R. Bassi. 2002. Chromophore organization in the higher-plant photosystem II antenna protein CP26. *Biochemistry.* 41:7334–7343.
29. Schägger, H., and G. von Jagow. 1987. Tricine-sodium dodecyl sulfate-polyacrylamide gel electrophoresis for the separation of proteins in the range from 1 to 100 kDa. *Anal. Biochem.* 166:368–379.

30. Cardol, P., B. Bailleul, …, G. Finazzi. 2008. An original adaptation of photosynthesis in the marine green alga *Ostreococcus*. *Proc. Natl. Acad. Sci. USA*. 105:7881–7886.

31. Borst, J. W., M. A. Hink, …, A. J. Visser. 2005. Effects of refractive index and viscosity on fluorescence and anisotropy decays of enhanced cyan and yellow fluorescent proteins. *J. Fluoresc*. 15:153–160.

32. van Hoek, A., and A. J. W. G. Visser. 1985. Artefact and distortion sources in time correlated single photon counting. *Anal. Instrum*. 14:359–378.

33. Digris, A. V., V. V. Skakoun, …, A. J. Visser. 1999. Thermal stability of a flavoprotein assessed from associative analysis of polarized time-resolved fluorescence spectroscopy. *Eur. Biophys. J*. 28:526–531.

34. van Oort, B., A. Amunts, …, R. Croce. 2008. Picosecond fluorescence of intact and dissolved PSI-LHCI crystals. *Biophys. J*. 95:5851–5861.

35. Ihalainen, J. A., P. E. Jensen, …, J. P. Dekker. 2002. Pigment organization and energy transfer dynamics in isolated photosystem I (PSI) complexes from *Arabidopsis thaliana* depleted of the PSI-G, PSI-K, PSI-L, or PSI-N subunit. *Biophys. J*. 83:2190–2201.

36. Ihalainen, J. A., F. Klimmek, …, J. P. Dekker. 2005. Excitation energy trapping in photosystem I complexes depleted in Lhca1 and Lhca4. *FEBS Lett*. 579:4787–4791.

37. Ihalainen, J. A., I. H. M. van Stokkum, …, J. P. Dekker. 2005. Kinetics of excitation trapping in intact Photosystem I of *Chlamydomonas reinhardtii* and *Arabidopsis thaliana*. *Biochim. Biophys. Acta*. 1706: 267–275.

38. van Amerongen, H., L. Valkunas, and R. van Grondelle. 2000. Photosynthetic Excitons. World Scientific Publishing, Singapore.

39. van Oort, B., A. van Hoek, …, H. van Amerongen. 2007. Aggregation of light-harvesting complex II leads to formation of efficient excitation energy traps in monomeric and trimeric complexes. *FEBS Lett*. 581:3528–3532.

40. Sandonà, D., R. Croce, …, R. Bassi. 1998. Higher plants light harvesting proteins. Structure and function as revealed by mutation analysis of either protein or chromophore moieties. *Biochim. Biophys. Acta*. 1365:207–214.

41. Morosinotto, T., R. Bassi, …, J. Barber. 2006. Biochemical and structural analyses of a higher plant photosystem II supercomplex of a photosystem I-less mutant of barley. Consequences of a chronic over-reduction of the plastoquinone pool. *FEBS J*. 273:4616–4630.

42. Yakushevska, A. E., P. E. Jensen, …, J. P. Dekker. 2001. Supermolecular organization of photosystem II and its associated light-harvesting antenna in *Arabidopsis thaliana*. *Eur. J. Biochem*. 268:6020–6028.

43. Santini, C., V. Tidu, …, R. Bassi. 1994. Three-dimensional structure of the higher-plant photosystem II reaction centre and evidence for its dimeric organization in vivo. *Eur. J. Biochem*. 221:307–315.

44. Broess, K. 2009. Primary photosynthetic processes: from supercomplex to leaf. PhD thesis. Laboratory of Biophysics, Wageningen University, Wageningen, The Netherlands.

45. Moya, I., M. Silvestri, …, R. Bassi. 2001. Time-resolved fluorescence analysis of the photosystem II antenna proteins in detergent micelles and liposomes. *Biochemistry*. 40:12552–12561.

46. Palacios, M. A., F. L. de Weerd, …, H. van Amerongen. 2002. Superradiance and exciton (de)localization in light-harvesting complex II from green plants? *J. Phys. Chem. B*. 106:5782–5787.

47. van Oort, B., A. van Hoek, …, H. van Amerongen. 2007. Equilibrium between quenched and nonquenched conformations of the major plant light-harvesting complex studied with high-pressure time-resolved fluorescence. *J. Phys. Chem. B*. 111:7631–7637.

48. Pascal, A. A., Z. F. Liu, …, A. Ruban. 2005. Molecular basis of photoprotection and control of photosynthetic light-harvesting. *Nature*. 436:134–137.

49. Miloslavina, Y., A. Wehner, …, A. R. Holzwarth. 2008. Far-red fluorescence: a direct spectroscopic marker for LHCII oligomer formation in non-photochemical quenching. *FEBS Lett*. 582:3625–3631.

50. Caffarri, S., R. Kouril, …, R. Croce. 2009. Functional architecture of higher plant photosystem II supercomplexes. *EMBO J*. 28:3052–3063.

## Supplementary material

This Supplementary material contains five sections: (i) details about the experimental conditions, (ii) fluorescence emission spectra, (iii) derivation of $\tau_{trap} = N_{eff}[\tau_{CS} + \tau_{RP}\exp(-\Delta G/kT)]$ and (iv) calculation of the decay associated spectra (DAS), and (v) a schematic overview of the macrostructure of the thylakoid membrane.

### (i) Experimental conditions

The sample was kept at 287 K in a flow cuvette and a sample reservoir (25-50 ml). The sample was flowing from the reservoir to the cuvette and back, with a flow speed of ~150 ml/min. The optical path length of the cuvette was 3 mm, the OD at the excitation wavelength was ~0.2/cm, and the size of the excitation spot was 2 mm. The excitation power was 0.5-4 µW. In this way each laser pulse excites 1 out of ~$5*10^7$ to $4*10^8$ Chls. In the time (~7 ms) to travel through the excitation spot ~$3*10^4$ pulses hit the sample, exciting 1 out of ~$2*10^3$ to $1.6*10^4$ pigments. Supposing equal excitation of PSI and PSII, and a PSII antenna size of ~200 pigments/RC, it follows that while passing through the excitation beam, pigments associated to ~0.6 to 5% of the RCs are excited. After passing through the beam, it takes ~10-20 s until the next passage. Experiments using higher or lower excitation power indicated that under the experimental conditions almost all RCs remain open. Figure S1 shows the WT fluorescence kinetics excited at 475 nm, and detected above 645 nm, at different excitation powers. The final experiment of a measuring series was always a repeat of the first experiment. The resulting decay curves were indistinguishable. Each sample was measured 2-5 times.

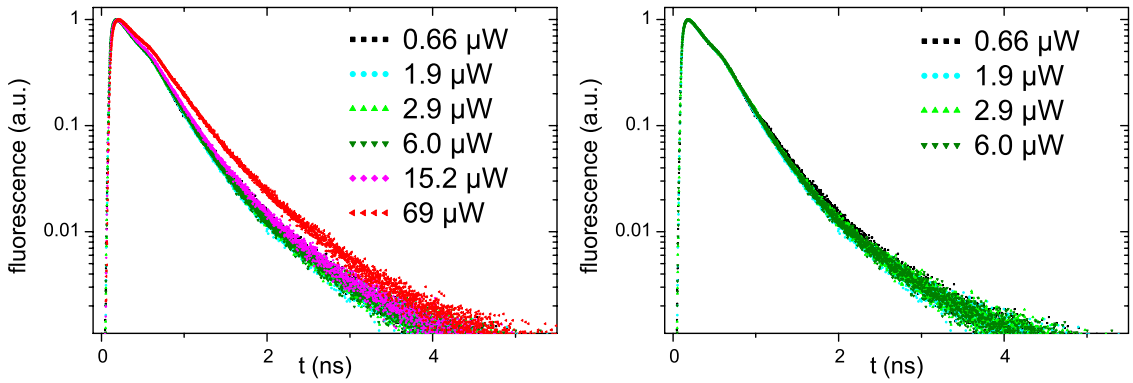


Figure S1. Fluorescence kinetics of thylakoid membranes of WT *Arabidopsis thaliana*, excited at 475 nm, and detected above 645 nm, at different excitation powers. The right figure shows the curves measured around the power range (0.5-4µW) used for the experiments described in the main text.

**(ii) Fluorescence emission spectra**

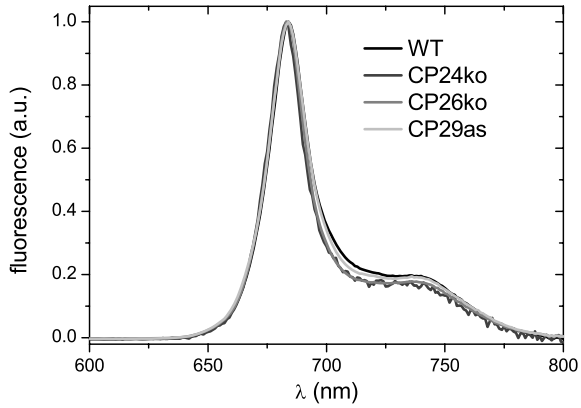


Figure S2. Room temperature fluorescence emission spectra of thylakoid membranes from WT and mutants of *A. thaliana*. The excitation wavelength is 412 nm.

**(iii) Derivation of** $\tau_{trap} = N_{eff}[\tau_{CS} + \tau_{RP}\exp(-\Delta G/kT)]$

Derivation of this equation: The system of linear kinetic equations for the antenna complex excitation probabilities (as presented in the Appendix of (1)) is mapped by Laplace transformation into a system of algebraic equations that can easily be solved. For the zero Laplace variable this system reduces into an algebraic system for the vector of partial lifetimes corresponding to the complexes of the coarse-grained model of PSII. The sum of the vector components gives the analytical expression for the average fluorescence lifetime depending on the model parameters like the hopping, CS and radical pair relaxation times as well as the free energy gap. Taking the zero hopping time limit we arrive at the trapping time expression.

**(iv) Calculation of decay associated spectra**

The calculations above require decay associated spectra (DAS). DAS are calculated from the steady-state spectra and the time-resolved experiments as follows: The relative amplitudes ($p_i^{\lambda}$) at detection wavelengths λ were scaled with factor $\alpha^{\lambda}$, such that for each detection wavelength, the area under the theoretical fluorescence decay curve equals the intensity of the steady-state spectrum at that wavelength (F(λ)): $F(\lambda) = \alpha^{\lambda}\int_0^{\infty}\sum_{i=1}^{3} p_i * e^{-t/\tau_i} = \alpha^{\lambda}\sum_{i=1}^{3} p_i^{\lambda} * \tau_i^{\lambda}$.

The resulting values $\alpha^{\lambda} * p_i^{\lambda}$ are the values of the DAS of decay component i at detection wavelength λ. F(λ) was calculated from the convolution of the steady-stated fluorescence emission spectrum and the transmission spectrum of the interference filters (measured on a Cary 5E UV-Vis-NIR spectrophotometer).

The longest fluorescence lifetime (> 1.7 ns, with very small amplitude, ≤1%) probably originated from free Chl, from closed RCs of PSII, or from antennae that are disconnected from the RCs. These are not the topic of interest, so the fit results were rescaled omitting this component.

**(v) Macrostructure of the thylakoid membrane**

The main components of the thylakoid membrane and their relative positions are schematically drawn in Figure S3. PSII and LHCII are present mainly in the stacked regions of the membranes, whereas PSI is mainly present in the unstacked regions and on the topmembranes of the granum stacks. Other complexes are cytochrome $b_6f$ and ATP synthase.

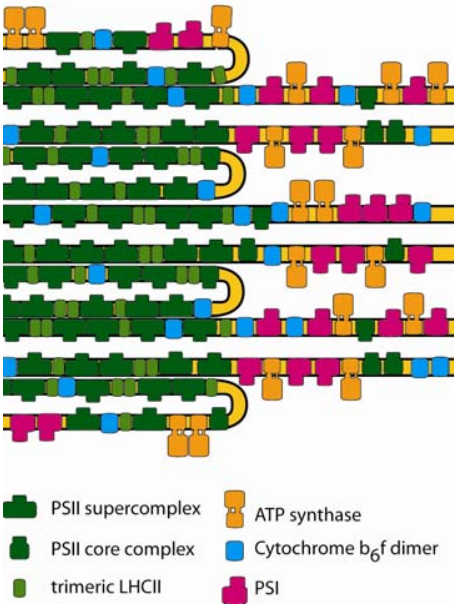


Figure S3 Schematic overview of the macrostructure of the thylakoid membrane, based on refs (2, 3).

**References**

1. Broess, K., G. Trinkunas, C. D. van der Weij-de Wit, J. P. Dekker, A. van Hoek, and H. van Amerongen. 2006. Excitation energy transfer and charge separation in photosystem II membranes revisited. Biophys. J. 91:3776-3786.
2. Allen, J. F., and J. Forsberg. 2001. Molecular recognition in thylakoid structure and function. Trends Plant Sci. 6:317-326.
3. Dekker, J. P., and E. J. Boekema. 2005. Supramolecular organization of thylakoid membrane proteins in green plants. Biochim. Biophys. Acta 1706:12-39.

# Section D

# A mutant without monomeric antenna proteins: towards a solution of the differential role of monomeric Lhcb proteins vs major LHCII in Non Photochemical Quenching.

## D.1 A mutant without monomeric antenna proteins: towards a solution of the differential role of monomeric Lhcb proteins vs major LHCII in Non Photochemical Quenching.

### D.1.1 Introduction

The dissipation of excess absorbed light energy as heat (NPQ) in PSII is an essential mechanism of photosynthesis, activated very rapidly upon illumination (Muller et al., 2001), which protects plants from severe photodamage under variable light conditions (Barber and Andersson, 1992; Demmig-Adams and Adams, 1992; Frank et al., 2000).
According to present understanding the major part of the energy quenching (qE) is strictly dependent on the presence of the PsbS protein, an integral PSII membrane protein, member of the Lhc-protein superfamily (Li et al., 2000), on a synergistic action of the lumen pH, xanthophyll conversion, binding activation (Demmig-Adams, 1990; Niyogi et al., 1998) and conformational changes in the antenna of PSII that have been proposed to control the efficient quenching of chlorophyll excited state ($^1Chl^*$) states (Horton and Ruban, 2005; Horton et al., 2008). The decrease in lumenal pH induces

the activation of the violaxanthin de-epoxidase enzyme (VDE) with zeaxanthin (Zea) production and accumulation into the thylakoids, correlated to NPQ amplitude for a wide variety of plants (Demmig-Adams and Adams, 1994; Niyogi et al., 1998). The key role of the PsbS protein has been assigned to two protonatable and lumen-exposed amino acids, enabling PsbS to act as sensor of the pH in the thylakoid lumen (Li et al., 2004). Recently PsbS was also suggested to modulate the interaction between PSII and LHCII, controlling PSII organization (Kiss et al., 2008; Betterle et al., 2009).
The molecular mechanism of NPQ is only partially elucidated. Although several components with an important role in the mechanism have been identified, still the identity of the quencher is the object of an intense debate. Such a protein should bind lutein and Zea or, at least, should interact tightly with a xanthophyll-binding protein, thus providing a quenching effect. Early works proposed that PsbS might bind both Chls and xanthophylls (Funk et al., 1995) or Zea alone (Aspinall-O'Dea et al., 2002), making it a candidate for the role of quencher. Nevertheless, further works pointed to the non-conservation of Chl-binding residues in PsbS (Dominici et al., 2002), while its properties both *in vivo* and *in vitro* were not consistent with binding of xanthophylls (Bonente et al., 2008). Once PsbS is ruled out as a quencher, Lhcb proteins appear to be ideal candidates for the role of quenching sites owing to their capacity to bind both Chls (the species to be quenched during NPQ) and xanthophylls, a class of molecules that are well known as good quenchers, owing to the short lifetime of their S1 excited state. One xanthophyll species has been shown to be important for quenching, and is Zea while another, lutein, has also an important role. Upon violaxanthin de-epoxidation, the newly synthesized Zea is distributed among LHCII and monomeric complexes: Zea is known to cause a conformational change able to switch Lhcs into a state with efficient thermal dissipation (Dall'Osto et al., 2005; Gilmore et al., 1995; Moya et al., 2001; Formaggio et al., 2001). A long standing discussion has been developed on whether the quenching site is located within the monomeric antenna proteins (Bassi et al., 1993; Avenson et al., 2008; Ahn et al., 2008) or in the major, trimeric, antenna complexes, called LHCII (Horton and Ruban, 2005; Pascal et al., 2005; Ruban et al., 2007). It has been proposed that quenching in Lhcb monomers is caused by charge transfer (CT) involving Zx to Chl (Holt et al., 2005; Ahn et al., 2008). Alternative mechanism being energy transfer from Chl to lutein (Ruban et al., 2007) or by formation of a Chl-Chl charge transfer state (Miloslavina et al., 2008). It is common to all models that pH- and PsbS-dependent rearrangements in the antenna structure and/or conformation of antenna proteins essentially control qE and that Zea is either directly or indirectly involved in the generation of total NPQ quenching. All these factors, combined with a reorganization of the PSII supercomplexes

may cause a conformational change able to switch Lhcs into a quenching state for $^1Chl^*$ de-excitation.
The role of individual light harvesting complexes (Lhcs) has been investigated using reverse genetics. Down regulation of Lhcb1+2 and knock-out for Lhcb3 did not significantly decrease NPQ amplitude or slow down its kinetic despite these gene products account for most of the antenna size of PSII (Andersson et al., 2003; Damkjaer et al., 2009). Targeting monomeric Lhcbs yielded into different results: Lhcb5 knock out plants retained qE (Andersson et al., 2001; de Bianchi et al., 2008) while the qI component (inhibitory quenching) of NPQ was down-regulated (Dall'Osto et al., 2005). qE was affected in Lhcb6 and Lhcb4 knock out plants (Betterle et al., 2009; de Bianchi et al., 2008; Andersson et al., 2001; Kovacs et al., 2006). In summary, although showing an NPQ phenotype, depletion of a single monomeric Lhcb gene products could not completely abolish NPQ, implying redundancy within the sub-family members (Avenson et al., 2008). The making of a mutant without all the three monomeric Lhcb4-6 would allow verifying if monomeric Lhcbs have the exclusive capacity for qE quenching. Alternatively, this function could be located in the major LHCII or be a common property of all Lhcs irrespective from their aggregation state. In this work, we attempted isolation of a mutant ko for all the monomeric Lhcbs. Lhcb5 (CP26) and Lhcb6 (CP24) are encoded by a single gene while three isoforms of Lhcb4 (CP29) are present in the *Arabidopsis* genome. Thus we looked for a five-gene mutant. This genotype would be useful in order to verify or falsify the hypothesis that the quenching site(s) is located within one of the monomeric Lhcb proteins.

### D.1.2 Materials and Methods

#### Plant material and growth conditions

*Arabidopsis thaliana* T-DNA insertion mutants (*Columbia* ecotype), GK Line ID282A07 with insertion in the At5g01530 locus (*lhcb4.1*), SAIL_910_D12 with insertion in the At3g08940 locus (*lhcb4.2*), SALK_032779 with insertion in the At2g40100 locus (*lhcb4.3*), SALK_077953 with insertion in the At1G15820 locus (*lhcb6*) and SALK_014869 with insertion in the At4G10340 locus (*lhcb5*), were obtained from NASC collections (Alonso et al., 2003) and were previously selected (de Bianchi et al., 2008; Dall'Osto et al., 2006, Section A.2). GK Line ID282A07 plants (*lhcb4.1* gene) were genotyped by PCR using the following primers: 5'-TCACCAGATAACGCAGAGTTTAATAG-3' and
5'-CACATGATAATGATTTTAAGATGAGGAG-3', giving rise to a
1378 bp fragment, and for the knockout allele the primers
5'-TCACCAGATAACGCAGAGTTTAATAG-3' and

5'CCATATTGACCATCATACTCATTGC-3', yielding a 700 bp fragment. The wild type allele of *lhcb4.2* (line SAIL_910_D12), was amplified with the following PCR primers 5'-GCGTTTGTGTTTAGCGTTTCGACATCTGTCTG-3' and 5'-GGTACCCGGGTGGTTTCCGACATTAGC-3', giving rise to a 520 bp fragment, and for the knockout allele of this line, the primers 5'-GCGTTTGTGTTTAGCGTTTCGACATCTGTCTG-3' and 5'-GCCTTTTCAGAAATGGATAAATAGCCTTGCTTCC-3' were used, yielding a 660 bp fragment. For the genotyping of SALK_032779 line the wild type allele of *lhcb4.3*, the sequences 5'-GTGAGCTGATCCATGGAAGGTGG-3' and 5'-GGCCGGTTTTGAACGATTGATGTGAC-3', amplified a 1050 bp fragment, and for the knockout allele, the amplification of a 770 bp fragment was performed with the primers 5'-GTGAGCTGATCCATGGAAGGTGG-3' and 5'-GCGTGGACCGCTTGCTGCAACT-3'. For the genetic characterization of the *lhcb5* locus (SALK_014869 line) were used the following primers: 5'-GGATTCTGTGCTTAAGGTTTATTGGTCTG-3', 5'-GGTGTAGCTTGTCCTCGAAATCCTACC-3' and LBb1 primer (GCGTGGACCGCTTGCTGCAACT) while for the *lhcb6* locus 5'-CTCATGGCGATGGCGGTCTCC-3', 5'-GCCTCGAGTGCTTAATCTCTGCC-3' and Ds3-4 primer (5'-CCGTCCCGCAAGTTAAATATG-3') were used. Genomic DNA was extracted according to Edwards et al., 1991. Mutants were grown for 4 to 6 weeks at 100 $\mu$mol photons $m^{-2}s^{-1}$, 21°C, 90% humidity, and 8 h of daylight.

## Plant's breeding procedure

For flowers of female parent the major considerations are that they should not be self-fertilized, although the stigma should be mature; this is usually achieved by choosing a flower in which the sepals are still closed, and a stigma is protruding from the end of the flower. Any siliques, open flowers, or open buds were removed and from the chosen flower sepals, petals and expose the anthers, were stripped away, carefully under magnification, leaving the pistil. Four flowers on the same inflorescence can be emasculated and crossed. The whole flowers of the male parent full-blown, and with visible pollen on the anthers were remove with forceps and the stigma of the emasculated female flower was dabbed with the whole male flower.
After about four days, it should be possible to see the stigma lengthening and swelling, which indicates that the cross was successful. Seeds were collected with forceps when siliques and stems turn yellow.

### Video imaging: *in vivo* fluorescence and NPQ measurements.

For the video imaging analysis on detached leaves we used a fluorometer equipped with a peltier-cooled charge-coupled device (CCD) camera, as described earlier (Oxborough and Baker, 1997).
Minimum fluorescence ($F_0$) was measured with a 0.15 $\mu$mol photons $m^{-2}s^{-1}$ beam, maximum fluorescence ($F_m$) was determined with a 0.8 s light pulse (4500 $\mu$mol photons $m^{-2}s^{-1}$), and white continuous light (1200 $\mu$mol photons $m^{-2}s^{-1}$) was supplied to induce the quenching.
The $F_v/F_m$ parameter was used as a measure of the maximal efficiency of PSII photochemistry (Kitajima and Butler, 1975) and NPQ was calculated according to the equation (Van Kooten and Snel, 1990) NPQ=($F_m$-$F_m$')/$F_m$', where $F_0$ is the fluorescence determined in darkness by a weak measuring beam, $F_m$ is the maximum chlorophyll fluorescence from dark-adapted leaves measured after the application of a saturating flash, $F_v$ is the difference between $F_m$ and the initial fluorescence level $F_0$ and $F_m$' the maximum chlorophyll fluorescence under actinic light exposure.

### DNA constructs

The *lhcb5* coding sequence (NM_117102) was amplified by polymerase chain reaction (PCR) using gene-specific primer with restriction site at the ends, giving rise to a sequence with a SpeI site at the 5'-end and an XhoI site at the 3'-end of the gene. This fragment was TA-cloned into pGEM-T-easy and sequenced. The binary transformation plasmid pER8 containing the two-component estrogen system (Zuo and Chua, 2000) was digested with XhoI and SpeI (Fermentas). The Lhcb5 coding sequence was thus isolates from pGEM-Lhcb5 following digestion with the same enzymes and cloned into the pER8 in an antisense orientation, giving rise to pER8-AsLhcb5.

### *Arabidopsis* transformation

Adult *Arabidopsis* plants were transformed by floral dipping with a solution containing *Agrobacterium tumefaciens* carrying the pER8-AsLhcb5 construct. The method was performed in according to Zhang et al., 2006 protocol. Transformed seeds were selected on Murashige and Skoog (1962) plates containing 25 $\mu$g/mL hygromycin. Hygromycin-resistant plants were collected and allowed to self-pollinate to get the T2 generation that was used for the experiments.
To test the estrogen induction we plates T2 transformed plants on agar medium with the addition of 5$\mu$M 17-$\beta$-estradiol (Sigma).

### Thylakoid Isolation, gel Electrophoresis and Immunoblotting

Unstacked thylakoids were isolated from leaves as previously described (Bassi et al., 1988).
SDS-PAGE analysis was performed with the Tris-Tricine buffer system as described in Schägger and von Jagow, 1987. For immunotitration, thylakoid samples corresponding to 15 $\mu$g of chlorophyll were loaded for each sample and electroblotted on nitrocellulose membranes. Filters were incubated with antibodies raised against the protein of interest and were detected with alkaline phosphatase-conjugated antibody, according to Towbin et al., 1979.

## D.1.3 Results

### First crossing and screening strategy for the isolation of the mutant without monomeric antenna proteins.

Two genotypes previously selected were the starting point for the crossing strategy: koCP24/26 mutant with the two *lhcb5* and *lhcb6* genes knocked out (ko) on both alleles (de Bianchi et al., 2008) and the triple koCP29 mutant (Section A.2) with all the three *lhcb4* genes carrying insertions, also in both alleles. The F1 progeny originated from this cross (koLhcb5/Lhcb6 x koLhcb4.1/Lhcb4.2/Lhcb4.3) is heterozygous at each of the five loci. We confirmed this genetic condition by performing PCR amplification of the five loci; the result is reported in Figure D.1.

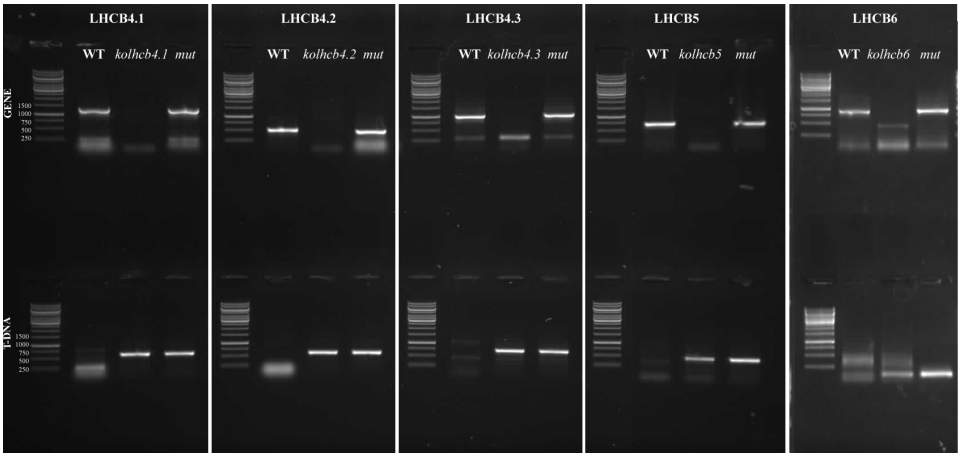


**Figure D.1:** *Genetic condition of the heterozygous plant at the five monomeric Lhcb loci. Amplification of lhcb4.1, lhcb4.2, lhcb4.3, lhcb5, lhcb6 loci with allele specific primer PCR. At the top, the amplification using gene specific primer: 1378 bp, 520 bp, 1046 bp, 591 bp, 918 bp for the amplification respectively of lhcb4.1, lhcb4.2, lhcb4.3, lhcb5 and lhcb6 locus. At the bottom amplification using a gene specific primer and the T-DNA specific primer: 697 bp, 661 bp, 773 bp, 546 bp, 197 bp for the amplification respectively of lhcb4.1, lhcb4.2, lhcb4.3 lhcb5 and lhcb6 knocked out loci. Details of primer sequence are reported in materials and methods.*

F2 seeds derived from self-pollination of F1 plants were sown on soil and grown in control conditions (100 $\mu$mol photons $m^{-2}s^{-1}$, 21°C). The fre-

quency of the five-loci homozygous ko genotype is 1/1024 (Figure D.5). For this reason we grew initially more than two thousand plants to be screened. The probability of finding the "only" plant with homozygous ko at the five genes is very low but this step allows for a first "enrichment" of the desired alleles. A pre-screening of the population in order to reduce the biochemical analysis to a restricted number of plants was performed by imaging pulse-fluorometry. From the analysis of single, double, triple monomeric antenna mutants we identified some fluorescence parameters correlated with the lack of antenna subunits (de Bianchi et al., 2008; Andersson et al., 2003; Kovacs et al., 2006), in particular, we expect higher $F_0$ and slower NPQ rise kinetic with respect to WT. The amplitude of $F_0$ is inversely related to the efficiency of energy transfer from antenna pigments to open PSII reaction centers. In different koLhcbs the increase in $F_0$ so far obtained was distinct depending on genotype. However this feature was present in all cases implying that a larger fraction of absorbed energy is lost as fluorescence and, thus, that the connection between the major LHCII complex and the PSII reaction center (RC) is less efficient in the absence of monomeric antenna proteins. Consistently, the $F_v/F_m$ value is lower. The increase in $F_0$, although significant, is rather small in koCP26 mutants. Instead, it is larger in koCP24, koCP29 and in the double mutant koCP24/26. Thus, we expect that a mutant without the three antenna proteins should have a higher $F_0$ and a smaller $F_v/F_m$ ratio with respect to WT. A second parameter affected in Lhcb mutants is NPQ. The correlation between the absence of antenna subunit and the amplitude of is not as strict as for $F_0$: NPQ of koCP26 is similar to WT while koCP24 has NPQ reduced by 50%, koCP29 is reduced by 30% and the kinetic of rise is slower (de Bianchi et al., 2008; Betterle et al., 2009 Section A.2). On these basis we expect a five-fold mutant with a strong reduction of the capacity for energy dissipation and with a strongly increased $F_0$.

We proceeded with the recording of the fluorescence emitted by dark-adapted detached leaves of F2 population using a video imager equipped with a CCD camera (Figure D.2) while WT and koCP24 were included as reference genotypes. $F_0$ was detected; then samples were illuminated with strong actinic light (4000 $\mu$mol photons $m^{-2}s^{-1}$) for 0,8 seconds, which close all the RCs, in order to determined $F_m$ and thus $F_v/F_m$ value. With this last parameter we can be sure that plant analyzed are healthy and well dark-adapted (for a healthy leaf, $F_v/F_m$ is around 0.78-0.8). Leaves were then illuminated with actinic light (1200 $\mu$mol photons $m^{-2}s^{-1}$) for 5 minutes in order to obtain the NPQ value. By choosing such a short time of illumination we can also distinguish mutants with a slower NPQ kinetic as koCP24/26 and koCP29, a property that might be shared by the five-fold mutant.

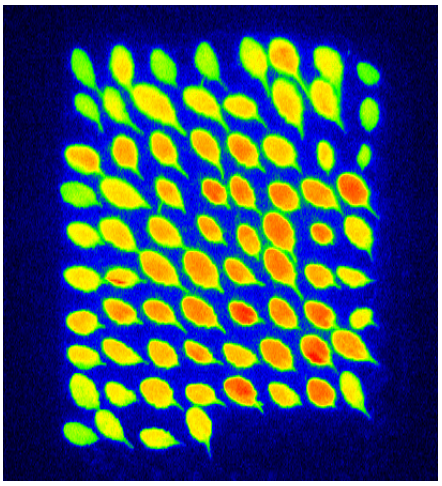

**Figure D.2:** *Fluorescence video imaging of the F2 population from the cross koLhcb5/Lhcb6 x koLhcb4.1/Lhcb4.2/Lhcb4.3. Chl fluorescence of detached leaves was measured during continuous illumination (1200 µmol photons $m^{-2}s^{-1}$) with a chlorophyll fluorescence monitoring system (FluorCam 700MF, Photon Systems Instruments, Brno, Czech Republic). We captured chlorophyll fluorescence images at the end of illumination (5 min) with a CCD camera.*

We analyzed 2748 plants of the F2 population and we selected 576 plants with a higher $F_0$ and a low NPQ value. In a second step, we analyzed the composition in antenna proteins of the selected 576 samples, resolving total proteins by SDS-PAGE separation. From the denaturating gels stained with Coomassie, the presence of the monomeric antenna proteins was quite simply detected, as shown in Figure D.3A, allowing a first, tentative, attribution of the mutant genotype. In order to simplify the screening and to restrict the number of samples we decided to select for the further characterization plants lacking CP26, whose Coomassie-stained band is sharp and simpler to recognize. We found 216 plants putatively koLhcb5 that we further analyzed by western blotting using specific antibody against CP24, CP26 and CP29 subunits (Figure D.3B). The results of the immunological detection are the following:

**Table I:** *Results of the immunological revelation with monomeric subunits' specific antibodies. The frequency of the detected and the expected genotype is reported*

| Phenotype | WT | KoCP26 | KoCP24 | KoCP29 | KoCP24/26 | KoCP29/24 | KoCP29/26 | KoCP24/26/29 |
|---|---|---|---|---|---|---|---|---|
| N° of plants detected | 3 | 121 | 5 | 0 | 85 | 2 | 0 | 0 |
| N° of plants expected | 0 | 159.5 | 0 | 0 | 53.1 | 0 | 2.5 | 0.9 |
| | | (189/256) | | | (63/256) | | (3/256) | (1/256) |

Some plants (ten) were not correctly selected in the previous SDS-PAGE screening for the lack of CP26 and are instead WT (three), koCP24 (five) or koCP29/24 (two) plants. We found more double mutant koCP24/26 and less single koCP26 mutant than expected because of the pre-screening by imaging pulse-fluorometry that preferentially selected plants with a higher $F_0$ and lower NPQ value. As reported in Section A.2 the CP24 protein, disappears for pleiotropic effect in plants without CP29 (CP29 is the binding

site for CP24) and for this reason we did not found plants lacking CP29 only but we found two putative koCP29/24. The definition of "putative" is, thus, due to the fact that the real genotype of plants lacking the CP24 protein can be assessed only by PCR analysis. What was surprising, also if expected with low frequency, was the completely absence of two genotypes: the four-site mutant koLhcb5/Lhcb4.1/4.2/4.3 (koCP29/26), and the five-site mutant koLhcb5/Lhcb4.1/4.2/4.3/Lhcb6 (koCP24/26/29). In the F2 population of the starting cross (koLhcb5/koLhcb6 x koLhcb4.1/Lhcb4.2/Lhcb4.3) the first four-sites mutant phenotype (koCP29/26) was expected with a frequency of 3/1024 (considering both homozygous WT and heterozygous Lhcb6 locus), while the five-site mutant (koCP24/26/29) is expected as 1/1024, thus respectively 8 plants of the quadruple mutant and 2-3 (2,5) plants of the five fold mutant, that we didn't find.

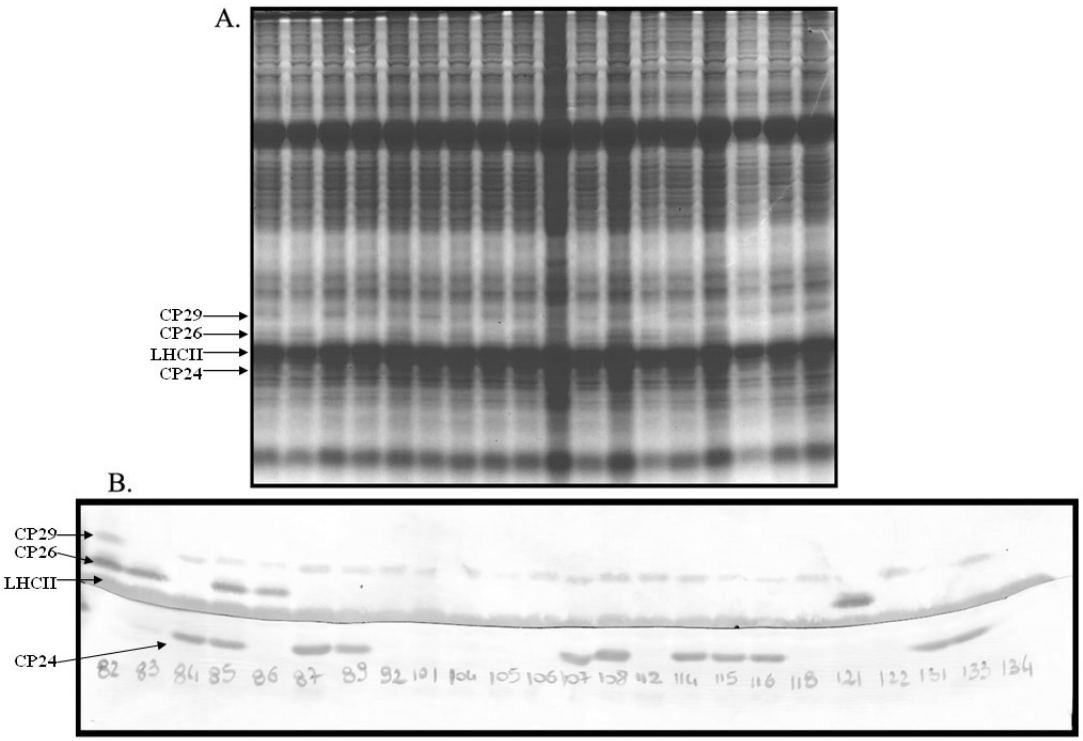


**Figure D.3:** *Minor antenna protein composition of F2 plants. Plants pre-selected by fluorescence video-imaging screening, are later analyzed for their antenna proteins content. A) Total proteins SDS/PAGE analysis with the Tris-Tricine buffer system of selected plants. Apoprotein bands are marked. B) Immunoblot analysis of thylakoid membranes with an antibody directed against Lhcb subunits that recognize minor antenna proteins CP26, CP29, CP24 and the LHCII complex.*

## Second crossing and screening strategy for the isolation of the mutant without monomeric antenna proteins

Based on the unsuccessful results of the above describe strategy, we used an alternative screening strategy starting with the identification of plants

knocked out for CP24 and CP29 genes, and with a *lhcb5* heterozygous locus (CP26 protein) (Figure D.5). We will henceforth refer to this genotype as QHet (quadruple koCP29/24 mutant heterozygous at *lhcb5* locus). In the F2 population of the cross koLhcb5/koLhcb6 x koLhcb4.1/Lhcb4.2/Lhcb4.3 we identified plant koCP29/24 that we tested for the *lhcb5* locus condition. We found plant with heterozygous at the *lhcb5* locus as confirmed with gene-specific PCR (Figure D.4). Upon the self-pollination of this genotype, we expected the segregation of the *lhcb5* alleles giving a population in which $\frac{1}{2}$ will be heterozygous, $\frac{1}{4}$ homozygous WT and $\frac{1}{4}$ homozygous ko at the *lhcb5* locus (Table II). Thus $\frac{1}{4}$ of the population should be constituted by the genotype we were looking for, lacking all the three subunits, CP24, CP26 and CP29 (Figure D.5). We analyzed by immunoblotting the protein composition of plants population derived from the self-pollination of QHet: among 105 plants, all koCP29/24, we expected 26, but instead none lacked the CP26 protein. When we checked the *lhcb5* locus of some of these plants, we noticed that only two genotypes were found: WT/WT and WT/kolhcb5 (heterozygous). Moreover the number of heterozygous plants are lower than expected (Table II).

This is an indication about a probable weaker heterozygous condition. A variant of this experiment was performed by concentrating on Lhcb4 and Lhcb5, disregarding Lhcb6. The starting genotype was homozygous ko at genes Lhcb4.1, Lhcb4.2 and Lhcb4.3 (koCP29) while heterozygous at the *lhcb5* locus (WT for CP24, *lhcb6* locus). The results obtained by selfing these genotypes were essentially the same as reported above: no progeny lacking both CP29 and CP26 (koCP29/26 plants) were detected by western blotting. Thus, it seems not possible to knock out at the same time genes encoding CP26 and CP29 subunits. Instead, koCP24/26 and koCP29/24 can be obtained with the expected frequency.

**Table II:** *The cross table of expected genotype form the selfing of genotypes with an heterozygous condition at the Lhcb5 locus (Aa). On the left the segregation of gametes. On the right the results of the lhcb5 locus amplification: the frequency of the detected and expected genotypes is reported.*

| Gametes | A | a |
|---|---|---|
| A | AA | Aa |
| a | aA | aa |

| | Homo WT lhcb5 | Heter lhcb5 | Homo ko lhcb5 |
|---|---|---|---|
| | AA | Aa-aA | aa |
| N° plants detected | 63 | 42 | 0 |
| N° plants expected | 26.25 | 52.5 | 26.25 |

## Seeds and siliques analysis.

It is clear that when a genotype homozygous ko for all the three Lhcb4 loci (CP29) and Lhcb6 (CP24) and heterozygous at site Lhcb5 (QHet) undergoes self-pollination, the homozygous koCP24/26/29 (koLhcb4.1/4.2/4.3/Lhcb6/Lhcb5) combination has to be present whit a frequency of $\frac{1}{4}$ in the first steps of zy-

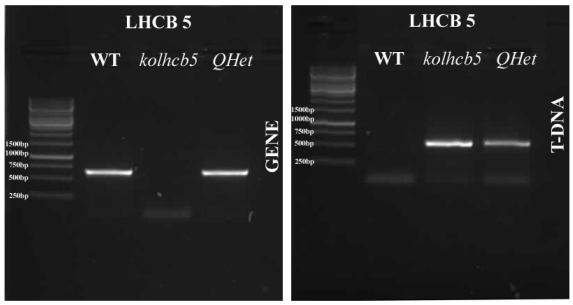


**Figure D.4:** *Amplification of the lhcb5 locus' of koCP29/24 plants with allele specific primer PCR.*
*At the top the amplification using gene specific primer, at the bottom amplification using a gene specific primer and the T-DNA specific primer.*

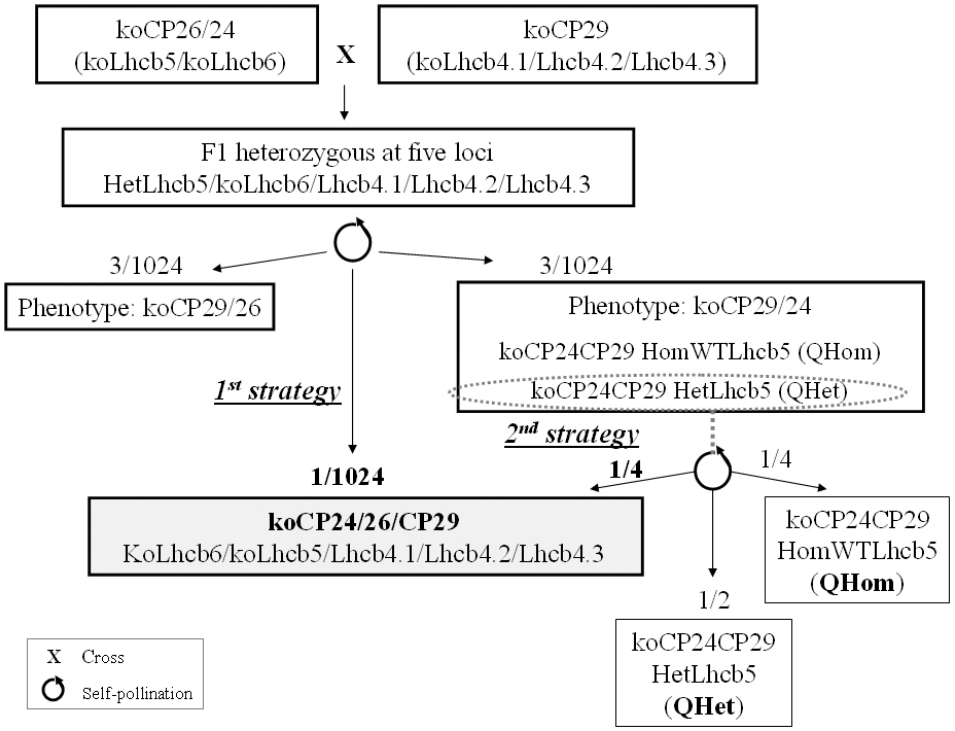


**Figure D.5:** *Schematic diagram of the crossing strategy. In the first strategy we screened the F2 population of the cross koLhcb5/koLhcb6 x koLhcb4.1/Lhcb4.2/Lhcb4.3. The five-site mutant koCP24/26/29 was expected with a frequency of 1/1024. In the second strategy we looked at the population derived from the self-pollination of the QHet; in this case the koCP24/26/29 was expected as a quarter of the population.*

gote formation. Since this is not the case, there should be a limiting step during the stages of development following zygote formation. In order to verify the occurrence of problems in seed germination, we plated mutant and WT seeds on agar plates, in the presence of sucrose. The agar plates simplify seeds counting and the presence of hexogen carbon source could support the initial phase of grow in the case of a weak growing phenotype due to mutations. We counted WT and mutant's seeds and we found the same percentage of germination (about 98-99%) for both populations: there are no problems in the vitality of mature seed.
How can the absence of the five-fold mutant be explained? We looked at the previous phases: flowering time, embryo development and seeds formation into the siliques, comparing WT, koCP29/24 (namely QHom - quadruple ko mutant homozygous WT at *lhcb5* locus; homozygous ko at sites *lhcb4.1/4.2/4.3*, *lhcb6* and homozygous WT at site *lhcb5*) and QHet (homozygous ko at sites *lhcb4.1/4.2/4.3*, *lhcb6* and heterozygous at site *lhcb5*) grown on soil in control condition (100 $\mu$mol photons $m^{-2}s^{-1}$). We observed that QHet showed some difficult in flowering: in the first phases after the appearance of inflorescences, buds didn't developed appropriately and there were no flowers. Only at later stage some buds gave rise to flowers (and to siliques), but very late respect to control genotype. At first sight the siliques of QHet are pale-green and shorter than those in QHom and WT (about 14 mm in QHom and WT, 9 mm in QHet) (Figure D.6). Upon dissection, we observed seeds: WT and QHom siliques had two long rows of green seeds with only few white seeds, less than 1%. In QHet siliques some seeds developed normally and were green and swollen while others remained small, transparent or brownish and shriveled, a phenotype typical for aborted embryos (http://www.seedgenes.org). The aborted seeds in the mutant were randomly distributed along the siliques, and were a little more than 25%; instead the total number of possible seeds per silique (normal seeds plus aborted seeds) was lower in QHet respect to QHom (and WT) (Table III).

**Table III:** *Statistic of normal and aborted seeds in silique of QHom and QHet.*

| Genotype | Silique Examined | Normal Seeds | Aborted Seeds | Total Seeds |
|---|---|---|---|---|
| **QHom** | 6 | 2376 | 15 | 2391 |
| **QHet** | 6 | 1638 | 447 | 2085 |

From these observations it appears that QHet genotype has some problems in flowering and in silique formation. The presence of aborted seeds suggests the presence of a lethal-embryo mutation. The aborted seeds were instead in a number higher than expected. It is difficult to explain why these embryos die, especially because the genes knocked down encodes chloroplast

antenna subunits, not involved in flowers or seeds formation. A possible explanation for this unexpected result could be a higher sensibility of the mutants in normal light condition that could lead to ROS generation, reactive species able to damage embryo structure and development (Cairns et al., 2006). This could be also the reason for the more stressed phenotype of the mutant inflorescence, with a late flowers formation, shorter and pale-green siliques and a lower amount of total seed.

In order to verify if the reason for the putative oxidative stress is the excess light intensity, we repeated the same observations on flower, siliques length/color and seeds formation, on plants grown at lower light intensity (25 $\mu$mol photons $m^{-2}s^{-1}$) but no improvements were observed in the phenotype, on the contrary, plants had more difficulties in flower development due to the low light intensity (Kim et al., 2008; Wollenberg et al., 2008). We also tried to shade the inflorescence using a neutral filter that cut by five times light intensity while leaves were left at normal light. However, it was not possible to rescue the flower/seed developmental defects by this method.

What is the meaning of this lethal phenotype? The unexpected genetic evidence shows that, for a correct and functional organization of the PSII supercomplexes, at least one of the two monomeric antenna subunits CP26 or CP29 needs to be present. Probably these two proteins can replace each other but none of the other monomeric antenna are able to takes their place in PSII $C_2S_2$ particles.

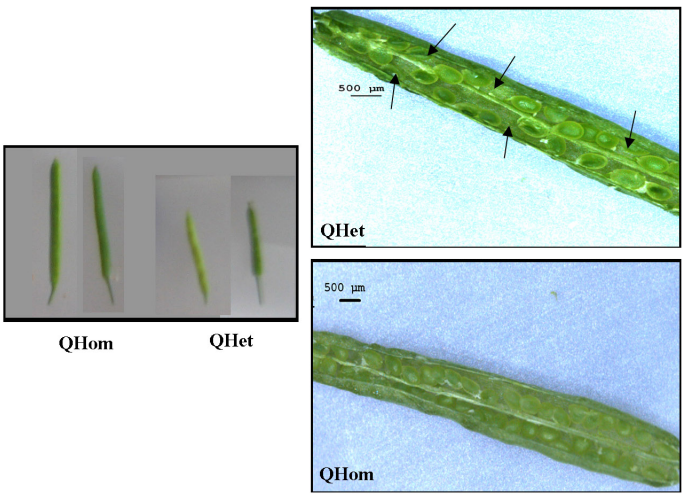


**Figure D.6:** *Siliques and seeds of QHom and QHet.*

## Composition of the minimal content in monomeric antenna proteins of PSII supercomplex.

Once accepted the (experimental) impossibility of obtaining a five gene homozygous mutant, we tried to determine the minimal unit that has to be expressed in order to assemble a functional PSII. Three different isoforms encode the CP29 protein (*lhcb4.1*, *lhcb4.2* and *lhcb4.3* genes) (Jansson, 1999) and only one for the CP26 subunit. We tried to understand if the minimal PSII monomeric antenna unit needs, in the absence of CP26, a specific CP29 isoform or if all the three isoforms can functionally replace CP26. This is interesting because the three *lhcb4* genes are expressed at different levels: the first two isoform (*lhcb4.1* and *lhcb4.2)* are found in equimolar amounts in the thylakoid and their expression levels are similar while the third isoform (*lhcb4.3*) is 20 times less expressed in control condition (Jansson, 1999) and no polypeptide of this isoform was detected so far (Section A.2).
Moreover, from our results (Section A.2) it seems that there are sites in PSII supercomplex specific for the first isoform; in fact in PSII of mutants where *lhcb4.1* is knocked out and thus Lhcb4.1 subunits is not present, the Lhcb4.2 cannot replace the empty site left by Lhcb4.1. In order to answer this question, we looked at the F2 population derived from the self-pollination of the mutant heterozygous at all the five loci (also analyzed above). We tested by gene specific PCR, the condition of the *lhcb4* loci in the 85 plants having phenotype koCP24/26 from immuno-blotting (Table I). We found plants with the following Lhcb4 composition: (a) only Lhcb4.1; (b) Lhcb4.1 + Lhcb4.2; (c) Lhcb4.1+ Lhcb4.3. Thus, all plants expressed the isoform Lhcb4.1 while we didn't find any koCP24/26 plant that expressed only Lhcb4.2 or Lhcb4.3. To further verify this result, we repeated the experiment within the population derived from a koCP24/26 mutant plant heterozygous at all the three *lhcb4* loci. Again all the F2 plants analyzed expressed the Lhcb4.1 isoform with or without Lhcb4.2 or/and Lhcb4.3. It seems that the minimal unit that has to be expressed in order to assemble a functional PSII is composed by CP26 and the first isoform of CP29 (Lhcb4.1). This implies that CP26 and Lhcb4.1, conserved in *Viride plantae* genomes (Alboresi et al., 2008), have a common function fundamental for the plant survival, that is not share by Lhcb4.2 and Lhcb4.3, whose genes appeared later in genomes of organisms of the green lineage.

## An alternative strategy for the obtaining of a (conditional) ko mutant for the five genes encoding Lhcb-monomeric proteins.

From the genetic data above we conclude that is not possible to isolate a stable genetic five-fold mutant without all the three monomeric antenna proteins. Thus we decided to use an alternative strategy to obtain, this time,

not a fully genetic five fold mutant but, more modestly, a phenocopy without monomeric antenna proteins. To this aim we transformed a koCP29/24 mutant with a construct aimed to silence the third and last monomeric antenna subunit (fifth gene), Lhcb5 (CP26). In this way we can avoid the genetic difficulty due to the lethal embryo phenotype. The expression of the silencing sequence needs to be inducible in order to yield into silencing only when plants are grown-up; in this way we can observe the five-mutant phenotype in the newly developed leaves, evading lethality problems in the first days after germination. For these purposes we chose the pER8 vector (Zuo and Chua, 2000), a chemically inducible receptor system, estrogen-based, in which we cloned the *lhcb5* (CP26) coding sequence in an antisense orientation. Thus, the antisense expression, once the two-component estrogen system is stably inserted in the genome, was under the control of an inducible promotor activated by treating plants with $\beta$-estradiol (Figure D.7).

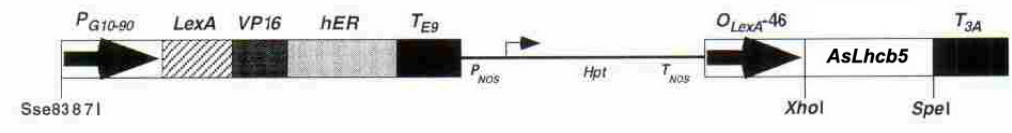


**Figure D.7:** *A schematic diagram of the XVE vector with the Lhcb5 coding sequence in antisense orientation (Zuo and Chua, 2000).*

## Plants transformation and results

We transformed, using the floral dipping protocol, WT and QHom plants with *Agrobacterium* carrying the CP26 (Lhcb5) antisense inducible plasmids. We tried also to transform QHet plants, but it soon appeared very hard and not convenient (they have very late and few flowers). Seeds of transformed WT and QHom plants were collected (T1 generation) and spread on hygromicin selection plates. The resistance plants were moved to soil and led to flowering. T2 seeds (from self-pollination) are then collected and tested on hygromicin plates for the maintenance of the resistance. The results are the following: among 17 WT resistant T1 lines, 15 conserved this property in the T2 generation. In the case, of QHom, instead, among 24 selected T1 plants, only 14 still conserved the antibiotic resistance. The loss of resistance in the F2 population could be due to false positive resistance of T1 plants selected or to rearrangements in the genome after the self-pollination.
As a preliminary characterization of transformed lines, we verified if the construct was complete and correctly inserted. To this aim we determined in which of these T2 resistance populations the CP26 antisense construct works properly in order to use a few such lines for further experimentation. This was obtained by testing the CP26 protein level: we spread WT T2 seeds

on hygromicin selection plates added with $\beta$-estradiol (5$\mu$M) and, once germinated and grown, we analyzed the CP26 level in at least 9 seedlings for each line by immunoblotting with CP26-specific antibody. We found that in 3 among 15 T2 WT lines, the CP26 amount was decreased (in some cases only weekly) yielding plants with a lower CP26 amount. In other cases the subunit was totally silenced (Figure D.8).

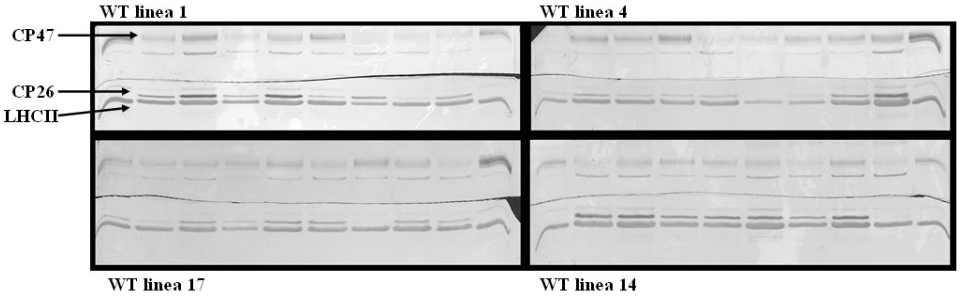


**Figure D.8:** *Immunoblot analysis.*
*Leaves protein, extracted from WT T2 plants, were immunoblotted using antibodies directed against minor antenna proteins CP26 and against the PSII core subunit CP47 (as a loading standard). In these plants the silencing construct worked well and with different efficiency.*

We also attempted the same approach with the QHom T2 resistant with the aim of verifying if the CP26 level was modulate in these lines. We spread QHom T2 seeds on hygromicin selection plates added with $\beta$-estradiol (5$\mu$M) and then we looked at the immunoblotting results: in this case we found that all the 14 T2 seedling analyzed showed the same level of CP26 expression. We can speculate that the reason for this result could be that (1) plants with an active antisense construction died because of the total absence of monomeric antenna proteins in the early phases of germination, as we observed above for embryos. In this case, however, the absence of any modulation of CP26 level in these lines appears somehow odd. Another explanation (2) is that the construct doesn't work in these QHom T2 plants or that (3) we failed to find a line because we screened too few of them. However in the case of T2 WT plants, the successful transformants were approx 20%, suggesting that a deviation from expected frequency is highly probable.
In a first approximation, we considered the hypothesis in (1) and further verified it. We sowed QHom T2 seeds of each population in two different media, with or without $\beta$-estradiol. Seedlings from lines with an active antisense should have a significant lower rate of germination in the $\beta$-estradiol medium. We counted the seeds number in the two conditions and we subtract at the fraction of non-germinated seeds in the medium with $\beta$-estradiol the fraction of non-germinated seeds in the medium without the inductor. The result expresses the increase in the "non-germinating seeds" in the $\beta$-estradiol medium with respect to the medium without the inductor. Lines

with a positive value should have a functional insertion, expression and full function of the antisense construct. Three lines showed a positive value in this experiment, as reported in Figure D.9.
The future prospect is to grow these three lines in hydroponic culture. This should allow separating two growth phases: in a first phase, during the first weeks after germination, we need to grow plants without the inductor in order to avoid the lethality factor; in the second phase, when the seedlings have six to eight leaves, we plan to add $\beta$-estradiol to the hydroponic medium, and then follow the development of newly formed leaves, that should be strongly reduced in CP26 (besides CP29 and CP24) and thus a phenocopy of the homozygous five-gene mutant. On these leaves we could verify the photoprotection capacity and NPQ.

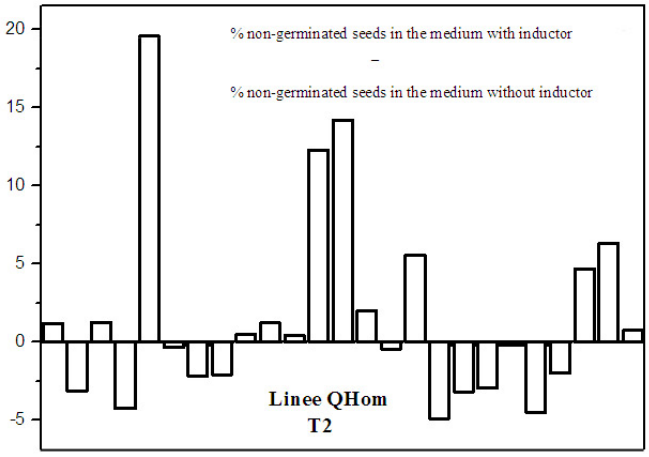


**Figure D.9:** *Difference in germination in presence and absence of $\beta$-estradiol. Seed of the T2 population of QHomo transformed plants were spread on two different medium, with and without $\beta$-estradiol. At the fraction of non-germinated seeds in the medium with the inductor was subtracted the fraction of non-germinated seeds in the medium without the inductor. The result expressed how much more seeds are not germinated in the $\beta$-estradiol medium respect in a medium without and is reported as percentage in the histogram.*

## CP26 content and quenching capacity (NPQ) in QHet and QHom mutants

QHet and QHom plants are different only for the condition at the Lhcb5 locus (heterozygous in QHet and homozygous WT in QHom), thus we expect they have both the same dominant phenotype, as already observed with other antenna mutants: for example, koCP24 mutants with an hetero or homo WT condition at the *lhcb5* locus have exactly the same phenotype. Instead as we mentioned above, we noticed a dose effect for the *lhcb5* gene. Some of these differences can be observed in the flowering process: (i) late buds and flowers formation; (ii) shorter and pale-green siliques and, (ii) the lower number of seeds per silique. How can we explain this pheno-

type? The only biochemical difference between these two genotypes could be the amount of CP26 whose mRNA is translated by only one allele in QHet and by two copies in QHom. We proceeded to determine the stoichiometry of CP26 subunit. This was obtained by the densitometry of its sharp Coomassie-stained band in a Tris-tricine gel, upon normalized to the LHCII content. We found that QHet has 20% less CP26 respect to QHom (QHom 100,0 ± 10,1; QHet 83,7 ± 3,9). Thus, there is an *lhcb5* allele-dose effect on the CP26 protein content: the presence of only one functional copy of *lhcb5*, in a koCP29/24 background, causes a small but significant reduction of the total CP26 content. As for the koCP29 NPQ phenotype, QHom shows a fast rise to a value of 1.0 in the first minute at 1200 $\mu$mol photons $m^{-2}s^{-1}$ and further rise of the quenching is then delayed by 2-3 minutes, after which, NPQ rise resumes without, however, reaching WT value at 8 minutes of illumination. The NPQ kinetics of koCP29/24 (QHom) is identical to that of the koCP29 phenotype (Figure D.10A) (Betterle et al., 2009, Section A.1). Thus the quenching capacity could be ascribe to CP26, the last monomeric antenna subunit remained in the PSII. Alternatively, (i) the major light-harvesting complex, LHCII, could also be involved or (ii) the quenching mechanism located within the PSII core complex (Finazzi et al., 2004). Because we cannot study the five fold mutant phenotype, these two mutants QHom and QHet could help us to give an answer to the question about the quenching site(s). Does the quenching capacity correlates with the amount of CP26 in a koCP29/24 background? In Figure D.10A the NPQ kinetic of these two genotypes is shown: QHet has a quenching curve a little lower than QHom and the NPQ value at the end of illumination is around 20% lower than in QHom (QHom 100,0 ± 5,7; QHet 86,9 ± 6,6). Thus CP26 amount and NPQ capacity seems to be strictly correlated as shown in Figure D.10B.

### D.1.4 Discussion

Monomeric antenna proteins are located in between the PSII core complex and the trimeric LHCII, acting as a connection between these two moieties. Their localization is important for the energy transfer to the reaction centre, having also an important role in photoprotection when light exceed the photochemical capacity to use it in the electron transport. Their position is also fundamental for the binding of LHCII trimer to the core, in fact when one of these subunits lacks, a higher disconnection of the trimer is observed and a larger fraction of absorbed energy is lost as fluorescence in the mutants, implying that the connection between the major LHCII complex and PSII RC is less efficient in the absence of monomeric antenna proteins (Kovacs et al., 2006; de Bianchi et al., 2008; Andersson et al., 2001). Some of the

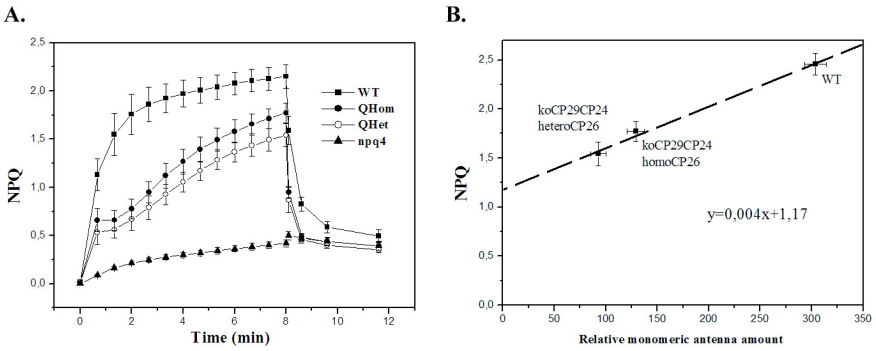


**Figure D.10:** *NPQ kinetic of WT, QHom and QHet mutants.*
*A. Kinetics of NPQ induction and relaxation were recorded with a pulse-amplitude modulated fluorometer. Chlorophyll fluorescence was measured in intact, dark-adapted leaves, during 8 min of illumination at 1200 µmol photons $m^{-2}s^{-1}$ followed by 4 min of dark relaxation. We put npq4 as a reference for the null NPQ phenotype. B. Correlation between the NPQ value after 8 min of illumination and monomeric antenna amounts calculated from densitometry of Coomassie-stained band in a Tris-tricine gel.*

interactions between monomeric subunits and LHCII are known, for example M-LHCII trimer requires CP24 for its binding (Kovacs et al., 2006; de Bianchi et al., 2008) and there are evidences that this specificity is due to the interaction between CP24 and Lhcb3, present only in trimer M (Betterle et al., 2009; Caffarri et al., 2009). Moreover, in a mutants without CP24, Lhcb3 is strongly depleted (de Bianchi et al., 2008; Caffarri et al., 2009) and, conversely, the content of CP24 in koLhcb3 is reduced (Caffarri et al., 2009). There are some specific interactions within the PSII that allows the stabilization of the supercomplex. This is true also for the interactions between the monomeric subunits: CP24 is connected through CP29 to the core complex and thus when CP29 is knocked out, CP24 is unable to bind stably to the photosystem and get degraded as observed in koCP29 mutant (Section A.2, Andersson et al., 2001). The CP24 position in PSII also suggests that CP24 cannot transfer excitation energy directly to the core, because there are no Chl of CP47 located near CP24, but the transfer from M trimer and CP24 to the core occurs through CP29 (Caffarri et al., 2009). The stable association of the S-LHCII trimer to the core complex through CP43 is instead mediated by the interaction with CP26 and CP29. The binding of S trimer in the absence of CP26 is controversial, it seemed to still be connected to the supercomplex (Yakushevska et al., 2003), but recent results indicate that this binding is much less stable when CP26 is missing (Caffarri et al., 2009). CP29 contributes to a general stabilization of the PSII dimer; thus it seems the key subunit for the stability of the supercomplex (van Oort et al., 2010, Section C.1). Thus, the present understanding of the role of monomeric antenna complexes is not only to play important roles in the assembly of PSII into the supercomplex, in the macroorganization of supercomplexes in the thylakoid membrane, in the maintaining of its high quantum efficiency and

the ability to transfer energy to the RC (Section C.1, van Oort et al., 2010; Harrer et al., 1998; Dekker and Boekema, 2005; Morosinotto et al., 2006; Yakushevska et al., 2003; Caffarri et al., 2009) but also that some of the complexes, namely CP26 and CP29 isoform one (Lhcb4.1) play an essential function, which is not yet fully identified, that is essential to the life of the embryo during seed development and germination. We are looking forward to obtain results from the experiment with inducible RNAi (see above) in order to understand is this function is also essential for the photosynthesis in fully developed chloroplasts in leaves. These results have both supporting and contrasting evidences from existing literature. As a support for an essential role of CP26 and CP29, it is well documented that they are highly conserved through evolution and have been defined as the PSII "functional core" antenna system conserved within the green lineage (Alboresi et al., 2008). Our results strongly confirm the fundamental role of monomeric subunits in the assembly and macroorganization of the PSII: when one of these complexes is missing, we observe a disconnection of LHCII from PSII core complex (de Bianchi et al., 2008, Sections A.2, B.2). Furthermore, when both CP26 and the Lhcb4.1 subunits lack, the embryo is unable to survive since the first phases of its formation. These antenna subunits are expressed in the reproductive tissue, in the meristematic cells and in young embryonic tissue (Sawchuk et al., 2008; https://www.genevestigator.com/gv/index.jsp; Figure D.11) and the lethal phenotype observed could be due to the their absence during the first phases of the zygote formation and seeds development. In fact, during seed development, increased levels of ROS occur and are normally controlled by increased levels of antioxidant compounds and activity of ROS scavenging enzymes (Bailly et al., 2004; Cairns et al., 2006). A contrasting evidence comes from Chl *b*-less mutants such as *Chlorina f2* in barley (Bassi et al., 1987) and *ch1* in *Arabidopsis* (Havaux et al., 2007; Dall'Osto et al., 2010) which miss Lhc proteins, including monomeric Lhcbs, and yet have a normal development. A residual CP26 level is conserved in *ch1*, however the double mutant ch1koCP26 is viable (Havaux et al., 2007; Dall'Osto et al., 2010). We conclude that lack of CP29 and CP26 is only lethal when LHCII is present. This implies that minor CPs are essential for the energy transfer from LHCII and PSII RC.

In our case the absence of monomeric antennas and the consequent LHCII disconnection could lead to a high ROS production not counteracted by the antioxidant mechanism present at that development stage. A relation between the chlorophyll content and the maturity of seeds has been well studied in seeds of oilseed rape (*Brassica napus L.*) and turnip rape (*Brassica rapa L.*) (Ward et al., 1992; Ward et al., 1995; Jalink et al., 1998). *Arabidopsis* belongs to the family of *Brassicaceae*, and probably a strong alteration in the PSII supercomplex assembly could compromise the maturation of the

seeds into siliques. It's important to note that in embryo, immature seeds and silique tissues are green and thus they posses photosynthetic proteins able to bind chlorophylls.

The phenotype of mutants obtained in the present work suggest some considerations about the role of monomeric antenna proteins in NPQ.
The comparison between QHom and QHet: both mutants lack CP24 and the three CP29 isoforms but differ for the condition at the *lhcb5* locus, homozygous WT in QHom and heterozygous in QHet. We observed a dose effect for the expression of Lhcb5 (CP26). The level of CP26 accumulated in the thylakoid membrane strictly correlates with the amplitude of quenching observed when plants are illuminated at saturating light intensity (1200 $\mu$mol photons $m^{-2}s^{-1}$). The correlation between the NPQ value and the amount of monomeric antenna protein is shown in Figure D.10B. If we ideally set to zero the amount of monomeric antenna subunits we expect a putative NPQ value of 1. The amount of the quenching due to the monomeric antenna represents thus most of the NPQ process. In the case of koCP29 (and koCP29/24) the majority of the quenching capacity is due to the quenching capacity of CP26 subunit.
The residual quenching capacity could be due to the LHCII supercomplex, still present. However, the results of the antisense suppression of LHCII (Andersson et al., 2003) and of the Lhcb3 knock out (Damkjaer et al., 2009), show that the quenching capacity is not affected when LHCII is absent. Clearly, we cannot exclude the hypothesis that monomeric subunits are able to functionally replace the putative LHCII quenching capacity when the major complex is suppressed.
From the experimental evidence is also clear that the LHCII complex can not be connected to the supercomplex without monomeric subunits. This indicate that for the correct connection of LHCII to the core, monomeric complexes are indispensable and this could be probably also true for LHCII putative quenching role.
Alternatively the residual fluorescence quenching in the absence of monomeric subunits can be attribute to a quenching mechanism located within the PSII core complex as reported in Finazzi et al., 2004.
From these considerations we can affirm that monomeric subunits have a major role in the non-photochemical quenching and that they seems to be the preferential site of the quenching as stated in different quenching models (Avenson et al., 2008; Ahn et al., 2008). At present, it is not possible, however to exclude that LHCII also has a role in quenching of PSII fluorescence in WT leaves.

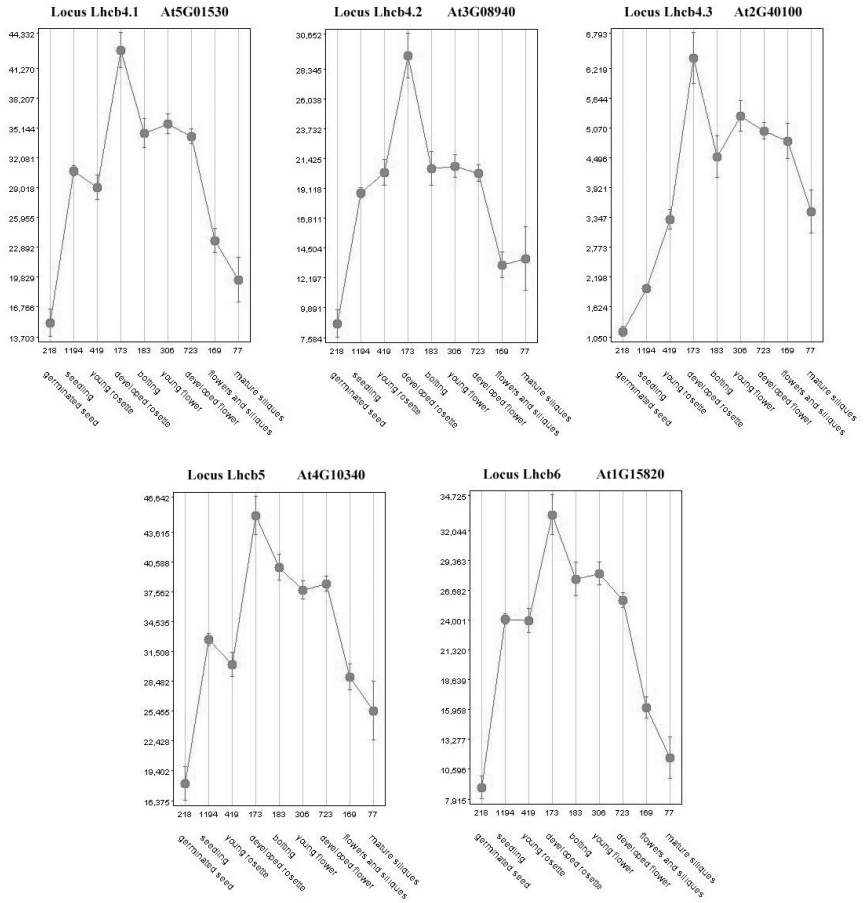


**Figure D.11:** *Lhcbs expression profile in different tissue.*
*Expression profile of monomeric Lhcbs in different Arabidopsis tissue. Data are collected from https://www.genevestigator.com/gv/index.jsp.*

## Abbreviation

NPQ, non photochemical quenching; qE, energy quenching; $^1$Chl*, chlorophyll excited state; VDE, violaxanyhin deepoxidase; Zea, zeaxanthin; Lhc, light harvesting complex; CT, charge transfer; qE, energy quenching; qI, inhibitory quenching; ko, knocked out; RC, reaction center; QHet, koCP29/24 quadruple mutant heterozygous at *lhcb5* locus; QHom, koCP29/24 quadruple mutant homozygous at *lhcb5* locus; ROS, reactive oxygen species.

## Acknowledgement

Dr. Chua as the provider of the plasmid pER8.

## Reference list

**Ahn,T.K.,** Avenson,T.J., Ballottari,M., Cheng,Y.C., Niyogi,K.K., Bassi,R., and Fleming,G.R. (2008). Architecture of a charge-transfer state regulating light harvesting in a plant antenna protein. Science 320, 794-797.

**Alboresi,A.,** Caffarri,S., Nogue,F., Bassi,R., and Morosinotto,T. (2008). In silico and biochemical analysis of Physcomitrella patens photosynthetic antenna: identification of subunits which evolved upon land adaptation. PLoS. One. 3, e2033.

**Alonso,J.M.,** Stepanova,A.N., Leisse,T.J., Kim,C.J., Chen,H., Shinn,P., Stevenson,D.K., Zimmerman,J., Barajas,P., Cheuk,R., Gadrinab,C., Heller,C., Jeske,A., Koesema,E., Meyers,C.C., Parker,H., Prednis,L., Ansari,Y., Choy,N., Deen,H., Geralt,M., Hazari,N., Hom,E., Karnes,M., Mulholland,C., Ndubaku,R., Schmidt,I., Guzman,P., Aguilar-Henonin,L., Schmid,M., Weigel,D., Carter,D.E., Marchand,T., Risseeuw,E., Brogden,D., Zeko,A., Crosby,W.L., Berry,C.C., and Ecker,J.R. (2003). Genome-wide insertional mutagenesis of Arabidopsis thaliana. Science 301, 653-657.

**Andersson,J.,** Walters,R.G., Horton,P., and Jansson,S. (2001). Antisense inhibition of the photosynthetic antenna proteins CP29 and CP26: Implications for the mechanism of protective energy dissipation. Plant Cell 13, 1193-1204.

**Andersson,J.,** Wentworth,M., Walters,R.G., Howard,C.A., Ruban,A.V., Horton,P., and Jansson,S. (2003). Absence of the Lhcb1 and Lhcb2 proteins of the light-harvesting complex of photosystem II - effects on photosynthesis, grana stacking and fitness. Plant J. 35, 350-361.

**Aspinall-O'Dea,M.,** Wentworth,M., Pascal,A., Robert,B., Ruban,A.V., and Horton,P. (2002). In vitro reconstitution of the activated zeaxanthin state associated with energy dissipation in plants. Proc. Natl. Acad. Sci. U. S. A 99, 16331-16335.

**Avenson,T.J.,** Ahn,T.K., Zigmantas,D., Niyogi,K.K., Li,Z., Ballottari,M., Bassi,R., and Fleming,G.R. (2008). Zeaxanthin radical cation formation in minor light-harvesting complexes of higher plant antenna. J. Biol. Chem. 283, 3550-3558.

**Bailly,C.,** Leymarie,J., Lehner,A., Rousseau,S., Come,D., and Corbineau,F. (2004). Catalase activity and expression in developing sunflower seeds as related to drying. J. Exp. Bot. 55, 475-483.

**Barber,J.** and Andersson,B. (1992). Too Much of a Good Thing - Light Can Be Bad for Photosynthesis. Trends Biochem. Sci. 17, 61-66.

**Bassi,R.,** Hoyer-hansen,G., Barbato,R., Giacometti,G.M., and Simpson,D.J. (1987). Chlorophyll-proteins of the photosystem-II antenna system. J. Biol. Chem. 262, 13333-13341.

**Bassi,R.,** Pineau,B., Dainese,P., and Marquardt,J. (1993). Carotenoid-Binding Proteins of Photosystem-II. Eur. J. Biochem. 212, 297-303.

**Bassi,R.,** Rigoni,F., Barbato,R., and Giacometti,G.M. (1988). Light-harvesting chlorophyll a/b proteins (LHCII) populations in phosphorylated membranes. Biochim. Biophys. Acta 936, 29-38.

**Betterle,N.,** Ballottari,M., Zorzan,S., de Bianchi,S., Cazzaniga,S., Dall'Osto,L., Morosinotto,T., and Bassi,R. (2009). Light-induced dissociation of an antenna hetero-oligomer is needed for non-photochemical quenching induction. J. Biol. Chem. 284, 15255-15266.

**Bonente,G.,** Howes,B.D., Caffarri,S., Smulevich,G., and Bassi,R. (2008). Interactions between the photosystem II subunit PsbS and xanthophylls studied in vivo and in vitro. Journal of Biological Chemistry 283, 8434-8445.

**Caffarri,S.,** Kouril,R., Kereiche,S., Boekema,E.J., and Croce,R. (2009). Functional architecture of higher plant photosystem II supercomplexes. Embo Journal 28, 3052-3063.

**Cairns,N.G.,** Pasternak,M., Wachter,A., Cobbett,C.S., and Meyer,A.J. (2006). Maturation of arabidopsis seeds is dependent on glutathione biosynthesis within the embryo. Plant Physiol 141, 446-455.

**Dall'Osto,L.,** Caffarri,S., and Bassi,R. (2005). A mechanism of nonphotochemical energy dissipation, independent from Psbs, revealed by a conformational change in the antenna

protein CP26. Plant Cell 17, 1217-1232.

**Dall'Osto,L.,** Cazzaniga,S., Havaux,M., and Bassi,R. (2010). Enhanced Photoprotection by Protein-Bound vs Free Xanthophyll Pools: A Comparative Analysis of Chlorophyll b and Xanthophyll Biosynthesis Mutants. Mol. Plant.

**Dall'Osto,L.,** Lico,C., Alric,J., Giuliano,G., Havaux,M., and Bassi,R. (2006). Lutein is needed for efficient chlorophyll triplet quenching in the major LHCII antenna complex of higher plants and effective photoprotection in vivo under strong light. Bmc Plant Biology 6, 32.

**Damkjaer,J.T.,** Kereiche,S., Johnson,M.P., Kovacs,L., Kiss,A.Z., Boekema,E.J., Ruban,A.V., Horton,P., and Jansson,S. (2009). The Photosystem II Light-Harvesting Protein Lhcb3 Affects the Macrostructure of Photosystem II and the Rate of State Transitions in Arabidopsis. Plant Cell.

**de Bianchi,S.,** Dall'Osto,L., Tognon,G., Morosinotto,T., and Bassi,R. (2008). Minor antenna proteins CP24 and CP26 affect the interactions between photosystem II subunits and the electron transport rate in grana membranes of Arabidopsis. Plant Cell 20, 1012-1028.

**Dekker,J.P.** and Boekema,E.J. (2005). Supramolecular organization of thylakoid membrane proteins in green plants. Biochim. Biophys. Acta 1706, 12-39.

**Demmig-Adams,B.** (1990). Carotenoids and photoprotection in plants: A role for the xanthophyll zeaxanthin. Biochim. Biophys. Acta 1020, 1-24.

**Demmig-Adams,B.** and Adams,W.W. (1992). Photoprotection and other responses of plants to high light stress. Ann. Rev. Plant Physiol. Plant Mol. Biol. 43, 599-626.

D**emmig-Adams,B.** and Adams,W.W. (1994). Capacity for energy dissipation in the pigment bed in leaves with different xanthophyll cycle pools. Aust. J. Plant Physiol. 21, 575-588.

**Dominici,P.,** Caffarri,S., Armenante,F., Ceoldo,S., Crimi,M., and Bassi,R. (2002). Biochemical properties of the PsbS subunit of photosystem II either purified from chloroplast or recombinant. J. Biol. Chem. 277, 22750-22758.

**Edwards,K.,** Johnstone,C., and Thompson,C. (1991). A simple and rapid method for the preparation of plant genomic DNA for PCR analysis. Nucleic Acids Res. 19, 1349.

**Finazzi,G.,** Johnson,G.N., Dall'Osto,L., Joliot,P., Wollman,F.A., and Bassi,R. (2004). A zeaxanthin-independent nonphotochemical quenching mechanism localized in the photosystem II core complex. Proc. Natl. Acad. Sci. U. S. A 101, 12375-12380.

**Formaggio,E.,** Cinque,G., and Bassi,R. (2001). Functional architecture of the major Light-harvesting Complex from Higher Plants. J. Mol. Biol. 314, 1157-1166.

**Frank,H.A.,** Bautista,J.A., Josue,J.S., and Young,A.J. (2000). Mechanism of nonphotochemical quenching in green plants: Energies of the lowest excited singlet states of violaxanthin and zeaxanthin. Biochemistry 39, 2831-2837.

**Funk,C.,** Schröder,W.P., Napiwotzki,A., Tjus,S.E., Renger,G., and Andersson,B. (1995). The PSII-S protein of higher plants: A new type of pigment- binding protein. Biochemistry 34, 11133-11141.

**Gilmore,A.M.,** Hazlett,T.L., and Govindjee (1995). Xanthophyll cycle-dependent quenching of photosystem II chlorophyll a fluorescence: Formation of a quenching complex with a short fluorescence lifetime. Proc. Natl. Acad. Sci. USA 92, 2273-2277.

**Harrer,R.,** Bassi,R., Testi,M.G., and Schäfer,C. (1998). Nearest-neighbor analysis of a photosystem II complex from Marchantia polymorpha L.(liverwort), which contains reaction center and antenna proteins. Eur. J. Biochem. 255, 196-205.

**Havaux,M.,** Dall'Osto,L., and Bassi,R. (2007). Zeaxanthin has Enhanced Antioxidant Capacity with Respect to All Other Xanthophylls in Arabidopsis Leaves and functions independent of binding to PSII antennae. Plant Physiol.

**Holt,N.E.,** Zigmantas,D., Valkunas,L., Li,X.P., Niyogi,K.K., and Fleming,G.R. (2005). Carotenoid cation formation and the regulation of photosynthetic light harvesting. Science 307, 433-436.

**Horton,P.,** Johnson,M.P., Perez-Bueno,M.L., Kiss,A.Z., and Ruban,A.V. (2008). Photosynthetic acclimation: does the dynamic structure and macro-organisation of photosystem II in higher plant grana membranes regulate light harvesting states? FEBS J. 275, 1069-1079.

**Horton,P.** and Ruban,A. (2005). Molecular design of the photosystem II light-harvesting antenna: photosynthesis and photoprotection. J. Exp. Bot. 56, 365-373.

**Jalink,H.,** van der Schoor,R., Frandas,A., van Pijlen,J.G., and Bino,R.J. (1998). Chlorophyll fluorescence of Brassica oleracea seeds as a non-destructive marker for seed maturity and seed performance. Seed Science Research 8, 437-443.

**Jansson,S.** (1999). A guide to the Lhc genes and their relatives in Arabidopsis. Trends Plant Sci. 4, 236-240.

**Kim,S.Y.,** Yu,X., and Michaels,S.D. (2008). Regulation of CONSTANS and FLOWERING LOCUS T expression in response to changing light quality. Plant Physiol 148, 269-279.

**Kiss,A.Z.,** Ruban,A.V., and Horton,P. (2008). The PsbS protein controls the organization of the photosystem II antenna in higher plant thylakoid membranes. J. Biol. Chem. 283, 3972-3978.

**Kitajima,M.** and Butler,W.L. (1975). Quenching of chlorophyll fluorescence and primary photochemistry in chloroplasts by dibromothymoquinone. Biochim. Biophys. Acta 376, 105-115.

**Kovacs,L.,** Damkjaer,J., Kereiche,S., Ilioaia,C., Ruban,A.V., Boekema,E.J., Jansson,S., and Horton,P. (2006). Lack of the light-harvesting complex CP24 affects the structure and function of the grana membranes of higher plant chloroplasts. Plant Cell 18, 3106-3120.

**Li,X.P.,** Bjorkman,O., Shih,C., Grossman,A.R., Rosenquist,M., Jansson,S., and Niyogi,K.K. (2000). A pigment-binding protein essential for regulation of photosynthetic light harvesting. Nature 403, 391-395.

**Li,X.P.,** Gilmore,A.M., Caffarri,S., Bassi,R., Golan,T., Kramer,D., and Niyogi,K.K. (2004). Regulation of photosynthetic light harvesting involves intrathylakoid lumen pH sensing by the PsbS protein. J. Biol. Chem. 279, 22866-22874.

**Miloslavina,Y.,** Wehner,A., Lambrev,P.H., Wientjes,E., Reus,M., Garab,G., Croce,R., and Holzwarth,A.R. (2008). Far-red fluorescence: A direct spectroscopic marker for LHCII oligomer formation in non-photochemical quenching. FEBS Letters 582, 3625-3631.

**Morosinotto,T.,** Bassi,R., Frigerio,S., Finazzi,G., Morris,E., and Barber,J. (2006). Biochemical and structural analyses of a higher plant photosystem II supercomplex of a photosystem I-less mutant of barley. Consequences of a chronic over-reduction of the plastoquinone pool. FEBS J. 273, 4616-4630.

**Moya,I.,** Silvestri,M., Vallon,O., Cinque,G., and Bassi,R. (2001). Time-Resolved Fluorescence Analysis of the Photosystem II Antenna Proteins in Detergent Micelles and Liposomes. Biochemistry 40, 12552-12561.

**Muller,P.,** Li,X.P., and Niyogi,K.K. (2001). Non-photochemical quenching. A response to excess light energy. Plant Physiol 125, 1558-1566.

**Niyogi,K.K.,** Grossman,A.R., and Björkman,O. (1998). Arabidopsis mutants define a central role for the xanthophyll cycle in the regulation of photosynthetic energy conversion. Plant Cell 10, 1121-1134.

**Oxborough,K.** and Baker,N.R. (1997). An instrument capable of imaging chlorophyll a florescence from intact leaves at very low irradiance and at cellular and subcellular levels. Plant, Cell and Environment 20, 1473-1483.

**Pascal,A.A.,** Liu,Z., Broess,K., van Oort,B., Van Amerongen,H., Wang,C., Horton,P., Robert,B., Chang,W., and Ruban,A. (2005). Molecular basis of photoprotection and control of photosynthetic light-harvesting. Nature 436, 134-137.

**Ruban,A.V.,** Berera,R., Ilioaia,C., van Stokkum,I.H., Kennis,J.T., Pascal,A.A., Van Amerongen,H., Robert,B., Horton,P., and van Grondelle,R. (2007). Identification of a mechanism of photoprotective energy dissipation in higher plants. Nature 450, 575-578.

**Sawchuk,M.G.,** Donner,T.J., Head,P., and Scarpella,E. (2008). Unique and overlapping expression patterns among members of photosynthesis-associated nuclear gene families in Arabidopsis. Plant Physiol 148, 1908-1924.

**Schägger,H.** and von Jagow,G. (1987). Tricine-sodium dodecyl sulfate-polyacrylamide gel electrophoresis for the separation of proteins in the range from 1 to 100 kDa. Anal. Biochem. 166, 368-379.

**Towbin,H.,** Staehelin,T., and Gordon,J. (1979). Electrophoretic transfer of proteins from polyacrylamide gels to nitrocellulose sheets: Procedure and some applications. Proc. Natl. Acad. Sci. USA 76, 4350-4354.

**Van Kooten,O.** and Snel,J.F.H. (1990). The use of chlorophyll fluorescence nomenclature in plant stress physiology. Photosynt. Res. 25, 147-150.

**van Oort,B.,** Alberts,M., de Bianchi,S., Dall'Osto,L., Bassi,R., Trinkunas,G., Croce,R., and Van Amerongen,H. (2010). Effect of Antenna-Depletion in Photosystem II on Excitation Energy Transfer in Arabidopsis thaliana. Biophys. J. 98, 922-931.

**Ward,K.,** Scarth,R., Daun,J., and Mcvetty,P.B.E. (1992). Effects of Genotype and Environment on Seed Chlorophyll Degradation During Ripening in 4 Cultivars of Oilseed Rape (Brassica-Napus). Canadian Journal of Plant Science 72, 643-649.

**Ward,K.,** Scarth,R., Daun,J.K., and Vessey,J.K. (1995). Chlorophyll Degradation in Summer Oilseed Rape and Summer Turnip Rape During Seed Ripening. Canadian Journal of Plant Science 75, 413-420.

**Wollenberg,A.C.,** Strasser,B., Cerdan,P.D., and Amasino,R.M. (2008). Acceleration of flowering during shade avoidance in Arabidopsis alters the balance between FLOWERING LOCUS C-mediated repression and photoperiodic induction of flowering. Plant Physiol 148, 1681-1694.

**Yakushevska,A.E.,** Keegstra,W., Boekema,E.J., Dekker,J.P., Andersson,J., Jansson,S., Ruban,A.V., and Horton,P. (2003). The structure of photosystem II in Arabidopsis: localization of the CP26 and CP29 antenna complexes. Biochemistry 42, 608-613.

**Zhang,X.,** Henriques,R., Lin,S.S., Niu,Q.W., and Chua,N.H. (2006). Agrobacterium-mediated transformation of Arabidopsis thaliana using the floral dip method. Nat. Protoc. 1, 641-646.

**Zuo,J.** and Chua,N.H. (2000). Chemical-inducible systems for regulated expression of plant genes. Curr. Opin. Biotechnol. 11, 146-151.

# Conclusions

A long standing discussion has been developed on whether the site of the photoprotection mechanism, including protection from photo-oxidation and excitation energy quenching (NPQ) was located within the monomeric antenna proteins or in the major light harvesting complex of PSII, called LHCII. This thesis work was aimed to elucidate the role of the monomeric antenna proteins in light harvesting and photoprotection with particular focus on NPQ. In order to investigate the role of individual monomeric Lhcbs, I used a reverse genetic approach with the aim to obtain *Arabidopsis* mutants specifically devoid of one or more Lhcb subunits. Following that, I characterized the photosynthetic phenotype and the capacity for photoprotection of these mutants. Moreover, capacity for chlorophyll fluorescence quenching was followed on leaves by ultra-fast Chl fluorescence, while changes in the organization of the PSII antenna during exposure to strong light and NPQ development were characterized by biochemistry and electron microscopy. The main features of knock out mutants isolated and other final considerations are listed below.

**KoCP24**. The absence of CP24 subunit in the PSII supercomplex leads to a destabilisation of the M-LHCII trimers leading to a $C_2S_2$ configuration of the PSII particles. CP24 is required for proper macro-organization of PSII complexes. Indeed, in its absence, the packing of PSII limits the plastoquinone diffusion rate and slows down the electron transport. Therefore koCP24 mutant shows a lower amplitude of the $\Delta$pH gradient across the grana membranes, a reduced capacity for non photochemical quenching (reduced by 50%), and a limited growth. As a consequence of the physical disconnection of LHCII form PSII, koCP24 has a decreased efficiency of energy transfer from LHCII to the PSII reaction centre. Ultra-fast Chl fluorescence analysis revealed that koCP24 plants lack one of the two major quenching components, called Q1, located in the major LHCII complexes and functionally detached from the PSII reaction centre in this mutant. These results are consistent with electron microscopy evidences, and suggest that CP24 subunit could act as specific quencher of LHCII domains that undergo dissociation from PSII during NPQ.

**KoCP26**. The absence of CP26 does not affect qE component of NPQ but

lead to a reduce qI. Thus CP26 plays a major role in qI, confirming the observed capacity to assume a quenched conformation upon Zea binding under high-light treated thylakoids. Although PSII organization is not disturbed in the absence of CP26 subunit, it likely shares vital functional features with CP29. I made many attempts to isolate a mutant lacking both CP26 and CP29 without success, implying that a specific function, indispensable for plant life and development and yet unknown, is associated to these two proteins.

**KoCP26/24**. The absence of both CP26 and CP24 subunits restored the macro-organization of PSII in the grana membranes with respect to koCP24, and re-established electron transport and $\Delta$pH build-up capacity. The NPQ kinetic is slower in the first phases of illumination but it reaches the WT value after 8 minutes of light, thus suggesting that the strong NPQ phenotype of the single mutant koCP24 is not caused merely by the absence of CP24 but, rather, to pleiotropic or compensatory effects (organization of PSII into arrays).

**KoCP29**. CP29 shows a specific effect in protecting PSII from photoinhibition, which could account for the higher sensitivity to high-light stress of koCP29 than wild-type plants. Probably the binding site for CP29, located in between LHCII trimers and reaction centre of PSII supercomplexes, is particularly effective in protecting PSII from ROS produced during photosynthetic process. Similarly to other monomeric Lhcbs, CP29 functions in bridging dimeric PSII core complexes to the major trimeric LHCII antenna both structurally and functionally, thereby, when it lacks, a large fraction of the LHCII becomes badly connected to the reaction centre. This subunit is determinant for the binding of CP24 to the core complex. Indeed, knockout of Lhcb4 genes yields into the complete absence of CP29 and CP24 (mutant koCP29 is a phenocopy of koCP29/24). No PSII arrays in grana membranes could be observed by electron microscopy as well as no defined PSII supercomplexes in the absence of CP29; these evidences suggest that CP29 is a key component for the stability of PSII supercomplexes. CP29 absence yields into a delay in NPQ induction, and ultra-fast Chl fluorescence analysis suggests that CP29 plays an important role in the second site of quenching (Q2) located in and connected to the PSII complex.

Regarding the functional role of minor antennae in NPQ regulation, results reported in the present thesis demonstrate that depletion of a single monomeric Lhcb protein does not completely abolish NPQ, implying a redundancy within the subfamily members, in agreement with previous results in isolated Lhcb proteins which showed radical cation formation in the Lhcb4-6. Although there is not strict specificity among the complexes with respect to the NPQ induction, there is a specificity regarding Lhcb

contribution to functional assembly and organization of PSII supercomplex, which affect electron transport processes, hence NPQ. If one antenna type is missing, others can probably take the place of the missing Lhcb, showing the high flexibility of the photosynthetic apparatus concerning the ability to maintain a functional and photoprotected structure of PSII.
Given the functional redundancy among Lhcb complexes, characterization of a mutant lacking all minors antennae (CP24, CP26, CP29) was awaited in order to verify whether a) NPQ can be sustained in the absence of these gene products, and b) if LHCII complex has a role in the energy quenching mechanism.
Any attempts to isolate a mutant knocked out for all the monomeric Lhcbs, a five-gene mutant, were unsuccessful: surprisingly, we discover that when both CP26 and the CP29 coding sequences were deleted, the embryo is unable to survive since the first phases of its formation.
Despite troubles in isolation of a mutant completely devoid of minor antennae, we can infer some considerations by analyzing NPQ capacity of two mutants retaining CP26 as monomeric subunit (koCP29/24), but in different amount due to their lhcb5 locus condition (heterozygous/homozygous WT).
CP26 level on thylakoids strictly correlates with the amplitude of quenching; we ideally extrapolate a putative NPQ value of 1 (vs 2.8 in WT) with the amount of monomeric antenna subunits at zero. We conclude that the quenching due to the monomeric antennas represents most of the NPQ process.
The residual quenching could be due to the LHCII supercomplex, still present or to the PSII core complex, to which a quenching capacity has been attributed by previous work. However, published results on qE phenotype of both LHCII antisense and Lhcb3 knock-out lines, clearly showed that the quenching capacity is not affected when LHCII is depleted. Experimental evidence reported in this thesis clearly show that LHCII subunits can not be efficiently connected to the PSII supercomplex without monomeric subunits. Thus, monomeric Lhcb complexes are necessary elements to allow a proper LHCII/core-complex connection, and this could be probably also true for its putative quenching role.

The results obtained with this work strengthen the evidences for a major role of the monomeric subunits in the non-photochemical quenching and the hypothesis that they are the preferential site of the quenching, as stated by different quenching models. At present, however, it is not possible to exclude that LHCII could directly participate in quenching of PSII fluorescence in WT leaves.

# Acknowlegdments

Non potevano mancare i ringraziamenti al termine di questi 3 anni di lavoro.

Ringrazio innanzitutto il prof. Bassi per avermi dato la possibilità di portare avanti questo progetto di ricerca, sostenendomi sempre con suggerimenti e con fondamentali intuizioni. Grazie anche per la disponibilità, per gli stimoli nel migliorare le mie capacità di scrittura e per la pazienza nelle correzioni!

Grazie a Luca che mi ha seguito da vicino in questi 3 anni di esperimenti e il cui aiuto e competenza si sono rivelati a dir poco determinanti nel portare avanti questo progetto. Grazie anche per le piacevoli ciacole in mensa, momento di stacco dalla giornata di lavoro.

Grazie a Giulia per gli aiuti e i preziosi consigli in biologia molecolare e per sua presenza in laboratorio così originale!

Grazie a Ale per la completa disponibilità in qualsiasi occasione, per le informazioni bibliografiche sempre puntuali e per sua pacatezza.

Grazie a Matteo per il suo knowhow scientifico, sicuro punto di riferimento per ogni informazione sui meccanismi NPQ, il cui aiuto è stato importante.

Grazie a Nico per la sua presenza in laboratorio, pacifica, simpatica e divertente: è davvero un piacere lavorare insieme a lui!

Grazie a Stefano per il prezioso supporto tecnico, per le idee "originali" e le chiacchierate "alternative".

Grazie a Simone per la sua conoscenza a 360°, in grado di soddisfare qualsiasi curiosità; grazie anche per il prezioso sostegno tecnico-informatico.

Grazie a Cinzia per la sua unicità, la sua indipendenza e capacità di approfondimento che lasciamo sempre stupiti.

Grazie a Michela per sua vivacità che dona un tocco di allegria “collinare” al laboratorio.

Grazie a Julien, troppo forte con le sue battute sempre puntuali! Grazie anche per l’aiuto nel creare l’originale copertina di questa tesi.

Grazie a Sara, compagna di laboratorio ma prima ancora cara amica; è un piacere e una fortuna per me averla in laboratorio!

Quante cose sono cambiate in questi 3 anni di dottorato! E quante nuove persone conosciute, tutte da ringraziare!!!!
Grazie a tutte le Sentinelle che ho avuto la fortuna di incontrare, un arricchimento continuo per la mia vita; grazie per aver condiviso e aver reso speciali le missioni di spiaggia, i ritiri, le riunioni e le serate e Desenzano.
Grazie agli amici della Salette del martedì sera.
Grazie a tutte le persone conosciute a Loreto nel 2008, a quelle conosciute in occasione del matrimonio (..e diventate così care!), a quelle incontrate “per caso” in questi anni e che hanno lasciato il segno e che tutt’ora fanno la differenza.. Antonio, Elisa e Paolo, Lucia e Giovanni, Sara e Francesco, Nicola, Daniele, Pacciaiapan e ancora tutte le famiglie speciali che ci sono vicine e sono dei sicuri punti di riferimento.
Grazie a tutti i compagni delle superiori per la voglia di vedersi, aiutarsi, condividere, incoraggiarsi e divertirsi insieme. E sempre un piacere organizzare un ritrovo con loro!

Grazie agli amici del Saval per il loro affetto e per la loro presenza.
Grazie a Glendy e Polly, le mie care testimoni, con cui condivido ogni esperienza e per cui farei qualsiasi cosa. Sono per me come sorelle!
Grazie alle mie compagne di squadra, soprattutto al gruppo storico, con cui si è creata una profonda amicizia e con cui c’è sempre un’intesa unica!

Grazie ai miei genitori per tutto l’affetto che mi dimostrano e su cui so di poter sempre contare. Sanno proprio fare la differenza!

Grazie a Stefano, insostituibile al mio fianco e con cui sento davvero di essere una cosa sola.

Ma più di tutti grazie a Colui che mi ha amato da sempre e il cui prezioso Amore ho scoperto solo in questi anni. In questa vita nuova con Lui ogni affetto, amicizia, intuizione, decisione, relazione, avvenimento acquista ogni giorno un “sapore” nuovo e un entusiasmo e una felicità sempre più veri.